Solar Probe+ Mission Engineering Study Report

March 10, 2008

NASA

APL

March 10, 2008

Solar Probe+ Mission Engineering Study Report

Prepared for NASA's Heliophysics Division

By The Johns Hopkins University Applied Physics Laboratory (Under Contract NNN06AA01C)

Approved By:

Andrew A. Dantzler
Study Lead, The Johns Hopkins University Applied Physics Laboratory

Robert D. Strain
Space Department Head, The Johns Hopkins University Applied Physics Laboratory

J. Walter Faulconer
Civilian Space Business Area Executive, The Johns Hopkins University Applied Physics Laboratory

DISCLAIMER: Note that all colors used on mechanical drawings contained in this report are for clarification of image content only and do not necessarily reflect the actual colors of the items depicted.

ACKNOWLEDGMENTS

STUDY TEAM AND SUPPORT

David Artis, *JHU/APL*
Scott Benson, *NASA/Glenn Research Center*
Stewart S. Bushman, *JHU/APL*
Andrew Dantzler, *JHU/APL*
Christopher Deboy, *JHU/APL*
Michelle M. Donegan, *JHU/APL*
David G. Drewry, *JHU/APL*
Peter Eisenreich, *JHU/APL*
Jacob Elbaz, *JHU/APL*
Martin Fraeman, *JHU/APL*
Daryl George, *JHU/APL*
Robert E. Gold, *JHU/APL*
Yanping Guo, *JHU/APL*
Meagan Hahn, *JHU/APL*
Roshanak Hakimzadeh, *NASA/Glenn Research Center*
Ray Harvey, *JHU/APL*
John Hickman, *NASA/Glenn Research Center*
Angela Hughes, *JHU/APL*
Jack Hunt, *JHU/APL*
Kelly Judge, *JHU/APL*
Anne King, *JHU/APL*
James D. Kinnison, *JHU/APL*
Geoffrey Landis, *NASA/Glenn Research Center*
Valerie Lyons, *NASA/Glenn Research Center*
Douglas Mehoke, *JHU/APL*
Chris Monaco, *JHU/APL*
Steve Parr, *JHU/APL*
David Persons, *JHU/APL*
Sandra Reehorst, *NASA/Glenn Research Center*
John Riehl, *NASA/Glenn Research Center*
Elliot Rodberg, *JHU/APL*
Lew Roufberg, *JHU/APL*
Paul Schmitz, *NASA/Glenn Research Center*
Richard K. Shaltens, *NASA/Glenn Research Center*
Hongxing Shapiro, *JHU/APL*
Rainee Simons, *NASA/Glenn Research Center*
Tom Sutliff, *NASA/Glenn Research Center*
Michael D. Trela, *JHU/APL*
Brian R. Tull, *JHU/APL*
Steve Vernon, *JHU/APL*
Joe Wagner, *MCR Technologies, LLC*
David R. Weir, *JHU/APL*
Melissa Wirzburger, *JHU/APL*
Larry Wolfarth, *JHU/APL*

SCIENCE AND TECHNOLOGY DEFINITION TEAM

Loren Acton, *Montana State University*
Marianne Balat, *Centre National de la Recherche Scientifique (CNRS)*
Volker Bothmer, *University of Goettingen*
Ray Dirling, *Science Applications International Corporation (SAIC)*
Bill Feldman, *Los Alamos National Laboratory*
George Gloeckler, *University of Michigan*
Shadia Habbal, *University of Hawaii*
Don Hassler, *Southwest Research Institute (SwRI)*
Ingrid Mann, *Westfalische Wilhelms-Universitat Muenster*
Bill Matthaeus, *University of Delaware/Bartol Research Institute*
Dave McComas (Chair), *SwRI*
Ralph McNutt, *JHU/APL*
Dick Mewaldt, *California Institute of Technology*
Neil Murphy, *Jet Propulsion Laboratory (JPL)*
Leon Ofman, *Catholic University of America*
Ed Sittler, *NASA/Goddard Space Flight Center*
Chuck Smith, *University of New Hampshire*
Marco Velli, *Florence/JPL*
Thomas Zurbuchen, *University of Michigan*

Solar Probe+ Mission Engineering Study Report

Mission Overview

Solar Probe+ will be a historic mission, flying into one of the last unexplored regions of the solar system, the Sun's atmosphere or corona, for the first time. Approaching as close as 8.5 solar radii above the Sun's surface, Solar Probe+ will employ a combination of in situ measurements and imaging to achieve the mission's primary scientific goal: to understand how the Sun's corona is heated and how the solar wind is accelerated. Solar Probe+ will revolutionize our knowledge of the physics of the origin and evolution of the solar wind.

Science Objectives

- Determine the structure and dynamics of the magnetic fields at the sources of the fast and slow solar wind
- Trace the flow of energy that heats the corona and accelerates the solar wind
- Determine what mechanisms accelerate and transport energetic particles
- Explore dusty plasma phenomena in the near-Sun environment and their influence on the solar wind and energetic particle formation

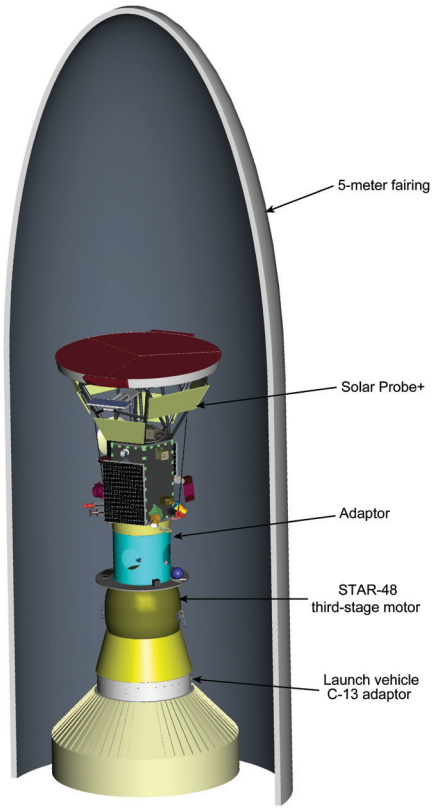

Solar Probe+ will launch on an Atlas V551 with a STAR-48BV third stage to achieve the required launch energy.

Mission Summary

Launch Vehicle	Atlas V 551
Third Stage	STAR-48BV
Launch Window	May 21 through June 9, 2015
First Perihelion	August 2015
First Min. Perihelion at 9.5 R_S	October 2021
Cost	$739.5 million (FY07$)

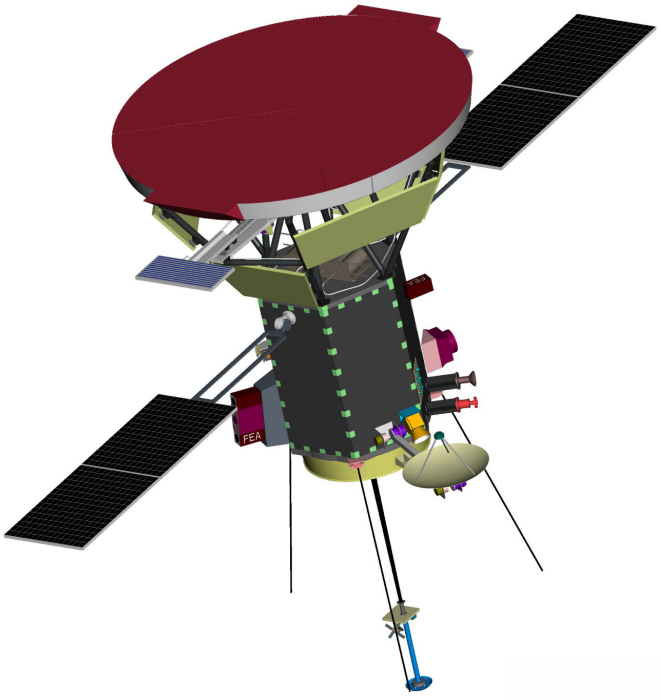

Solar Probe+ shown with primary solar array panel in the deployed position.

Spacecraft Summary	
Wet Mass	481 kg (lift mass: 610 kg for 30% margin)
Power	• 482 W for high-power mode; includes 34% margin • Dual solar array system
Configuration	Three-axis-stabilized
Propulsion	Hydrazine monopropellant 190 m/s ΔV
Attitude control	Reaction wheels and thrusters
Thermal Control	Passive thermal control using blankets and active cooling for secondary solar arrays
Telecommunications	• Dual-frequency X-band and Ka-band through articulated HGA • Dual 128-Gbit solid-state recorders for redundant data storage prior to downlink

Solar Intensity

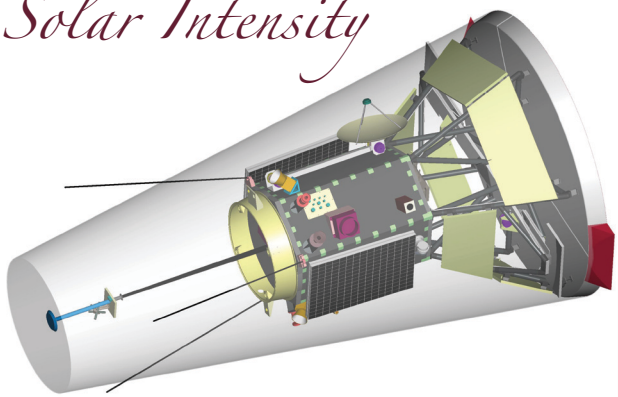

Instruments will be retracted inside the umbra of the Thermal Protection System to limit solar exposure.

Power Generation

Solar Probe+ uses two sets of solar cell arrays, each optimized to work over a different range of Sun–probe distances.

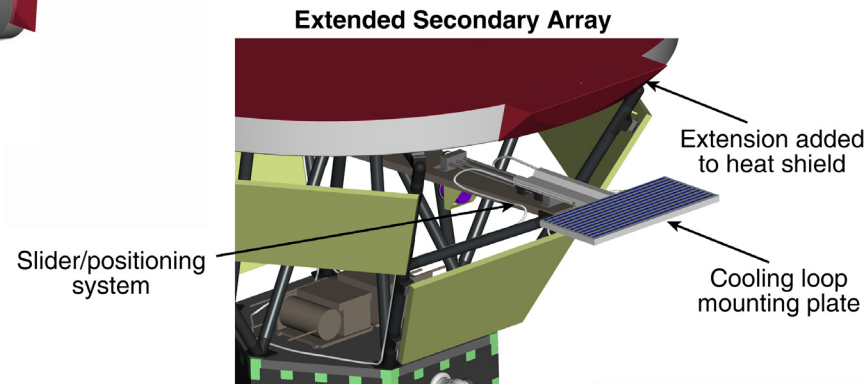

Mission Enablers

Challenge	Solution
Solar Intensity	Thermal Protection System
Power Generation	Secondary Solar Arrays
Temperature Control	Support Structure
Mission Design	Multiple Venus Gravity-Assist Trajectories

Temperature Control

The transition structure assembly provides the mechanical support structure that couples the bus to the Thermal Protection System.

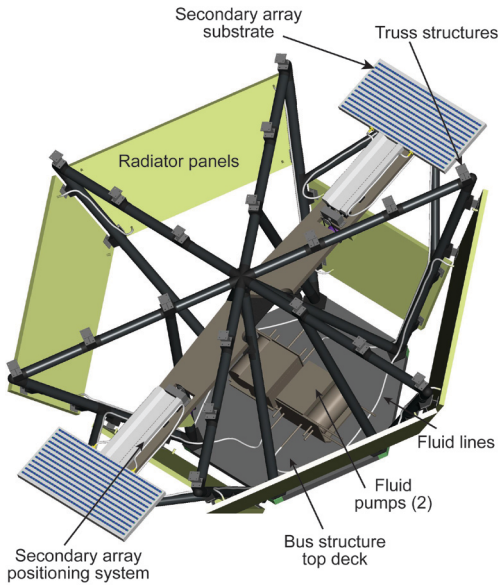

Mission Design

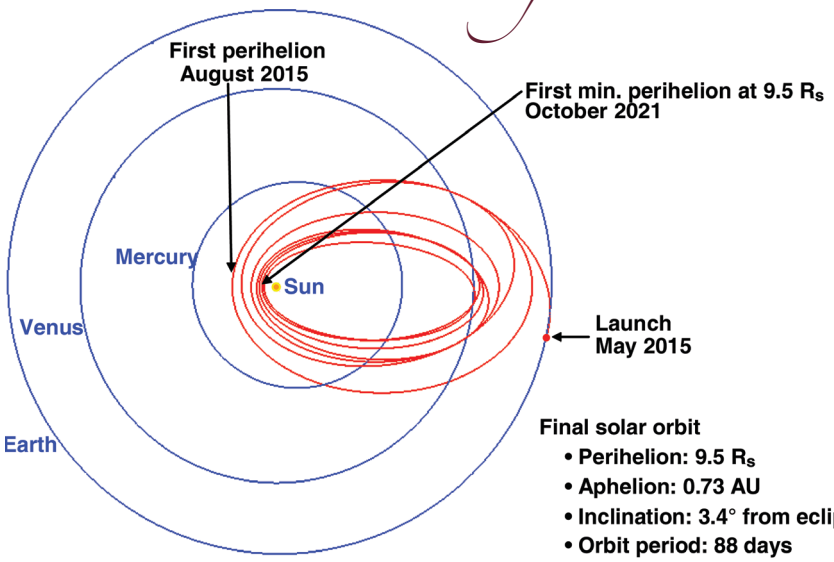

Final solar orbit

- **Perihelion: 9.5 R_S**
- **Aphelion: 0.73 AU**
- **Inclination: 3.4° from ecliptic**
- **Orbit period: 88 days**

The baseline Solar Probe+ trajectory uses Venus flybys and no deep-space maneuvers to reach a minimum perihelion of 9.5 R_S in 6.4 years.

TABLE OF CONTENTS

1.0. EXECUTIVE SUMMARY

The concept of a probe to investigate the close regions of the Sun has been studied for more than 40 years. In 2005, NASA tasked The Johns Hopkins University Applied Physics Laboratory (APL) to work with an independent Science and Technology Definition Team (STDT) to determine the optimum concept for such a Solar Probe mission. The results of that study[1] described an exciting mission to the Sun that would meet all of the science objectives laid out by the STDT. Unfortunately, the overall cost of the described mission and its required use of plutonium for power production made the mission unrealizable within available resources.

On August 27, 2007, NASA tasked APL to conduct a new study, called Solar Probe Lite, to determine the feasibility of a non-nuclear mission that would retain as much of the 2005 Solar Probe concept's science as possible, for a total mission cost of less than $750M. In performing this study, APL worked in tandem with the original STDT to ensure that the new concept remained commensurate with the intended science. The result is a mission called Solar Probe+, so dubbed by the STDT because of the potential gains in science of the current concept over its predecessors.

This report presents the engineering concept and cost estimate basis for the Solar Probe+ mission. The science objectives, justification, and science implementation plan, as well as comparisons to the objectives and implementation presented in the 2005 study, for the Solar Probe+ mission will be described in a partner report to this one,[2] written in parallel by the STDT. Table 1.0-1 provides a summary of this study's compliance with the requirements laid out in the NASA Task Order (NNN07AA15T of Contract NNN06AA01C) that initiated the study. All requirements are met, with the exception of meeting the mass margin of 35%. The 30.1% margin we present, however, is within the industry standard. In addition, methods to increase this margin exist and warrant further study. Mass margin is discussed further in Section 3.4.3.

[1] *Solar Probe: Report of the Science and Technology Definition Team*, NASA/TM—2005–212786, National Aeronautics and Space Administration, Goddard Space Flight Center, Greenbelt, MD (2005).

[2] *Solar Probe+: Report of the Science and Technology Definition Team*, Southwest Research Institute, San Antonio, TX, in press (2008).

1.1. Solar Probe+ Spacecraft and Mission Design Summary

In two full Science and Technology Definition Team (STDT) meetings and several smaller discussions, the STDT and engineering team members refined science and measurement objectives from previous Solar Probe studies, defined instrument resource and accommodation requirements, developed orbit geometries and concepts of operations, and identified risk mitigation measures and cost savings options. The STDT encouraged the engineering team to draw on their own extensive internal experience with space missions, along with examining external ideas and solutions, to develop the most detailed and technically complete engineering study possible. Key requirements that flow down from the study ground rules and science objectives are summarized here:

Mission Requirements

- ***Achieve at least three orbits with perihelion distance less than 10 R_S***
- ***Achieve the above within 10 years***
- ***Return all data collected from each perihelion pass***

Spacecraft Requirements

- ***Survive solar intensity during perihelion pass (with a solar intensity of ~510 Suns)***
- ***Provide reliable power over the distance range of 0.04–1 AU***
- ***Accommodate the STDT-provided strawman payload***

Table 1.0-1. Summary of study concept performance against task order requirements.

Item from Task Order NNN07AA15T	Study Report Compliance
"Total mission lifecycle cost shall not exceed $750 million in FY07 dollars including the launch vehicle."	Total mission cost is estimated at ~$740M in FY07$.
"Use the earliest technically feasible launch readiness date, assuming a April 2009 Phase A start with no constraints on funding profile."	Mission design work has yielded May 2015 as the optimum launch date. Schedule and costing assumes April 2009 Phase A start.
"The instrument costs shall not exceed $100 million, and NASA shall specify the reduced payload content from the Solar Probe STDT reports."	The STDT has reached consensus on a strawman payload suite. Cost is assumed to be $100M, all-inclusive.
"The launch vehicle is an Evolved Expendable Launch Vehicle (EELV)."	The launch vehicle is an Atlas V 551.
"The cost estimate shall include at least one independent, parametric estimate."	An independent cost estimate was performed by MCR Technologies, LLC, and reconciled with independent APL cost analysts to ensure validity.
"The cost estimate shall include 30 percent reserves on Phases B through D excluding the EELV."	The report cost estimate includes 30% on Phases B–D, as well as 5% on Phase A and 15% on Phase E. Reserves are on total mission excluding the launch vehicle, Deep Space Network (DSN), and payload suite.
"The schedule reserves for mission shall include at least one month per year for Phases B and C and two months per year for Phase D."	The report schedule includes 9.5 months of funded reserve. Reserve in each phase meets or exceeds the requirement.
"Margins for mass and power shall be at least 35 percent."	Mass margin is 30.1%. Possibilities for increase of margin, if necessary, exist and can be studied in Phase A. Power margin is 34.4% (worst case).
"The mission pre-concept shall not use Multi-mission Radioactive Thermoelectric Generators"	Solar Probe+ uses photovoltaics.

The result of this study is a technically feasible, acceptably low-risk and affordable mission that can survive in the unique thermal and dust environment near the Sun and that will fully achieve all of the Solar Probe+ science objectives.

Trajectory trade studies were conducted aimed at developing a feasible mission concept for Solar Probe+ under NASA's new direction and guidelines. Trajectory design is the key that defines the scope of the mission and determines how the mission will be implemented, what can be accomplished for science, and how much it will cost. A wide range of trajectory options were explored with various mission scenarios. Representative trajectory design options were presented to the STDT and discussed between the APL engineering team and the STDT science team. After discussions and comparison, a baseline trajectory design was selected from six alternative trajectory design options, including a Jupiter gravity assist trajectory design.

The baseline mission design (Figure 1.1-1) meets the above-listed mission requirements and program constraints. This design features

- Launch in May 2015, with total mission duration of ~7 years
- First perihelion at ~0.16 AU (35 R_S) in 3 months after launch
- 24 orbits over 6.9 years, 19 perihelia within 20 R_S , yielding 961 hours within the 20-R_S region
- Three perihelia at 9.5 R_S (heliocentric distance), with an orbital period of 88 days
- Frequent visits of the near-Sun region over 6 years, providing extensive science measurements over a half solar cycle

In addition to providing nearly 1000 hours of science collection opportunity within the near-Sun region, the baseline mission design also

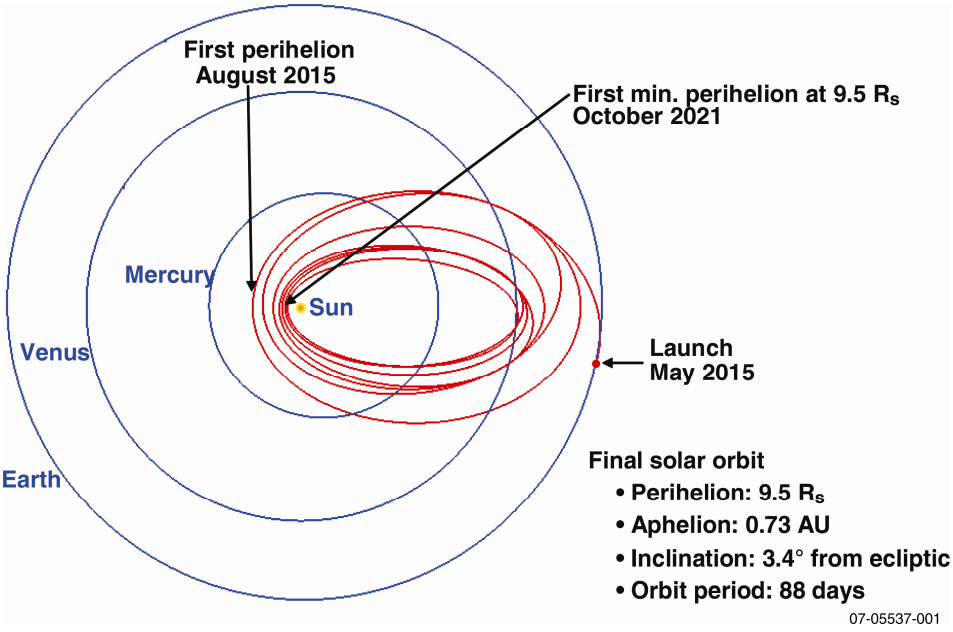

Figure 1.1-1. Baseline Solar Probe+ trajectory.

has several advantages in mission implementation. For example

- Perihelion gradually decreases to 9.5 R_S, allowing for "practice," leading to successively closer perihelia
- Aphelion is less than 1 AU, ensuring sufficient solar power without the need for radioisotope thermoelectric generators (RTGs)

The baseline Solar Probe+ is a three-axis-stabilized spacecraft designed to survive and operate successfully throughout its many orbits around the Sun. The spacecraft concept utilizes a Thermal Protection System (TPS) that features a large 2.7-m diameter carbon–carbon low-conductivity, low-density shield. The TPS protects the spacecraft bus and instruments within its umbra during the solar encounter. The bus consists of a hexagonal equipment module and a cylindrical adapter. It provides an efficient mechanical structure that accommodates the instruments and spacecraft subsystems and handles the loads from the TPS and the launch loads. Solar Probe+ will be powered by two sets of photovoltaic arrays. The two primary arrays are deployed when the spacecraft is more than 0.25 AU from the Sun and are retracted at closer distances. Within 0.25 AU, two smaller, high-temperature-tolerant photovoltaic arrays provide power. These arrays are cooled by a pumped liquid system and gradually are retracted behind the TPS as the spacecraft approaches the Sun, effectively keeping the incident solar power approximately constant. A simple blowdown hydrazine monopropellant propulsion system will be used for ΔV maneuvers and attitude control. The guidance and control system consists of three star trackers and a high-precision, internally redundant inertial measurement unit that provide attitude knowledge, and attitude control is provided by four reaction wheels and 12 thrusters. The spacecraft is equipped with three antennas: a high-gain antenna (HGA) mounted to a dual-axis gimbaled mast and two hard-mounted low-gain antennas (LGAs). The HGA is the prime antenna for the Ka-band science return downlink, whereas X-band uplink and downlink capability is provided through all antennas. When the spacecraft is within 0.59 AU of the Sun, communications are maintained through the LGAs.

Although the benefits of the Solar Probe+ are numerous, it is necessary to note that there are important issues that must be more fully addressed in Phase A in order to help ensure a successful mission. Among these issues are the multiple-flyby trajectory and the detailed design and qualification of the Thermal Protection System and the secondary solar arrays.

1.2. Solar Probe+ Summary

Solar Probe+ is an exciting mission of exploration and discovery. It will journey to one of the last unexplored regions of the solar system and reveal how the corona is heated and the solar wind is accelerated, solving two fundamental mysteries that have been top-priority science goals for many decades. The mission described in this study report is based on a rigorous engineering study performed in concert with the Science and Technology Definition Team (STDT). The described mission is technically feasible, can be accomplished within realistic resources, and can fully achieve all science objectives, thus transforming our understanding of the Sun and its sister Sun-like stars and enabling exploration.

2.0. SCIENCE OBJECTIVES AND INSTRUMENTATION

The Solar Probe+ Science and Technology Definition Team (STDT) has written a partner report to this one,[1] describing in detail the science objectives, justification, and science implementation plan for the Solar Probe+ mission. The purpose of the present engineering study report is to describe how these science objectives will be met. To set the context for the engineering description, a top-level summary of the Solar Probe+ science objectives is presented here.

- ***Determine the structure and dynamics of the magnetic fields at the sources of the fast and slow solar wind***
- ***Trace the flow of energy that heats the corona and accelerates the solar wind***
- ***Determine what mechanisms accelerate and transport energetic particles***
- ***Explore dusty plasma phenomena in the near-Sun environment and their influence on the solar wind and energetic particle formation***

The Solar Probe+ science objectives will be addressed through a combination of in situ and remote-sensing observations made from a near-ecliptic heliocentric orbit at progressively closer distances to the Sun, with the spacecraft achieving a minimum perihelion distance of ~9.5 R_S in roughly 6.5 years after launch.

To meet the Solar Probe+ science objectives, the STDT has recommended an integrated strawman payload comprising in situ and remote-sensing instruments. For the purposes of assigning resources to the components of payload suite, the STDT started with the baseline of the 2005 Solar Probe STDT report,[2] in which mass, power, and peak data rate are provided. The payload suite will be serviced by a common data processing unit (CDPU) and a low-voltage power supply (LVPS). A single integrated payload has been assumed in the engineering study and cost estimate. The strawman payload consists of the following instruments:

In Situ Instrumentation

- ***Fast Ion Analyzer (FIA)***
- ***Two Fast Electron Analyzers (FEAs)***
- ***Ion Composition Analyzer (ICA)***
- ***Energetic Particle Instrument (EPI)***
- ***Magnetometer (MAG)***
- ***Plasma-Wave Instrument (PWI)***
- ***Neutron/Gamma-Ray Spectrometer (NGS)***
- ***Coronal Dust Detector (CD)***

Remote-Sensing Instrumentation

- ***White-Light Hemispheric Imager (HI)***

In addition, the STDT has assumed resources (within the overall allocation for the suite) for an additional instrument, in the event that an unforeseen beneficial component is proposed.

The entire payload suite connects to a CDPU, which integrates the data processing and LVPS for all of the payload science instruments into a fully redundant system that eliminates replication, increases redundancy, and reduces overall payload resources.

The CDPU provides a unified interface to the payload for the spacecraft. The spacecraft selects which side of the CDPU will be powered, leaving the redundant side off as a cold spare. The payload CDPU communicates with the spacecraft over a MIL-STD-1553 bus, accepting commands and producing Consulta-

[1] *Solar Probe+: Report of the Science and Technology Definition Team*, Southwest Research Institute, San Antonio, TX, in press (2008).

[2] *Solar Probe: Report of the Science and Technology Definition Team*, NASA/TM—2005–212786, National Aeronautics and Space Administration, Goddard Space Flight Center, Greenbelt, MD (2005).

tive Committee for Space Data Systems (CCSDS) packets ready for final processing by the spacecraft for telemetry to the ground. Accommodation of the payload suite is covered further in Section 3.

3.0. MISSION IMPLEMENTATION

Throughout the Solar Probe+ study, an engineering team from The Johns Hopkins University Applied Physics Laboratory (APL) and Glenn Research Center has worked closely with the Science and Technology Definition Team (STDT) to define the technical mission implementation described in this section. The ground rules for implementation defined by NASA for this study are as follows:

- Preserve Solar Probe science to the maximum extent possible
- Power the spacecraft with a non-nuclear power source
- Develop a mission with duration of less than 10 years
- Launch in 2015
- Maintain mass and power margins of at least 35%
- Keep total mission cost below $750M

In two full STDT meetings and several smaller discussions, the STDT and engineering team members reexamined the science and measurement objectives from previous Solar Probe studies[1,2,3,4,5] in light of the current study ground rules, defined instrument resource and accommodation requirements for this new concept, developed a new orbit geometry and concept of operations, and identified risk mitigation measures and cost savings options for the new concept. The STDT encouraged the engineering team to draw on their own extensive internal experience with space missions, and to examine external ideas and solutions, in order to develop the most detailed and technically complete engineering study possible.

Our approach has been to examine the 2005 Solar Probe mission implementation in light of the NASA ground rules and science requirements flow-down and only address areas of the previous implementation that have changed. For example, the previous study included design detail for the avionics suite. Only minor changes to this suite are needed to meet the requirements for the Solar Probe+ concept; the avionics description in Section 3.9 focuses on the changes to the subsystem to respond to revised requirements rather than including a detailed design description. Other areas where the changes from the 2005 Solar Probe study are more significant include correspondingly more description.

Key requirements that flow down from the study ground rules and science objectives are summarized below.

Mission Requirements

- At least three orbits with perihelion distance less than 10 R_S
- A Sun–spacecraft–Earth encounter geometry that supports simultaneous Earth-based observations to support Solar Probe+ observations
- Minimum perihelion orbits achieved within 10 years
- Return of full data collected in a solar encounter in each orbit

Spacecraft Requirements

- Survive solar intensity during perihelion (~510 Suns)
- Provide reliable power over the distance range of 0.044–1 AU

[1]Gloeckler, G., *et al*., *Solar Probe: First Mission to the Nearest Star, Report of the NASA Science Definition Team for the Solar Probe Mission*, The Johns Hopkins University Applied Physics Laboratory, Laurel, MD (1999).

[2]*Solar Probe: An Engineering Study*, prepared by The Johns Hopkins University Applied Physics Laboratory, in partnership with the Jet Propulsion Laboratory, under contract NAS5-01072, Laurel, MD (November 12, 2002).

[3]*Solar Probe: Report of the Science and Technology Definition Team*, NASA/TM—2005–212786, National Aeronautics and Space Administration, Goddard Space Flight Center, Greenbelt, MD (2005).

[4]*Solar Probe Risk Mitigation Study*, prepared by The Johns Hopkins University Applied Physics Laboratory, 2006 Mid-Year Report.

[5]*Solar Probe Thermal Protection System Risk Mitigation Study: FY 2006 Final Report*, prepared by The Johns Hopkins University Applied Physics Laboratory under Contract NAS5-01072, Laurel, MD (November 30, 2006); and *ITAR-Restricted Annex* (September 17, 2007).

- Protect instruments and spacecraft systems from dust environment near the Sun
- Provide large total science data return (~128 Gbits per orbit)
- Accommodate significant payload mass (~50 kg) and power (57 W)
- Provide science boom for magnetometer and plasma-wave search coils
- Provide actuations of instruments and antennas for proper placement and field of view (FOV) orientations during science collection

These requirements differ from previous Solar Probe studies in that the science objectives are satisfied by repeated passes through the near-equatorial coronal regions rather than one to two passes through the region using a polar approach, as described in Section 2. The new mission concept results in several changes to mission and spacecraft requirements that offered opportunities for simplification of aspects of the mission. For instance, the 2005 Solar Probe study identified real-time science data downlink as a mission requirement to reduce the risk of data loss given that only two opportunities for science collection exist in that mission concept. The Solar Probe+ mission concept achieves the same risk mitigation by using more data collection opportunities and a softer walk-in to the critical region that allows an opportunity to practice for the required encounters and to repeat measurements interrupted by anomalies. This change in approach allows the use of a simpler store-and-downlink concept of operations where data collection and data downlink are decoupled. Each section below includes a description of these changes from the 2005 Solar Probe concept.

These requirements, and the new mission design, led to three major challenges addressed by the engineering team. The *first challenge* was to develop a power system concept not centered on the use of radioisotope thermoelectric generators (RTGs), which led to an extensive trade study on systems able to generate power near the Sun as well as at aphelion. The *second challenge* was to survive the thermal environment of the near-Sun portions of the orbit, achieved through adaptation of previous Thermal Protection System (TPS) designs. The *third challenge* was to develop a lightweight spacecraft concept that fits within the performance of current launch vehicles. Solar Probe+ is planned for an Atlas V 551 launch with positive mass margin, yet retains compatibility with the Delta IVH for risk mitigation. Each section below includes a summary of trade studies conducted in the development of this concept as well as a description of trade studies and analyses to be conducted early in the Solar Probe+ program.

The result of this study is a technically feasible and affordable mission with acceptable risk that can survive in the unique thermal and dust environment near the Sun and that will fully achieve all of the Solar Probe+ science objectives. The sections that follow describe this baseline Solar Probe+ mission. Additional supporting material is presented in the Appendices.

3.1. Baseline Mission Design

3.1.1. Mission Design Overview

The engineering team conducted studies of trajectories to develop a feasible mission concept for Solar Probe under NASA's new direction and guidelines. In order to meet these requirements, significant change is required to the Solar Probe mission concept developed during the last several Solar Probe study efforts, the last one being the 2005 *Solar Probe: Report of the Science and Technology Definition Team*.[6] Trajectory design is the key that defines the scope of the mission and determines how the mission will be implemented, what can be accomplished for science, and how much it will cost. A wide range of trajectory options were explored with various mission scenarios. Representative trajectory design options were presented to the STDT and discussed between the APL engineering

[6] *Solar Probe: Report of the Science and Technology Definition Team*, NASA/TM—2005–212786, National Aeronautics and Space Administration, Goddard Space Flight Center, Greenbelt, MD (2005).

team and the STDT science team. After discussions and comparison, a baseline trajectory design was selected from six alternative trajectory design options, including a Jupiter gravity assist (JGA) trajectory design. Details of this trade study are given in Section 3.1.9.

The baseline mission design meets the above-listed mission requirements and program constraints. The baseline trajectory design presents a new mission concept with more thorough and repeated exploration of the near-Sun region:

- Launch in May 2015, with total mission duration of 6.9 years
- First solar pass at ~0.16 AU (35 R_S) in 3 months after launch
- 24 solar encounters over 6.9 years, 19 encounters within 20 R_S, 961 hours within 20 R_S region
- Minimum perihelion at 9.5 R_S
- Baseline three perihelia at 9.5 R_S, occurring every 88 days
- More orbits are possible in extended mission, requiring no orbit maintenance
- Frequent visits at the heliosphere region over 6 years, providing extensive science measurements over a half solar cycle

In addition to offering more science opportunity as described in Section 2, the trajectory design also has several advantages in mission implementation:

- Perihelion gradually decreases to 9.5 R_S, lowering mission risk
- Aphelion is less than 1 AU, ensuring sufficient solar power without the need of RTG
- Minimum perihelion of 9.5 R_S reduces the solar flux and corresponding thermal environment, allowing use of photovoltaics for power generation through the entire orbit
- Avoidance of JGA simplifies power system and allows for multiple solar encounters

3.1.2. Launch

The baseline mission design calls for Solar Probe+ to be launched in May–June 2015 during a 20-day launch period from May 21 through June 9, 2015. On each day, up to 30 minutes is planned for the launch window. Preliminary trajectory analysis shows the launch time for May 21, 2015, as 06:10 UTC. As with other interplanetary missions, the spacecraft will be placed into a low-Earth parking orbit after lift-off from the launch pad by the launch vehicle, coasting in the parking orbit for ~34 minutes, and then will be injected into the desired heliocentric trajectory. Candidate launch vehicle and upper stage are described in Section 3.1.7.

3.1.3. Baseline Mission Trajectory

The baseline trajectory uses seven Venus flybys and no deep-space maneuvers to reach a minimum perihelion of 9.5 R_S in 6.4 years in October 2021, as shown in Figure 3.1-1. The baseline mission will end after three orbits with at the minimum perihelion of 9.5 R_S. From launch to the end of mission, the baseline trajectory consists of

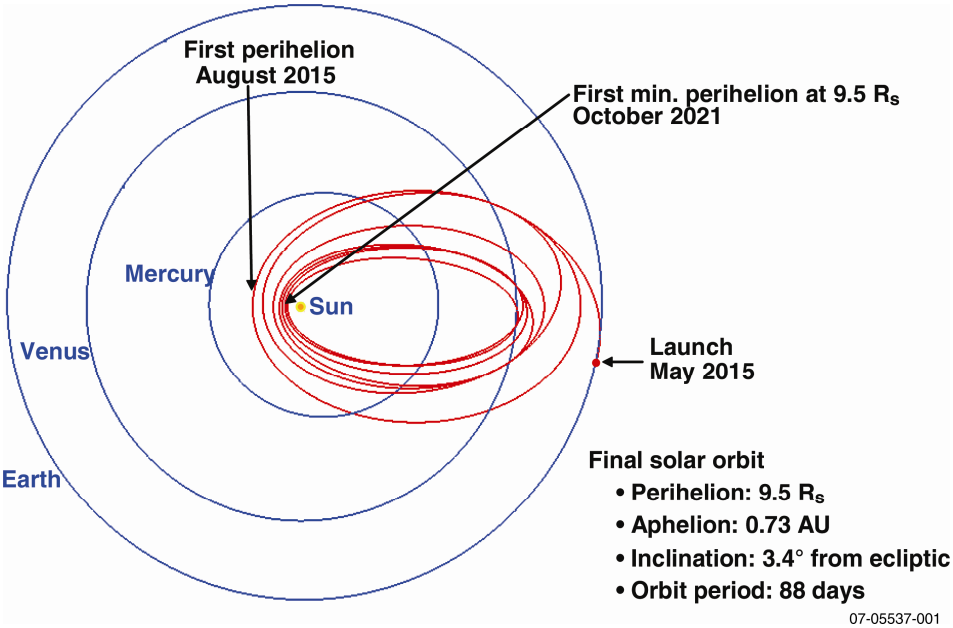

Figure 3.1-1. Baseline Solar Probe+ trajectory.

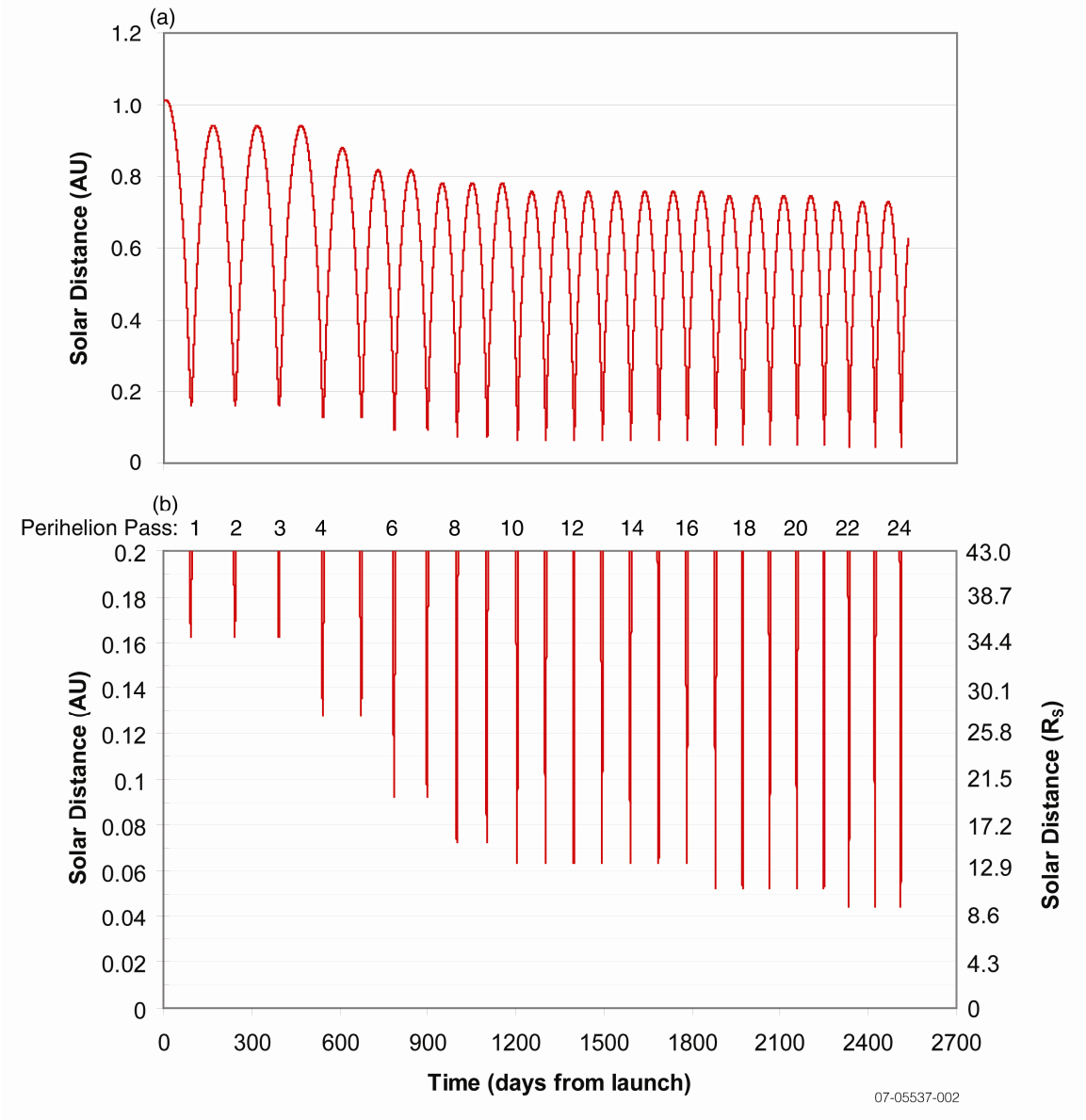

Figure 3.1-2. Solar distance profile for baseline trajectory.

24 solar orbits whose perihelia gradually decrease, from 35 R_S down to 9.5 R_S. Figure 3.1-2 plots the solar distance over the entire mission and the perihelion distances of the 24 solar orbits. The first perihelion occurs only 3 months after launch. The Sun–Earth–probe (SEP) angle and Sun–probe–Earth (SPE) angle as functions of time are plotted in Figure 3.1-3.

A completely integrated trajectory of the baseline mission from launch through the end of the nominal mission (after three 9.5-R_S perihelion orbits) was computed with a full gravity field model including the Sun and all planets. The results of the trajectory were verified by different mission design software used for trajectory design, flyby targeting, and trajectory correction maneuver (TCM) planning for the ongoing interplanetary missions [New Horizons, MESSENGER (Mercury Surface, Space Environment, Geochemistry, and Ranging), and STEREO (Solar Terrestrial Relations Observatory)] managed by APL for NASA.

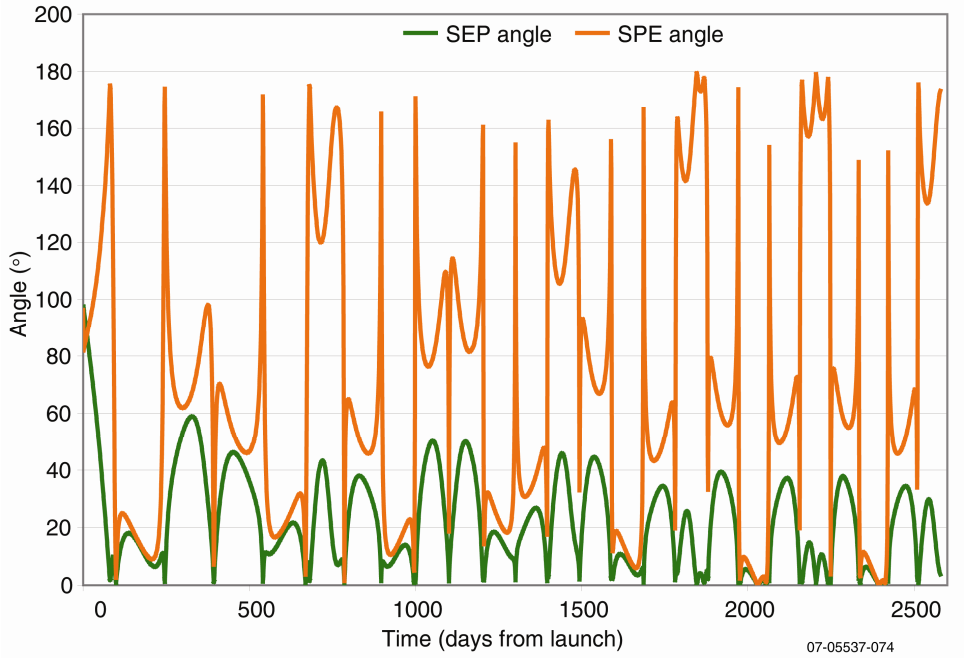

Figure 3.1-3. Sun–Earth–probe (SEP) angle and Sun–probe–Earth (SPE) angles for the baseline Solar Probe+ trajectory.

3.1.4. Solar Encounters

Figure 3.1-4 shows a solar encounter trajectory with perihelion at 9.5 R_S, viewing from the north pole of the Sun. The time duration within 20 R_S is 57 hours. The perihelion velocity with respect to the Sun will approach 200 km/s. Trajectories of other perihelion orbits are similar with a greater distance and a slower speed.

At each solar encounter, the geometry of Earth with respect to the encounter trajectory is of great interest to science, because of the intent to conduct observations remotely from the Earth while the onboard in situ measurements are performed. With 24 solar encounters, this mission design allows for various observation geometries from the Earth when Solar Probe+ is passing in front of the Sun at perihelion. The Earth positions at the three 9.5-R_S perihelion orbits are shown in Figure 3.1-5 as an example. The range between the spacecraft and Earth is illustrated in Figure 3.1-6 for those and all other orbits.

As indicated in Figure 3.1-2*b* and Table 3.1-1, Solar Probe+ will spend a significant amount of time in the near-Sun region, covering more than half of the 11-year solar cycle, with three to four encounters per year. In 24 orbits over the 6.9-year mission duration, the perihelion distance decreases from 35 R_S to 9.5 R_S. In 21 of the orbits, the distance from the center of the Sun will be less then 30 R_S, and in 19 of the orbits, the distance from the center of the Sun will be less than 20 R_S. The total accumulated

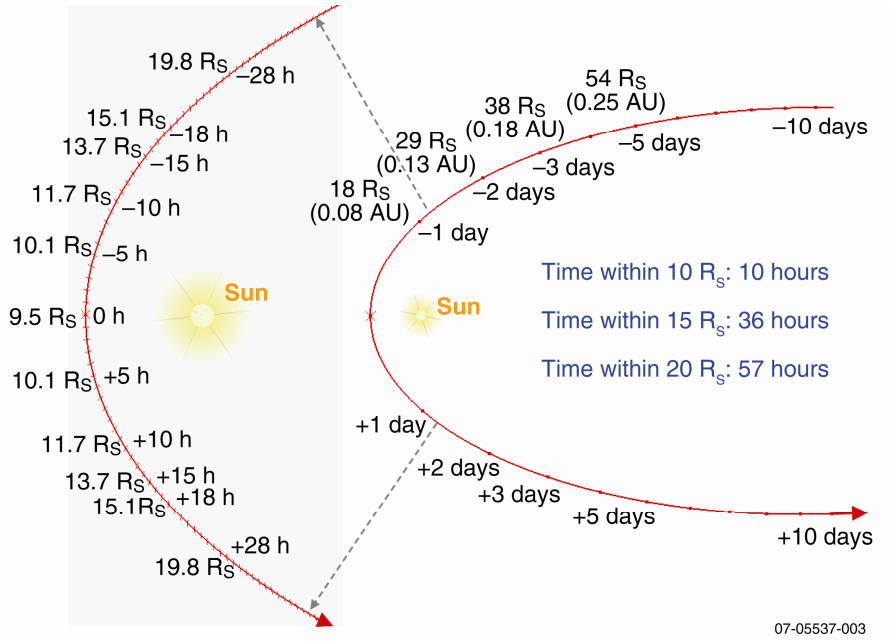

Figure 3.1-4. Near-Sun trajectory for baseline mission.

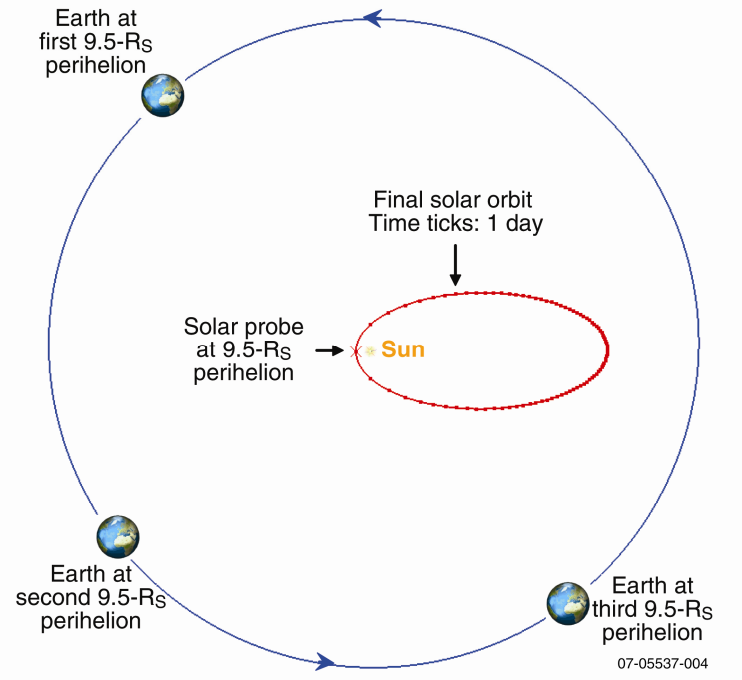

Figure 3.1-5. Location of Earth during solar encounters with perihelion below 10 R_S.

time of Solar Probe+ within the regions of less than 30 R_S, 20 R_S, 15 R_S, and 10 R_S is summarized in Table 3.1-1.

Table 3.1-1. Times in various solar distance regions.

Solar Pass Number	Time within			
	30 R_S (hr)	20 R_S (hr)	15 R_S (hr)	10 R_S (hr)
4	67			
5	67			
6	105	10		
7	105	10		
8	109	50		
9	109	50		
10	108	55	23	
11	108	55	23	
12	108	55	23	
13	108	55	23	
14	108	55	23	
15	108	55	23	
16	108	55	23	
17	105	57	33	
18	105	57	33	
19	105	57	33	
20	105	57	33	
21	105	57	33	
22	102	57	36	10
23	102	57	36	10
24	102	57	36	10
Total	2149	961	434	30

3.1.5. Comparison with 2005 Solar Probe

The 2005 Solar Probe mission concept used a JGA trajectory to achieve a pole-to-pole near-Sun orbit with perihelion at 4 R_S. The aphelion of the final heliocentric orbit was 5.5 AU, about the distance of Jupiter. Two solar encounters were baselined and were separated by the orbital period of 4.6 years, which resulted in mission duration of 8.8 years, ending after the second solar encounter. The first Sun encounter would have occurred 4.1 years after launch in October 2014.

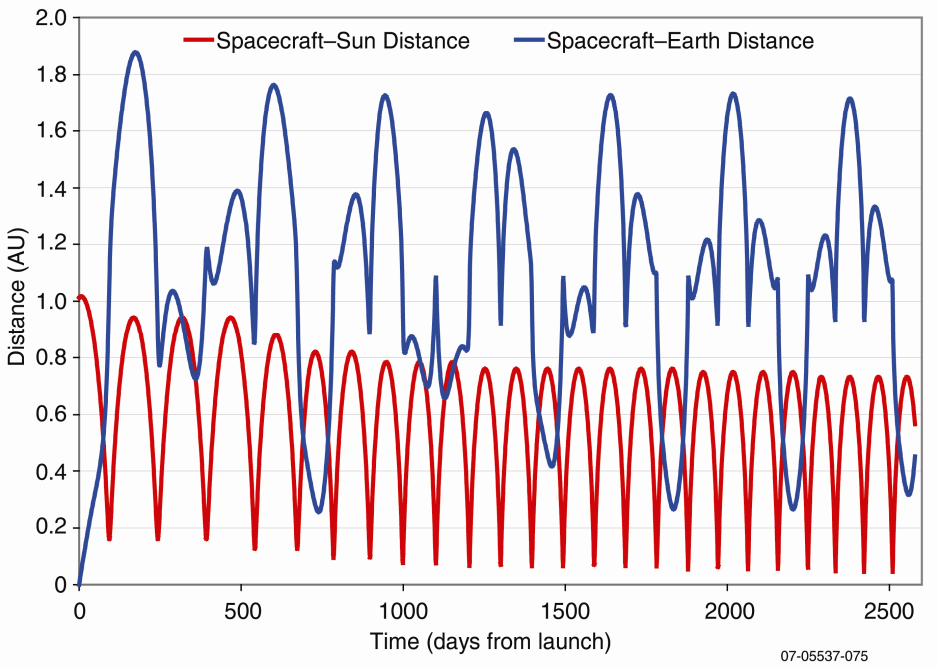

Figure 3.1-6. Distance of the spacecraft from Earth.

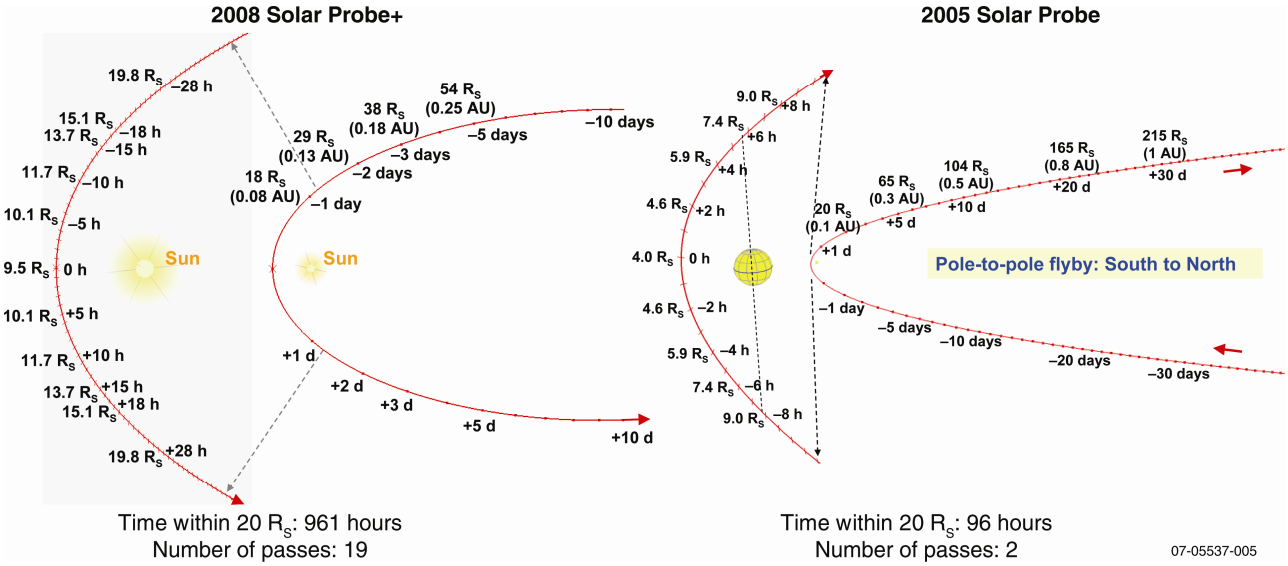

Figure 3.1-7. Comparison of 2008 Solar Probe+ and 2005 Solar Probe trajectories.

Constrained by solar power at aphelion, the current Solar Probe+ mission concept excludes a fly out to Jupiter for gravity assist. Instead, an inward route is taken to reach minimum perihelion at 9.5 R_S through the use of multiple gravity assists from Venus flybys. A side-to-side comparison of the near-Sun encounter between the current and the 2005 concept is shown in Figure 3.1-7. More comparisons are summarized in Table 3.1-2.

The first in situ measurements within the heliospheric region will occur only 3 months after launch. Starting the mission's science investigation right after launch and continuing for 6+ years is unprecedented for planetary missions. With three to four solar encounters per year, the heliosphere will be thoroughly and timely probed. Although perihelion is not as close as 4 R_S and the orbit is not polar, the total time within 20 R_S is 10 times that obtained with the 2005 concept. In addition, the 24 solar encounters provide various perihelion viewing geometries from Earth, allowing for simultaneous Earth observations on different parts of the Sun, as was previously illustrated in Figure 3.1-5. Reducing the perihelion gradually in multiple orbits results in lower operational risk than the JGA trajectory approach, which directly lowers the perihelion to 4 R_S at the first near-Sun orbit.

3.1.6. ΔV Budget and Navigation

The baseline mission trajectory requires no deep-space maneuvers from launch to final heliocentric orbit with perihelion at 9.5 R_S, and all the Venus flybys are not powered. Therefore, no deterministic ΔV is required throughout the entire mission. Currently, a total of 190 m/s is allocated for the ΔV budget to cover the injection errors at launch, the targeting of seven Venus flybys, and momentum control. Launch error correction includes significant ΔV for all launch

Table 3.1-2. Comparison of 2008 Solar Probe+ and 2005 Solar Probe mission designs.

	2008 Solar Probe+	2005 Solar Probe
Minimum Perihelion	9.5 R_S	4 R_S
Inclination	3.4° from ecliptic	90° from ecliptic
Number of Solar Encounters	24	2
Total Time within 20 R_S	~ 961 hours	~ 96 hours
Time Between Perihelia	88–150 days	4.6 years
Time from Launch to First Perihelion	3 months	4.1 years
Mission Duration	6.9 years	8.8 years
Aphelion	1 AU	5.5 AU

Table 3.1-3. Preliminary ΔV/fuel budget.

Usage	Event	ΔV (m/s)
Trajectory Correction Maneuver	Launch Error Correction	90
	Venus Flyby 1	8
	Venus Flyby 2	12
	Venus Flyby 3	12
	Venus Flyby 4	12
	Venus Flyby 5	12
	Venus Flyby 6	12
	Venus Flyby 7	12
Attitude Maneuver	Momentum Management	6
Margin		14
Total ΔV		190
Usable Propellant (kg)		52.3
Residual (kg)		0.3
Pressurant (kg)		0.1
Total Propellant Mass (kg)		52.7
Spacecraft Wet Mass (kg)		610

days. Table 3.1-3 presents the ΔV budget for Solar Probe+. The budget for momentum management includes an estimate of the frequency of momentum dumping based on the expected solar pressure imbalance and also impulses from dust impacts. In this design, the propellant tank is not full, and extra tank capacity is not included in the margin cited in Table 3.1-3. A detailed navigation analysis associated with ΔV requirement refinement will be conducted in Phases A, B, and C/D.

To simplify spacecraft attitude management and maintain the thermal protection attitude, we have designed the Solar Probe+ mission to avoid burns during solar encounters. All TCMs will be performed near aphelion, at distances greater than 0.5 AU. The TCMs for Venus flyby targeting will be placed before the Venus flyby. Table 3.1-4 presents the schedule for Venus flybys and TCMs.

Navigation has no special requirements and will be straightforward. Optical navigation is not required. The radiometric Doppler range and range rate data will be used for spacecraft trajectory determination. Delta differential one-way range (Delta-DOR) tracking data may be used before the Venus flybys to enhance the orbit determination (OD) accuracy. From launch (L) to L+2 weeks, there will be continuous Deep Space Network (DSN) tracking, followed by five 10-hour passes per week from L+2 to L+4 weeks. At each Venus (V) flyby there will be five 10-hour passes per week from V–5 weeks to V–1 week and one 10-hour pass per day from V–1 to V+1 week.

Table 3.1-4. Venus flybys and planned TCMs.

Event	Date
Launch	05/21/15
TCM 1	06/05/15
TCM 2	07/05/15
Venus Flyby #1	07/19/15
TCM 3	09/20/16
Venus Flyby #2	10/11/16
TCM 4	01/25/17
TCM 5	04/16/17
Venus Flyby #3	04/26/17
TCM 6	09/10/17
TCM 7	11/27/17
Venus Flyby #4	12/07/17
TCM 8	07/11/18
Venus Flyby #5	08/01/18
TCM 9	08/09/19
TCM 10	05/15/20
Venus Flyby #6	06/05/20
TCM 11	05/23/21
TCM 12	08/12/21
Venus Flyby #7	08/22/21
Perihelion	10/10/21

3.1.7. Launch Vehicle and Third Stage

Because of cost restrictions, the candidate launch vehicle currently under consideration is the Atlas V 551 with a STAR-48BV third stage built by ATK. Solar Probe+ retains compatibility with the Delta IVH as a backup vehicle and with the Boeing STAR-48B as a backup third stage. Based on the lift capability provided in the *Atlas Launch Systems Mission Planner's Guide*[7] and performance for the STAR-48BV provided by ATK, the estimated launch mass is 610 kg, assuming a 20-

[7] *Atlas Launch Systems Mission Planner's Guide, Rev. 10a*, Lockheed Martin Corporation (January 2007).

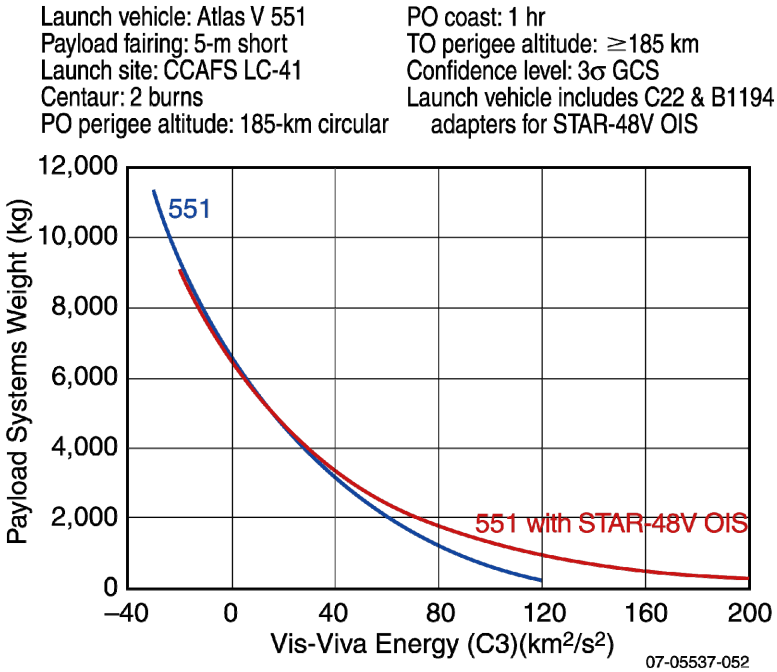

Figure 3.1-8. Launch vehicle performance.

day launch period. Launch vehicle performance is shown in Figure 3.1-8.

The ATK STAR-48BV stage is a thrust-vector-controlled motor offering a simple control system and higher performance than the spinning STAR-48B, which has been used in programs such as New Horizons. The STAR-48BV uses a loaded motor case from the flight-proven STAR-48B, with nozzle design qualified for the Conestoga program and a newly developed thrust vector actuator (TVA) control system currently being qualified to support vectorable nozzles across the STAR product line. The nozzle and thrust vector control system will be used on a STAR-37FMV in mid-2008, and the STAR-48BV upper stage currently is under contract and scheduled for a first flight as part of the Minotaur IV launch vehicle. The first flight is scheduled for September of 2009 as part of the TacSat-4 mission. Planned Phase A activities include significant engagement with the NASA launch services, the launch vehicle provider, and the third stage provider for finalization of the launch configuration, refinement of the lift mass estimate, and identification and development of mitigations for technical risks.

3.1.8. Launch Opportunity

The synodic period of Venus is 584 days, which results in a launch opportunity occurring approximately every 19 months. Besides the baseline mission launch time of 2015 suggested by the NASA guidelines for this study, launch opportunities before 2015 and beyond in a reasonable timeframe for near-term mission planning were analyzed. Details of the trajectory design for the four launch opportunities from 2013 through 2018 are summarized in Table 3.1-5, where the 2015 baseline launch also is included for comparison. The C3 requirement

Table 3.1-5. Launch opportunity summary.

Launch Opportunity		2013	2015	2017	2018
Launch	Date	10/25/13	05/31/15	01/10/17	08/09/18
	Optimum C3 (km^2/s^2)	170.0	155.6	177.2	157.0
Trajectory	Flybys	7 Venus	7 Venus	7 Venus	7 Venus
	Deep Space Maneuver (ΔV)	None	None	None	None
	Max. aphelion (AU)	1	1	1	1
Final orbit	Perihelion (R_S)	9.5	9.5	9.5	9.5
	Aphelion (AU)	0.73	0.73	0.72	0.73
	Inclination from ecliptic (°)	3.4	3.4	3.4	3.4
	Orbital period (day)	88	88	87	88
Near-Sun Pass	Total no. of solar passes (<0.2 AU)	24	24	24	24
Timeline	Launch to minimum perihelion (year)	6.4	6.4	6.4	6.4
	Mission duration (including three 9.5-R_S passes) (year)	6.9	6.9	6.8	6.9

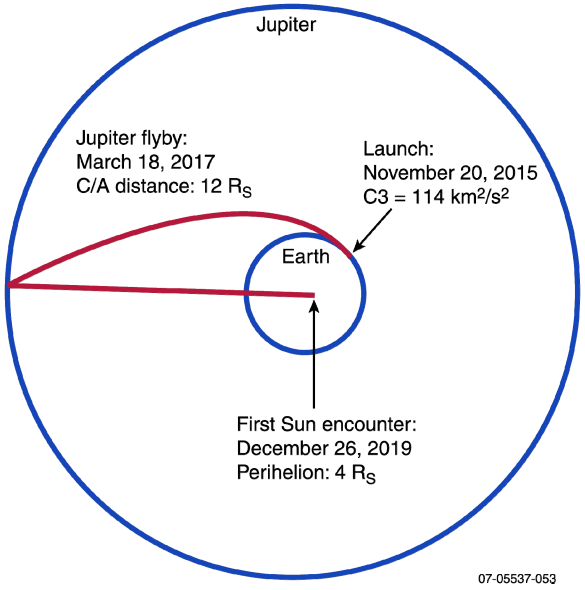

Figure 3.1-9. Trajectory Option 1: Trajectory design.

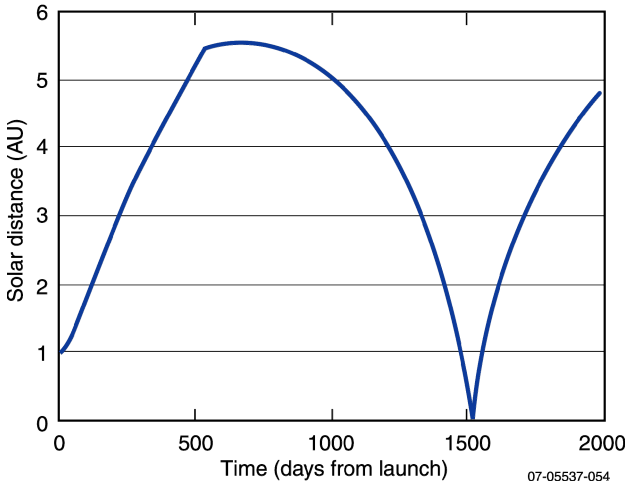

Figure 3.1-10. Trajectory Option 1: Solar distance profile.

shown is for the listed launch date chosen near the optimal launch time of that launch opportunity. Higher C3 will be required if a launch window, for example, a 20-day launch period, needs to be reserved. Trajectory analyses for launch opportunities in more extended timeframes in the future and with other types of trajectories included are planned for Phase A study.

3.1.9. Mission Design Trade Study

The 2005 Solar Probe concept cannot be implemented without significant changes to mission design under the new guidelines for the current study. In particular, NASA has directed that this study develop a concept without use of a nuclear power source. This restriction forces the use of solar arrays for power generation outside the solar encounter. Arrays sufficient to generate power at Jupiter, even if the spacecraft enters a lower-power "hibernation" state, are too large to protect during the solar encounter. In this concept, portions of the primary solar arrays must be ejected before entering the near-Sun regions of interest and cannot be used to power the spacecraft for a second orbit. In addition, energy storage is impractical to implement and more massive than can be launched into the JGA orbit with current launch vehicles. Therefore, a fundamental requirement of the 2005 study to perform two solar encounters cannot be met with the non-nuclear restriction. A major activity of the current Solar Probe+ study has been to develop alternative mission designs (including a single-pass JGA mission) that will accomplish most of the science objectives from the 2005 study while meeting the constraints as described in previous sections.

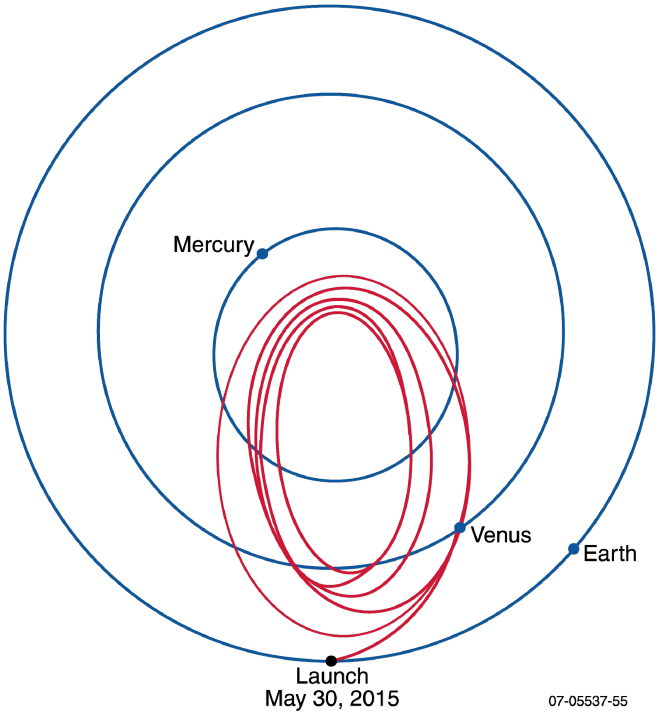

Figure 3.1-11. Trajectory Option 2: Trajectory design.

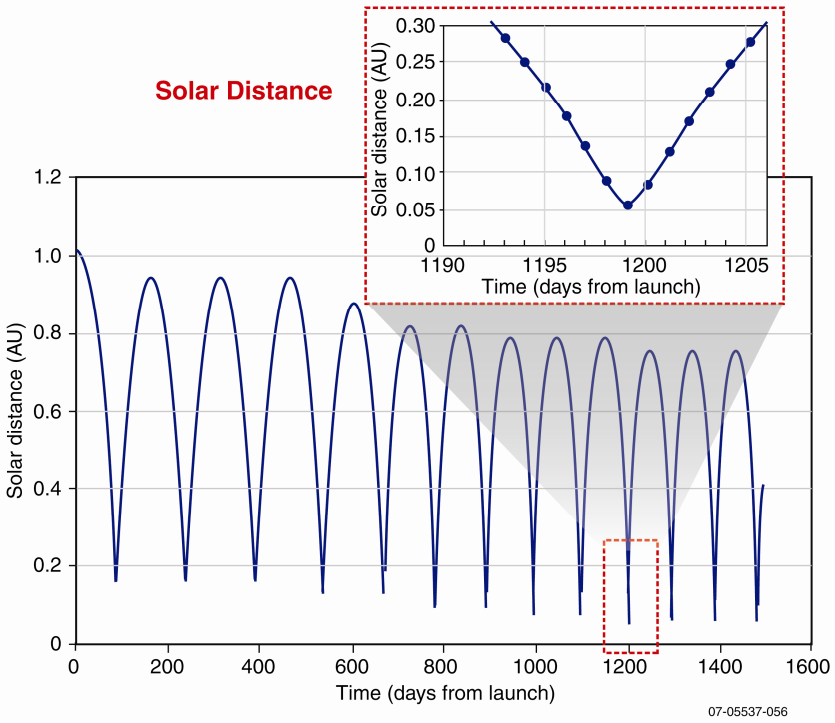

Figure 3.1-12. Trajectory Option 2: Solar distance profile.

3.1.9.1. Trajectory Study

The trajectory study explored various mission scenarios and trajectory options using gravity assists from the inner planets: Mars, Earth, Venus, and Mercury, or their combinations in search for the alternative Solar Probe+ mission trajectory and answers to the following questions:

- How close to the Sun can Solar Probe+ get without the JGA under current implementation ground rules with currently available launch vehicle capability?
- How high from the ecliptic plane of the inclination can Solar Probe+ reach without the JGA?
- Is it possible to achieve perihelion at 4 R_S and inclination at 90° for the solar flyby with the gravity assists from the inner planets?

On September 24, 2007, the engineering team gave the first trajectory study report at the STDT meeting. Representative trajectories of different trajectory types, named Trajectory Option 1 (Figures 3.1-9 and 3.1-10), Trajectory Option 2 (Figures 3.1-11 and 3.1-12), Trajectory Option 3 (Figures 3.1-13 and 3.1-14), and Trajectory Option 4 (Figures 3.1-15 and 3.1-16) were presented as potential candidate trajectories for Solar Probe+. These trajectory options were selected from the various trajectories analyzed since the Solar Probe+ study was initiated. Findings from these

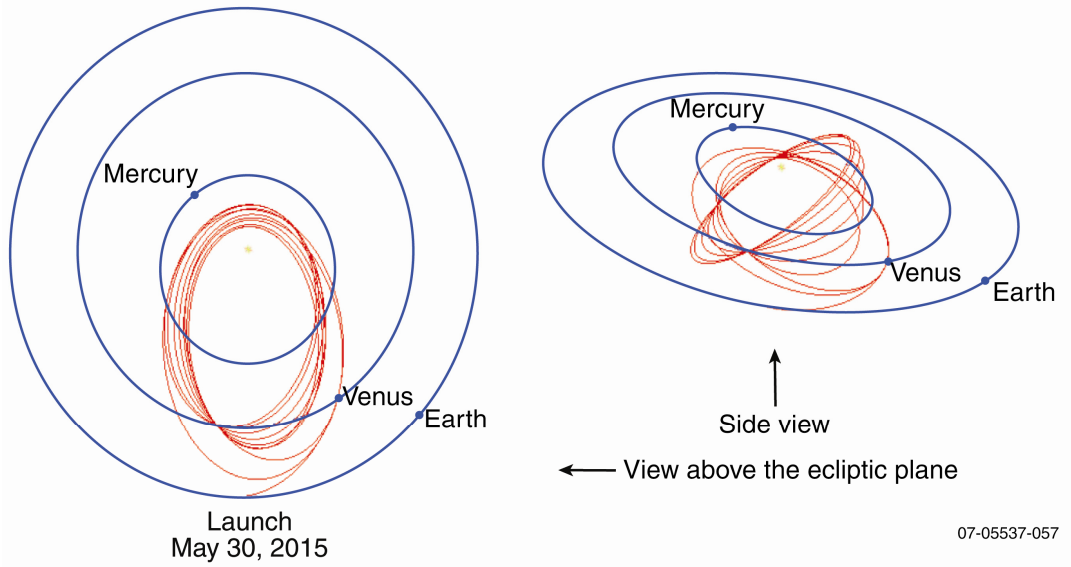

Figure 3.1-13. Trajectory Option 3: Trajectory design.

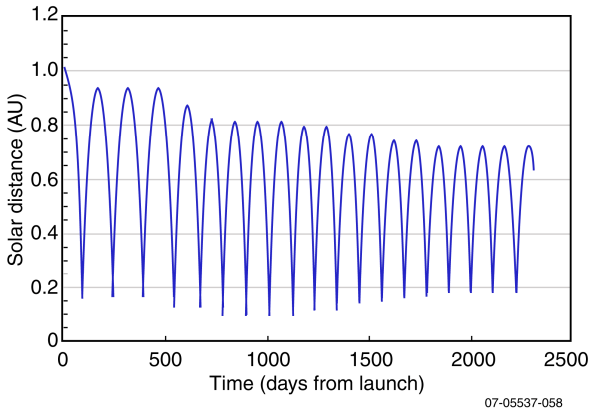

Figure 3.1-14. Trajectory Option 3: Solar distance profile.

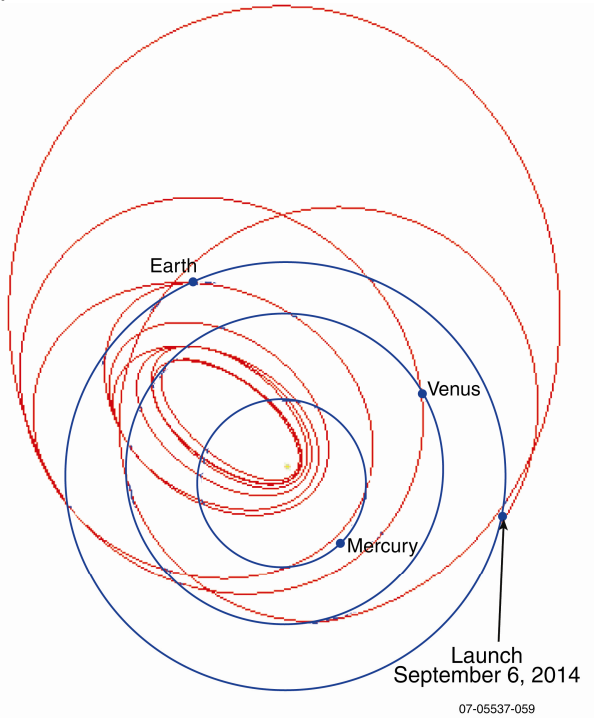

Figure 3.1-15. Trajectory Option 4: Trajectory design.

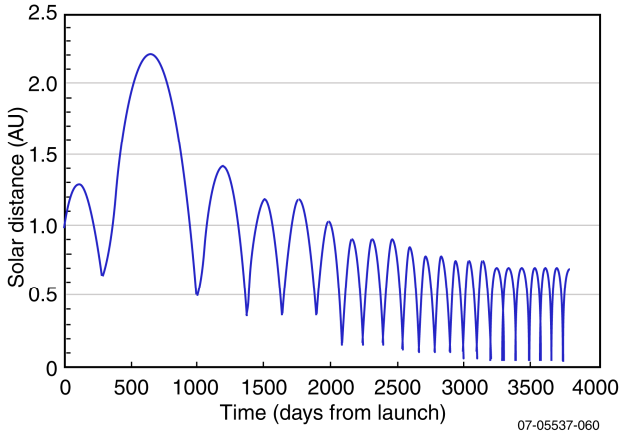

Figure 3.1-16. Trajectory Option 4: Solar distance profile.

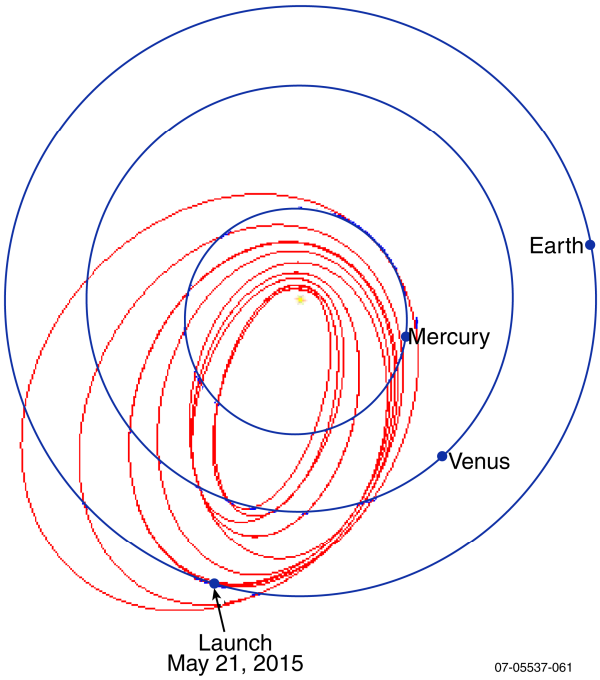

Figure 3.1-17. Trajectory Option 6: Trajectory design.

preliminary trajectory analyses were described in the summary remarks of the presentation:

- To achieve a solar pass with perihelion at 4 R_S and 90° inclination requires JGA flyby.
- The 2015 launch JGA trajectory (Trajectory Option 1) can achieve the same Sun encounter geometry as the 2005 study's baseline trajectory, but engineering issues limit spacecraft functionality to one orbit only.
- Preliminary trajectory analysis shows that using Venus and Earth gravity assists (Options 2, 3, and 4) can get perihelion down to ~0.05 AU and inclination up to ~38° from the ecliptic plane.

After discussion, the STDT down-selected the trajectory options to two mission concepts, Option A and Option B, for further study of implementation feasibility:

- Option A: A JGA trajectory with a single flyby of perihelion at 4 RS
- Option B: A new trajectory consisting of three orbits of perihelion less than 10 R_S and mission duration less than 10 years

Trajectory Option 3 was not pursued further because the STDT determined that a close perihelion outweighed higher latitudes at farther distances.

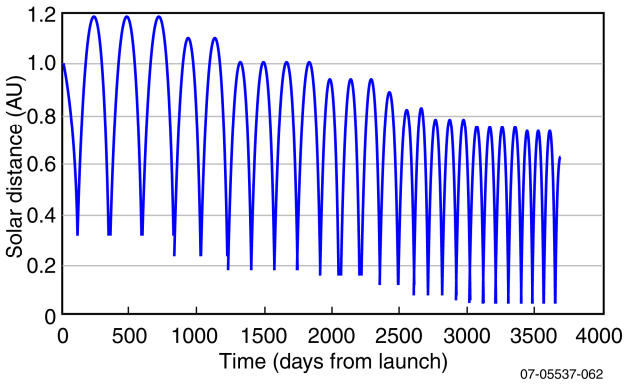

Figure 3.1-18. Trajectory Option 6: Solar distance profile.

Two trajectory options, Trajectory Option 5 and Trajectory Option 6 (Figures 3.1-17 and 3.1-18), were developed for mission concept Option B. Ultimately, Option 5 was chosen as the mission baseline. Table 3.1-6 gives a comparison of the trajectory options considered.

3.1.9.2. Rationale for Selection

The primary science considerations for selections were (*i*) minimum perihelion must be below 10 R_S and (*ii*) minimum perihelion must be achieved in less than 10 years in order to fit within the cost constraints as established for this study. In addition, the study guidelines

Table 3.1-6. Comparison of trajectory options.

Trajectory Option		Option 1	Option 2	Option 3	Option 4	Option 5	Option 6
Launch	Date	11/20/15	05/30/15	05/30/15	09/06/14	05/21/15	05/24/15
	C3 (km^2/s^2)	114	156	156	108	158	128
Trajectory	Flybys	1 Jupiter	5 Venus	9 Venus	3 Earth, 7 Venus	7 Venus	1 Earth, 9 Venus
	Deep Space Maneuver (ΔV)	None	None	None	1 (232 m/s)	None	1 (397 m/s)
	Max Aphelion (AU)	5.56	1	1	2.29	1	1.19
Final Orbit	Perihelion (R_S)	4	11.8	39.8	9.5	9.5	9
	Aphelion (AU)	5.56	0.75	0.725	0.73	0.73	0.73
	Inclination from Ecliptic (°)	90	3.4	37.9	2.9	3.4	3.4
	Orbital Period	4.6 year	94 days	112 days	88 days	88 days	88 days
Timeline	Launch to Min. Perihelion	4.1 year	3.3 year	2.1 year	10 year	6.4 year	9.5 year
	Mission Duration	4.5 year	3.8 year	5.8 year	10.5 year	6.9 year	9.95 year
Orbits	Total no. of solar encounters (<0.2 AU)	1	12	18	16	24	21
Pros		Pole-to-pole solar flyby at 4 R_S	Short mission duration; multiple, frequent solar flybys; aphelion <1 AU	Short mission duration; multiple, frequent solar flybys; aphelion <1 AU	Good perihelion distance; multiple, frequent solar flybys; moderate C3	Good perihelion distance; multiple frequent solar flybys; short mission duration; no deep space maneuver; aphelion <1 AU	Good perihelion distance; multiple, frequent solar flybys; moderate C3
Cons		Single solar flyby; great aphelion distance; long cruise; long orbit period	Low inclination; high C3	Large perihelion distance; high C3	Long mission duration, requiring deep space maneuver	Low inclination; high C3	Long mission duration, requiring deep space maneuver

require significant science return. Finally, the chosen mission must support a spacecraft implementation that can fit in the launch capability of the trajectory with acceptable margins. From these criteria, we were able to choose the optimal mission among those considered.

Options 2 and 3 were eliminated immediately because of failure to achieve acceptable minimum perihelion. Option 4 also was eliminated because this mission does not reach minimum perihelion within 10 years. Option 6, although it achieves the minimum perihelion within 10 years, requires more planetary flybys and much longer mission duration than Option 5 and therefore was eliminated to reduce cost and complexity.

Spacecraft conceptual designs were developed for the remaining options. Trajectory Option 1 includes a JGA, while Option 5 remains within 1 AU for the mission. This difference in trajectory led to a major difference in power subsystem concept for the two options. Option 1 requires the use of a large solar array that cannot be completely retracted behind the TPS for the solar encounter. Therefore, the extra solar panels associated with travel outside 1 AU must be ejected, limiting the science opportunity to a single solar pass. Option 5 can be powered throughout the mission without this restriction, and repeated solar encounters give significantly more science data. Given that equivalent scientific objectives can be accomplished with these two mission options, Trajectory Option 5 was selected as the baseline mission.

3.2. Mission Concept of Operations

3.2.1. Overview

The baseline mission consists of 24 solar orbits, all of which are very similar. Operations during an orbit are distinguished by events that occur on the orbit timeline, each of which is a discrete set of actions and conditions. The operations for events are similar for all orbits. For example, seven orbits include a Venus flyby. If we define that portion of an orbit of 40 days around a Venus encounter as a Venus flyby event, spacecraft operations for that event are consistent across orbits where flyby events occur. This mission concept lends itself well to modular operations with predefined sequences that are consistent throughout the mission. Solar Probe+ will take advantage of the event-driven nature of the mission timeline by modularizing operations for events, allowing for lower risk in operating the spacecraft and for savings in planning and operations costs. Any differences from orbit to orbit in modularized operations will be captured through parameters that can be set independently for an event in each orbit. For example, trajectory correction maneuvers (TCMs) are events that will occur in each orbit, yet the specific details of each burn change with each orbit. Parameterizing the command sequence allows the team to fully develop a tested set of commands once and modify that set through parameter updates for each orbit instead of developing a full set of commands for each orbit. The STEREO mission has successfully used this methodology for operations.

Solar Probe+ science instruments do not require specific pointing of the spacecraft beyond ram-pointing of certain instruments, nor does the payload depend on mechanisms operated by the spacecraft beyond single-shot deployable antennas and boom. Measurement sequences are self-contained and can be carried out simultaneously with little or no impact on spacecraft or other instruments. This leads to a concept for science measurement planning that is decoupled from spacecraft operations. The spacecraft design fully supports the decoupled operations concept by providing sufficient resources for payload operations. The Solar Probe+ operations concept takes full advantage of this decoupling to simplify operations, resulting in reduced risk, more efficient use of operations staff and resources, and reduced cost.

3.2.2. Launch and Early Operations

Solar Probe+ will be launched from Cape Canaveral within a 20-day launch window on an Atlas V 551 with a STAR-48 third stage.

The nominal launch date is May 21, 2015. Except for launch vehicle dispersion and navigational corrections, the entire ΔV necessary for achieving orbit will be supplied by the launch vehicle.

The spacecraft will be three-axis-stabilized by the launch vehicle and third stage for the entire launch ascent and third stage flyout. No despin maneuver is needed after third stage separation. After separation, Solar Probe+ will be oriented in Sun-pointing attitude. The low-gain antenna (LGA) will be the primary antenna for communications until the high-gain antenna (HGA) is deployed and checked out.

The first Venus flyby will occur approximately 6 weeks after launch. The time from launch until first encounter will be devoted to spacecraft systems checkout and preparation for that event. Time between the first Venus flyby and the first solar encounter will be devoted to science instrument checkout, encounter preparations, and the first changeover from primary power to secondary power. During the first 7 days after launch, DSN coverage will be continuous. After this period, DSN coverage will consist of approximately five 8-hour contacts per week.

3.2.3. Mission Events

Figure 3.2-1 shows a typical orbit for Solar Probe+ that includes all events to be used except for early operations, which were discussed in Section 3.2.2. This orbit starts at aphelion, includes a Venus flyby, periods when downlinking data, transition to science for the near-Sun pass, science collection, and transition back to data downlink.

Data Downlink. The default activity for the spacecraft outside of all other events is to downlink data collected from the previous science event. Contacts using Ka-band and a DSN 34-m disk on the HGA will be conducted for an average of 10 hours per day. All data from one science event will be downlinked before the next science event occurs.

When not in contact, the spacecraft maintains the default pointing with ram-pointing instruments in the correct attitude. When in contact, the spacecraft will maintain Sun-pointing directionality while rolling the spacecraft to allow the HGA to point to Earth as needed. No science measurements requiring specific pointing will be collected during contacts; however, low rate science on some instruments will be conducted between contacts.

Venus Flyby/TCM. Seven Venus flybys are used to lower perihelion to below 10 R_S. The period extending from 30 days before to 10 days after a Venus encounter are designated a Venus flyby event. Except for early operations before the first Venus flyby, all TCMs are expected to occur within the period leading up to Venus flyby or at aphelion. Operations during this period are limited to

- Downlink of science data from previous solar encounter.
- Contacts to allow analysis, execution, and evaluation of a navigation burn planned be-

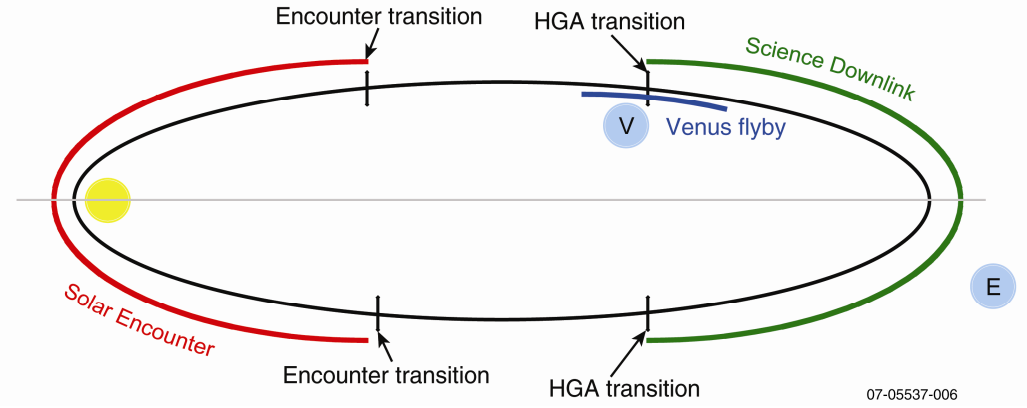

Figure 3.2-1. Typical Solar Probe+ orbit indicating events and operational modes.

fore the encounter and a burn after encounter to correct any residual errors.
- Monitoring of spacecraft health and safety through encounter.

Science. At ~0.25 AU (~5 days before perihelion), Solar Probe+ will transition from the standard configuration to science configuration. While maintaining the correct Sun-pointing, the primary solar arrays are retracted inside the umbra formed by the TPS, and the spacecraft is powered only by the secondary solar arrays, which are fully extended. As the spacecraft nears perihelion, the secondary solar arrays are retracted behind the TPS shield to maintain constant power. Science data collection is carried out throughout this event; however, the instruments in use and the measurement rates vary, with highest use near perihelion. All data are stored on each solid-state recorder (SSR) for downlink outside the science event; however, a low-rate link is maintained through the low-gain antenna (LGA) for command uplink and housekeeping telemetry downlink except during solar conjunction. During science collection, instruments do not require off-pointing of the spacecraft or specific pointing about the Sun–probe axis with the exception of a small number of instruments that require ram-pointing. After Solar Probe+ passes perihelion, the secondary solar arrays are slowly extended to maintain constant power, followed by transition to the downlink configuration when the spacecraft is farther than 0.25 AU from the Sun (~5 days after perihelion).

3.2.4. Operations

The mission operations concept for Solar Probe+ is based on the modular nature and similarity of events across orbits as described above. Operations for recurring events are executed using predefined sequences that are repeated with only small changes from one orbit to the next. This allows significant reuse in operations planning and tasking, resulting in lower risk to the mission at lower cost than for mission with less repetitive operations.

Spacecraft operations are devoted to functions needed to support the collection and downlinking of science data to execute the mission science:
- Maintaining safe orientation of spacecraft at all times
- Generating sufficient power for spacecraft subsystems and instruments
- Transitioning from one mode to another as described above
- Conducting Venus flybys to lower perihelion and trajectory corrections as needed
- Collecting and storing data from the payload and downlinking data to the ground
- Receiving and executing payload and spacecraft commands

Unlike many missions such as New Horizons where planning observational sequences requires a high degree of integration between instruments and spacecraft to deconflict resources and coordinate issues such as spacecraft attitude, the Solar Probe+ mission is designed for simple operations. Instrument operations do not affect spacecraft attitude or operating mode, nor are sequences of pointing maneuvers needed to perform science measurements. Therefore, spacecraft and payload operations are decoupled. Detailed sequencing of instrument commands will be produced by the instrument teams themselves and provided to mission operations for upload after testing. As with the modular nature of spacecraft operations, this decoupling of payload planning and mission operations simplifies the science and mission operations interface, reduces risk to the mission, and provides a cost-effective means of accomplishing the science objectives. The decoupled operations concept has been successfully used in missions such as STEREO.

Another aspect of Solar Probe+ mission operations designed to reduce costs is the unattended mode of operations within the Mission Operations Center (MOC). Outside of critical events such as TCMs, flybys, and encounters, the MOC is capable of supporting the downlink of science data during contacts through the DSN without the need for staffing within the MOC. The ground system monitors spacecraft

health and status and supports remote notification of predefined alarm conditions to Mission Operations Team members. Although the notification comes with an initial indication of severity, the ground system is designed to allow team members to access additional information remotely. Depending on the issue, the web-based planning and scheduling system may allow the situation to be resolved remotely. Unattended operations is another concept successfully used on the STEREO mission.

3.3. Mission Environment

Solar Probe+ must be able to survive and operate under extreme environmental conditions, which present significant challenges for the engineering design of the spacecraft. As the spacecraft approaches and flies past the Sun, it will be exposed to intense solar flux and bombardment by particles from the circumsolar dust cloud. In addition, the effects of coronal lighting and solar scintillation in the near-Sun environment must be included in the design of attitude control and telecommunications systems.

3.3.1. Solar Flux

The most challenging spacecraft design driver is the intense solar flux to which Solar Probe+ will be exposed. At perihelion, the flux will be roughly 510 times that at Earth orbit. As discussed in detail in Section 3.6, the TPS, consisting of a ceramic-coated carbon–carbon (C-C) shield, protects the instruments and spacecraft bus from direct exposure to this flux. Immediately after launch and spacecraft separation, the TPS will point toward the Sun, and this attitude will be maintained through the mission. Except for the secondary solar arrays and the plasma-wave instrument (PWI) electric field antennas, instruments and spacecraft components will reside within the umbra of the TPS at all times during solar encounter. The only other components intended to extend beyond the umbra are the primary solar arrays and high-gain antenna (HGA), which are extended only in portions of the orbit away from the solar encounter.

3.3.2. Radiation

The radiation environment is dominated by solar energetic protons that are responsible for total dose damage in components and galactic cosmic rays that are the source of most single-event effects experienced by spacecraft. In addition, protons produced in solar flares also will contribute to the single-event effects rate during periods when the Solar Probe+ spacecraft experiences this elevated environment.

Most of the Solar Probe+ mission will occur during solar minimum conditions. During this period of the solar cycle, the total dose is negligible, and significant radiation damage will occur only in the later years when the Sun becomes active during the solar maximum period. The total dose requirement for Solar Probe+ is 30 krad behind 100 mils of aluminum shielding, based on the 95% worst-case Jet Propulsion Laboratory solar proton model for the 2 years of maximum conditions and correcting for Sun–spacecraft distance through the orbit as defined above. The total dose requirement is the same as that of the MESSENGER mission and is achievable through a parts screening and qualification test similar to that used for MESSENGER and other recent programs. During the design phase, a three-dimensional shielding analysis will be conducted to allow mass reduction in electronics enclosures and spacecraft structure without compromising total dose survivability.

Outside of exposure to energetic charged particles during a solar event, the single-event effects environment is worst near aphelion, where single-event effects rates are similar to that of near-Earth missions. Solar flare exposure also is expected to be no worse than flare environments experienced by missions such as MESSENGER and STEREO. Parts used in Solar Probe+ are similar to those used in previous missions with equivalent or worse environments, and the parts screening and qualification program used for recent interplanetary missions will assure that single-event effects requirements are met and that the system will function as needed for the life of the mission.

3.3.3. Coronal Lighting

Coronal lighting near the Sun is an environmental factor that can have significant consequences for maintaining attitude control. Excessive coronal lighting can increase background noise and degrade a star tracker's ability to detect star constellations needed to determine spacecraft attitude. Although coronal lighting conditions can be estimated from data acquired by remote-sensing instruments in orbit from 1 AU, uncertainty about the actual lighting conditions will remain until a mission near the Sun is performed. Because of this uncertainty, Solar Probe+ uses three star trackers facing in orthogonal directions, a high-precision inertial measurement unit (IMU), and a solar horizon sensor (SHS) used to detect faults in attitude control and initiate corrective autonomous recovery. The guidance and control (G&C) subsystem is described further in Section 3.12.

3.3.4. Solar Scintillation

The effects of solar scintillation have been well characterized based on mission data from the Near Earth Asteroid Rendezvous (NEAR) mission as well as from the Magellan and Galileo missions. During the NEAR mission, measurable telemetry losses in the X-band downlink were experienced around solar conjunction once the angle among the Sun, the Earth, and the spacecraft came within 2.3°. Although chosen for its increased data rate, Ka-band also is less sensitive to scintillation effects; thus, Solar Probe+ will use Ka-band for telecommunications, both for low-rate command and telemetry during the solar encounter as well as during high-rate science data downlink outside the solar encounter. X-band communication is baselined in the telecommunications subsystem design as a backup for periods when Ka-band is unavailable because of ground station conditions; however, a Phase A study will be conducted to determine whether a dual-frequency system is required.

3.3.5. Spacecraft Charging

The Solar Probe spacecraft described in the 2005 *Report of the Science and Technology Definition Team*[8] and the 2006 *Solar Probe Thermal Protection System Risk Mitigation Study* and *ITAR-Restricted Annex*[9] include a cone-shaped, ceramic-coated primary heat shield. This design produced a temperature reduction of ~200 K and was an essential enabler for the mission. The Solar Probe+ mission retains the ceramic coating but replaces the cone-shaped heat shield with a disc. Additionally, the trajectory no longer carries the spacecraft to a Jovian encounter, and it now experiences a closest approach of ~9.5 R_S rather than 4 R_S. Therefore, the charging situation with respect to both spacecraft safety and the likelihood of disruption of data collection must be reevaluated for the new design and trajectory; preliminary results are given in this report. Previous efforts also included an investigation of charging mitigation and early investigations of particle tracking; such work would need to be reevaluated for Solar Probe+.

The equilibrium process of spacecraft charging balances the current into the spacecraft (incident ions and electrons) with the current out of the spacecraft (photoemission, secondary electron emission, and backscattered electrons). A potential may develop on the spacecraft relative to the surrounding plasma "ground" (absolute charging), or different parts of the spacecraft may charge to different potentials (differential charging). For example, in the case that part of the spacecraft experiences Sun exposure while another part is shaded, the Sun-exposed side will undergo photoemission and therefore acquire a net positive charge relative to the shaded side, resulting in differential charging

[8] *Solar Probe: Report of the Science and Technology Definition Team*, NASA/TM—2005–212786, National Aeronautics and Space Administration, Goddard Space Flight Center, Greenbelt, MD (2005).

[9] *Solar Probe Thermal Protection System Risk Mitigation Study: FY 2006 Final Report*, prepared by The Johns Hopkins University Applied Physics Laboratory under Contract NAS5-01072, Laurel, MD (November 30, 2006); and *ITAR-Restricted Annex* (September 17, 2007).

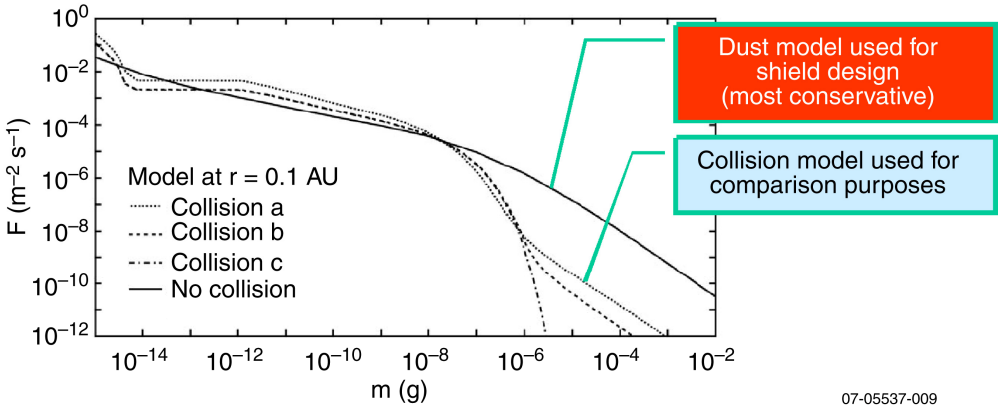

Figure 3.3-1. Predicted dust environment at 0.1 AU (from Mann *et al.*[10] and Ishimoto and Mann[11]).

unless the parts of the spacecraft are well grounded to each other.

Modeling of the charging effects was performed by using the charging analysis program NASCAP-2K, which was created by Science Applications International Corporation (SAIC) and has the capability to model spacecraft potentials. Details of this study are presented in Section 3.14.1.

3.3.6. Micrometeoroid and Dust

Over the years of Solar Probe studies, a description of the near solar dust environment has been developed by leading solar scientists from throughout the world. This description predicts that a Solar Probe spacecraft following either a polar or ecliptic orbit would encounter dust particles ranging from submicrometer up to several hundred micrometers in diameter traveling at relative speeds as high as 350 km/s. For the Solar Probe+ trajectory, it is expected that spacecraft would encounter mostly small particles consisting of carbon and some refractory silicate material with a bulk density of ~2.5 g/cm^3. Mann *et al.*[10] estimated that significant dust-particle collisions (see Ishimoto[11]) occur in the inner heliosphere that redistribute the particle flux greatly in favor of smaller particles, as illustrated in Figure 3.3-1. However, to account for uncertainties in the actual circumsolar dust environment, it has been conservatively assumed that there are no collisions between particles. The model employs the following assumptions:

- The number density of the dust in ecliptic orbits (within ±30° inclination) varies with distance as $1/r$ between 10 R_S and 1 AU.
- 5% of the dust within 30° of the ecliptic is in retrograde orbits.
- Beyond 30° inclination, the flux is 10% that of ecliptic orbits for particles smaller than 5 μm and 5% that of ecliptic orbits for particles larger than 5 μm.
- 50% of the flux at >30° inclination is in retrograde orbits.
- All dust trajectories close to the Sun are circular.
- As the distance from the Sun decreases to within 10 R_S, the number density of dust particles remains constant because of dust destruction.

While a comprehensive study will be done as part of the Solar Probe+ effort, a preliminary comparison of the Solar Probe+ trajectory with those from the earlier studies shows a potentially larger dust exposure. For the proposed Solar Probe+ mission, the spacecraft is planned to follow 24 elliptical orbits with each perihelion lowering from 35 R_S to 9.5 R_S. During one encounter, the Solar Probe+ trajectory will encounter about five to six times more particles than the

[10]Mann, I., *et al.*, Dust near the Sun, *Space Sci. Rev.* **110,** 269–305 (2004).
[11]Ishimoto, H., Mann, I., Modeling the number density distribution of interplanetary dust on the ecliptic plane within 5 AU of the Sun, *Astron. Astrophys.* **362,** 1158–1173 (2000).

earlier study, based primarily on the elliptical trajectory path, and the Solar Probe+ trajectory includes 10 times more orbits. Therefore, the total dust exposure will be about 50 to 60 times higher for the Solar Probe+ trajectory than for that defined in the 2005 STDT study. Despite this increase in the environment, the mitigation factors baselined in the 2005 STDT study are sufficient to protect the spacecraft. A detailed analysis is given in Section 3.14.

3.3.7. Electromagnetic Interference, Electromagnetic Compatibility, and Magnetic Cleanliness

Solar Probe+ is intended to measure electrical and magnetic fields near the Sun. We expect that spacecraft systems will be required to meet electromagnetic compatibility (EMC), electromagnetic interference (EMI), and magnetic cleanliness requirements like those in other missions with similar instruments such as STEREO and Radiation Belt Storm Probes (RBSP). Generally, these requirements necessitate the use of hardware mitigation, e.g., synchronized DC/DC converters and filters in the power system electronics (PSE). In the case of Solar Probe+, the fields to be measured are larger than for missions performing similar measurements; preliminary analysis indicates that requirements will be no worse than for previous missions such as STEREO. Detailed requirements will be developed in Phase A. The baseline concept includes EMI/EMC and magnetic cleanliness mitigations that we anticipate using, and we have included EMI/EMC testing and verification activities in the program cost and schedule reported in this study.

3.4. Spacecraft Overview

The Solar Probe+ spacecraft will operate in environments ranging from 0.044 to 1 AU from the Sun and will accommodate the payload defined by the STDT. The spacecraft concept is illustrated in Figure 3.4-1, and the major components are shown in the block diagram in Figure 3.4-2. This section provides an overview of the baseline design, discusses the fault management approach, and summarizes the Solar Probe+ mass and power requirements. Individual subsystems are discussed in subsequent sections.

3.4.1. Spacecraft Description

Solar Probe+ is a three-axis-stabilized spacecraft. Its most prominent feature is the Thermal Protection System (TPS), a large flat ceramic-coated carbon–carbon (C-C) shield that is 2.7 m in diameter, with associated structure used to attach the shield to the spacecraft. The TPS protects the bus and payload within its umbra during solar encounter. The science instruments are mounted either directly to the bus, on a stand-off bracket near the fairing attachment, or on a science boom extended from the rear of the spacecraft. The science boom also carries the solar horizon sensor (SHS) for backup attitude safing during the solar encounter. Three deployable C-C plasma-wave antennas are mounted 120° apart on the side of the bus. These antennas will protrude beyond the umbra during encounter.

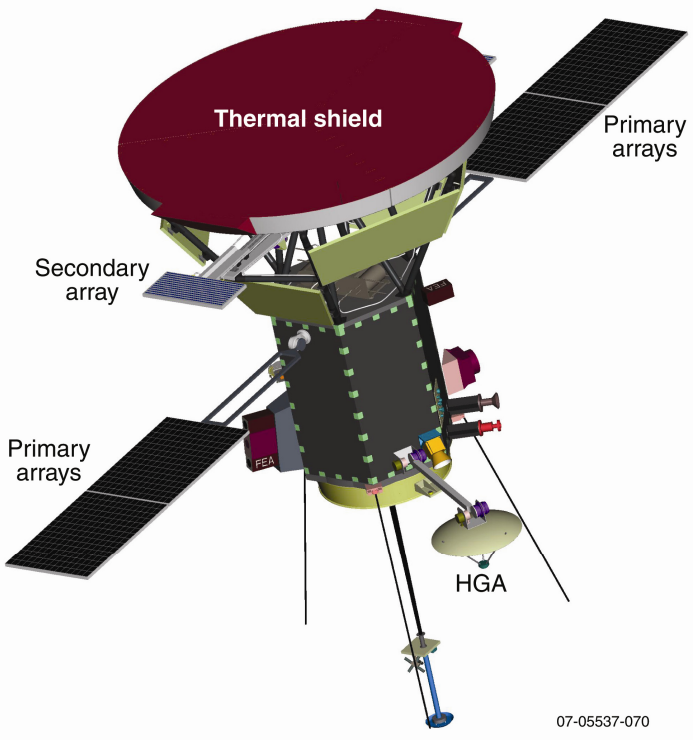

Figure 3.4-1. Spacecraft configuration.

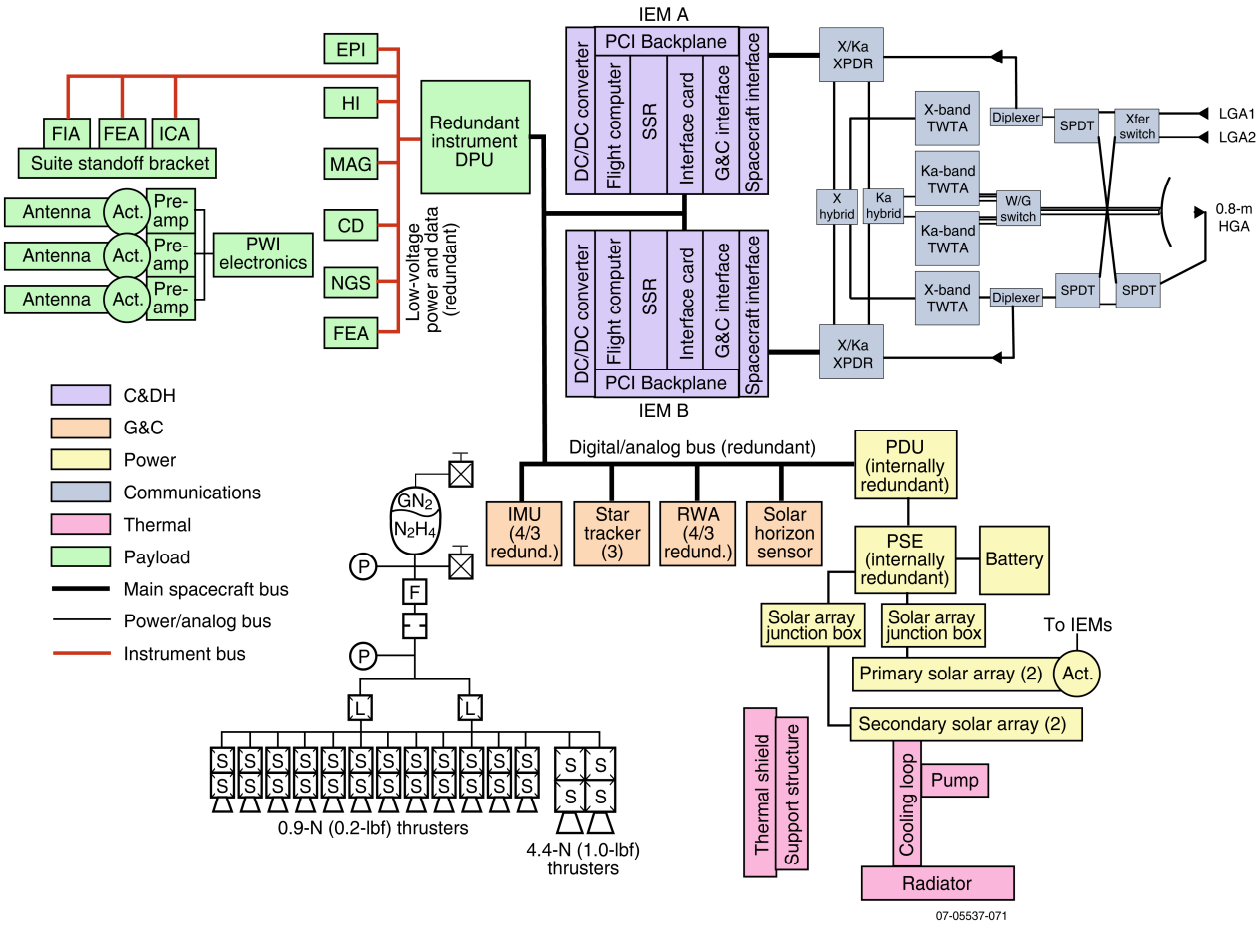

Figure 3.4-2. Solar Probe+ block diagram

Instrument data processing is provided by a common data processing unit (DPU). The baseline design includes instrument power distribution through the DPU. A Phase A study will be conducted to optimize payload power distribution in light of electromagnetic interference (EMI)/electromagnetic compatibility (EMC) and magnetic cleanliness requirements. The hexagonal bus carries the spacecraft subsystems and provides an efficient mechanical structure to handle launch loads and integrate with the launch vehicle.

Power is provided by two separate solar array systems. The primary solar arrays, used outside 0.25 AU, are MESSENGER-heritage panels. Array temperature is controlled by including optical surface reflectors (OSRs) with cells and rotating the arrays with respect to the Sun to keep the cell temperature within qualification limits. Inside 0.25 AU, the primary arrays are folded inside the umbra formed by the TPS. During solar encounter, power is generated by the secondary solar arrays, two panels of high-intensity solar cells mounted on moveable, liquid-cooled base plates. At 0.25 AU, the start of solar encounter, the panels are fully extended outside the TPS, and as the spacecraft approaches the Sun, panels are partially retracted behind the TPS to maintain constant temperature and power output. A lithium-ion battery is included as a secondary power source to handle transient loads and power the spacecraft during launch and ascent until the primary solar arrays are deployed. The power system electronics (PSE) box controls spacecraft power and battery recharge, and provides the primary power bus voltage for the bus.

The Solar Probe+ avionics suite centers on redundant integrated electronic modules (IEMs) that house the command and data han-

dling (C&DH) processor, solid-state recorder (SSR), guidance and control (G&C) instrument interface, and payload interface. The avionics suite also includes the power distribution unit (PDU), an internally redundant box that includes all power switching as well as pulsed loads to thrusters and single-event actuators. Remote input/output (RIO) devices are used to collect spacecraft telemetry and communicate with the avionics suite through serial data links.

The G&C subsystem consists of three star trackers and one internally redundant inertial measurement unit (IMU) as the primary attitude determination sensors, with an internally redundant SHS used as a check on the primary G&C sensors and as a backup safing sensor. Four reaction wheels are used for attitude control.

The telecommunications subsystem consists of a gimbaled high-gain antenna (HGA) mounted on an arm used to extend the HGA beyond the umbra for Earth-pointing and two low-gain antennas (LGAs). Because the geometry of each solar encounter is different, no real-time science data downlink is planned inside 0.25 AU. In this region, command and housekeeping telemetry links will be on Ka-band through the LGAs, because the HGA must be stowed within the umbra formed by the TPS. Science data collected in a solar encounter is stored on the SSR and downlinked outside the solar encounter where the temperature constraints on the HGA are satisfied. X-band communication through the LGAs is provided as backup for periods when Ka-band communication is not available.

The propulsion subsystem consists of a blowdown monopropellant hydrazine system consisting of a single tank, 12 0.9-N (0.2-lbf) and two 4.4-N (1-lbf) thrusters used for momentum control and trajectory correction maneuvers (TCMs), and associated plumbing and electrical hardware. The hydrazine propellant tank is central to the bus.

3.4.2. Spacecraft and Mission Reliability

Solar Probe+ uses both hardware and functional redundancy to reduce the risk of failure and ensure mission reliability. The fault management approach adopted for the mission is based on several considerations. First, during a solar encounter, attitude control must be precisely maintained to avoid exposing instruments and spacecraft to direct solar flux. At perihelion, the maximum off-pointing allowed is 2°. Inability to recover quickly from an attitude control fault could result in loss of mission. Attitude control is rendered more difficult by uncertainties in the solar environment such as coronal lighting effects on star trackers or torques induced by high-speed dust impacts. Second, the nature of science data collection requires a significant amount of onboard autonomy and the ability to quickly switch to backup systems. In addition, the nearly 7-year mission lifetime influences hardware selection and redundancy decisions.

Hardware redundancy is incorporated in all spacecraft components and subsystems that can practically be made redundant (Table 3.4-1). In addition, Solar Probe+ incorporates functional redundancy in many critical areas,

Table 3.4-1. Hardware redundancy.

Functional Area	Hardware Redundancy
Avionics	2 IEMs Internally redundant PDU
Payload	Internally redundant payload DPU
Attitude Determination	3 star trackers Internally redundant IMU Internally redundant SHS
Attitude Control	4 reaction wheels
Propulsion	Redundant thrusters in each axis
Data Bus	Redundant 1553 bus Redundant serial interfaces
Data Storage	2 SSRs
Telecommunications	2 uplink/downlink cards 2 LGAs 2 each X-band and Ka-band TWTAs
Thermal Control	2 thermistor harnesses 2 heater harnesses
Power	Internally redundant PSE Extra solar cell strings on each array

Table 3.4-2. Functional redundancy.

Functional Area	Primary System Failure	Functional Redundancy	Mission Impact
C&DH Processing	C&DH software fault	Second IEM operates in safe mode	Software must be promoted back into operational mode
G&C Processing	G&C software fault	Second IEM operates in safe mode	Software must be promoted back into operational mode
Attitude Determination	Star tracker	IMU: short duration Sun Horizon Sensor	Communications through LGA instead of HGA
	IMU	Star tracker: low rates Sun Horizon Sensor	Degraded pointing performance
Attitude Control	Reaction wheels	Thrusters	Increased propellant usage Increased outgassing
Telecommunications	Ka-band downlink	X-band downlink	Loss of communications P ± 8 hours Reduced science data volume
	HGA	LGA	Significant reduction in data rate
Power	Battery	Solar arrays	More difficult management of switch-over between primary and secondary solar arrays.

as shown in Table 3.4-2. Mechanisms represent a potential source of failure, which will be addressed in the detailed Solar Probe+ design. In particular, the primary solar arrays must be stowed during solar encounter and then extended following encounter, the secondary solar arrays must be retracted through perihelion and then extended as the spacecraft travels away from perihelion, and the HGA must move to point to Earth and also be stowed during solar encounter. One major driver during this effort has been to reduce the number of mechanisms needed. This effort will continue in further design phases. The remaining mechanisms incorporate fail-safe features to guarantee mission reliability.

The Solar Probe+ fault management system is distributed throughout the spacecraft design as hardware, software, autonomy, and mission operations requirements. The primary objective of the fault management system is to maintain a thermally safe attitude during the solar encounter. In addition, the fault management system is responsible for responding to time-critical fault scenarios, maintaining a power-positive spacecraft configuration, and, if necessary, reconfiguring the telecommunications system for emergency data rate communications. Some of the fault detection and fault response sequences will be designed into the flight software with the APL heritage rule-and-macro-based autonomy system. During the detailed mission design, the engineering team will determine the necessary operating modes to satisfy the safety requirements for each orbital phase while minimizing software and operational complexity.

APL has successfully demonstrated their ability to operate a spacecraft in a thermally sensi-

Table 3.4-3. Mass summary.

Name	Current Best Estimate (kg)
Instruments	47.2
Accommodation Hardware	7.4
Telecommunications	31.8
G&C	30.4
Power	119.2
Thermal Protection System	68.5
Thermal Control	15.7
Avionics	12.7
Propulsion	20.5
Structure	58.9
Harness	18.5
Dry Mass	428.3
Propellant	52.7
Wet Mass	533.3
Launch Mass	610
Total Mass Reserve	77
Total Margin	**30.10%**

Table 3.4-4. Mass margin risk mitigation.

ID No.	Subsystem	Task Description	Current Best Estimate Expected Mass (kg)
1	Launch Vehicle	Identify launch vehicle mass hold-backs, etc., based on historical experience and comparison of mission-unique items across programs	23.00
2	TPS	Decrease the shield diameter via a bus repackaging	5.00
3	Power, Solar Array	Decrease the substrate required area/perform a cell-string layout	2.00
4	Power, Solar Array	Perform a historical margin analysis for in-flight systems and decrease the derating penalties	3.00
5	Thermal	Investigate lightweight radiators	2.00
6	Thermal/Mechanical	Perform design cycle on transition structure assembly (TSA) fluid/mechanical system	3.00
		Total Potential Savings	**38.00**

tive environment with the MESSENGER spacecraft flying through perihelion distances of approximately 0.3 AU. Because of the similarity in the mission fault management requirements, the Solar Probe+ fault management system will utilize numerous design components and lessons learned from the MESSENGER mission.

3.4.3. Mass and Power Budget Summaries

3.4.3.1. Mass Budget

Table 3.4-3 shows the mass summary for Solar Probe+. Mass is summarized for instruments, instrument support hardware, mechanisms, and each spacecraft subsystem. Masses given in Table 3.4-3 are current best estimates representing the best current assessment of mass for that item at launch. Launch mass is based on performance for an Atlas V 551 launch vehicle with a STAR-48BV third stage, the baseline for Solar Probe+. The mass summary includes 30.1% margin to account for unanticipated growth and any launch reserves. Because specifics of the launch vehicle have not yet been set, propellant mass is based on the need to achieve the required ΔV after inclusion of the full margin. A more detailed mass budget is provided in Appendix A.

Mass data are developed for Solar Probe+ by using a bottom-up methodology where lead engineers responsible for their subsystems generate current best estimates of mass. The maturity of the system is assessed, historical data are compared with the current best estimate, and an appropriate allocated margin is added at the spacecraft system level. Unallocated margin is then carried at the system level for distribution from the system engineering team to the various subsystems as the need arises during the program. The engineering team has identified a collection of Phase A trade studies, shown in Table 3.4-4, to increase mass margin beyond 30% within 6 months of Phase A start.

3.4.3.2. Power Budget

The power subsystem is designed to provide 482 W of load power between 0.9 AU and 0.044 AU distance from the Sun. Between 0.9 AU and 1 AU, less power is available, and spacecraft operational requirements in this regime will be reduced primarily by lowering power allocated to the telecommunications subsystem. Sun–probe distance is greater than 0.9 AU only immediately after launch and around aphelion of the first few orbits, so no impact on science return is expected. Table 3.4-5 summarizes the average power needed during the solar encounter based on current best estimates. A more detailed breakdown of the power budget for all modes of spacecraft operation is provided in Appendix A.

3.5. Mechanical Systems

Mechanical systems for the Solar Probe+ mission are organized into three areas of responsibility: the bus structure, mechanisms supporting both the telecommunications and thermal/power subsystems, and science instrument accommodations (including mechanisms and interfaces).

Table 3.4-5. Power summary.

Name	Post-separation	Maneuver	Cruise	Checkout	Approach	Science
Instruments	0.0	0.0	0.0	28.6	0.0	57.2
Accommodation Hardware	0.0	0.0	0.0	0.2	0.0	0.0
Telecommunications	49.7	97.7	97.7	49.7	49.7	49.7
G&C	95.2	95.2	95.2	95.2	95.5	95.5
Power	18.8	18.8	18.8	18.8	18.8	18.8
Secondary Array Thermal Control	0.0	43.2	43.2	43.2	43.2	43.2
Avionics	35.0	35.0	35.0	35.0	35.0	35.0
Propulsion	2.9	35.9	2.9	2.9	2.9	2.9
Heaters	0.0	27.4	60.4	51.6	80.1	22.7
Harness Loss	3.0	5.3	5.3	4.9	4.9	4.9
Total	204.6	358.5	358.5	330.1	330.1	329.9
Available Load Power	0.0	482.0	482.0	482.0	482.0	482.0
Power Reserves	–204.6	123.5	123.5	151.9	151.9	152.1
Margin	–100%	34.4%	34.4%	46.0%	46.0%	46.1%

3.5.1. Bus Configuration and Structure Design

The configuration of the mechanical system is driven primarily by the launch vehicle and third-stage-generated environments, science payload field of view (FOV), subsystem requirements, and the Thermal Protection System (TPS) design. Figures 3.5-1, 3.5-2, and 3.5-3 identify the significant components and the baseline bus system mechanical configurations. Figures 3.5-4 and 3.5-5 depict the flight configurations, and Figure 3.5-6 depicts the launch configuration.

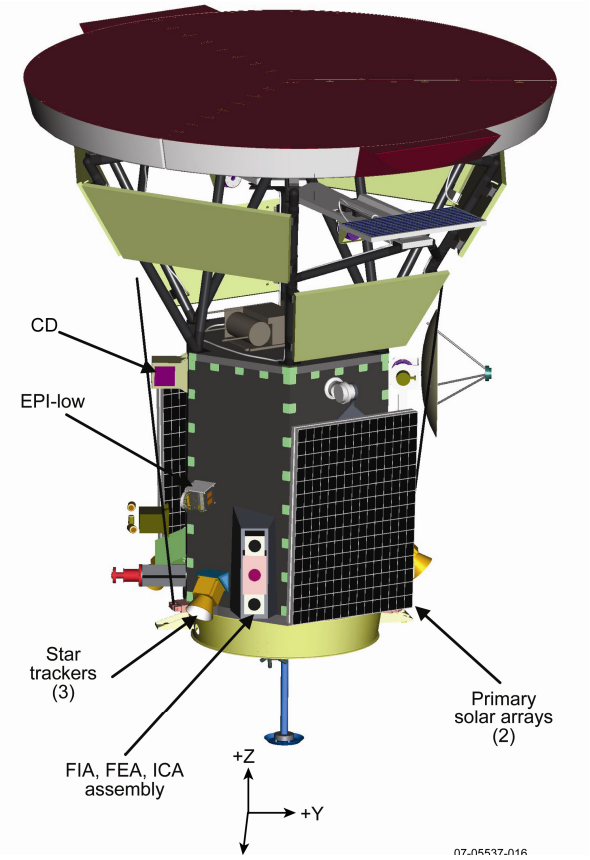

Figure 3.5-1. Solar Probe+ solar encounter configuration.

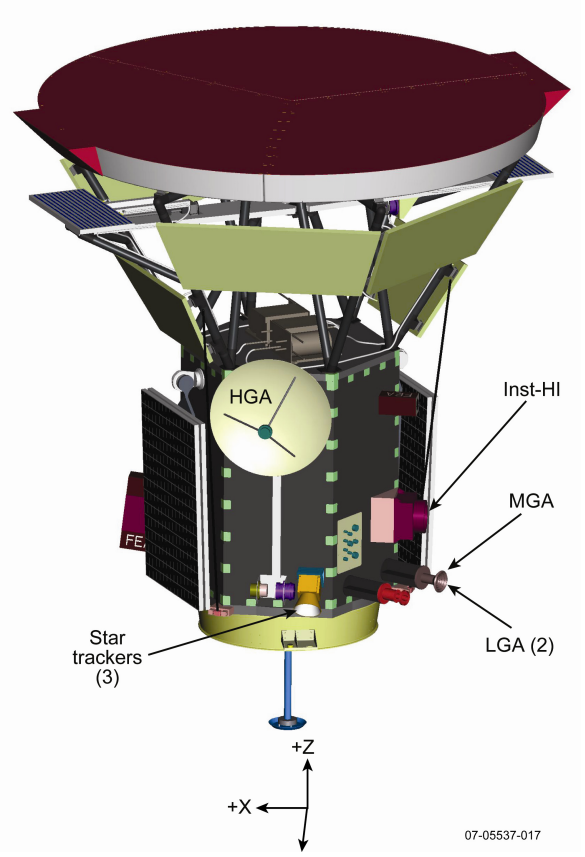

Figure 3.5-2. Alternate view of solar encounter configuration.

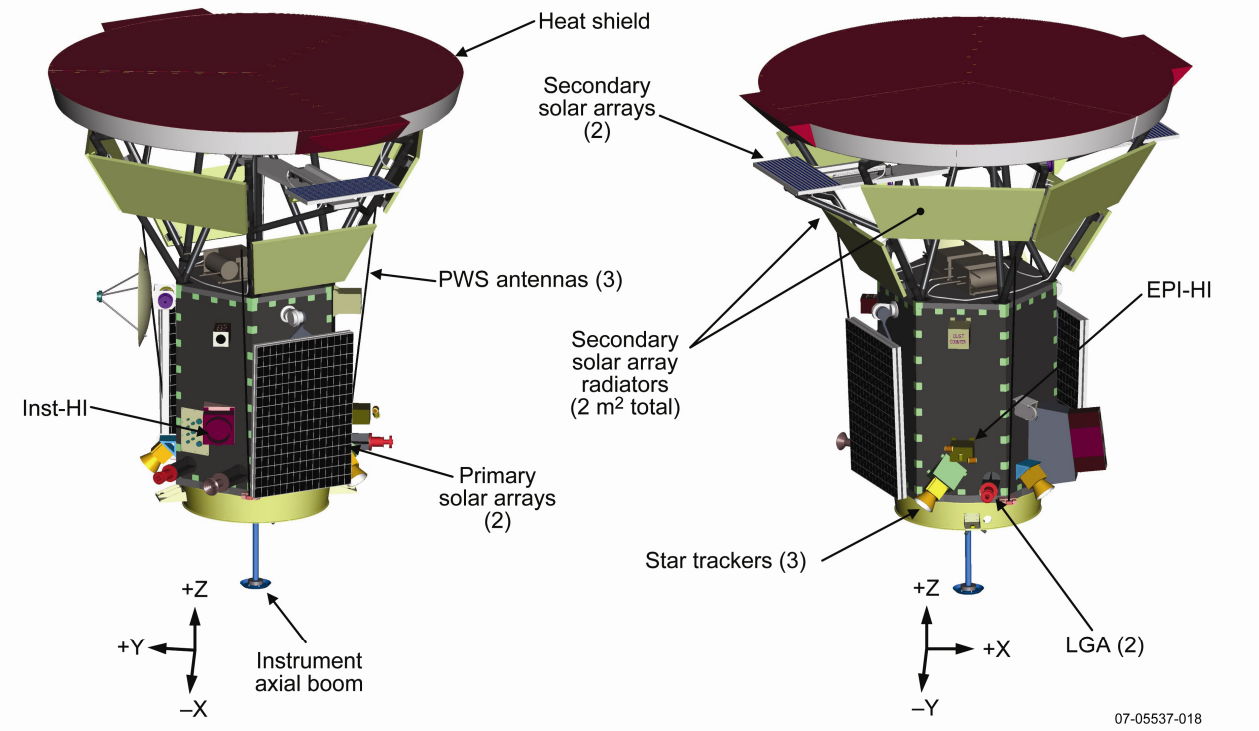

Figure 3.5-3. Alternate views of solar encounter configuration.

The bus structure design chosen is a conventional aluminum design that employs no technology development and presents a very low-risk approach to the mission. Aluminum honeycomb panels employ both embedded-edge members and bonded clips to attach the panels in a manner very similar to the approach used for several recent successful missions, including STEREO and New Horizons. Clean load paths

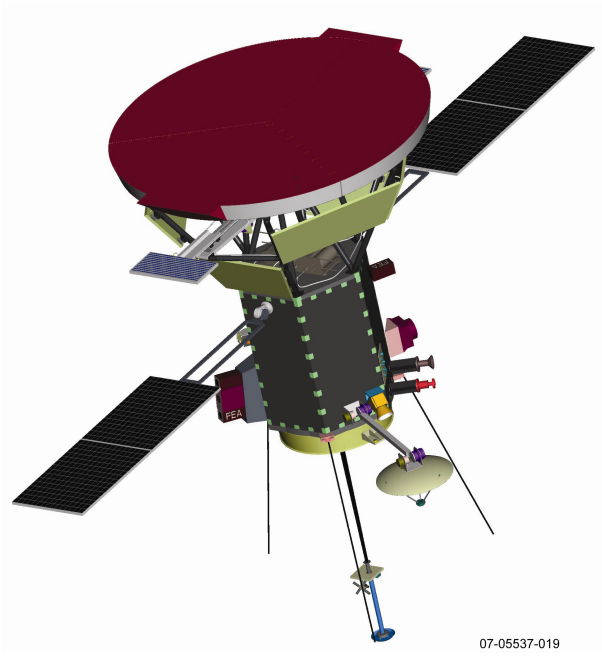

Figure 3.5-4. Science downlink configuration.

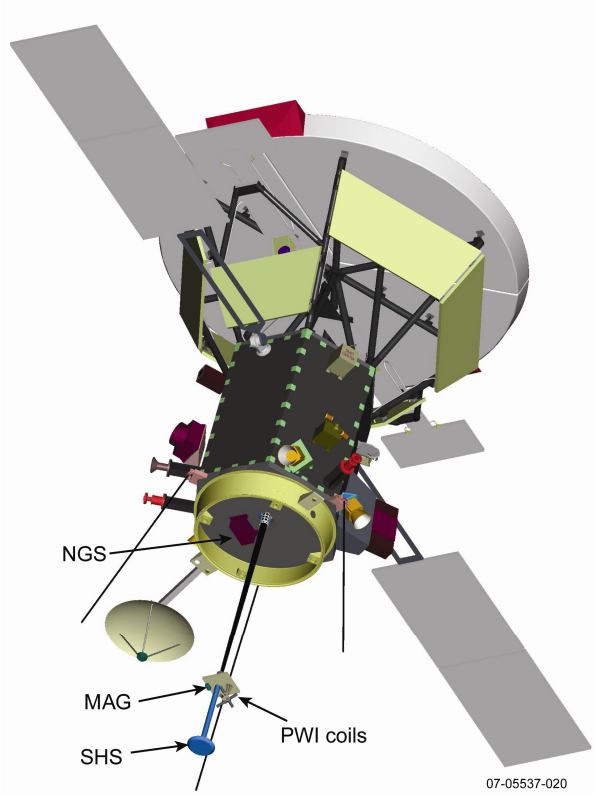

Figure 3.5-5. Alternate view of science downlink configuration.

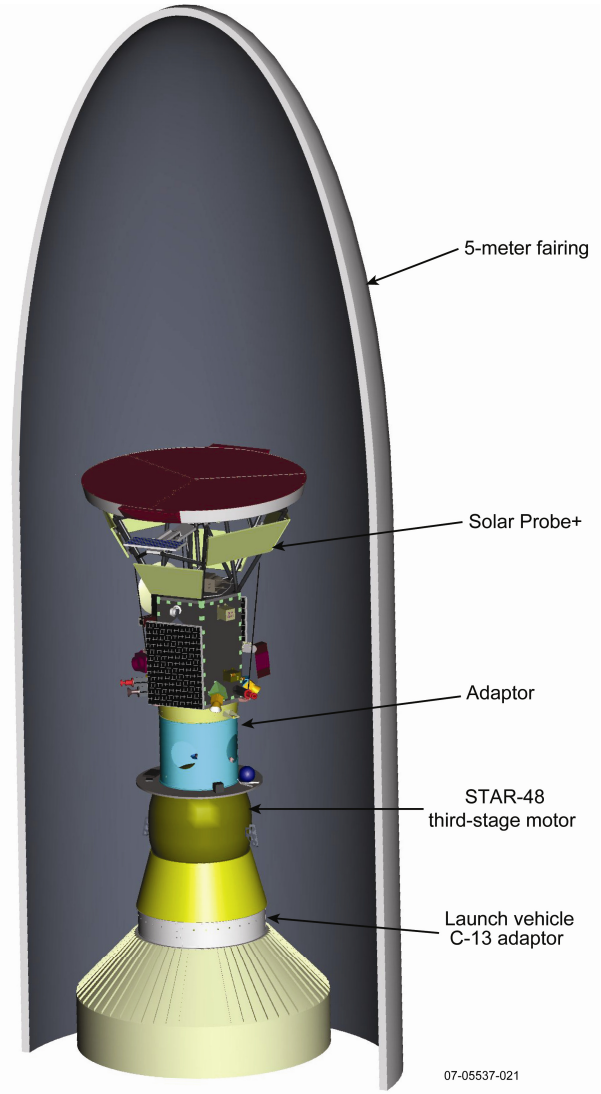

Figure 3.5-6. Launch configuration shows compatibility with volumetric stage.

efficiently transfer the launch and flight loads from the TPS interface trusses and from bus-mounted components through the bus structure corners and into the payload adaptor. The structural design approach for the bus-centric propulsion tank mount consists of a simple machined and assembled bracket support structure. Ample access to the interior of the spacecraft is provided by three removable panels.

The 37-in. diameter third-stage STAR-48 interface and clamp band are industry-standard components and are very well understood technologies. The adaptor interface to the third stage incorporates all needed electrical and instrument purge interfaces for the spacecraft.

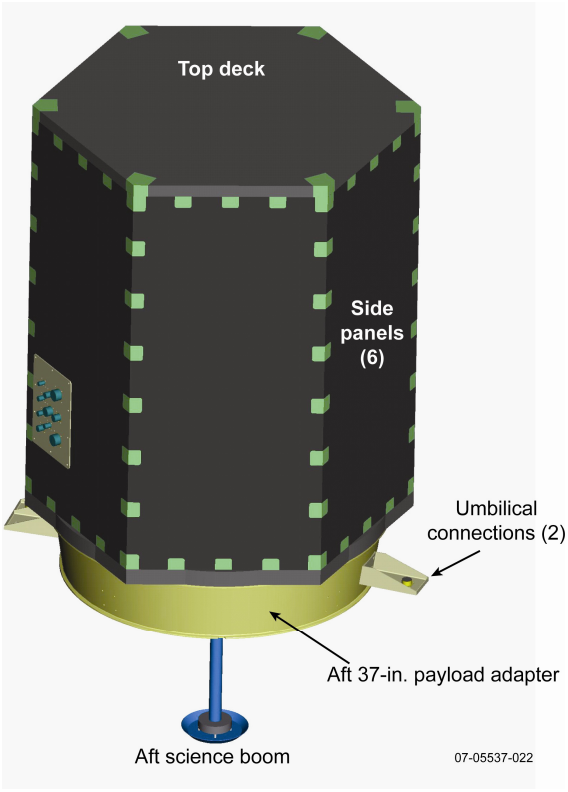

Figure 3.5-7. Spacecraft bus layout.

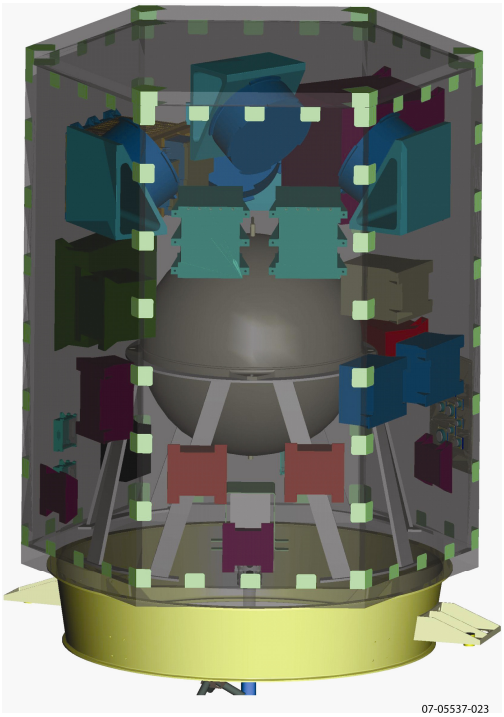

Figure 3.5-8. Interior view of spacecraft bus layout.

Figure 3.5-7 depicts the significant bus structure elements. Figure 3.5-8 illustrates the preliminary layout of the interior bus components,

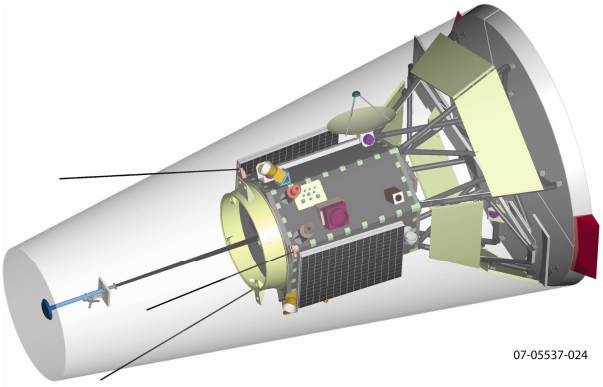

Figure 3.5-9. Solar encounter flight configuration showing umbra.

demonstrates adequate volumetric space for harness and connectors, and provides an illustration of the propulsion tank mounting concept. Figure 3.5-9 illustrates the stowed spacecraft configuration within the umbra.

There are no new technology development tasks outside the usual design process for the aluminum bus structure. The bus structure mass has been calculated based on the current design presented, and the values stated for components have been favorably compared with experience spanning several recent missions. All mechanical ground handling equipment (MGSE) support equipment for spacecraft handling, transfer, shipping, and testing operations is planned to be either currently available equipment or, in the case of lift fixtures and transportation dollies and containers, typical mission unique hardware of standard design.

The bus structure proposed development schedule and cost baseline support a conservative and low-risk approach successfully used on recent previous programs. The structure follows a proto-flight approach with a single-flight structure. There are no engineering models planned for the bus structure. The baseline test and qualification program will include a static load test before shipment to the propulsion vendor. After propulsion system integration, a thermal balance and propulsion system thermal vacuum test will be performed. To obtain modal information and to qualify major package interfaces, component mass models will be integrated and a three-axis sine vibration test of the bus structure will be performed before delivery for spacecraft system-level integration. A mass simulator of the TPS and the engineering model support trusses will be used for these preintegration tests, enabling development of the bus and the transition structure assembly (TSA) support trusses in parallel with the carbon–carbon (C-C) TPS. The bus structure, TSA and TPS subsystem testing, and flow into the spacecraft system-level integration and testing (I&T) phase is discussed in detail in Section 3.5.5.

Phase A design and development activities planned for the bus structure include the usual configuration, science instrument, and subsystem accommodation tasks. An investigation into both a hybrid composite and an all-composite structure design is planned to ensure that the bus structure optimization of cost, mass, and schedule has been achieved for this mission and matched to the system-level requirements. A calculated mass rollup, detailed schedule and revised cost estimate, and draft bus structure requirements document for the system are included in Phase A tasks.

3.5.2. Transition Structure Assembly Design Overview

The TSA provides the mechanical structure that couples the bus structure to the TPS shield and also serves as a platform to support the secondary solar array system and its associated thermal fluid cooling subsystem. Figure 3.5-10 depicts the significant components of the TSA.

The baseline structure design consists of a set of graphite-based structural members connecting the TPS, the secondary power system thermal system, and mechanism components. The mechanisms are discussed in Section 3.5.3. Thermally isolated flat-panel exterior radiators provide heat rejection for the secondary solar array fluid circulation system. These are tied to the six carbon graphite/cyanate ester (Gr/CE) trusses by short flexures that accommodate thermal expansion mismatch. The current baseline design and mass estimates of the radiators

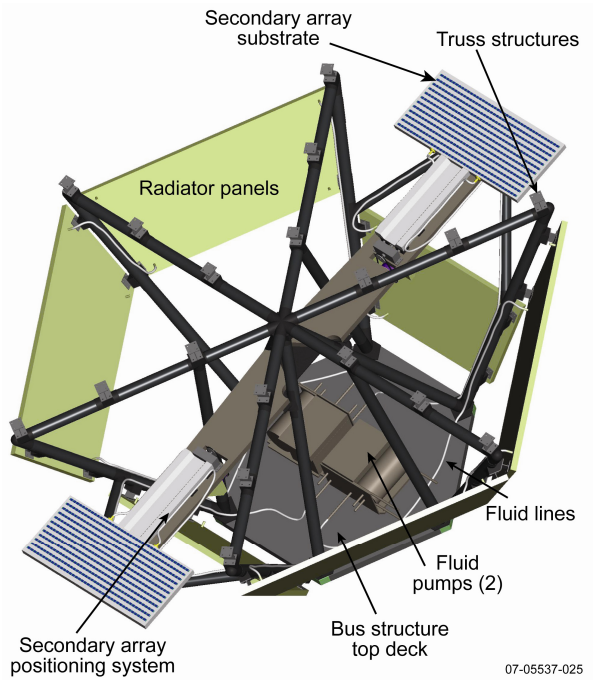

Figure 3.5-10. TSA components.

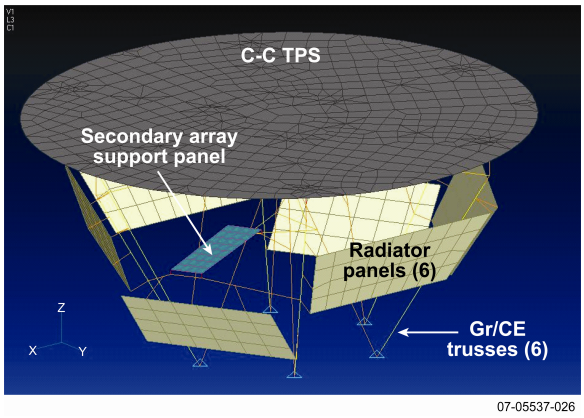

Figure 3.5-11. Both pinned and fixed-boundary conditions were evaluated. Fifteen iterations were completed to maximize stiffness while minimizing mass. All elements show positive margins of safety.

Table 3.5-1. Data analysis summary. MEMF, model equivalent mass fraction.

Frequency	Direction	MEMF	Comments
18.1 Hz	Lateral 1	16% *X* 30% *Y*	Truss bending
19.2 Hz	First *Z*	10% *X* 26% *Y* 20% *Z*	Bending of secondary array support panels and tubes
23 Hz	Lateral 2	36% *X* 13% *Y*	Truss bending

employ heat pipes embedded within aluminum honeycomb panels and face sheets. The spacecraft forward deck, trusses, radiator panels, circulation pumps, secondary solar arrays, slider mechanism, plumbing, and control electronics are assembled, processed, and qualified as a single assembly, all included in the TSA. The integration, testing, delivery, and integration into the spacecraft system of this assembly is discussed in Section 3.5.5.

A preliminary structural analysis has been performed on the TSA system. The results confirmed the mass values estimated for these elements. A finite element model was used to establish truss geometry and sizing needed to meet launch vehicle requirements. Three static load cases—15 *g* separately in *X*, *Y*, and *Z*—were run, and 15 iterations were completed, resulting in a completion of the baseline geometry and member sizing tasks. The design meets all requirements with positive margins. Figure 3.5-11 illustrates the primary components modeled from a finite element model analysis perspective. Figure 3.5-12 depicts several of the finite element model analysis runs. Table 3.5-1 summarizes the data analysis results.

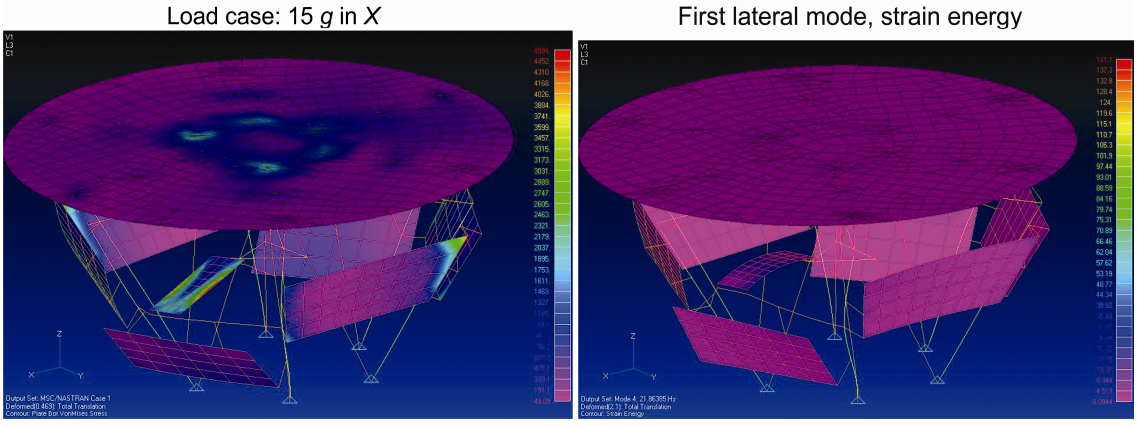

Figure 3.5-12. Results from fixed-boundary conditions are shown. All elements show positive margins of safety.

3.5.3. Bus and Transition Structure Assembly System Mechanisms

Mechanisms and mechanical systems supporting the power and TPS subsystems are discussed in this section, and thermal and electrical performance of these systems are discussed in their respective subsections

3.5.3.1. Primary Solar Array Design Overview

The primary solar array system consists of two identical wings, each comprising two panels. The wing design interfaces to the spacecraft via a two-axis Schaffer-Moog Type II bi-axial harmonic drive stepper motor, a set of interface brackets, and a pyrotechnic-activated Hi-Shear pin puller (SP-1214) device that provides a preload to the wing and postlaunch release for subsequent mission operations. The wing design is a retractable design, driven out to the deployed position after launch release and retracted back to the stowed position when the spacecraft is within 0.25 AU of the Sun. The drive motor system baseline is a bi-axial Schaeffer-Moog Type I harmonic drive stepper motor design with extensive flight heritage. After the full deployment position is reached, the array wings then are capable of rotation by the second axis of the motor in order provide the array angular relationship to the Sun as needed for thermal and power system control.

The retractable, rotating wing, two-panel system design combines flight-heritage components from the TIMED (Thermosphere, Ionosphere, Mesosphere Energetics and Dynamics) four-panel design with the additional Solar Probe+ requirement added for a retractable design. A similar design incorporating a retraction and redeployment capability similar to the Solar Probe+ requirement was proposed for the TIMED mission and developed to the preliminary design review (PDR) level by a vendor but was not used in flight as the mission design evolved. A design trade study for the Solar Probe+ retractable feature that will trade independently driven hinge lines using a geared stepper motor against the cable synchronized hinge lines of the earlier TIMED study will be conducted in Phase A. A full-scale, high-fidelity engineering model test program is planned and costed with a schedule that precedes the flight build. The required *g*-negation system, the dynamics analysis tasks, and deployment data collection system are all heritage processes tracing their roots to the deployment testing of the TIMED four-panel solar array system. The substrates and their associated high-temperature array technology use materials and process technology from the MESSENGER solar array and differ only in geometric shape and area. In order to further minimize the risk to the flight build cycle, several qualification and test panels are planned and costed to ensure previous fabrication and cell lay-down processes used on MESSENGER have been retained by the fabrication and cell lay-down vendors. Primary solar array mass has been calculated based on the current system requirements and uses MESSENGER measured masses and packing factors for the panels where appropriate.

Primary Solar Array Subsystem Qualification. The primary array flight system buildup and qualification testing duplicates the flow and processes developed for the TIMED solar array wing assemblies. The flight system design cycle starts with the fabrication and testing of a full-scale, high-fidelity engineering model. The engineering model is used to ensure that the dynamic behavior (deployments and retractions) correlates with the dynamic modeling analysis, so that flight system calculated mass, inertias, and physical size are matched to the flight design. The engineering model also functions as the development model for harness routing and thermal blanketing. The engineering model program uses the same mechanical ground handling hardware, including the gravity negation system as the flight system. Mechanism life testing at both hot and cold temperature extremes also is planned for both the engineering model system model and for the mechanism subassembly level. Once the engineering model system performance is correlated to the dynamics analysis models, the flight build can proceed. This identical engineering model development

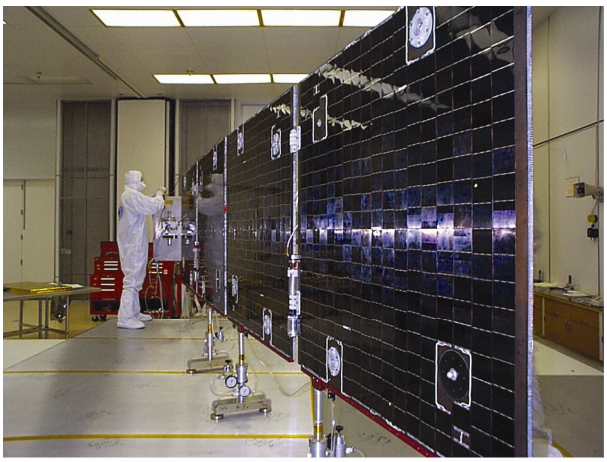

07-05537-028

Figure 3.5-13. TIMED flight wing and *g* negation system.

program methodology lead to the successful TIMED solar array in flight deployments that correlated closely with predictions.

The flight build and test program starts with the fabricated substrates delivered to the cell vendor for cell lay-down and wiring. After receipt and power system electrical performance testing, the flight substrates then are assembled and deployment-tested with the identical off-loading *g*-negation fixture used for the engineering model development program as described above. The TIMED solar array wing and *g*-negation system (Figure 3.5-13) are well understood and more complex than that needed for Solar Probe+. Data recovered during deployment testing of the flight system is compared against the engineering model kinematics analysis to ensure that the behavior of the system is fully understood and a baseline performance set of characteristics is captured before wing environmental testing. Proto-flight vibration testing (at levels above predicted flight levels) is followed by an additional set of deployment tests to ensure no changes in dynamic deployments occur as a result of vibration testing. The system is then ready for spacecraft-level integration where it will undergo spacecraft system-level vibration, acoustic, shock, and pop-and-catch deployments to ensure first motion occurs.

3.5.3.2. Secondary Solar Array and Transition Structure Assembly Mechanism Design Overview

The secondary power-generation system mechanical system design is driven by the mission power generation needs within 0.25 AU. Under the intense solar flux during solar encounter, an active cooling loop system is required to cool the secondary solar arrays. As the solar distance decreases, a positioning system pulls the concentrator arrays inboard, shadowing more strings behind two knife edges in the TPS. This operation provides constant power generation while maintaining the heat on the concentrator array to manageable levels. The secondary power-generation system design is an integrated part of the TSA, which couples the TPS into the conventional bus system. Figure 3.5-10 depicts the TSA assembly and identifies the significant components.

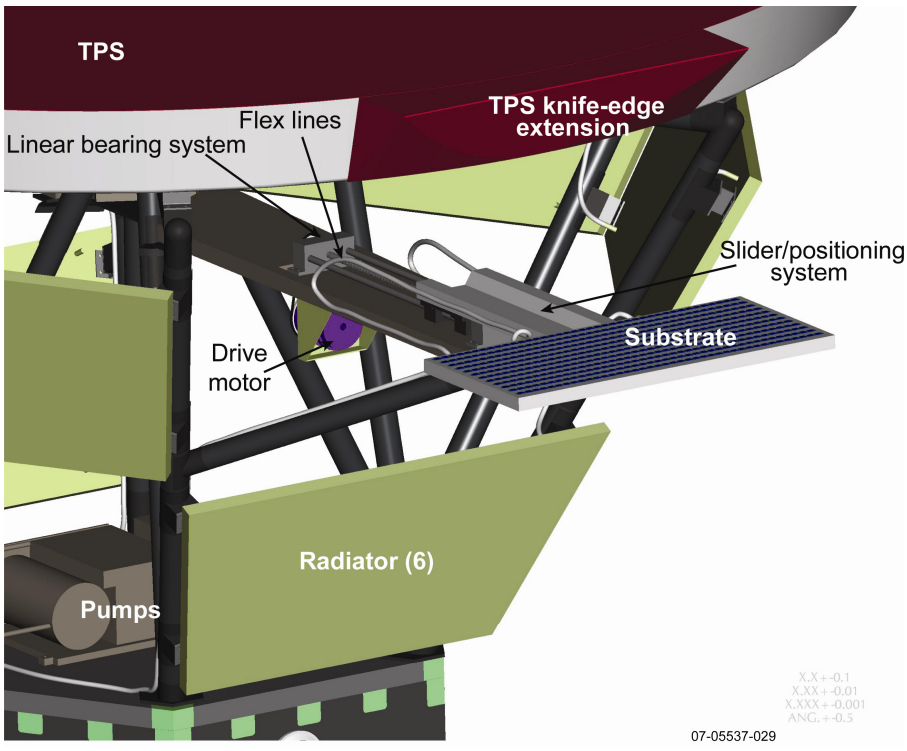

Figure 3.5-14. TSA mechanism components.

Figure 3.5-14 identifies the major mechanical components of the TSA and secondary power subsystem. Two identical retractable panel/cooling systems are used for the Solar Probe+ spacecraft. The release of each system from the launch (stowed) configuration is accomplished by the activation of a single flight-qualified Hi-Shear pin puller (SP-1214) device used successfully on previous spacecraft. Once the launch lock is released, the system is capable of flight deployment/retraction operations. During operations outside 0.25 AU, the secondary solar arrays are fully extended to maintain temperature and minimize heater power needed for thermal balance. At 0.25 AU, the secondary system is fully extended, and the primary solar array system (both wings) is then stowed. The temperature of the cell substrates (and resulting power conversion efficiency) is controlled as the spacecraft gets closer to the Sun by a closed-loop fluid management system. The system is designed to keep the cells, mechanisms, drive motors, and other components within typical operating temperature limits.

The slider mechanism baseline design consists of linear bearings and a recirculating ball lead screw system adapted from commercial machine tool systems. Features include a simple, robust mechanism derived from numerical controlled machine tools where debris tolerance, millions of problem-free cycles, precision, and tolerance of thermally induced misalignments are the normal operating requirements. The modifications planned for the slider are primarily made to reduce mass and ensure lubricants and selected components meet spaceflight requirements. The drive motor selected for the system is a Schaeffer-Moog stepper motor with extensive flight heritage. The rated life, available torque, and positional accuracy (resolution) of the motor exceed mission requirements.

The copper used to hold the secondary solar array cells is attached to the slider and extracts heat from the cells via internal passages through which fluid passes. Input and output flex hoses transfer the fluid between the plate and the radiator panels. Aluminum fittings and tubing (0.015-in. wall thickness × 0.500-in. diameter) are the baseline for mass calculations and preliminary sizing of the system. The use of fittings to connect tubing to components is minimized where possible. Preliminary runs for plumbing have been developed to identify first-order challenges as illustrated in several TSA-related figures. Development and optimization of the flight plumbing and harness will occur using a full-scale mockup.

Phase A mechanical system tasks identified for the TSA mechanisms development include trade studies on selection of mechanical components, a fabrication and testing development program for several subassemblies, a design trade study on radiator design, and evaluation of alternatives for plumbing components. Included in Phase A tasks is a trade study to compare a design that moves the knife edge with the baseline design, which moves the array.

Secondary Solar Array Subsystem Qualification. The secondary solar array system mechanisms are managed under a test and qualification program very similar to the primary solar array system, with additional testing planned for the fluid components and elevated temperatures attributable to the operating environment imposed by the proximity to the TPS shield. A high-fidelity, full-scale engineering model fabrication and testing program is planned. The engineering model test plan starts at the component level for the critical motion components. Mockups of all flexible components (harness, cooling lines, etc.) are tested over temperature extremes for both physical behavior (routing changes resulting from repeated motion) and, in the case of fluid components, fluid integrity under pressure. Once the testing for performance and lifetime are complete, a test to failure is planned for both the flexible harness and flexible fluid components to ensure that the limits of performance are well understood and compared to the expected mission requirements. Torque changes of all flexible service loops resulting from lifecycle testing also are measured again, duplicating the solar array system testing and qualification plan

methodology. After the component-level testing is completed, the full-scale engineering model secondary array system (less cells) is assembled and tested as a subsystem. Again, the system is exercised over predicted temperature extremes. Vibration testing and postvibration deployment testing is planned for the mechanism subassemblies.

The flight secondary power generation system will be qualified and delivered to the spacecraft I&T program as a complete subsystem in the configuration illustrated in Figure 3.5-10. The system will be vibrated and strength-tested by using a TPS mass simulator attached to the forward plane of the Gr/CE support trusses using titanium flexures. After vibration and release testing, the system will be thermally cycled, and a thermal balance test will be performed with solar cell simulators and a TPS heat-source simulator. During thermal testing, the mechanisms will be life-tested (~50 cycles through the motion extremes). Subsequent to solar cell installation, solar array testing will be conducted as with the primary solar arrays.

3.5.3.3. Science Instrument Payload Mechanical System Accommodations

3.5.3.3.1. Aft-Mounted Science Boom

The bus system will supply an aft-mounted boom for science instrument accommodation. The integration of the boom-mounted science instruments into the boom system will require significant accommodation efforts and interface definition early in the bus development cycle. The bus mechanical team will lead this effort. The current location of the boom on the bus eliminates unnecessary bus structure mass by taking advantage of significant open space available in the payload adaptor fitting.

3.5.3.3.2. Mechanical System Interfaces and Science Instrument Accommodations

Mechanical interfaces for the instruments consist primarily of flat surfaces with standard, threaded fasteners used to attach the components to the bus structure. Where pinning is required for alignment stability, it can easily be accommodated with the bus design. Phase A tasks include a drafting of a preliminary alignment budget and verification plan. Baseline instrument purge requirements are unexceptional and easily accommodated with existing support systems.

Physical locations of the science payload instruments on the bus and the resulting instrument requirements for clear FOV (CFOV) are compliant based on information provided by the STDT. As actual instruments are selected for the mission, accommodation requirements for each will be met; no significant issues with instrument accommodation are expected. The science instrument CFOV are illustrated in Figures 3.5-15 through 3.5-19.

3.5.3.4. High-Gain Antenna Mechanical Mechanism Overview

High-Gain Antenna Mechanical Design Overview. The mechanical motion components of the high-gain antenna (HGA) system are dis-

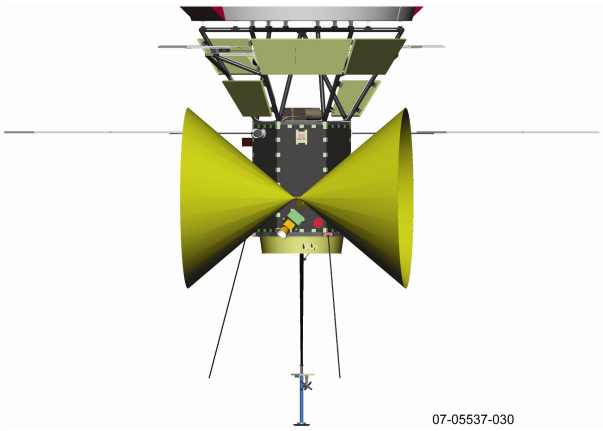

Figure 3.5-15. Instrument CFOV.

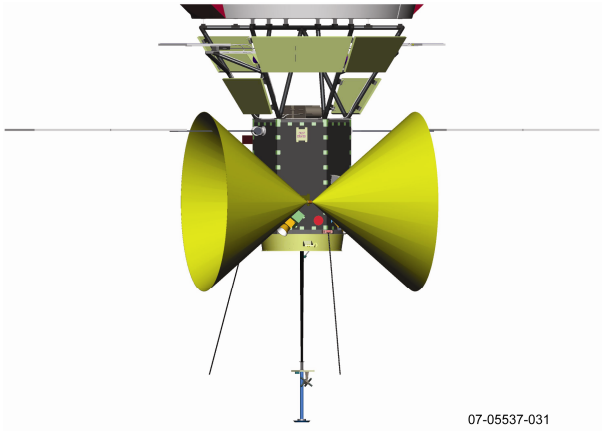

Figure 3.5-16. Alternate view of instrument CFOV.

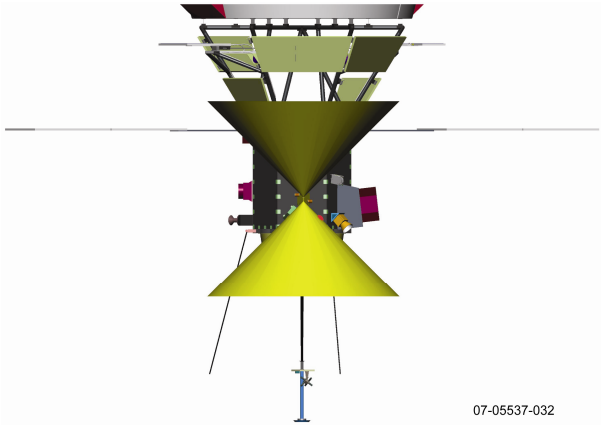

Figure 3.5-17. Alternate view of instrument CFOV.

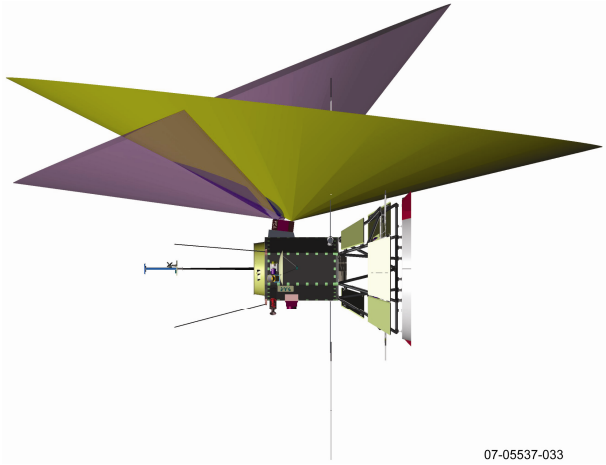

Figure 3.5-18. Alternate view of instrument CFOV.

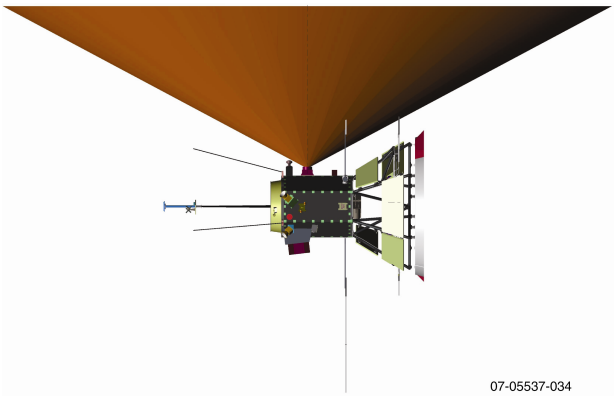

Figure 3.5-19. Alternate view of instrument CFOV.

cussed in this section, and the antenna element and the radio frequency (RF) system performance are discussed in Section 3.10. The FOV coverage requirements of the mission coupled with the requirement to stow and deploy the antenna multiple times during the mission are the driving requirements. Preliminary layouts

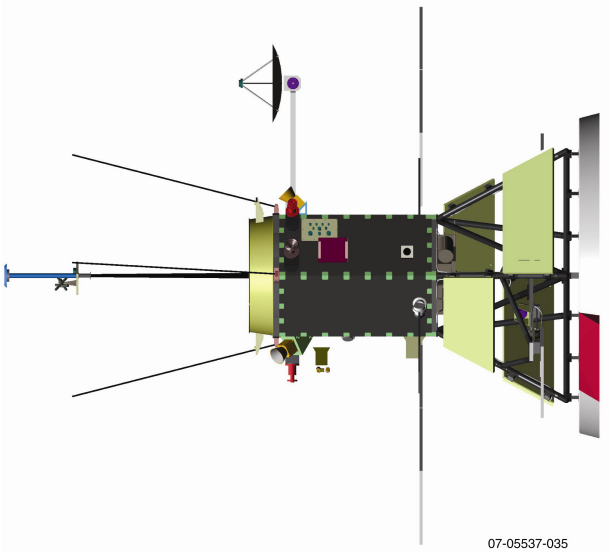

Figure 3.5-20. HGA/bus layout.

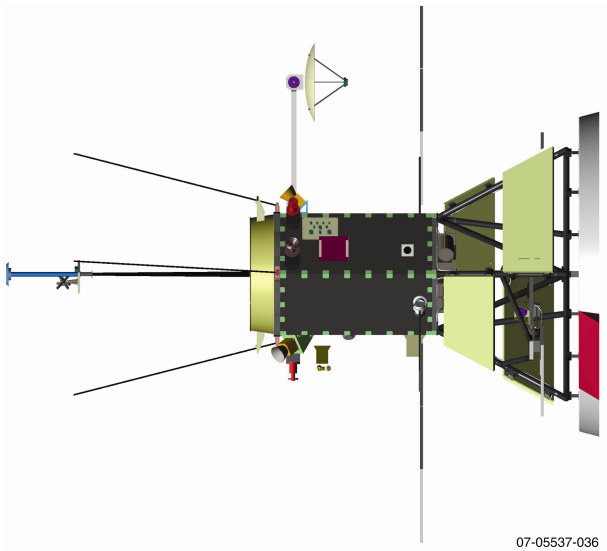

Figure 3.5-21. Alternate view of HGA/bus layout.

(Figures 3.5-20 and 3.5-21) have been performed to establish the required HGA system geometry needed to achieve the CFOV needed for communications. A Schaeffer-Moog harmonic drive actuator is the baseline motor for both motion joints. The motors chosen have demonstrated lifetimes well in excess of the mission requirements. RF signals are transmitted across the rotary joints via spaceflight heritage rotary joints and along the mast via rigid waveguide. The arm baseline design is of a normal flight-heritage design using a lightweight carbon-composite tube with bonded titanium end fittings at the attachment points.

HGA Mechanical System Test and Qualification Plan. The methodology used to design and implement the HGA mechanical test and qualification plan follows closely the successful experiences of both the HGA systems used on the Midcourse Space Experiment (MSX) and the STEREO spacecraft. A high-fidelity engineering model will be mechanically integrated and tested for proper motion employing the existing TSA and the full-scale wiring model. Measurements of drag torque resulting from temperature effects on all motion components, life-cycle testing, and other testing is planned on all motion components and on the engineering model system. Following the completion of the engineering model testing, the flight build will start, and it also will follow a test and qualification plan that uses hot and cold deployment and operational testing, sine vibration, and other subsystem-level mechanical testing before delivery to both the RF system and spacecraft I&T team. The flight antenna element will be included for all subsystem flight hardware testing before the spacecraft integration.

3.5.4. Spacecraft System Structural Analysis and Launch Environments

The preliminary design loads for the spacecraft system are derived according to the most recently available *Atlas Launch System Mission Planner's Guide*.[12] The expected flight levels provided in the launch guide are specified as quasi-static accelerations for the spacecraft center of gravity. Design loads for subsystems are initially based on a mass acceleration curve, superseded later in the program by the coupled loads analysis (CLA).

Spacecraft and subsystem design loads are more accurately computed by the launch vehicle manufacturer during the CLA cycles, in which reduced dynamic models of the spacecraft are combined at the launch vehicle interface with the flight-verified vehicle dynamics model. The coupled model is then excited with flight forcing functions for various dynamic loading events. CLA loads succeed the preliminary design loads and have customarily proven to be lower than the *Atlas Launch System Mission Planner's Guide* loads. There typically are two CLA cycles during a program, the first performed with a preliminary spacecraft dynamics model to aid spacecraft design and the second with a test-verified spacecraft dynamics model to finalize flight margins. Loads analysis is performed by using the requirements levied in NASA-STD-5002, *Load Analysis of Spacecraft and Payloads*.[13]

The spacecraft also is exposed to an acoustic environment during takeoff and through transonic flight. This external acoustic environment is transmitted through the vehicle fairing to impinge onto the spacecraft and affects large-area, low-weight surfaces such as the TPS, the radiator panels, and solar arrays. The acoustic sound pressure levels are provided in the *Atlas Launch System Mission Planner's Guide* and vary according to spacecraft volume, payload fairing dimensions, and acoustic blanket placement. Results from preliminary acoustic analysis of the TPS, solar arrays, and lightweight radiator panels under effective root-mean-squared (RMS) pressures indicate that the quasi-static design loads based on a typical mass acceleration curve remain the predominant load cases. Other analytical methods involving finite element, boundary element, and statistical energy methods will be used to more accurately determine the response of these lightweight structures over the entire acoustic frequency spectrum.

The *Atlas Launch System Mission Planner's Guide* requires a minimum natural frequency of the spacecraft to be 8 Hz in the two lateral directions and 15 Hz in the thrust direction. To avoid coupling, the subsystem minimum frequencies typically are set higher. For the TPS mounted on its flexure system, the fundamental frequency design goals are set at 15-Hz lat-

[12] *Atlas Launch Systems Mission Planner's Guide, Rev. 10a*, Lockheed Martin Corporation (January 2007).

[13] *Load Analyses of Spacecraft and Payloads*, NASA-STD-5002, National Aeronautics and Space Administration (June 21, 1996).

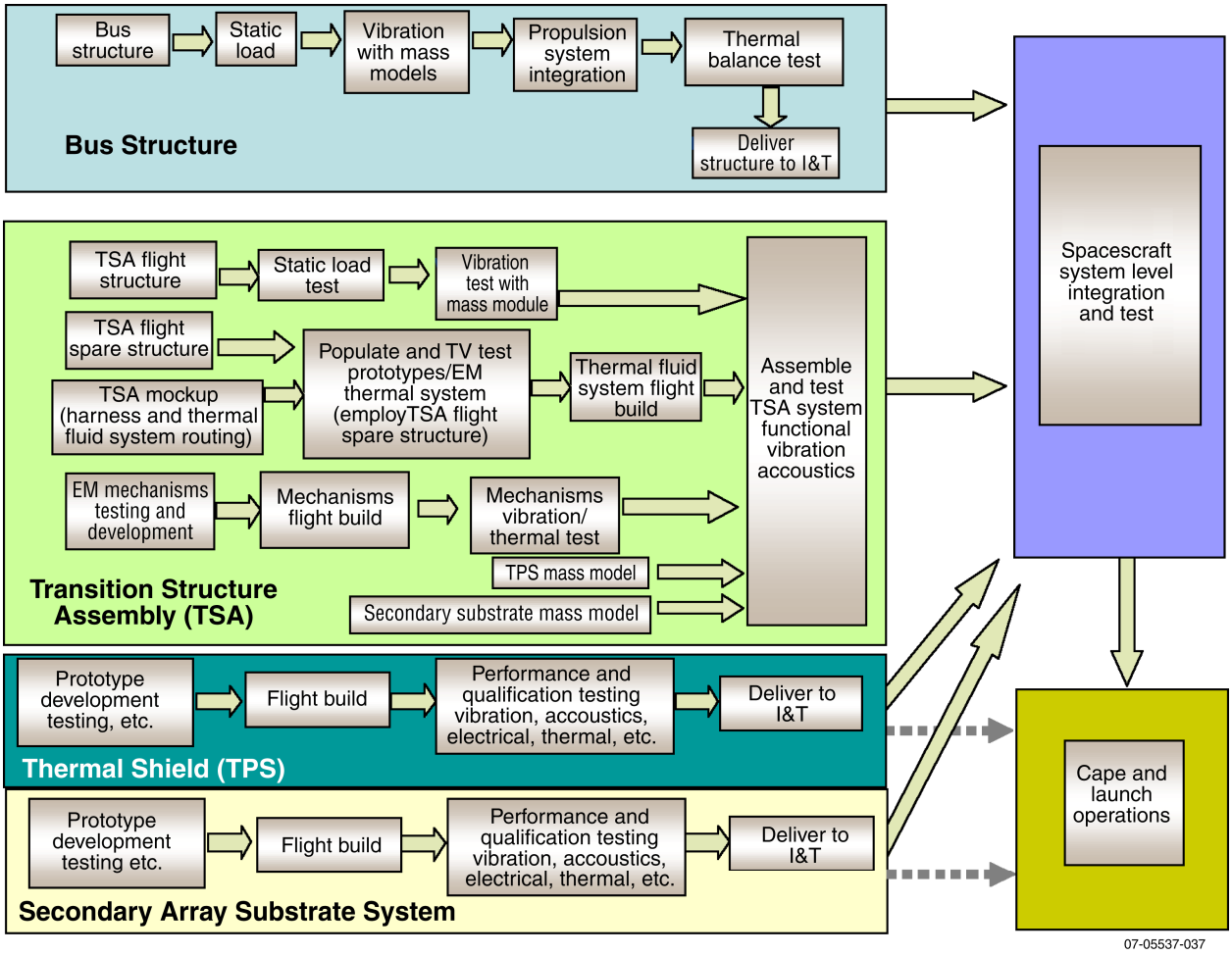

Figure 3.5-22. Systems test flow.

eral and 25-Hz axial. Solar array and radiator panels will be designed for frequencies above 25 Hz. Instruments and components shall have fundamental frequencies above 50 Hz.

The 2005 study included an analysis showing that the 2005 design met all Atlas requirements for stiffness. The current study uses a flat-plate TPS, a truss structure, and a bus essentially unchanged (from a load path standpoint) from that previous study—a more favorable design. The minimum frequency of the Solar Probe+ stack also will meet Atlas stiffness requirements.

3.5.5. Spacecraft System Mechanical Thermal Test and Qualification Plan

3.5.5.1. Rationale and Test Flow

The Solar Probe+ testing, qualification, and integration plan for the bus structure and TSA is designed to decouple the three significant development items of the spacecraft mechanical system: the bus structure, the transition structure, and the top circular-shaped TPS. The rationale for this design and development approach is offered for each element as follows:

- The *bus structure element* is considered to be a well understood, simple design using traditional materials and fabrication techniques. Its development cycle will closely follow the flow established for the STEREO and New Horizons missions.
- The *transition structure element* is composed of the secondary power-generation system and its associated thermal-cooling system as well as the structural support for the thermal shield. The development of this system is more challenging than the development of a standard solar array power sys-

tem because of the addition of the liquid-cooling feature. The subsystem requires qualification testing different than that of a typical solar power system.
- The *thermal shield* development program has the lowest technology readiness level (TRL) of the three mechanical elements. The program leverages heavily the work done for the 2006 *Solar Probe Thermal Protection System Risk Mitigation Study*.[14]

Decoupling the development cycles of the three primary elements reduces the risk of delayed hardware development schedules. Planning via design to decouple these elements provides schedule flexibility and allows each element of the program to manage its specific schedule independent of the system, provided delivery dates are ultimately met in I&T. The decoupled hardware development, testing, and qualification plan presented here lowers schedule risk and provides the best structure for these particular program challenges. Figure 3.5-22 illustrates the flow of the significant elements and captures the significant qualification tests of the systems. Note provisions have been made (illustrated by dashed arrows) to decouple the most technically challenging two items (the TPS and the cell substrates for the secondary array) from the spacecraft system, thus providing for their arrival at the launch site should unforeseen development problems surface.

3.5.5.2. Bus Structure Qualification Plan

The bus structure schedule ties significant interface definition milestones to the other elements to ensure all systems interface properly in form, fit, function, and delivery. Fabrication of the structure follows a traditional schedule.

After initial assembly of the bus structure, preliminary measurements and alignments are performed. Testing then commences with a static load and vibration test using mass models. The structure is then cleaned and bagged and shipped to the propulsion vendor for propulsion system I&T. After return of the structure to APL, a thermal balance test is performed. At that point, the top deck is removed and delivered to the TSA team to be used for their flight buildup, and the remaining bus structure is delivered to the I&T team for harness installation and population with the flight components.

3.5.5.3. Transition Structure Assembly Qualification Plan

Transition Structure Assembly Mockup. The TSA consists of the structural support truss elements, the thermal-cooling system (radiators, pumps, cooling hoses, etc.), and the secondary power-generation system. A similar developmental approach to that used for spacecraft bus development begins with a high-fidelity mockup. The engineering mockup is populated with a mix of simulators and engineering model components in order to identify harness and plumbing issues before the flight build. The mockup will be thermal vacuum-chamber-compatible and of high enough fidelity to support any thermal system subassembly and component performance testing required.

Secondary Power-Generation System Mechanisms. The design of the secondary power-generation system lends itself to a modular approach and a conventional mechanism development plan employing a high-fidelity engineering model. After assembly of the drive and release components, baseline current and torque margin performance measurements are made. The engineering model cell positioning mechanism (EMCPM) systems then will undergo vibration testing as subassemblies. After postvibration current and torque measurements are completed, the EMCPMs will be life-tested to two times the predicted number of cycles, under both hot and cold conditions, with current and torque trending performed.

[14] *Solar Probe Thermal Protection System Risk Mitigation Study: FY 2006 Final Report*, prepared by The Johns Hopkins University Applied Physics Laboratory under Contract NAS5-01072, Laurel, MD (November 30, 2006).

The design approach will use simulators of the solar cell/substrate assembly in order to decouple the solar cell/substrate development and delivery schedule from the mechanism test and qualification program. The flight build will commence after completion of the engineering model development and testing in order to incorporate any design changes uncovered in the mechanisms during testing. The flight-build CPMs will undergo the same testing sequence as the engineering model units, with the exception of life testing. When the flight cell/substrate assemblies are delivered, they can be assembled to the flight mechanisms without disturbing the cooling fluid loop integrity.

Transition Structure Assembly. Slightly overlapping the transition structure mockup development and secondary power subsystem testing, the flight truss elements will be fabricated and assembled with mass models in preparation for a static load test where the interfaces are structurally test-qualified to the worst-case expected loads. After the static load test, a vibration test will be performed with mass models of the TPS and components to complete the structural test program for the structural elements of the TSA. The modal data obtained from the vibration test will be used to correlate the CLA finite element model. Population of the TSA with flight components will then begin with various functional and electrical tests planned to exercise the motion components. The thermal-cooling system will be installed, the fluid system will be loaded, and thermal cycling and thermal balance testing will be performed. After successful completion of all functional and performance testing, the TSA flight system will be delivered to I&T for system-level testing.

3.5.5.4. Thermal Shield Development

The thermal shield development is discussed in a separate section of the report, yet the plan for integrating the shield into the bus system as well as the assumptions covering the integration plan will be discussed in this section. The shield possesses no electrical interface to the bus system. The sole interface is a conventional mechanical bolted joint. A template will be fabricated, and a fit check will be performed early to ensure successful integration of the flight TPS. The TPS will be delivered to the bus as a fully tested and qualified component. The program mechanical integration plan has the TPS arriving and assembled to the spacecraft as late as just before mass properties operations at the launch site. This sequencing provides the maximum development time to the element with the lowest TRL.

3.5.5.5. Spacecraft System-Level Mechanical Test Campaign

System-level testing is conducted by using NASA-STD-7002, *Payload Test Requirements*,[15] and GSFC-STD-7000, *General Environmental Verification Standard (GEVS)*.[16]

Verification that the transition structure and the spacecraft bus will withstand the design loads is achieved through low-frequency (5–100 Hz range) swept sinusoidal testing. The levels for the system-level sine vibration test are given in the *Atlas Launch System Mission Planner's Guide*.[17] These levels typically are notched to match spacecraft responses derived from the final CLA cycle. A minimum natural frequency for the spacecraft is specified in the *Atlas Launch System Mission Planner's Guide* to ensure that design loads and displacements are not exceeded. Minimum natural and actual frequencies are verified during the fixed-base sine test sequence of the spacecraft. With the TPS qualified separately and integrated before mass property testing, a mass simulator of the TPS will be used during spacecraft-level environmental testing.

---

[15] *Payload Test Requirements*, NASA-STD-7002, Rev A, National Aeronautics and Space Administration (September 10, 2004).

[16] *General Environmental Verification Standards (GEVS) for GSFC Flight Programs and Projects*, GSFC-STD-7000, Goddard Space Flight Center (April 2005).

[17] *Atlas Launch Systems Mission Planner's Guide, Rev. 10a*, Lockheed Martin Corporation (January 2007).

Verification that the spacecraft will withstand the acoustic environment is achieved through acoustic testing. The levels for the acoustic test are given in the *Atlas Launch System Mission Planner's Guide*. Testing is conducted by using NASA-STD-7001, *Payload Vibroacoustic Test Criteria*.[18]

Mass properties testing is conducted at the spacecraft level, generating a full inertia matrix of the test article. Measured in separate tests, the mass properties of the solar arrays, the TPS, and the instruments in their deployed condition are added analytically to generate the full-up spacecraft mass properties matrix in the various configurations encountered during launch and flight. Shock testing—including clamp-band separation and local sources of shock such as solar array release, instrument doors, etc.—is performed twice at the system-level. Final launch site operations include a launch configuration weighing and center of gravity measurement before third stage integration.

3.6. Thermal Protection System

3.6.1. System Design Requirements

The present system requirements for the Thermal Protection System (TPS) are shown in Table 3.6-1. These requirements are very similar to those developed in the 2005 STDT[19] study. The Solar Probe+ closest approach is 9.5 R_S, compared with 4 R_S in earlier Solar Probe studies. At that solar distance, the TPS does not require a large conical shield. Slightly lower temperatures are achieved for the Solar Probe+ design, using a coated, flat-front sunshield, than were obtained with the conical design and the closer solar distances of the earlier studies. ***Therefore, a significant part of the design, analysis, and testing done as part of those study efforts remains valid for the Solar Probe+ design.*** The design requirements listed bound the expected environmental exposures that will be encountered over the mission, define the required TPS configuration, and support the scientific measurements being made.

Table 3.6-1. TPS requirements.

Requirement	Value
Environmental requirements	
Structural requirement	15 Hz lateral 35 Hz thrust
Ionizing Radiation	44 krad Si
Solar Flux	Max. 70 W/cm^2 Min 0.13 W/cm^2
Mission Duration	7 years
Configuration	
TPS Mass	70.5 kg
Shield Diameter	2.72 m
Primary Shield Thickness	15 cm
Spacecraft Orientation	Sun-pointing
Science measurements	
Mass Loss	2.5 mg/s
Primary Shield Surface α/ε	0.6
Surface Conductivity	Conductive
Heat Flow into Spacecraft	<50 W

Compared with the TPS design presented in the 2005 STDT and 2006 TPS Risk Mitigation[20] reports, the key difference is the change in the Sun distance. At closest approach, 9.5 R_S, the peak flux is 70 W/cm^2, compared with 400 W/cm^2 at 4 R_S in the previous studies. The largest distance from the Sun also has changed. The Solar Probe+ aphelion is less than 1 AU, compared with 5 AU in the earlier studies. At 1 AU, the minimum solar flux is 0.13 W/cm^2, resulting in a minimum sunshield temperature of ~0°C.

The current Solar Probe+ sunshield design is based on the secondary shield design developed in the Risk Mitigation Study.[21] With the Solar Probe+ mission peak flux, the sunshield design achieves similar temperatures to the earlier Solar Probe studies without the conical primary

[18] *Payload Vibroacoustic Test Criteria*, NASA-STD-7001, National Aeronautics and Space Administration (June 21, 1996).

[19] *Solar Probe: Report of the Science and Technology Definition Team*, NASA/TM—2005–212786, National Aeronautics and Space Administration, Goddard Space Flight Center, Greenbelt, MD (2005).

[20] *Solar Probe Thermal Protection System Risk Mitigation Study: FY 2006 Final Report*, prepared by The Johns Hopkins University Applied Physics Laboratory under Contract NAS5-01072, Laurel, MD (November 30, 2006).

[21] *Solar Probe Risk Mitigation Study*, prepared by The Johns Hopkins University Applied Physics Laboratory, 2006 Mid-Year Report.

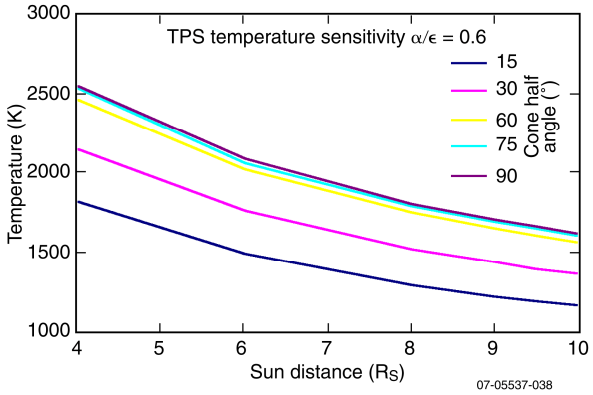

Figure 3.6-1. TPS temperature sensitivity.

shield. The Solar Probe+ TPS design includes a carbon–carbon (C-C) shell surrounding an insulating carbon foam. The front surface of the shield includes an optical coating to reflect some of the incident solar energy. The resulting peak temperature expected at closest approach is ~1700 K.

TPS temperatures are a function of the shield configuration and optical properties. Shield temperatures for different cone geometries and Sun distances are shown in Figure 3.6-1. The key optical property is the ratio of the solar absorptance to the IR emissivity, α/ε, set at the design value of 0.6 in Figure 3.6-1, which shows that the shield temperatures are reduced as the Sun distance increases or the cone angle is decreased. It also shows that there is very little impact on temperature until the cone angle is below 45°. At 9.5 R_S, the shield temperature is ~1700 K. In the earlier Solar Probe studies with the conical TPS, the shield temperature was a little over 1800 K. Based on the complexity of making a large C-C structure, the Solar Probe+ TPS design is simplified by using a flat shield.

Other requirements from the earlier Solar Probe studies are affected by the change in the mission aphelion. When the Solar Probe mission included a Jupiter gravity assist (JGA), the spacecraft spent a long period in which the direction of the sunshade relative to the Sun was unconstrained. The Solar Probe+ mission keeps the spacecraft inside 1 AU throughout the mission. At those distances, the spacecraft must always be positioned to keep the shield in front of the Sun.

The Solar Probe+ mission trajectory reduces the program risks by incorporating multiple encounters at progressively closer distances to the Sun. In the earlier studies, the first solar encounter was high risk because the first time the TPS was used, it was at its peak temperatures. The Solar Probe+ mission duration is seven years. During this time, the spacecraft makes 24 orbits, gradually decreasing the closest approach to the Sun from 35 R_S to 9.5 R_S. This movement of perihelion toward the Sun allows the TPS system to be tested incrementally. Should some performance degradation be found, the mission trajectory can be altered, keeping the spacecraft at a safe Sun distance.

The spacecraft heat flow requirement is based on the fact that the spacecraft has a range of power dissipations that it can absorb and still maintain temperature control. At closest approach, the spacecraft sunshield has a total incident flux of ~4 MW. Heat is transferred to the spacecraft both radiatively from the bottom of the shield and conductively through the shield supports. The shield is required to reduce the heat flow transmitted to the spacecraft to 50 W, or 0.001% of the original flux. At this effective shield requirement, it is difficult to adjust the heat leak. Our inaccuracy in analyzing and testing the shield performance is such that the goal of the shield design is to provide large margins and then verify the important parameters by realistic testing.

3.6.2. Design Approach

Sun Shield. The Solar Probe+ sunshield is a 2.7-m diameter shell, approximately 15 cm thick. It consists of a pan and a top cover. The shell is filled with carbon foam insulation that provides the thermal protection to the spacecraft bus. The material selection for the sunshield is driven by the expected exterior temperature of 1700 K. C-C was the baseline material for the TPS structure in the 2005 STDT report. It is one of the few structural materials that can survive the high temperatures, provide acceptable specific strength, and meet the outgassing requirements. The top cover is flat and

coated with a low α/ε coating. An additional micrometeoroid layer has been added into the sunshield to provide particle impact protection.

For a structure of this size to meet its tight mass estimate, it is required to be made of very thin-walled shell sections. The nominal lay-up for the C-C shell is a six-layer isotropic laminate, approximately 0.076-cm thick, and made of T300 carbon fabric. Coupon testing of a variety of C-C materials has been performed to define their material and mechanical properties. Thicker-walled sections will be used at fastener locations.

In earlier Solar Probe studies, fabrication oven volume limited the size of C-C pieces that could be made. As part of the new Constellation Program, a larger oven is being installed at one vendor, giving them the ability to make the shell in one piece. From a mechanical perspective, the choice between single and multiple piece construction will be defined in a Phase A trade study. The positive benefits of one-piece fabrication include a simpler structure and less assembly. The negatives include a higher reliance on cobonded stiffeners and limiting the vendor pool. For a multiple-piece shield design, the number of joints is a function of oven size and spacecraft symmetry. In the earlier radioisotope thermoelectric generator (RTG)-based designs, the three-piece shield worked better than a four-piece because of the cutouts needed for the six jack stands. With the elimination of the RTGs and the jack stands supporting the cone in the previous concept, the truss structure design has been simplified, and a new symmetry will emerge.

The shield shell encloses the insulation foam that provides the thermal protection for the spacecraft below. The shell encapsulates the foam, providing contamination protection. Should the launch environment generate any particulates from the foam, they will be captured by the pan and lid. The side of the shell is angled so that the Sun, at closest approach, does not impinge on the side of the shell. The angle also keeps the spacecraft body from viewing the side of the shell, simplifying the radiative heat transfer between the shell and spacecraft. This angle is an important part of the thermal control of the shield. The temperatures on the front surface are conductively tied to the side surface, which is free to radiate to space. This heat loss from the side wall reduces the bottom edge temperatures enough to be locally cooler than the rest of the bottom surface.

Coating. The Solar Probe+ shield design includes an optical coating on the forward-facing surface. The specific requirements for that optical coating include the following:

- Optical properties—ratio of solar absorptivity to IR emissivity, $\alpha/\varepsilon < 0.6$
- Resistance to radiation damage—inert to radiation damage including proton and electron bombardment and extreme ultraviolet (EUV) exposure
- Chemical stability—thermodynamically stable in the mission environments
- Charging—no impact to spacecraft or instrument operation or disturbance of local plasma environment
- Structural properties—able to maintain structural integrity after surviving launch vibroacoustic loads, temperature extremes (273 to 1700 K), and temperature cycling
- Particulate impact—able to survive solar wind particulate impact with minimal degradation to optical–thermal performance

Because the temperature of the shield is driven by its optical property, even using bare C-C requires that these properties be defined. Because of the importance of coatings on system temperatures, our inability to test these coatings in a flight-like environment, and the uncertainty in the effect of the mission environments on the coating, a factor of safety of 2 has been used for the optical properties. Generally, the measured values of α/ε have been in the 0.2 to 0.3 range, making the design requirement 0.6. While both the measurements and the margin will be reviewed over the course of the program, the present limit of 0.6

represents an achievable and conservative requirement on a critical design parameter.

As part of the TPS Risk Mitigation effort, two potential ceramic coatings were found that met the requirements of the Solar Probe+ mission. Ceramic materials that are visibly white generally provide the optical characteristics compatible with the proposed shield passive thermal management strategy. These characteristics are low solar absorptivity and high IR emissivity. Thermodynamic stability and chemical compatibility with C-C are additional differentiators that further narrow the list of candidate ceramics. At the end of the study, both aluminum oxide (Al_2O_3), commonly called alumina, and pyrolytic boron nitride (PBN) were found to notionally satisfy these basic characteristics.

During the Risk Mitigation Study, both coatings were subjected to testing that ensured their viability when exposed to environmental extremes beyond those required for the Solar Probe+ mission. Testing was done to demonstrate thermodynamic stability and to ensure a strong interface with the underlying C-C substrate. Optical property performance was successfully demonstrated through coupon testing after exposure to vacuum, temperature, and radiation environments. Coating mass loss and chemical interactions were characterized over temperature. The impact of the application process on adhesion also was investigated. Finally, the effectiveness of nondestructive evaluation techniques in finding coating defects was explored.

Insulation. The main insulating material in the shield is a 15-cm-thick layer of reticulated vitreous carbon (RVC) C-C foam. RVC insulation is an open-pore foam of pure carbon. It has very low density and can withstand very high temperatures. The foam is manufactured in 2.5-cm-thick sheets that are cut into the various shapes needed to fill the required volume. The foam packing configuration is designed to eliminate thermal shorts; i.e., nowhere in the TPS will there be joints between foam pieces coincident through all of the layers. Testing is planned to determine whether the foam sheets can be bonded together or whether an interstitial carbon felt is required. The target temperature for the bottom of the TPS is 350°C. The thickness of the foam is driven by both the surface temperature and the allowable heat flow through the shield.

Heat transfer through the C-C foam is a combination of conduction through the carbon structures and radiation across the empty spaces. At low temperatures, conduction dominates and the material conduction is nearly constant with temperature. At higher temperatures, radiation dominates and the effective material conduction rises rapidly with temperature. The thermal conductivity of the carbon foam has been measured, and a temperature-varying thermal conductivity is used in the analyses. The thickness of the sunshield has been kept at the value from 2006 the Risk Mitigation Study. Similar front surface temperatures, coupled with the uncertainties in the shield performance, form an argument for the present design to be kept "as is" until the system can be tested. As part of the TPS development effort, a representative section of the shield will be built and tested. Based on these results, the shield thickness will be reassessed. Because this testing is planned to be completed by preliminary design review (PDR), the mass savings resulting from a reduced shield thickness will be available to be used elsewhere in the Solar Probe+ system.

Thermal Protection System Supports. The supports that connect the TPS to the spacecraft need to be thermal isolators to protect the spacecraft bus from the high temperatures of the shield. Because the temperatures at the base of the sunshield are expected to be below 350°C, titanium flexures can be used to support the entire shield. These flexures transfer the mechanical loads to a truss system supported off the spacecraft bus. The titanium flexures also provide an additional thermal resistance, so temperatures at the top of the

truss supports are beneath 300°C. At these temperatures, normal composites can be used to reduce the mass of truss members.

In the Risk Mitigation Study, a trade was made of potential truss materials. The materials examined were high-temperature composites, C-C, titanium, and AlBeMet. The results of that trade show that composites are the best option. C-C has a slightly lower density and could be higher strength. However, the uncertainty in the cobonded joints and material properties make this material higher risk. Titanium has very good strength but almost doubles the mass. Finally, AlBeMet has good strength and mass capabilities but is disqualified by the higher heat leak because of its large thermal conductivity.

Structural Analysis. The Solar Probe+ TPS design meets all the stiffness and strength requirements. The elimination of the primary shield and jack stands greatly simplifies the design from the earlier Solar Probe studies. The structural analyses from those studies with respect to the secondary shield has been updated for the Solar Probe+ design. A key result from that earlier work is the requirement that all highly loaded C-C joints are bolted. Cobonded joints have been shown to be problematic but will continue to be evaluated. All highly stressed joints use conventional materials such as titanium and carbon fiber/polyimide with metallic fasteners.

As part of the detailed Solar Probe+ design effort, the analysis of the TPS finite element model under comprehensive thermal profiles will be made. This analysis is required to assess the stresses induced in the different parts of the structure caused by coefficient of thermal expansion (CTE) mismatch. Vibroacoustic analyses will be performed with the TPS finite element model to verify that current design loads are not exceeded. Broadband acoustic loads on the sunshield are required to assess coating adherence and C-C matrix integrity. A comparable level of detailed analysis will be performed on the truss after the material down-select process. Detailed truss analyses will be performed to optimize cross-section stresses and weight. The truss finite element model will be validated with static tests of a single truss under limit loads predicted from the TPS finite element model.

A key part of the structural design is the fact that the driving load case is the launch environment. Because this case occurs at ambient temperatures, the TPS design is testable.

Thermal Analysis. The TPS Risk Mitigation Study thermal design and analysis has been updated for the Solar Probe+ configuration and shows the TPS can meet all of its thermal design requirements. Temperatures and spacecraft heat flows are well within their limits. All key thermal design drivers have been simplified and addressed satisfactorily. Enough options continue to be available to adjust the design in the future, if unforeseen contingencies make that necessary.

The key issue with the thermal design is verifying the performance of the shield in its operating conditions. With its very low thermal conductivity, the effectiveness of the insulation is particularly sensitive to variations in the material properties, thermal shorts, and spaces between the foam blocks. System sensitivity to perturbations in all of these items will be included in the detailed thermal analyses of the TPS. As noted above, the design approach ensures that the heat flow through the shield is well below the required value. That fact, coupled with the incremental approach to the Sun, ensures that the TPS performance will be well characterized before the Solar Probe+ closest approach. As part of the developmental testing program for the TPS, a prototype shield section will be built up and tested.

As part of the work done in the Solar Probe STDT and TPS Risk Mitigation studies, much of the needed materials property work has been started. The thermal stability of the foam has been measured up to 2000 K. Two companies made thermal conductivity measurements at high temperatures. It was found that

just measuring the conductivity of the foam was very complicated. One of the normal approaches used did not work well because of the inability of the test plates to remain in contact with the foam without damaging it. Data was obtained by using an alternative approach, which will be repeated during the flight program. Alternative insulation materials, such as the aerogel infiltrated carbon foam (AICF) were identified that have a lower thermal conductivity but a higher density. The combination may allow a thinner shield, reducing the overall TPS mass. Many C-C, thin-shell property measurements have been made. The test methodology for making these measurements has been developed and will be used as part of the flight program material test program.

Trades. The following are the trades that are planned in Phase A of the Solar Probe+ study. These trade studies will be undertaken to develop options for saving mass and increasing reliability in the overall system.

Micrometeoroid Protection Layer. The spacing, thickness, and protection of the micrometeoroid protection layer will be analyzed by the University of Texas, El Paso. They were a part of the earlier studies, and they will update the dust model for the new trajectory and perform the micrometeoroid protection analyses.

Pan-Cover Connections. The number, configuration, and attachment of the connections between the shield pan and the top cover will be defined.

Layered Insulation Materials. The Solar Probe+ design assumes that the insulating foam is all carbon. There may be options to save mass by moving to lower-temperature materials near the bottom of the shield.

Bottom Side Surface Emissivity. A high emissivity [no multi-layer insulation (MLI)] design is the baseline approach. This study will look at potential savings through the use of low-emissivity coatings or high-temperature MLI on the bottom of the shield.

Flexure Support Details. The baseline design includes three titanium flexures on each of the six truss elements. The number, configuration, and material of the flexures supporting the shield from the truss elements will be defined.

Truss Design. The truss design will be examined as part of the spacecraft bus design study. The trade study will include the heat leak to the bus from the TPS, the mounting of the TPS, and a function of truss material, numbers of elements, and their configuration.

3.6.3. Thermal Protection System Development Program

The TPS development effort is aimed at reducing the risk associated with the Solar Probe+ TPS by performing a design, fabrication, and testing cycle early in the program. This section describes the development of the Solar Probe+ TPS. There are three broad steps. The first step is the analog and coupon testing necessary to provide the basic engineering information needed for the TPS design. The second step is the development of full-size system prototypes. Finally, the last step is to build the spare and flight units and integrate them into the spacecraft.

3.6.3.1. Coupon and Analog Testing

The Solar Probe+ TPS will include the first use in space of a variety of C-C and insulating materials. Although no new development of any materials is required by the program, the existing materials do not have the large databases of material properties needed for design purposes. Furthermore, some of the design questions involve applications where material property data are inadequate to provide the full design performance of the system. In these cases, analog testing is done on representative structures to get specific design information.

3.6.3.1.1. Material Test Program

C-C Coupon Testing. The Solar Probe+ will include a material test program to produce specific mechanical property measurements on the C-C structural materials being used in the design. The Risk Mitigation Study, along with several external databases, has collected some mechanical properties for thin-shell C-C and

high-modulus materials. The Solar Probe+ coupon test program will build on these efforts and produce material coupon test data for all C-C materials used in the design. Some high-temperature material property testing will be done.

Insulation Testing. It is difficult to make thermal conductivity measurements at the high temperature needed for the Solar Probe+ mission. Some testing has been done of the baseline carbon foam. That testing effort will be extended to carbon aerogels and AICF. Testing will include material CTE and thermal conductivity over the range in temperatures from 200 K to 2000 K.

3.6.3.1.2. Analog Element Testing

Flexure Interface. Support for the sunshield comes through the titanium flexures into the C-C shell. The local area of the shell will have to be reinforced to provide the local strength needed in the C-C laminate. This joint will include a variety of complex failure modes, so an analog test is the best method to verify the design in the early stages of the program. A full-size section of the flexure and shell will be built up and strength tested to verify the load path from the top of the flexure into the C-C shell.

Cobonded Joints/Carbon Bolts. Some parts of the C-C structure pieces require attachment with fasteners. The use of metallic materials at these high temperatures is complicated by the CTE differences. Metallic fastener designs that use flexible elements will be developed during Phase A. Other options that do not involve the use of different materials will be evaluated in Phase A. Two such options are available for C-C.

The first is a cobonded joint where the two C-C pieces are built separately and then carbonized together during processing to produce a functional bond. The capabilities of the resulting bond joints depend greatly on the specific joint configuration and the particular load directions. To verify the capabilities of the joint, a full-size analog test item is built and structurally tested. By combining test data and structural analyses of the test item, the "as delivered" capabilities of the joint can be determined and included in the analysis of the flight system.

Alternatively, C-C bolts can be used as an attachment method. Some C-C bolts have been tested already in the Risk Mitigation Study but have been shown to have very poor performance. Some of the failures have been traced to the bolt head design. Alternatives such as the Starfire bolts were not tested because of schedule limitations. However, the availability of a C-C bolt with a significant strength capability would provide a valuable option in the design of large C-C structures.

Carbon Foam, Interstitial Material. The carbon foam insulation provides the primary thermal block in the TPS. To function correctly, the foam must be packaged in a way that limits thermal shorts and prevents foam abrasion during testing and launch. To accomplish both these goals, analog testing of the assembled foam is planned. A vibration test of the packaged foam is planned to ensure that the interstitial material used is optimized for the sunshield. The issue to be defined is the minimum mass than can provide the required protection during vibration testing.

3.6.3.2. Prototype Development

Prototype shield development is aimed at bringing the TPS to a technology readiness level (TRL) of 6 by the system PDR. To accomplish this goal, two parallel development projects are planned. The first effort is to build and mechanically test a full-size TPS. The second is to build and thermally test a shield segment. The dual approach is based on the limitations of the available test facilities and the fact that the driving mechanical and thermal design cases are different.

Shell Prototype Development. The shell development brings the TPS to a TRL of 6 by building and testing a full-size prototype shield. A complete TPS will be subjected to vibration and acoustic testing at room temperature. This testing will verify that the me-

chanical design of the TPS is adequate to survive the launch environment. The test also will be used to correlate the associated analytical models. This work will be completed by the program PDR, allowing any design modifications to be incorporated into the flight units. Both APL and Goddard Space Flight Center (GSFC) have test facilities that are capable of supporting this developmental testing.

Shield Prototype Development. The second of the developmental prototypes is used to verify the thermal performance of the shield. This unit is aimed at verifying the protection the shield will provide during the closest approach to the Sun and the resulting heat leak to the spacecraft. The configuration is required to include only a representative section of the shield because there are no test facilities presently capable of taking the entire shield front surface to the required temperature via an applied radiative heat flux. As noted above, in flight, there will be ~4 MW incident on the shield's front surface.

There is a test facility at Johnson Space Center (JSC) that is used for thermally testing the Space Shuttle surfaces protected by insulating tiles. The facility includes a "hot wall," ~30 in. square, inside a vacuum chamber. The limited size of the hot area requires a section of the shield be built as a test specimen. The test section would contain the C-C pan and cover, including an edge section. Several foam packing approaches would be included. The test unit would include truss and spacecraft bus simulators that would allow the heat flow through the test item to be measured

As with the mechanical prototype unit, the thermal testing would be completed and the test data correlated with the analytical models by program PDR. This timing of the prototype unit would allow any design updates to be included into the flight designs.

As part of the planning for the developmental testing, a discussion was held with the Mars Science Laboratory TPS team to review their testing efforts. The bulk of their high-temperature testing has been aimed at defining the ablation parameters and quantifying material erosion. Testing was performed by using arc jets in a high-enthalpy flow field. They also used the Sandia Solar Tower for testing the radiation transmission of TPS coupon materials, but they have not tested the TPS there. The consensus was that it will be extremely difficult, if not impossible, to subject the full-size probe to heating on the order of 100 W/cm^2. The best option would be to use a radiant lamp facility, such as the ones at NASA JSC or NASA Dryden, as described in the preceding paragraph.

3.6.3.3. Spare and Flight Shield Fabrication, Assembly, and Testing

Directly after PDR, the final design effort for the TPS would begin. Because of the long lead time for the fabrication of the C-C parts, the final design is required before critical design review (CDR). The TPS plan includes spare and flight units to be designed, fabricated, assembled, and tested in a sequential manner. By sequencing the two builds, the first unit acts as a pathfinder for the second. However, the overall schedule does not allow the two builds to be in done in series. Therefore, the lessons learned during the first build will be more in the fabrication, assembly, and testing areas. The first build will be important in trying out procedures and facilities.

During spacecraft-level testing, a shield simulator is required to support the thermal vacuum testing of the spacecraft bus. As noted above, it is not possible to take the entire shield to temperature in any existing test facility. Therefore, a shield thermal simulator will be designed and built that will represent the temperature predicted on the bottom surface of the shield. The spacecraft test will verify the performance of the bus thermal control system in the presence of the shield environment. The capability of the shield to produce those temperatures will be verified by the "hot-wall" testing at JSC.

3.7. Thermal Control System

3.7.1. Spacecraft Bus

3.7.1.1. Requirements

The spacecraft bus is required to operate between 0.044 AU and 1 AU, with protection from the Thermal Protection System (TPS). The spacecraft is broken up into eight thermal zones, which include the bus, battery, high-gain antenna (HGA), star trackers, TPS, primary solar array, secondary solar array, and secondary solar array cooling system. The temperature ranges listed below are both operational and survival: they must be maintained throughout the Sun distances listed above and a mission duration of 7 years. The orbit period during the closest approaches to the Sun is approximately 88 days.

Because the propulsion system is an integral part of the bus, the bus temperature limits are 20°C to 40°C. All bus components (including the instrument interfaces) will be held to these temperature limits with the exception of the battery, HGA, and star trackers, which will be independently controlled. The battery temperature limits are 5°C to 30°C, the HGA temperature limits are –90°C to 250°C, and the star tracker temperature limits are –20°C to 60°C.

The primary array temperature limits are –90°C to 180°C. These arrays will be tilted off the Sun at closer solar distances in order to limit the incident solar flux. At 0.25 AU, they will be retracted inside the umbra and will stay in the shadow until the spacecraft reaches 0.25 AU again, at which point they will be redeployed. This sequence will occur during every orbit in order to provide the necessary power to operate the bus and limit the required battery size.

The secondary solar cells will be on a paddle that (starting at 0.25 AU) is retracted as the spacecraft gets closer to the Sun, in order to maintain as constant a solar flux and power output as possible while attempting to maintain the cells below 100°C. In order to maintain them below this temperature, a heat exchanger and mechanical pump loop will remove heat and transfer it to radiators solely designed for this purpose. The cells will remain exposed to the Sun at all times when the spacecraft is outside 0.25 AU, in order to limit their cold temperature to above 20°C. The cooling system is designed to maintain the cells within acceptable temperature ranges at all times. It will consist of the heat exchanger, mechanical pumps, tubing, radiators, and heat pipes. There will be a valve in the pumped loop system to keep the fluid out of the radiator during the cold case, which will keep the fluid from freezing and reduce the required heater power.

3.7.1.2. Thermal Protection System Interface

The spacecraft must keep the TPS pointed toward the Sun at all times but is allowed to roll as needed. The TPS interface with the bus will be at the end of the truss structure that is used to support the TPS from the bus. The TPS has a requirement to have no more then 50 W of heat flow to the spacecraft bus from the combination of radiation and conduction. The interface has been designed to minimize the transition structure assembly (TSA) conduction from the TPS into the bus. The bus and TPS also will include blanket "blockers" in order to reduce the radiation interchange between elements as much as possible. The items supported by the TSA must be mechanically supported but thermally isolated from the truss system. The attachment scheme will require a detailed analysis of the trusses to determine the truss temperature at the mounting location. This temperature will have the biggest influence on the material chosen for the isolation system. Preliminary temperature estimates indicate the industry-standard carbon fiber cyanate ester materials have sufficient high-temperature strengths at 230°C. Newer polyimide matrix composites are available if design trades indicate a lower mass system can be achieved by reducing the amount of thermal isolation available in the titanium flexures.

3.7.1.3. Block Diagram

Figure 3.7-1 shows a preliminary block diagram of the thermal subsystem, including all thermal hardware. All hardware depicted in

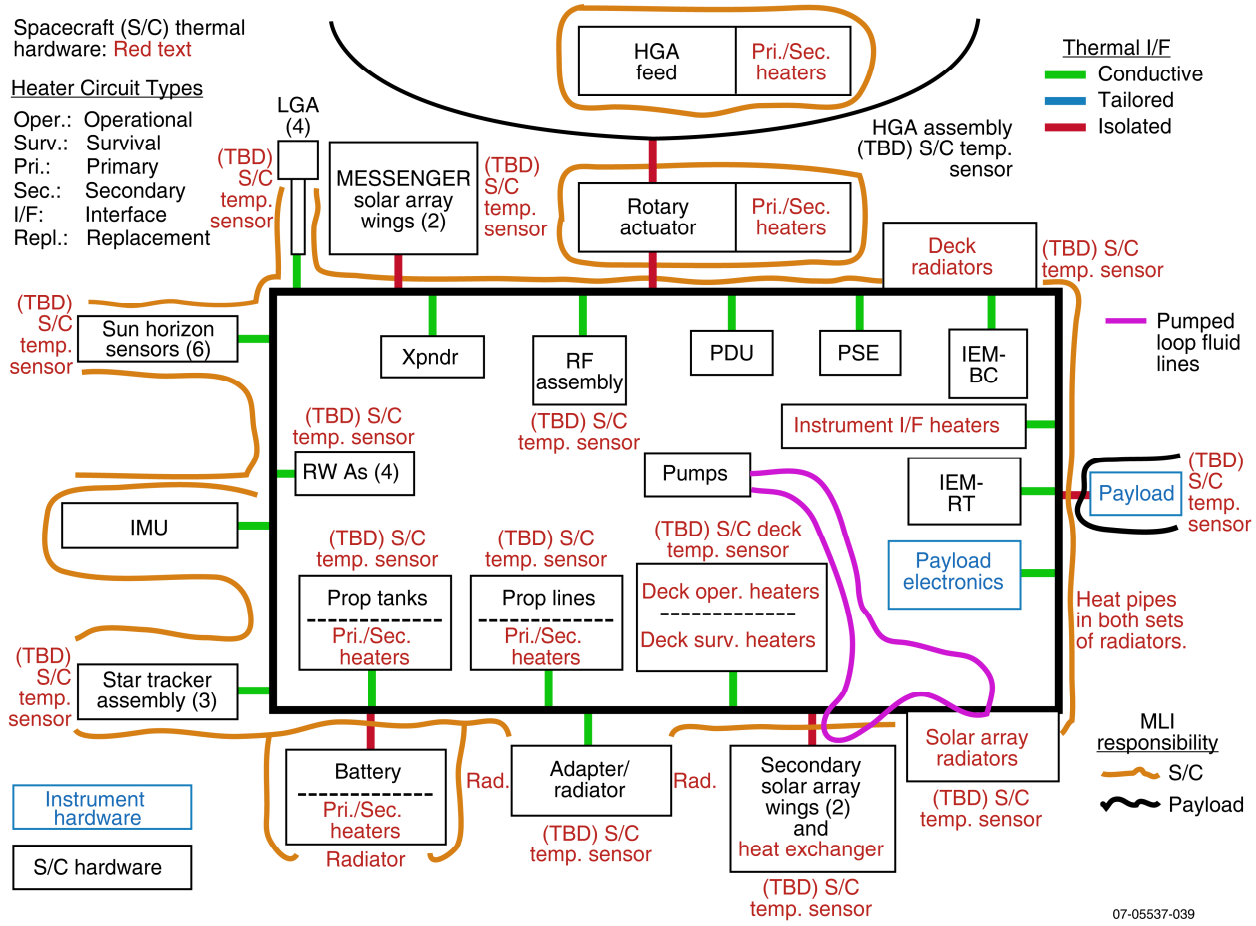

Figure 3.7-1. Thermal control system block diagram.

red is considered thermal hardware. This includes all temperature sensors, heaters, multilayer insulation (MLI), heat pipes, radiators, heat exchangers, mechanical pumps, and tubing. The thermal interfaces for all components (conductive or isolative) and blanket requirements also are shown. The component placements are not representative of the actual placement on the spacecraft.

3.7.1.4. Thermal Analysis

A worst-case hot and cold thermal analysis has been completed on the bus. This analysis determined the sizing of radiators and required heater powers and is summarized in Table 3.7-1 and shown graphically in Figure 3.7-2. The table and plot show that in order to maintain the bus temperature below 40°C in the hot case, the bus requires at least 0.64 m^2 of radiator area. With that much radiator area, in order to maintain the bus temperature above 20°C in the cold case, the overall power in the bus cannot go below 270 W, meaning that when the bus power is below 270 W, heaters must be turned on to maintain 270 W in the bus at all times. The baseline currently has a mini-

Table 3.7-1. Spacecraft bulk temperature (°C) as a function of heat into the bus.

Heat Source	Baseline	
	9.5 R_S	Cold Case
Electrical Dissipation	300	170
Strut (Conduction)	4.0	0.0
Strut (Radiation)	6.1	0.0
TPS Through Bus Sides	4.0	0.0
TPS Through Top MLI	10.0	0.0
PWI	19.0	0.0
Heater Power	0.0	100.0
Total	343.1	270.0
Spacecraft Bulk Temperature	38	20

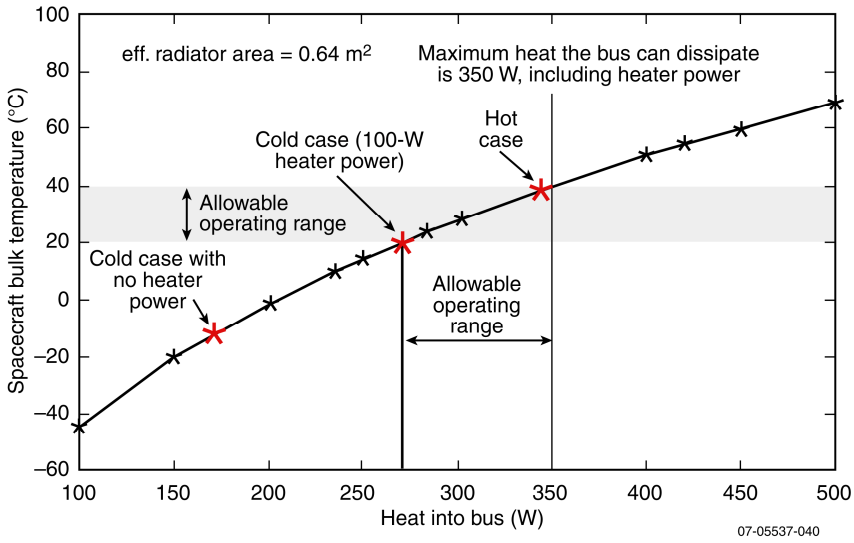

Figure 3.7-2. Spacecraft bulk temperature as a function of heat into the bus.

mum bus power of 190 W, and therefore the maximum heater power required is 80 W.

As stated above, the required radiator area is 0.64 m^2. In order to reduce the heat load from the TPS into these radiators, they will be placed as low on the bus (away from the TPS) as possible. Once all components are placed and the TPS final design is completed, the heat load from the TPS and the instruments will be analyzed again, and the final radiator size and placement will be determined.

The electronics box placement inside and outside the spacecraft will depend on box footprints, field of view (FOV), and thermal criteria. All the high-powered electronics should be placed as close to the radiator as possible and may need either doublers or heat pipes to spread the heat evenly into the radiator. The battery will have its own radiator and will be controlled separately from the rest of the bus. The star trackers also are independently controlled from the bus and will have their own heater power.

3.7.1.5. Instrument Interface

The instruments will be conductively tied to the bus with an interface temperature range of 20°C to 40°C. The only instrument expected to input to the bus any heat attributable to solar exposure is the plasma-wave instrument (PWI) antennas. The antennas will stick out of the umbra into the sunlight and will heat up to approximately 1500°C at the hot end. The antennas are designed in order to have a long distance inside the umbra before reaching the bus, which allows them to cool to close to bus temperatures before reaching the bus and therefore limits the heat conducted into the bus. The long distance to the bus also limits the amount of radiation from the hot end into the bus radiators (which are near the bottom of the bus, close to the mounting location of the antennas). The current calculations show that the three antennas will input ~19 W total into the bus in the hottest case.

3.7.1.6. Trades

One possible trade study to be conducted in Phase A is an optimization of the secondary power array temperature control through moving a part of the TPS structure instead of moving the secondary solar array. This move would eliminate the need for flexible hoses in the cooling system, but it also would require a mechanism that could work at 1500°C. Because of the complexity of any mechanism at such an elevated temperature, the moving array panel was chosen as a baseline but further studies will be completed.

Another trade study still to be completed involves the working fluid in the secondary solar panel cooling system. Ammonia was baselined, but other fluids will be studied to determine the best solution. The study will look at heat capacity and operating temperatures among other factors like corrosive properties and chemical interactions with the pipe material.

A third trade study involves the material for the secondary solar panel cooling system radiator panels. The current baseline is heat-pipe-

embedded honeycomb panels with aluminum face sheets. The trade study will look at composite, AlBeMet, and solid aluminum radiators. A composite radiator was flown on the Compact Reconnaissance Imaging Spectrometer for Mars (CRISM) instrument on the Mars Reconnaissance Orbiter (MRO) spacecraft. It was able to save a factor of over 3.5 on mass over the aluminum alternative. The directionality of heat flow sometimes presents challenges for interfacing with composite radiators, which could to be problematic in the current Solar Probe+ configuration because of the mechanical pump loop interface (although further definition of the interface still is needed). AlBeMet has higher thermal conductivity and specific heat than aluminum and therefore is the thermally preferred choice between those two. However, AlBeMet is heavier then aluminum and health hazards involved in working with beryllium may make this approach less effective than aluminum.

3.7.2. Primary Solar Panels

The primary spacecraft solar panels are based on the MESSENGER high-temperature solar array panels. The panels have a 33% packing factor in order to survive at higher solar flux. This means that the substrate surface contains 33% solar cells and 67% optical surface reflectors (OSRs). The arrays will be tilted off the Sun as the Sun distance decreases, which will allow the temperature to remain below the 180°C temperature limit for the array. An analysis was completed to determine if a different packing factor could be used to allow MESSENGER-like arrays to get closer to the Sun, but the increased mass because of the larger solar arrays (and the fact that they could not reach 0.044 AU, meaning some form of secondary power generation still was required) made this a nonviable option.

It will be possible to use these arrays in to 0.25 AU, but past that solar distance they would get too hot and therefore have to be retracted and stored within the umbra. At the present time, it is believed that the array can be tilted to approximately 75° off the Sun and still get power off the arrays (the MESSENGER arrays have produced power up to 74° off the Sun). A primary panel test bed is planned and will be used to test the tilt angle at which the arrays will no longer produce power.

3.7.3. Secondary Solar Array

A secondary solar array will be used to generate the power needed for the spacecraft when it is in close to the Sun (from 0.25 AU to perihelion and back to 0.25 AU). This solar distance was chosen because, as stated above, the current state-of-the-art solar array technology (the MESSENGER spacecraft) is capable of withstanding solar fluxes up to 0.25 AU (the MESSENGER arrays have already survived solar distances of 0.33 AU).

A knife-edge extension has been added to the TPS shield structure in two places. There will be one secondary panel under each knife edge. Both the knife-edge and secondary array panel radial and axial positions have been designed so that, at 9.5 R_S, one row of exposed cells will see half of the solar disk, which cuts down the solar flux hitting the panel by almost a factor of two and allows the cooling system to reject the heat. The secondary panel will use high-intensity solar cells, which are similar to those used for Earth-based concentrator array applications and will be qualified for use in space with an extensive test program planned for Phase A. The cells will be cooled with a mechanical pump loop to transport the heat to radiators with heat pipes in them to further spread the heat. Each secondary panel will have its own mechanical pump and pump loop as well as 1 m^2 of radiator area split into three separate panels.

The solar cell stack-up will be a critical area in this design because of thermal gradients built up through the different layers and the maximum allowable temperature of the cell, which is 100°C according to the manufacturer. A test program will be put in place to determine the actual maximum temperature for the cell as well as the efficiency at that temperature. The baseline stack-up is a triple-junction solar cell

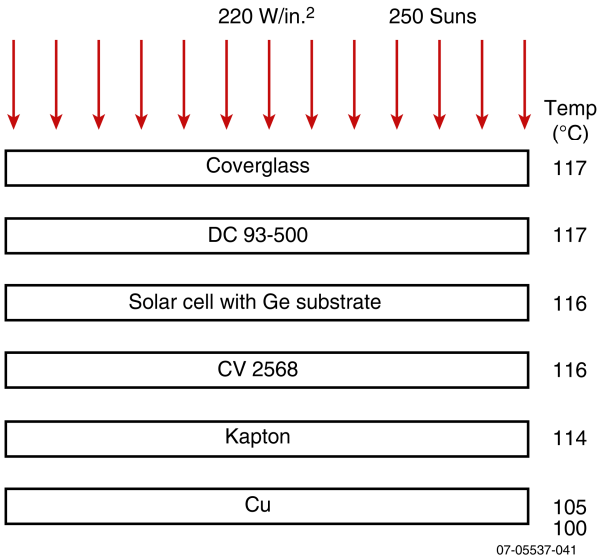

Figure 3.7-3. Baseline solar concentrator cell temperature stack-up.

with a germanium substrate, Kapton, cell, and coverglass (with adhesive in between layers). Figure 3.7-3 shows the expected Solar Probe+ temperature difference through the baseline stack-up.

A test setup will be created to test other possible cell stack-ups to determine which one will result in the lowest cell temperature and the lowest temperature difference through the stack. This test setup will be exposed to solar illumination at various levels to determine thermal gradients in both the 1-AU case and the 0.0443-AU case. Also, a subcontract is planned with one of the manufacturers of this technology for terrestrial applications in order to use their expertise in the design and qualification.

Another critical area is the cooling system, which will be composed of the heat exchangers underneath the cells, mechanical pumps, flexible hosing, and multiple radiators with embedded heat pipes. The current baseline for the heat exchangers is copper because of its coefficient of thermal expansion (CTE) match to the cell substrate and its thermal conductivity. Other materials are being considered in order to reduce mass. The leading candidates are currently AlBeMet and aluminum.

The heat exchangers will have channels or pipes under each string of cells through which the fluid from the mechanical pump will pass to remove the heat. The fluid then will go through the radiators to be cooled and back to the pump. The current baseline for the fluid is ammonia, although many other fluids will be looked at in the next phase to determine the best possible solution.

To ensure that the concept works as expected, the heat exchanger system will be built up into a solar array substrate fluid test bed. This test bed will be used to ensure that the design can get the heat out of the solar cells and into the fluid without a large temperature difference. It also will be used to determine the fluid flow rate required to keep the thermal gradients between cells in the same strings as low as possible.

The mechanical pumps that have been chosen for the baseline are built by Pacific Design Technology (PDT) and have heritage from the Mars Exploration Rovers (on which they have been working for several years). There also is a life test ongoing at PDT in which the pumps have been operating continuously for 5.5+ years. A development plan would be put in place to develop the system required for Solar Probe+, and a life test would be put into place. PDT also will be consulted in the determination of the fluid and the fluid line lengths to ensure that the pumps can handle the load.

Flexible hoses currently are a part of the baseline design. The flexible hoses are required because the secondary solar panel must be retracted as the spacecraft gets closer to the Sun. An extensive test program is planned to ensure that the hoses will work in all different configurations and over the required number of cycles.

As stated previously, the radiators currently are heat-pipe-embedded honeycomb panels with aluminum face sheets, but other materials, such as composite, AlBeMet, and solid aluminum also will be considered. Composite has the advantage of much lower mass but the disadvantage that it is difficult to get the heat into the fibers, unless you can add it to the fiber end, because the across-fiber conductivity

is ~10% or less of the in-fiber conductivity. AlBeMet has a high thermal conductivity and a high specific heat, which make it a better choice then aluminum, but the disadvantage is that it is heavier and there are safety concerns when working with the material.

The radiators will have embedded heat pipes in order to spread the heat and make the radiator more efficient. This network will be designed in order to get the maximum possible heat transfer across the surface for the lowest possible mass. Also, the interface between the pump piping and the radiator will be studied to find the most efficient way to get the heat out of the piping and into the heat pipes.

The final test bed will be a solar concentrator test bed. It will consist of all the pieces of the full system put together to make sure that everything works together as designed. It will use qualification units of hardware and will be built up and tested in a flight-like environment.

3.8. Power System

The power subsystem is based on a peak power tracking architecture using photovoltaic solar array panels for power generation and a lithium-ion battery for energy storage. Two different types of solar arrays are used, each optimized for a different range of distances from the Sun. Power electronics are contained within the power system electronics (PSE) box and the solar array junction boxes (SAJBs). A block diagram of the power subsystem is shown in Figure 3.8-1. A detailed trade study on the secondary solar array concept was performed, and the results are presented in Appendix C.

The power bus voltage is unregulated, and all subsystems attached to the bus will be designed to work between 22 V and 35 V. The actual battery-dominated bus voltage will vary less than these subsystem requirements. The peak power tracking electronics, with flight heritage from the MESSENGER and STEREO spacecraft, isolates the bus voltage from the solar array voltage and maximizes solar array output over the mission's widely varying operating conditions.

Normally, only the primary solar array or the secondary solar array is used as the main

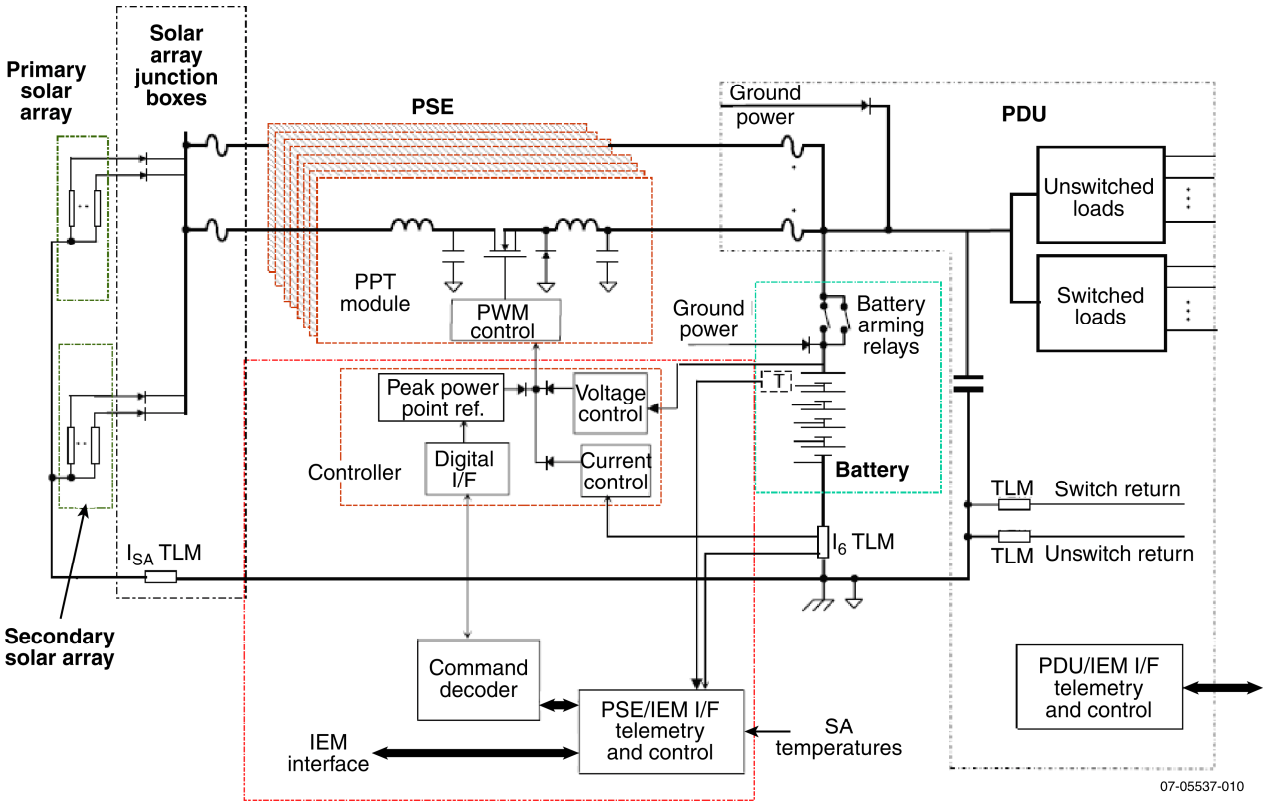

Figure 3.8-1. Power system block diagram.

source of power at any particular time, depending on the distance from the Sun. When the primary solar array is not in use, it is retracted and not exposed to the Sun. The two solar array systems are diode-isolated from each other, and both feed the common set of peak power tracker (PPT) modules within the PSE.

The power subsystem is designed to provide 482 W of power between 0.9 AU and 0.044 AU distance from the Sun. Between 0.9 AU and 1 AU, less power is available. Spacecraft operational requirements in this regime will be reduced primarily by lowering power allocated to the telecommunications subsystem. Sun–probe distance is greater than 0.9 AU only immediately after launch and around aphelion of the first few orbits, so there will be no impact on science return.

The power subsystem is single-fault tolerant. Full redundancy is provided for power control electronics and command/telemetry paths. Subsystem sizing is such that the loss of a battery cell or a string of solar cells would not affect mission performance. The mission requirements would still be met even with a failure of one of the multiple, parallel peak power tracking modules.

3.8.1. Power System Electronics

The power system electronics (PSE) box implements solar array peak power tracking and battery charge control. The PSE provides primary power to the power distribution unit (PDU) and has a serial digital command/telemetry interface with the integrated electronic module (IEM). The PDU and IEM are part of the avionics subsystem. Within the PSE, there are six PPT modules, two PPT controller slices, two command/telemetry interface slices, and battery interface slices. Power bus filtering also is included within the PSE.

Each PPT module contains a pulse-width-modulated buck-topology DC/DC converter and can support up to 90 W at its output. The use of current mode control within each PPT and centralized control (on primary and redundant sides) of all PPTs ensures current sharing among the modules. This approach also allows the PSE to continue functioning, even if one of the PPT modules fails, although with less total output power. The PPT modules and controller design were flown successfully on MESSENGER and the two STEREO spacecraft. The peak power tracking algorithm, proven on those missions, is contained within the IEM main processor. The STEREO PSE is shown in Figure 3.8-2.

07-05537-011

Figure 3.8-2. STEREO PSE.

The battery charge control electronics minimizes stress on the lithium-ion battery by reducing charge current when the battery approaches a high state of charge, based on ampere-hour integration. Also, battery voltage limiting causes the battery current to taper to a low value close to the end of charge. The battery charge control parameters are command-adjustable as a contingency in case of drift in the control electronics or to help compensate for battery aging. Bus overvoltage protection also is provided as an additional control loop.

The PSE box is constructed as a modular slice design, where each slice consists of a printed circuit board housed in its own mechanical frame. The slices are mechanically stacked and bolted together to form the box. The slices are electrically connected by using a wiring harness external to the box for power and signals.

Two SAJBs are used with the PSE. Each SAJB receives power from two solar array wings. One SAJB is used for the primary solar array and the other for the secondary solar array. Each SAJB feeds power to the PSE PPT modules. Included in the SAJB are solar array string isolation diodes and solar array current sensors. The SAJB design is similar to that flown on MESSENGER and STEREO.

3.8.2. Solar Arrays

Solar Probe+ uses two solar cell arrays, each optimized to work over a different range of Sun–probe distances. The primary array is used between 1 AU and 0.25 AU and is based on the MESSENGER solar array design. The secondary array uses high-intensity concentrator solar cells mounted on an actively cooled panel and is used to generate power within 0.25 AU.

3.8.2.1. Primary Solar Array

The primary solar array consists of two deployable, articulated wings. The primary solar array wings are deployed from behind the heat shield and oriented at an angle to the Sun as shown in Figure 3.8-3. As the spacecraft approaches the Sun, the primary array is tilted to maintain the array within flight-allowable thermal limits while meeting spacecraft power requirements.

Each solar panel contains 32 strings of solar cells. Each string has 39 series cells and a string isolation diode. The solar cells are triple-junction, gallium arsenide (GaAs)-based cells with an active area of 12 cm^2, and each cell includes an individual bypass diode. The coverglass is 0.15-mm-thick cerium-doped microsheet, type CMG, with dual antireflective coating. The total active area of cells on all of the solar panels is ~1.5 m^2.

Optical surface reflectors (OSRs) are evenly distributed among the cells at a ratio of two OSRs for each solar cell. This is the same technique that is used on the MESSENGER solar array. As successfully demonstrated on MESSENGER, the use of OSRs and the tilt of the panels help to maintain the primary array solar cell temperature below 180°C, which is well within the temperature range to which this design has been qualified. The MESSENGER solar array is shown in Figure 3.8-4.

The primary solar array wings are retractable by command. At Sun distances less than

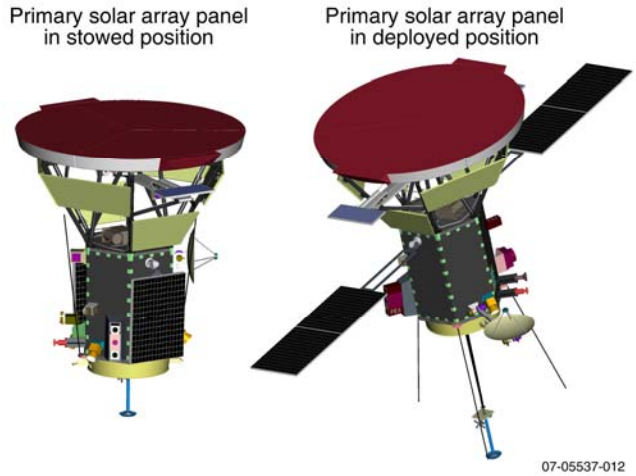

Figure 3.8-3. Primary solar array configuration (both stowed and deployed).

Figure 3.8-4. MESSENGER solar arrays.

0.25 AU, the secondary solar array is used and the primary array must be retracted behind the spacecraft heat shield because of the high temperature.

Although improved solar cells with increased efficiency are expected in the future, the power analysis conservatively assumes a 28% minimum average efficiency (under standard test conditions of 28°C, 1 Sun, air mass zero, beginning of life), as such space-flight-quality production-run cells are presently available and have been qualified and flown. Although the spacecraft performance will benefit from further improvements in solar cell efficiency, it is recognized that any newly developed cells will need to be qualified for the unique environment of this mission. High-intensity, high-temperature testing will be performed on sample solar cells and a non-flight-qualification solar panel. This panel also will be subjected to thermal cycling and electrical performance tests.

3.8.2.2. Secondary Solar Array

Used at Sun distances between 0.044 AU and 0.25 AU, the secondary solar array consists of two small retractable panels. The panels contain a planar array of concentrator photovoltaic cells on an actively cooled substrate that maintains cell junction temperatures below 120°C (see Sections 3.5 and 3.7 for details of the mechanical and thermal designs). The cells on the secondary solar array are designed and optimized for operation at high solar flux, as described later in this section. Each panel is attached to its own linear positioner actuated by a stepper motor. The panels can be completely retracted behind the spacecraft heat shield, extended beyond the shield, or positioned in between in fine increments (a small fraction of a cell width) by command. As the positions of the panels are adjusted, the quantity of solar cell strings exposed to direct sunlight will vary. The amount of exposure is therefore controlled as a function of Sun distance. The quantity of strings that are illuminated is minimized to reduce heat load but sufficient to meet the power requirements. This concept is illustrated in Figure 3.8-5.

A preliminary design of the secondary solar array panels contains 50 parallel strings of solar cells with 27 cells per string and an isolation diode in series. These array design parameters are preliminary and will be updated with data collected during the cell qualification testing described later in this section. A bypass diode is connected in parallel with each cell, and the diodes are located on the back side of the panel. The cell strings are arranged on the panel so that their series direction is parallel to the edge of the heat shield, thus ensuring that all cells within each string will be exposed to approximately the same illumination level, which becomes more important closer to the Sun, where only one or two strings are exposed on a panel and the illumination level on those strings is varied by fine positioning of the panel. The portion of the spacecraft heat shield just above each secondary solar array panel forms a straight knife edge, which improves the uniformity of illumination on the cells within the strings that are in the penumbra between full exposure and the umbra.

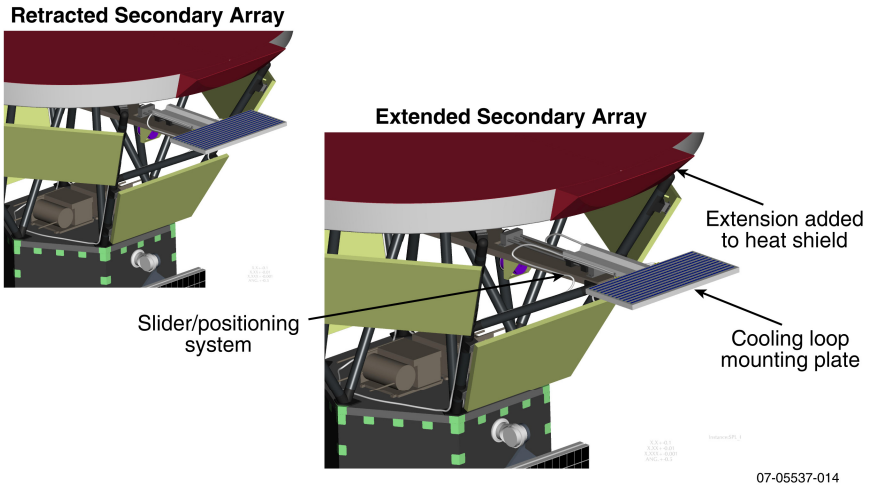

Figure 3.8-5. Secondary solar array concept.

The solar cells used for the secondary solar array

are triple-junction GaAs-based cells optimized for high-intensity illumination and high current density. These cells use the same epitaxial growth as high-efficiency cells with spaceflight heritage. The gridlines and contact metallization is the same as used for concentrator photovoltaic cells, which have been used for terrestrial applications with optics having a very high concentration ratio. Although optical concentration is not being used on this solar array, the close proximity to the Sun results in high flux, which the cell must accommodate. For this application, the illumination intensity varies between 16 and ~250 equivalent Suns. This intensity is well within the range for which concentrator photovoltaic cells have been designed. Characterization tests for concentrator photovoltaic cells have been performed at up to 1000 equivalent Suns.

Each cell has an active "aperture" area of 0.989 cm^2. The cell front-side metallization, dual bus bars, and gridlines are designed to minimize resistive losses to accommodate the relatively high current. Wide electrical interconnects with stress-relief and multiple-welded contact points are used to conduct the relatively high current between cells. OSRs and electrical insulation cover the cell-to-cell electrical interconnects to minimize thermal load.

The coverglass, which is cerium-doped microsheet with dual antireflective coating, is used for radiation protection and optical filtering. Tradeoffs will be performed to optimize the coverglass thickness and type of coating. The thermal effects of the coverglass thickness and filter coating are much more dominant than typical for this application because of the high solar flux and will be studied as part of tradeoffs to determine specifics of the coverglass design.

Under the predicted range of operating conditions, the effective conversion efficiency varies between 13% and 20% with a junction temperature of 120°C, resulting in additional 2259 to 1897 W of thermal energy absorbed by the cells. Effective conversion efficiency was estimated by using a conservative combination of specifications for spaceflight-qualified solar cells and concentrator photovoltaic cells at a 120°C operating temperature. Estimated efficiency included derating for losses caused by assembly, coverglass and coating, ultraviolet radiation, charged particle radiation, and micrometeoroid impacts. The power calculations for the concentrator photovoltaic cells also include a loss factor to account for the difference in spectral characteristics between the terrestrial (air mass 1.5) conditions for which these cells have been characterized and the space environment (air mass zero). In addition, the effect of peak power tracker inaccuracy was included.

At 0.25-AU Sun distance, both secondary solar array panels are almost fully exposed. In addition to the required load power margin, the design includes two extra strings of cells. At closest approach to the Sun of 0.044 AU, the secondary arrays are retracted to expose a total equivalent cell area of 34.04 cm^2.

Although the specific cell design proposed for the secondary solar panels has not been space-qualified, the epitaxial growth is the same as next-generation triple-junction solar cells that have spaceflight heritage on an experimental satellite. These solar cells have low series resistance and are well suited for operation at high intensity. The cell manufacturer has stated that, during 2008, these next-generation cells will undergo spaceflight-qualification according to American Institute of Aeronautics and Astronautics (AIAA) standard S-111.[22] This qualification testing includes temperature/humidity exposure, top and bottom contact-weld integrity, electron and proton irradiation, and accelerated life.

The cell-interconnect-cover (CIC) assembly qualification testing includes electrostatic discharge sensitivity, mechanical strength, and

[22] *Qualification and Quality Requirements for Space Solar Cells*, AIAA Standard S-111-2005, American Institute of Aeronautics and Astronautics (January 2005).

UV radiation effects. Solar cell characterization tests include postradiation current–voltage (*I–V*) over temperature, dark *I–V*, quantum efficiency, thermo-optical properties (absorptance and emittance with cover), and capacitance.

For the proposed cells, to use gridlines and contact metallization as is used for concentrator photovoltaic cells, most of the same cell-qualification tests will be performed. However, it is expected that abbreviated radiation testing can be performed, because the contact metallization should not have a major effect the radiation performance. Sample cells will be radiation-tested under several conditions for verification that the performance matches the full characterization testing performed for the next-generation solar cells.

In addition, a comprehensive test program has been planned to ensure that the cells and related components will withstand the space environment unique to this mission. The test program includes the use of a close-match air-mass-zero-spectrum solar simulator and high-concentration optics with a space simulation thermal vacuum chamber. The solar cells will be tested for electrical performance after exposure to charged particle radiation as a function of temperature and intensity. In addition to cell-level testing, a non-flight-qualification solar panel with multiple strings of cells will be constructed and subjected to thermal vacuum cycling and thermal vacuum balance tests. Structural integrity, thermal gradients, and electrical performance will be verified. At higher levels of assembly, acoustic and vibration testing will be performed.

3.8.3. Battery

The battery has a nameplate capacity of 20 Ampere-hours and contains space-flight-qualified lithium-ion cells. Advantages of lithium-ion cells are their high-energy density, good cycle life, nonmagnetic materials, and successful spaceflight heritage. The battery consists of multiple parallel strings, with each string containing eight ABSL 18650HC cells in series. This modular, parallel string approach for lithium-ion batteries has been successfully flown on many spacecraft, including NASA's five THEMIS spacecraft. It also has been selected for NASA's Living With a Star Solar Dynamics Observatory (SDO; a 12-year geosynchronous orbit mission) and the Lunar Reconnaissance Orbiter (LRO). In addition, this battery type has flown on many European Space Agency spacecraft, including Rosetta (an 11-year interplanetary mission), Mars Express, and Venus Express.

Each cell includes built-in safety features to open-circuit the cell in case of excessive current or high temperature, and the cell and battery designs meet the range safety requirements. The quantity of parallel strings has been selected to provide fault tolerance so that the battery requirements can be met even with a failed string of cells.

Because of the relatively large-scale production runs for this type of lithium-ion cell, their manufacturing uniformity, and the use of computer-aided cell selection and matching, the cells within the battery are very well matched in performance. The vendor has performed lifecycle testing and demonstrated the uniformity and self-balancing of the cells with cycling so that external cell-balancing electronics are not required. If a cell were to fail or have an anomalous voltage divergence, a switch within the cell is designed to open and isolate the string from the others in the battery.

Under normal conditions, the most significant discharge for the battery will be during launch. The battery is conservatively sized so that the depth of discharge (DOD) will not exceed 50%, even if there was no solar array power until the primary solar array panels are deployed and oriented to the Sun. The battery also supports short-term peak loads. In addition, the battery provides a low impedance source to clear a fuse in case of a load current fault. There are no repetitive eclipses expected, and there is no shadowing from appendages under normal conditions.

A nonflight "work" battery is used during initial spacecraft integration and testing (I&T). The flight battery is installed before spacecraft envi-

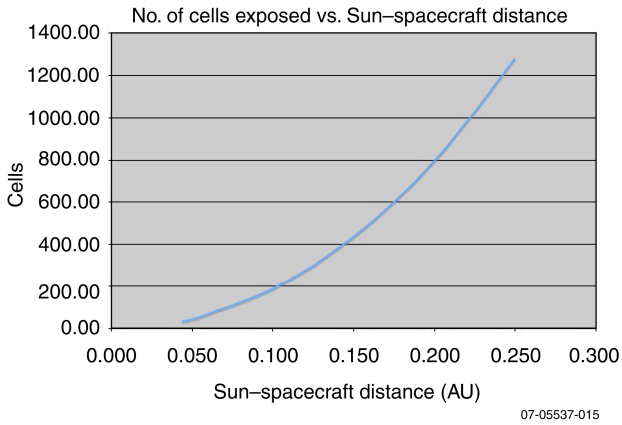

Figure 3.8-6. Solar cells illuminated as a function of solar distance.

ronmental testing. The battery conditioning/test equipment has multiple protective features to meet the safety requirements, and the battery is operated in accordance with the established battery-handling plans and procedures.

3.8.4. Power System Performance

Power analysis was performed taking into account solar array optical, assembly, and wiring losses; temperature effects; degradation due to ultraviolet radiation; and charged particle radiation. The analysis also includes the effects of intensity variations with Sun distance and other power system losses, including solar array string isolation diodes, PPT conversion efficiency, power subsystem wiring, and spacecraft wiring harness.

The power subsystem was designed to provide 482 W of load power between 0.044 AU and 0.9 AU distance from the Sun. The Sun–probe distance is greater than 0.9 AU only immediately after launch and around aphelion of the first few orbits. During these times using X-band rather than Ka-band will reduce power used by the telecommunications subsystem. The amount of data transferred to the ground also will be reduced. However, because the spacecraft spends relatively little time at these greater distances, there will be no impact on science return.

Between 0.9 AU and 0.25 AU the angle of the primary array is adjusted to deliver adequate power to the spacecraft. Inside of 0.25 AU, the primary array is folded into the umbra behind the spacecraft heat shield. As the spacecraft approaches the Sun and illumination intensity increases, the secondary array is retracted behind the shield as needed to expose enough photovoltaic cell area to maintain the desired electrical power output level. Figure 3.8-6 shows the equivalent number of cells on the secondary panel that are illuminated as a function of distance of the spacecraft from the Sun.

3.9. Avionics System

3.9.1. Avionics Suite

The Solar Probe+ avionics system, as shown in Figure 3.9-1, consists of the integrated electronic module (IEM), remote interface units (RIUs), and the power distribution unit (PDU). The IEM contains the main processor and interfaces to instruments and other subsystems. The off-the-shelf RAD750 processor supports commanding, data handling, data storage [using the solid-state recorder (SSR)], and guidance and control (G&C). The IEM is an evolutionary design based on the compact peripheral component interface (cPCI) backplane bus that has flown on MESSENGER and STEREO and is planned for use on RBSP. The standard cPCI bus allows great flexibility in combining appropriate processor, memory, and interface cards.

The Solar Probe+ IEM contains five 6U cPCI cards: a RAD750 CPU, a spacecraft interface card, a G&C interface card, a SSR card, and a DC/DC converter card. The IEMs are block-redundant.

The avionics subsystem also collects analog and digital telemetry via RIUs, which are based on the RIO application-specific integrated circuits (ASICs) flown on several previous missions. These small, lightweight units collect and digitize telemetry points and transmit the data to the IEM using the industry standard I2C bus.

The PDU switches loads and controls thrusters via command from either IEM. The PDU is internally redundant with two field-effect transistors (FETs) in each solid-state switch to ensure that every load can be turned

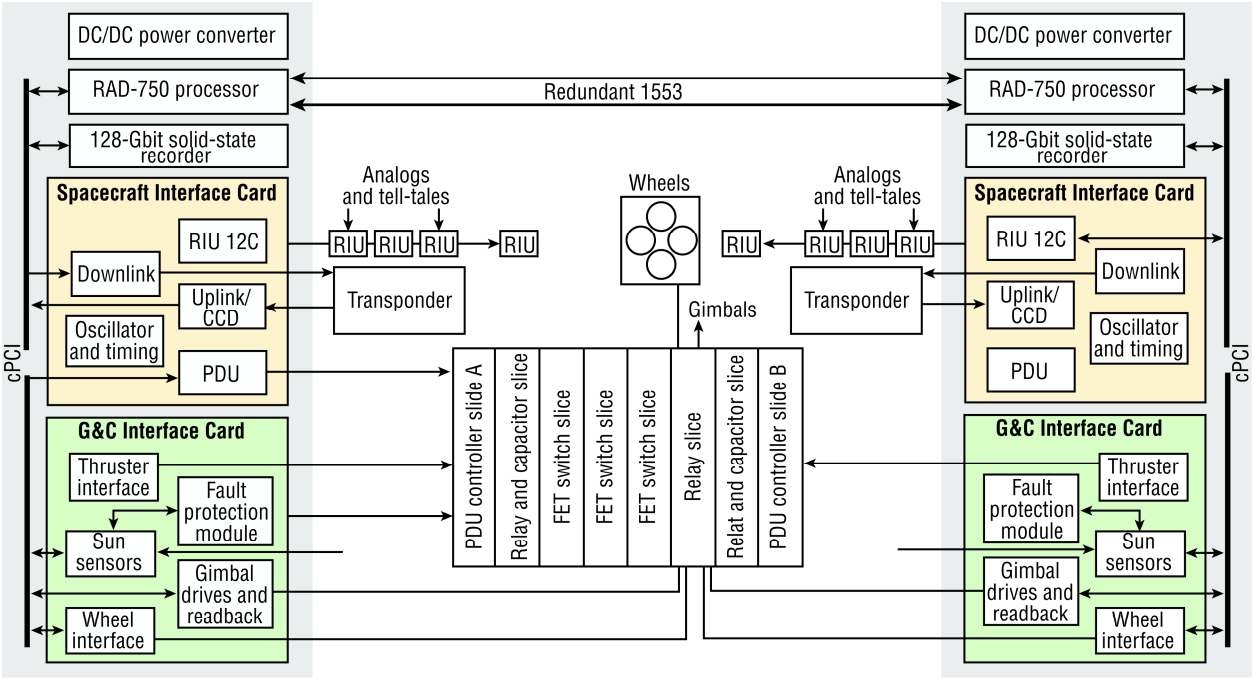

Figure 3.9-1. Avionics system block diagram.

off. The slice-based design from RBSP contains redundant slices for power, command, and telemetry. Slices based on relays and FET switches are stacked as appropriate. FET switches incorporate resetable circuit breakers based on the power remote input/output (RIO) (PRIO) ASIC.

The RAD750 CPU card is an existing design with 16-MB SRAM, 4-MB EEPROM, and 64-KB Fuse Link boot PROM. Various configurations are available, including SDRAM-based configurations that provide significantly more main memory, and can be selected as needed.

The 128-Gbit SSR is based on stacked SDRAM modules. BAE has proposed such a design for several missions. An alternative approach is to use a flash-based SSR based on that of New Horizons.

The spacecraft interface card is the only IEM card that contains the "standard" spacecraft interfaces that are not mission-specific. Much of the design is heritage from previous programs. It contains the critical command decoder, which executes some commands directly in hardware and passes some directly to the PDU. It also contains the PDU, downlink, RIU interface circuitry, backup oscillator, and clock/timing circuitry for the card.

The G&C interface card contains the interfaces to the engineering instruments, reaction wheels, and gimbal drive circuitry for the solar arrays. Also included is the interface to the aft horizon sensors used to detect a fault in attitude control and the fault protection module (FPM) that autonomously switches IEMs in response to the Sun being seen by the aft Sun sensors or other fault conditions. Each IEM contains an FPM, which, on the spacecraft interface card, is powered by unswitched power. The FPM in the "off" IEM monitors health signals from the "on" IEM. When the FPM detects a fault, it follows a decision tree and can command the PDU to switch IEMs. The FPM disables itself after use with a latching relay in the PDU. The FPMs can be enabled or disabled by critical command via either IEM (powered or unpowered) at any time.

3.9.2. Flight Software

The Solar Probe+ command and data handling (C&DH) software has direct heritage from RBSP and significant component heritage from previous missions, including MES-

SENGER, New Horizons, and STEREO. The software is implemented by using the C programming language and makes use of the core Flight Executive (cFE) middleware by NASA Goddard. The flight software system uses the VxWorks™ real-time operating system. This software environment facilitates hosting several concurrently executing software applications on a single processor. The Solar Probe+ flight processor executes C&DH, G&C, and autonomy and fault protection flight software. G&C attitude estimation and attitude control algorithms are implemented as tasks that execute concurrently within a single G&C application. The C&DH flight software is composed of several applications that manage, among other things, Consultative Committee for Space Data Systems (CCSDS) telecommand protocol uplink, downlink, command execution, SSR, parameters, peak power tracking, and the 1553 bus.

Among the two identical flight processors, the selection of the primary flight processor is made based on a discrete signal set by command via the critical command decoder hardware. A second discrete signal selects which one of the two software images to boot for the two flight processors. The primary flight processor acts as the 1553 bus controller and actively controls the spacecraft, performing all G&C, C&DH, and autonomy and fault protection software functions. The secondary flight processor, when powered, boots to a flight software configuration that operates as a remote terminal on the 1553 bus and will record science data to the standby SSR in parallel with the primary flight processor on the primary SSR. In critical phases of the orbit, the secondary flight processor acts as a hot spare in standby mode in the event of a fault in the primary flight processor. As a hot spare, the standby flight processor executes the same G&C application software as the primary flight processor. Attitude information is received by both processors via the 1553 bus from the three star trackers and the inertial measurement unit (IMU). The G&C application executing on the primary flight processor is responsible for attitude estimation and attitude control, while the standby instance of the G&C application is a hot spare. Attitude control of the spacecraft is necessarily limited to the primary flight processor, which is enforced in the 1553 bus application software.

The G&C attitude estimation and control algorithms are developed by using MATLAB Simulink™ models. MATLAB Real-Time Workshop (RTW) is used to generate C code from the Simulink™ models that is then compiled into the G&C flight software application. Several previous missions have successfully used this model of G&C software development.

The primary flight processor C&DH software manages the telecommunications uplink and downlink using CCSDS protocols for data handling. Commands are received in CCSDS telecommand packets and, according to an operation code contained in the packet header, are either processed by the primary flight processor software or dispatched to the other subsystems on the 1553 bus, including the secondary flight processor. The C&DH software supports storage of command sequences, or macros, which can be executed by a ground command, an autonomy event, or a time-tagged command stored in the flight processor's memory.

Instrument housekeeping and science data are routed through a common data processing unit (DPU) remote terminal on the 1553 bus to the flight processor. The DPU compresses and packetizes these data prior to their being sent to the flight processor where the C&DH software manages the storage of the data packets on the SSR in the form of files.

The C&DH software is configured to interleave CCSDS transfer frames of real-time telemetry packets with frames of SSR playback data based on a commandable ratio. SSR playback is managed using the CCSDS File Delivery Protocol (CFDP) software that was successfully used on MESSENGER. CFDP provides a mechanism to downlink files from the SSR by using a "handshake" with the CFDP client in the

ground system software. This protocol automatically manages retransmission of any file fragments lost because of data dropouts without requiring retransmission of the entire file. In addition, file transmissions may be easily suspended and resumed between contacts. The CFDP protocol helps automate contacts by ground stations, which increases reliability and reduces operating costs.

In addition to the C&DH and G&C flight software applications, the flight processor also hosts an autonomy and fault protection application. Data collected from all subsystems are stored in a memory buffer and can be referenced by uploaded autonomy rules to detect and respond to faults. Each rule can monitor one or more telemetry points, perform computations, and execute a specified command if the premise of the rule evaluates "true" for a designated number of consecutive evaluations. Typically, the command is an instruction to execute a stored macro that performs a corrective or maintenance action. This design facilitates the ability to develop, test, and upload autonomy rules without requiring software changes. Not only does this reduce the development cost of the flight autonomy system, but it also provides the flexibility to easily change the system behavior at any point during the mission, which is of particular interest in the event of a component failure or simply to allow operators to adapt as more experience is gained with the operational spacecraft. This system increases reliability, reduces risk, and reduces cost for autonomy system changes. This type of autonomy and fault protection software system has been successfully used on several previous missions.

The C&DH software supports receipt and storage of code, parameter, command, macro, and autonomy rule uploads, as well as downlink of these items or flight software data structures. Additionally, the flight software maintains a number of history logs, event logs, and anomaly logs that may be downlinked to support anomaly investigation. The C&DH flight software system performs health monitoring of the various software subsystems and may initiate a failover to the secondary flight processor in the event of a critical software anomaly. The system also makes use of a hardware watchdog timer that triggers a reset of the processor and failover to the secondary flight processor should the software become unable to service the watchdog timer within a programmed timeout.

3.10. Telecommunications

The design of the Solar Probe+ telecommunications system is driven by several primary requirements. First, the spacecraft remains near the ecliptic plane throughout the mission, which dictates antenna-pointing requirements and establishes the Sun–Earth–probe (SEP) geometry throughout the orbit. Second, the desired science data volume (128 Gbits) and the limited data-return time between subsequent perihelia (spaced ~88 days apart) set a high downlink data rate. Finally, the high-gain antenna (HGA) must remain within thermal requirements during use to maintain pointing and must be protected from temperatures exceeding survival limits at all times during the mission. These requirements ultimately establish the subsystem design and data management strategy to return the required science data. Figures 3.1-3 and 3.1-6, previously presented in the mission design overview, give the SEP angle and Earth–probe distance for the baseline mission.

3.10.1. Trade Studies

3.10.1.1. Frequency Selection

Solar Probe+ assumes use of the DSN 34-m subnet for routine (nonemergency) operations. The DSN 34-m subnet possesses both X-band and Ka-band communications capabilities. With Solar Probe+ remaining in the ecliptic plane, roughly half the postperihelion series of contacts will be on the far side of the Sun (Earth range greater than 1 AU), and the Sun will interfere in downlinks when the SEP angle is small (less than 3° for X-band, less than 1° for Ka-band). Ka-band science links provide an approximately four to five times increase in achievable data rate over X-band (including weather effects) in

the 34-m subnet. This advantage is critical to meeting science return requirements for post-perihelion contacts greater than 1 AU from Earth, with reasonable radio frequency (RF) transmit power levels and HGA diameters. The lower minimum 1° SEP angle limit at Ka-band adds several days of contact time to each post-perihelion series versus X-band operation. To maximize the data return, a Ka-band system is set as the primary science return link. Nevertheless, the advantages of also including a parallel X-band downlink system outweigh the costs: better emergency performance, the ability to utilize the 70-m subnet (which does not have a Ka-band capability), greater insensitivity to weather, greater technological maturity and flight heritage, and a more forgiving pointing requirement for the same aperture size. The Solar Probe+ telecommunications system uses both Ka-band and X-band downlinks. The uplink is at X-band, given the lower data rate requirements needed for commanding.

3.10.1.2. High-Gain Antenna Design

Several designs for the HGA system were considered. The maximum size of the antenna is limited by the size of the umbra, mounting locations along the spacecraft structure, and the pointing mechanism. A Ka-band phased array antenna was considered and but not selected because of its complexity in the number of elements required, its mass inefficiency, and performance losses over the range of required pointing angles. Two leading HGA candidates were considered at length: a body-mounted, shaped parabolic antenna with a single axis of rotation (the spacecraft roll would provide the additional axis), and a mast-mounted, circular parabolic antenna requiring two axes of rotation along with spacecraft roll: one axis to position the antenna outside the umbra and a second axis to point to Earth.

The body-mounted antenna is always in the umbra of the sunshield when the shield is pointed at the Sun. However, the range of possible Sun–probe–Earth (SPE) angles over which this antenna can support a link is limited by the body of the spacecraft, the distance to the umbra, and obscurations caused by the shield. A smaller HGA can point across a wider range, but at a cost in downlink rate capability. For example, with a 0.65-m HGA diameter, the range of possible SPE angles is limited to $38° < SPE < 142°$. Smaller antennas than 0.65 m provide greater coverage in the antisunshield direction but are limited by the shield in the sunshield direction, and they fall off in data rate capability inversely proportional to the square of the diameter.

The mast-mounted HGA extends the antenna out of the umbra and, along with controlling the roll angle of the spacecraft, permits pointing to Earth across all SPE angles (0 to 180°). However, the HGA can only be deployed outside the umbra when the spacecraft's distance to the Sun is greater than 0.59 AU, because of thermal limitations.

Table 3.10-1 charts the idealized data return from each of the HGA configurations for primary perihelia with closest approach at 9.5 R_S. This comparison uses the same assumptions for each HGA design under consideration, for the purposes of determining the best HGA configuration, but does not represent the actual data management for these perihelia. In both cases, a minimum SEP angle of 1° was assumed for Ka-band operation, as was one 8-hour effective pass per day with the DSN 34-m subnet. After the first and second principal perihelia, the

Table 3.10-1. Idealized post-perihelion data volume returned for principal perihelia.

Data Return	Mast	Body-Mounted
Perihelion 1 (worst-case SPE profile)	45 Gbits (1° SEP sets return limit to 40 Gbits)	0 Gbits (SPE always <15°)
Perihelion 2 (SPE < 90°, far side)	109 Gbits (0.59 AU limits otherwise 110-Gbit return)	111 Gbits (0.65-m dish diameter)
Perihelion 3 (SPE >90°, near-Earth return)	>1000 Gbits	510 Gbits

spacecraft remains on the far side of the Sun from the Earth. For the first perihelion, the SPE is always less than 15°, and no high-speed downlink is possible from the body-mounted antenna. For the second perihelion, the return from both antenna cases is approximately the same. For the third principal perihelion, where the spacecraft is on the same side of the Earth after closest approach, both antenna schemes provide downlink return in excess of 500 Gbits.

In order to retrieve science results from all perihelia, the mast-mounted 0.8-m antenna is selected. This case has a higher mass and greater number of components but maximizes science return. For orbits during which the spacecraft is on the far side of the Sun after perihelion, the number of passes in the inter-perihelion period must be increased beyond the one 8-hour pass per day assumption used here in order to meet the 128-Gbit data-return requirement.

3.10.2. Subsystem Implementation

The Solar Probe+ Telecommunications Subsystem architecture is shown in Figure 3.10-1. The subsystem uses three antennas: a HGA mounted to a dual-axis gimbaled mast and two hard-mounted low-gain antennas (LGAs). The HGA is the prime antenna for the Ka-band science return downlink, and X-band uplink and downlink capability is provided through all antennas. The HGA deployment system remains stowed within the shadow of the umbra while the spacecraft is within 0.59 AU of the Sun. When the spacecraft is farther than 0.59 AU from the Sun, the HGA mast is deployed, and the antenna pointed to Earth for science playback. The main reflector is 0.8 m in diameter and uses a dichroic subreflector to transmit a right-hand circularly polarized (RHCP) wave at Ka-band. A horn behind the subreflector provides bidirectional communications at X-band through the HGA. The 0.8-m aperture at Ka-band does set the required pointing error for the HGA boresight axis to Earth at 0.2°.

When the spacecraft is within 0.59 AU of the Sun, communications are maintained through the X-band LGAs hard-mounted to the spacecraft structure, separated by 180° and canted forward and aft, respectively. The LGAs provide some directivity, allowing for telemetry reception within the 0.59-AU limit and for emergency rate command and telemetry communications to 1.7 AU.

The Ka-band (32-GHz) high-power transmitters are 40-W RF output power traveling wave tube amplifiers (TWTAs). The TWTAs are ~50% efficient (DC power of 80 W) and build on heritage from TWTAs on the Kepler (35 W at 32 GHz) and LRO (40 W at 26 GHz) missions. The X-band transmitters are 13-W TWTAs that are heritage from the New Horizons mission and are ~40% efficient (32 W of primary DC power).

The two RF transponders are based on the advanced digital receiver flown on the New Horizons mission and on digital and Ka-band hardware developed for NASA on the CoNNeCT program. The transponders each require only

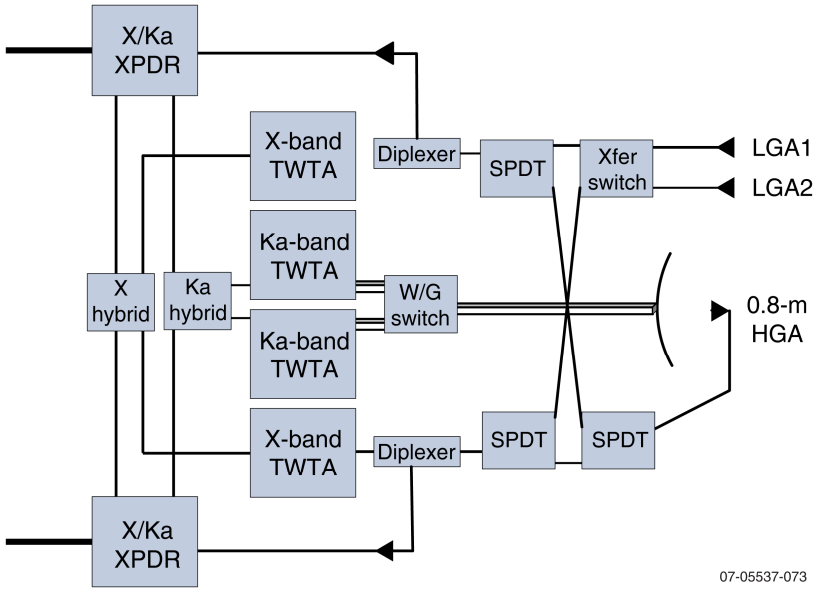

Figure 3.10-1. Solar Probe+ telecommunications system.

Table 3.10-2. Maximum telemetry rates vs. Earth range.

Downlink Rates vs. Earth Range			
	Estimated Maximum Telemetry Rate		
Earth–Spacecraft Distance (AU)	0.8-m HGA, X-band to 34 m, 13- W TWTA	0.8-m HGA, Ka-band to 34 m, 40-W TWTA	LGA, X-band to 70 m, 13-W TWTA
0.5	92 kb/s	932 kb/s	167 bps
1	23 kb/s	233 kb/s	42 bps
1.5	10 kb/s	104 kb/s	10 bps
1.8	7 kb/s	72 kb/s	6 bps

Table 3.10-3. Maximum command rates vs. Earth range.

Uplink Rates vs. Earth Range		
	Estimated Maximum Command Rate	
Earth–Spacecraft Distance (AU)	34-m to 0.8-m HGA, X-band	70-m to LGA, X-band
0.5	>10 kb/s	389 bps
1	>10 kb/s	97 bps
1.5	>10 kb/s	43 bps
1.8	>10 kb/s	30 bps

4 W of primary power in receive-only mode, 8.7 W in receive/X-band transmit mode, 9.7 W in receive/Ka-band transmit mode, or 14.1 W in receive/X- and Ka-band transmit mode. Other higher-power transponder options are available for consideration. A Phase A trade study will be conducted to determine the optimal transponder choice by balancing factors such as solar array size through the use of lower power systems, development status of the options, and overall system cost.

The output from either of the X-band TWTAs may be steered to any of the antennas through a network of single-pole-double-throw (SPDT) and transfer (XFER) switches, which are themselves configured for redundant operation. Similarly, the Ka-band TWTAs are switched to the HGA. Hybrid couplers are used with each of the X-band and Ka-band TWTA pairs to increase downlink system reliability.

3.10.3. Performance

Link performance is determined primarily by the antenna used and by the relative distance from the spacecraft to the Earth. Table 3.10-2 summarizes the estimated telemetry performance for the different antennas at varying distances. Table 3.10-3 summarizes maximum command rates. No significant solar interference and the use of a 34-m deep space mission system (DSMS) antenna for the ground link are assumed. In the case of the low-gain antenna (LGA), a 70-m DSN antenna is assumed along with a worst-case LGA orientation (random tumble) to cover an emergency situation.

3.11. Data Management

Even though the baseline instrument suite is fundamentally the same, the Solar Probe+ data management concept is different from the 2005 Solar Probe concept in two important ways. First, the nature of the Solar Probe+ mission design allows for repeated solar encounters at fairly regular intervals, while the 2005 concept is based on two solar encounters spaced widely apart. Second, the 2005 concept included real-time downlink of critical science data for risk mitigation. The Solar Probe+ concept reduces risk through critical perihelia farther away from the Sun and through the use the previously mentioned repeated encounters to allow extensive preparation for critical encounters and recovery from unanticipated problems, and no real-time science data downlink is used.

From an operational perspective, Solar Probe+ orbits are broken into aphelion segments and perihelion segments. Although some science data are taken throughout an orbit, the great majority of science data are taken during solar encounters around perihelion. During this time, the payload stores data onto the solid-state recorders (SSRs) through the payload data processing unit (DPU) and integrated electronic module (IEM). The aphelion segment is defined by the time in which the HGA can be used, nominally outside 0.59 AU, and is primarily when all data stored on the SSR during the previous encounter and during cruise since the last aphelion segment is downlinked.

Table 3.11-1. Instrument and housekeeping average data rates.

Instrument	Raw Data Rate (bps)	Data Rate to Recorder (bps)
Fast Ion Analyzer (FIA)	10,000	13,650
Fast Electron Analyzer (FEA)	20,000	27,300
Ion Composition Analyzer (ICA)	10,000	13,650
Energetic Particle Instrument (EPI) Low Energy	5000	6825
EPI High Energy	3000	4095
Neutron/Gamma-Ray Spectrometer (NGS)	500	683
Coronal Dust Detector (CD)	100	137
Magnetometer (MAG)	1100	1502
Plasma-Wave Instrument (PWI)	10,000	13,650
White-Light Hemispheric Imager (HI)	40,800	55,692
Housekeeping	1800	2457
Total	**10,230**	**139,640**

3.11.1. Science Data Collection

The Solar Probe+ payload, as discussed in Section 2.0, is essentially the baseline payload from the 2005 Solar Probe study. Science data collection will be conducted in much the same manner as in the previous study, and instrument data rates are currently baselined to be very similar to those presented in the previous study. Table 3.11-1 gives the average instrument/housekeeping data rates, where the raw data rates represent the actual science data and the data rate to the recorder includes 30% margin and a 5% overhead for packetization performed in the data processing unit (DPU). Actual data rates from the instruments will vary during the encounter, and detailed data volume allocations for each instrument in each orbit will be established in Phase A. The resulting required data rate of 139.6 kbps will be achieved by using a standard 1553 data bus to transfer data packets from the payload and housekeeping data from the various subsystems. Over the encounter period (and including any low-rate science collection outside encounter), the nominal 128-Gbit SSRs on Solar Probe+ will be simultaneously filled. Two recorders are used to provide redundancy.

3.11.2. Data Return

For each Solar Probe+ orbit, the period extending from 0.59 AU solar distance as the spacecraft leaves the Sun through aphelion back to 0.59 AU as the spacecraft approaches the Sun is designated primarily for data downlink. As shown previously in Figure 3.1-6, the Earth–probe distance varies from 0.3 AU to 1.9 AU, depending on the specific orbit. Based on 10-hour contacts and average downlink rates for each aphelion downlink period, we have developed a day-by-day downlink schedule that allows for downlinking the full SSR data volume within the aphelion segment as well as supporting other operational aspects of the mission (such as navigational requirements to support Venus flybys). Table 3.11-2 gives a summary of this contact plan and total data volume downlinked in each

Table 3.11-2. Orbit data return summary.

Orbit	1	2	3	4	5	6	7	8	9	10	11	12	13	14	15	16	17	18	19	20	21	22	23	24	Total
Days in Orbit	168	149	139	119	112	108	101	99	99	96	95	95	96	95	95	94	92	91	91	87	87	87	87	87	**2554**
Venus Flyby	Y			Y	Y		Y			Y							Y				Y				**7**
Downlink Days	81	42	42	81	6	42	59	6	6	56	54	6	6	54	42	6	42	37	42	6	42	29	42	6	**844**
Ave. Data Rate (kbps)	44	86	86	44	583	86	44	583	583	44	44	583	583	44	86	583	86	44	86	583	86	44	86	583	**92**
Data Return (Gbits)	128	128	128	128	128	128	94	128	128	90	86	128	128	86	128	128	128	59	128	128	128	46	128	128	**2765**

Table 3.12-1. Overall system pointing budgets.

Payload	Pointing Requirements (per axis)		
	Control degrees, 3σ	Knowledge degrees, 3σ	Jitter degrees, 3σ
Communication (HGA)	²0.2 *x*, *z*	N/A	N/A
In Situ Instruments <0.3 AU	²1 *x*, *y*, *z*	²0.3 *x*, *y*, *z*	²0.3 *x*, *y*, *z* over 10 s
Magnetometer <0.3 AU	²1 *x*, *y*, *z*	²1 *x*, *y*, *z*	²1 *x*, *y*, *z* over 0.05 s
Plasma Wave Sensor <0.3 AU	²1 *x*, *y*, *z*	²1 *x*, *y*, *z*	N/A
Hemispheric Imager <20 R_S	²1.0 *y*, *z*	²1.0 *y*, *z*	²0.03 *y*, *z* over 1 s

aphelion segment. Solar Probe+ is able to downlink the full dataset from each perihelion except for six orbits where the SEP geometry is least favorable. This calculation uses the average data rate for each orbit and assumes only a single 10-hour DSN contact for each day when contacts are planned. Therefore, the estimated data volume return is worst case. More detailed modeling of the daily data rate in Phase A is expected to show an increase in data volume returned for the worst-case orbits, and a trade study to be conducted in Phase A will optimize the return for these orbits by balancing science data cadence, DSN cost and schedule requirements, high-gain antenna (HGA) thermal design to increase the window for HGA deployment, telecommunications system topology, and radio frequency (RF) transmit power.

3.12. Guidance and Control System

The Solar Probe+ guidance and control (G&C) subsystem is designed to maintain the spacecraft attitude required to protect the spacecraft bus from the harsh solar environment, point antennas for communications with Earth, provide desired viewing geometry for science instruments, and point thrusters for trajectory correction maneuvers (TCMs). Three star trackers and a high-precision, internally redundant inertial measurement unit (IMU) provide attitude knowledge, and attitude control is provided by four reaction wheels and 12 0.9-N thrusters. The attitude determination and accuracy requirements derived from these different activities are summarized in Table 3.12-1. Pointing control is driven by the need to point the HGA within

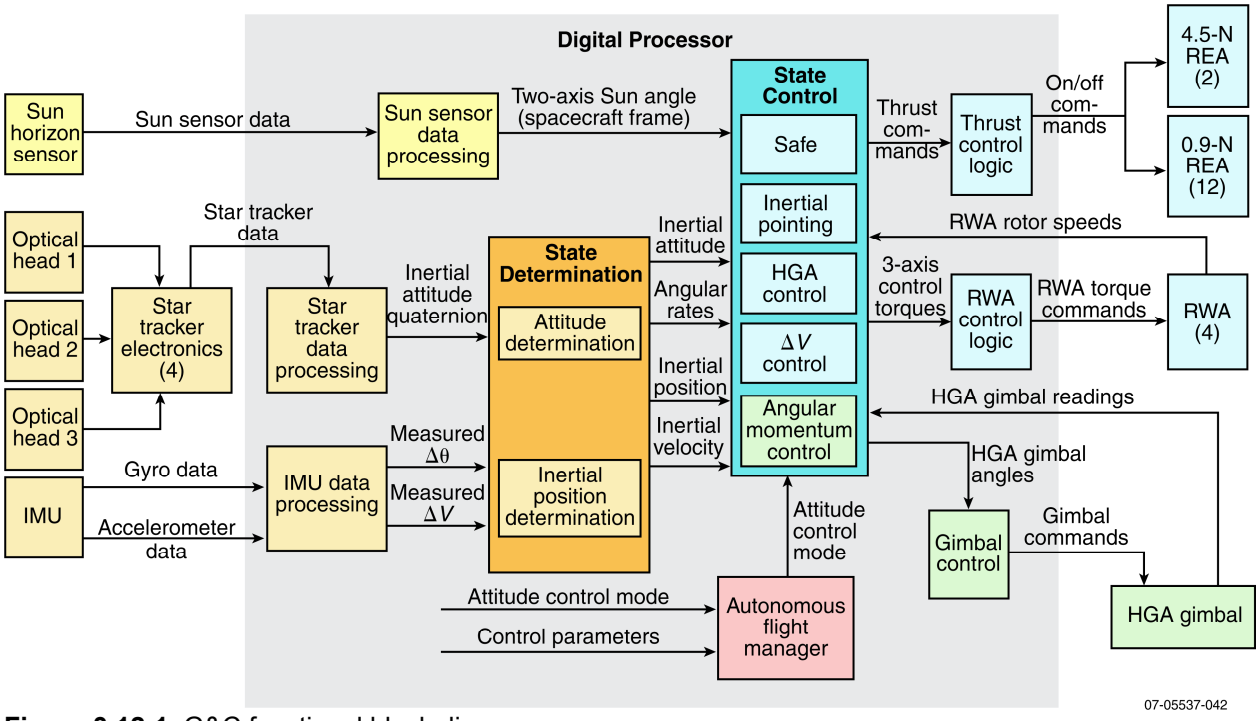

Figure 3.12-1. G&C functional block diagram.

0.2° when downlinking using the communication system. The pointing knowledge and jitter budget is driven by the remote sensing instrument. A functional block diagram of the system is shown in Figure 3.12-1.

3.12.1. Attitude Determination

Spacecraft attitude will be determined by three star trackers and an internally redundant inertial measurement unit (IMU). Using star trackers in the near-Sun corona presents a unique design challenge, which the baseline design addresses by mounting the star trackers so that their field of view (FOV) are approximately orthogonal to the Sun as well as to each other. This configuration minimizes the chance that all three units will be blinded by a localized coronal lighting event at the same time. Special care must be taken in the selection of the star trackers to ensure that they will perform properly with the elevated background noise of the near-Sun environment.

The IMU will provide the spacecraft rate and translational acceleration information necessary for maintaining attitude control as well as for closed-loop control during trajectory correction maneuver (TCMs). The IMU also can be used as a backup to the star trackers to propagate attitude for a brief period during a solar encounter if all three star trackers are temporarily blinded. The baselined IMU is a single integrated box with internal redundancy, although two separate units also would meet the needs of the mission.

In the event of long-duration star tracker blinding, system resets, or other attitude control anomalies, a new sensor design, the solar horizon sensor (SHS), is proposed for attitude safing when the spacecraft needs to be protected behind the Thermal Protection System (TPS) umbra. The detector would be mounted at the end of the science boom and would consist of a conical ring of carbon–carbon (C-C) material, a mirrored conical reflector, and a detector array with a pinhole lens. The detector array resides in a small electronics box, which contains readout electronics for both the detector and a set of thermistors. If an attitude error that reaches a designated threshold should occur, the edge of the conical ring would become illuminated and projected onto the detector. The processed signal could be used to provide attitude control for safing during the solar encounter.

Most currently available attitude control hardware should meet the needs of Solar Probe+ with little or no custom modifications. Special care must be taken to select star trackers that will perform well in the intense coronal lighting environment. During the engineering study, one or more potentially suitable candidate star trackers were identified in existing product lines. The SHS will be the only attitude determination device that will need to be developed for Solar Probe, and it is conceptually simple.

3.12.2. Attitude Control

Although the overall pointing requirement for the spacecraft is 0.2°, the G&C system was preliminarily budgeted to ~0.05° because much of the error budget will go to HGA misalignments and actuator setting errors. Consequently, reaction wheel control, which offers very tight pointing control and can easily maintain spacecraft attitude at better than the budgeted 0.05°, has been baselined. Wheel control also interacts less with flexible modes and would be more likely to control them to meet the jitter budget. Thrusters are used to control attitude during TCMs and for dumping accumulated angular momentum from the wheels when necessary.

A brief trade study was performed to determine whether reaction wheels or thrusters should be used as the primary method of attitude control. Dead-band thruster control using small minimum impulse bit rocket engines such as are used on Cassini and New Horizons was considered because it appeared to offer a means of reducing mass and average power during the encounter. Thruster control might possibly reduce overall mass slightly; however, it also has some disadvantages. First, as mentioned earlier, the required dead band for the G&C system is budgeted to ~0.05°. This small dead-band value would require frequent thruster firings, thus

driving up the total propellant requirement and negating most of the mass savings of removing the wheels. Overly frequent thruster firings also were a concern because of possible instrument contamination, valve lifetimes, and possible thruster-induced structural excitation that may exceed the jitter requirements. Because there are several components that could induce low-frequency modes such as the TPS, science boom, and plasma-wave antennas, dead-band thruster control appears less attractive but will be retained as a trade for Phase A.

3.12.3. Environmental Considerations

Several environmental factors are drivers for the Solar Probe+ G&C design and will require more detailed study in Phase A. First, as the spacecraft approaches perihelion, sunlight reflected off of dust particles will be seen by a star tracker looking away from the Sun through the solar corona. Coronal lighting reduces the signal-to-noise (S/N) ratio for a tracker using a charge-coupled device (CCD), thereby reducing the number of detectable stars and degrading the performance of the star tracker. This restricts the choice of star trackers and also drives the design to operate multiple star trackers at perihelion.

Solar pressure will be very high and will change rapidly during the solar encounter. Because the center of photon pressure is ahead of the center of mass, the solar pressure torque is destabilizing and is an important part of the dynamics of the spacecraft near perihelion. The solar pressure torque, which decreases with distance r from the Sun as $1/r^2$, will require multiple momentum dumps on the day of perihelion passage. Relatively small misalignments of the heat shield could induce significant torque and momentum build-up, potentially forcing more frequent use of thrusters for momentum management, consequently the center-of-pressure/center-of-mass offset will have to be carefully monitored during the design phase. The ΔV propellant budget includes an estimate of momentum dumping frequency during perihelion. A Phase A study will be conducted to optimize center of aerodynamic pressure (CP)/center of gravity (CG) requirements to reduce solar pressure effects.

Solar dust impacts also are an important attitude control consideration, especially near perihelion. Dust particles that impact Solar Probe+ will impart an instantaneous momentum impulse that the wheels must take out. In the event that the momentum impulse is too large for the wheels to handle, the thrusters will be fired to maintain the sensitive spacecraft systems safely in the umbra of the heat shield. During Phase A, more detailed analysis of the dust environment will be carried out and thruster selection optimized, as necessary.

3.12.4. Pointing Strategy

During all phases of the mission, the probe's attitude nominally changes so that the TPS points toward the Sun, keeping the instruments and subsystems within its protective umbra. TCMs will be planned for aphelion when the spacecraft TPS can be off-pointed from the Sun.

Momentum dumping will occur much more frequently during perihelion because of the intense solar radiation pressure. Each momentum management maneuver will be completed quickly taking typically on the order of 3–5 minutes. For these short periods, the thrusters will fire to remove angular momentum, and the control requirements for instrument pointing may not be maintained.

Solar pressure torques are often used as a means of passive momentum control. This option was considered as a possible augmentation of Solar Probe+ attitude control during the closest approach periods. It would require an intentional pointing offset of the heat shield that is adjusted automatically by the feedback control system. An advantage of passive dumping using solar pressure torques is that it could reduce the number of thruster momentum dumps needed. However, instrument pointing requirements might limit the range of offsets that could be used, reducing the overall contribution of a passive dumping mechanism. In addition, successful employment of this method also depends greatly on accurate modeling of the solar pressure effects. Thus, the

sizing of the baseline propulsion system assumes that all momentum control must be done with thrusters, given the uncertainties in the environment models.

During TCMs, the attitude of the spacecraft will be off-Sun pointed to use the larger, 4.4-N thrusters to impart the desired change in velocity. These maneuvers will occur near aphelion where it is permissible to have the spacecraft outside of the TPS umbra for the duration of the TCM. Upon completion of the maneuver, the TPS will again be pointed sunward.

3.12.5. High-Gain Antenna Control

The HGA will be pointed by rotating the spacecraft about the spacecraft sunline and rotating the antenna using the rotary actuator to keep it oriented toward Earth. The second axis of motion for the HGA is used to deploy the HGA mast to a fixed position to give the HGA a clear field of view to Earth. The G&C subsystem will compute the necessary positioning of the gimbal for the HGA based on onboard ephemeris models for the Earth, Sun, and spacecraft. In the event of loss of onboard ephemeris knowledge or other fault conditions, the HGA will be commanded to its safe stowed position.

3.12.6. Guidance and Control Changes Since Previous Study

There have been only minimal changes to the G&C design since the previous Solar Probe study.[23] The digital solar attitude detectors of the previous study, which were to be used as safing sensors for the periods of the mission when the spacecraft was outside of 0.8 AU, have been deleted from the design because the majority of the Solar Probe+ mission will be carried out within that distance. To replace those sensors and further add system robustness, a third star tracker was added to the design to maximize the probability of having at least one star tracker operational at all times. The internally redundant IMU, the SHS, and the reaction wheels are all carried over from the previous design.

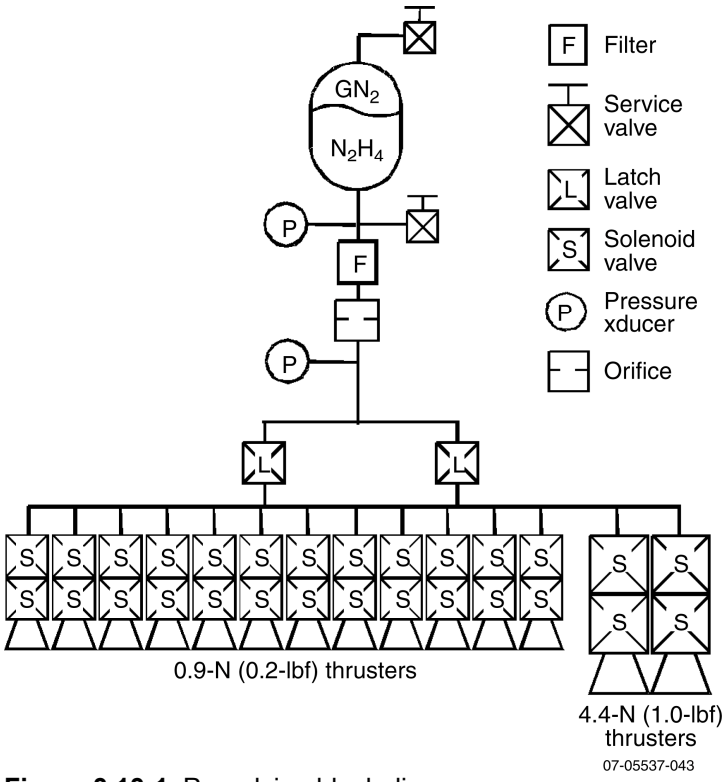

Figure 3.13-1. Propulsion block diagram.

3.13. Propulsion System

The Solar Probe+ propulsion subsystem is a blowdown monopropellant hydrazine system that provides ΔV and attitude control capability for the spacecraft. The system consists of 12 0.9-N (0.2-lbf) thrusters, two 4.4-N (1.0-lbf) thrusters, and components required to control the flow of propellant and monitor system health and performance. The propellant and pressurant are stored in the same tank, separated by a diaphragm. As propellant is expelled, the pressure of the pressurant decreases; thus, the thrust and specific impulse of the thrusters decrease as the mission progresses. All valves will maintain temperatures above 5°C to protect the soft seals. The propulsion system schematic is shown in Figure 3.13-1.

[23] *Solar Probe: Report of the Science and Technology Definition Team*, NASA/TM—2005–212786, National Aeronautics and Space Administration, Goddard Space Flight Center, Greenbelt, MD (2005).

07-05537-044

Figure 3.13-2. Baseline 0.2-lbf thruster.

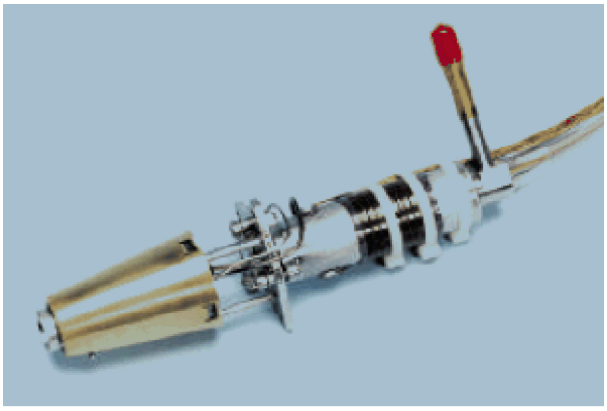

07-05537-045

Figure 3.13-3. Baseline ΔV thruster.

The baseline propellant load for Solar Probe+ is 49.7 kg of hydrazine. For a 554-kg wet mass launch, this translates to 190 m/s of ΔV. Several flight-proven options exist for each component of propulsion subsystem. A representative set of heritage components has been identified for preliminary performance evaluation and demonstrates that system requirements can be achieved.

The propellant tank is a 5555-in.^{3} (91.0-liter) titanium tank manufactured by ATK-PSI. This 22.14-in. diameter, vacuum-rated spherical tank (ATK P/N 80259) contains an elastomeric diaphragm that pushes propellant out the bottom of the tank through the tank outlet. The maximum expected operating pressure for the Solar Probe+ mission is 300 psi. The tank has flight heritage on the Defense Satellite Communications System (DSCS) III spacecraft.

The thrusters on the Solar Probe+ spacecraft are of the catalytic monopropellant hydrazine type; when the thruster valve is opened, propellant flows through the thruster into a catalyst bed, where the hydrazine spontaneously decomposes into hot gases, which then expand through a nozzle and exit the thruster, producing thrust. The baseline attitude control system thrusters are all Aerojet model MR-103G (Figure 3.13-2), which is a member of the MR-103 family of thrusters, used on Voyager, Magellan, New Horizons, Cassini, and several other missions. The baseline ΔV thrusters are both Aerojet model MR-111C (Figure 3.13-3). This thruster has heritage on the New Horizons, STEREO, and MESSENGER spacecraft. The actual steady-state thrust produced from both thrusters varies as the tank pressure decreases. Figure 3.13-4 illustrates thruster steady-state performance between beginning of life and end of life.

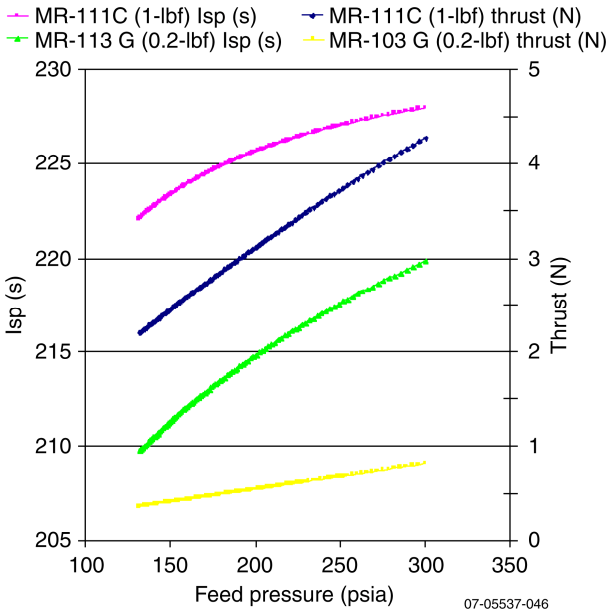

Figure 3.13-4. Blowdown curve.

The remaining components used to monitor and control the flow of propellant—latch valve, filter, orifice, and pressure and temperature transducers—have substantial heritage on spacecraft, including New Horizons, STEREO, and MESSENGER.

Latching valves isolate the thrusters from the tank for safety and system reliability (i.e., in case of a thruster leak). The Vacco ¼-in. latch valve (Figure 3.13-5), part number

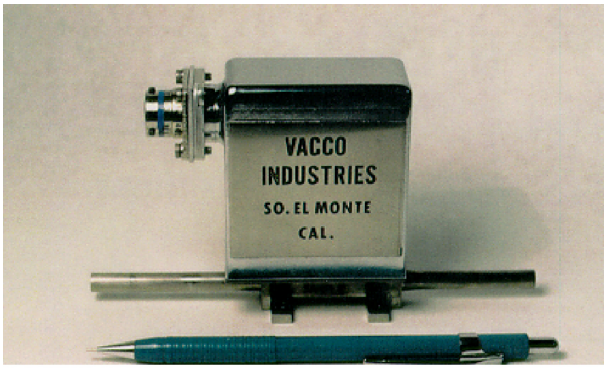

07-05537-047

Figure 3.13-5. Latch valve.

V1E10747-01, will be used to isolate the thrusters from the tank. These latch valves are proof-tested to 1000 psig with a burst pressure of 2400 psig. This item is fully flight-qualified and has heritage on both STEREO and New Horizons as well as flight heritage on numerous other missions.

Filters ensure propellant purity. The Vacco propellant filter, part number F1D10767-01, is a 10-µm filter composed of stacked etched titanium discs. This filter has flight history on STEREO and New Horizons. Manual service valves are used for testing and loading the system on the ground. The Vacco V1E10701-01 ¼-in. fill and drain valve will be used to load the hydrazine and pressurant on to Solar Probe+. This service valve design has a two-seat seal and a maximum expected operating pressure of 500 psig. It is proof-tested to 1750 psi and burst-tested to 2000 psi. This valve has flight heritage on STEREO and New Horizons.

3.14. Environmental Mitigation

3.14.1. Charging

3.14.1.1. Charging Analysis Methodology

Studies of the Solar Probe charging problem date to the 1980 Starprobe report.[24] That analysis only crudely accounts for the material properties of the heat shield, which was expected to be constructed from an uncoated carbon–carbon (C-C) composite rather than the ceramic-coated version now under study. Electron emission characteristics were accounted for with a rough analytical estimate only, and geometrical effects were ignored. Furthermore, there was no estimate of the differential charging of the spacecraft; only charging relative to the plasma "ground" was considered. Finally, only the closest approach case was evaluated, which may not be the region of greatest concern for a ceramic-coated heat shield.

The analysis described here is a continuation of the work reported previously, adapted for the Solar Probe+ mission design. Our analysis with NASCAP-2K provides estimates of differential charging, taking the spacecraft geometry into account. We have considered a range of trajectory points, including closest approach and the range from 0.5 AU down to 0.1 AU. Furthermore, our modeling efforts make use of the material properties for the coatings of interest. These properties include elevated temperature-resistivity estimates and room temperature secondary electron emission and backscattered electron emission measurements. It should be noted that the NASCAP results depend on the accuracy to which these material properties are known. In particular, because resistivity is the material property that most drives the charging behavior, more precise temperature-dependent resistivity measurements are desirable.

3.14.1.2. Charging Results

The baseline coatings for this effort are alumina (Al_2O_3) and pyrolytic boron nitride (PBN). We have considered the charging problem at the following trajectory points: 0.5, 0.4, 0.3, 0.2, 0.1, and 0.0443 AU (closest approach). This analysis was conducted for a solar absorptivity-to-infrared (IR) emissivity ratio (α/ε) of 0.6; previous efforts also included the lower α/ε of 0.2. The temperature of the heat shield will be lower for smaller

[24]Goldstein *et al*., *Spacecraft Mass Loss and Electric Potential Requirements for the Starprobe Mission*, A Report of the Starprobe Mass Loss Requirements Group Meeting of September 29–30, 1980, NASA Jet Propulsion Laboratory, California Institute of Technology, Pasadena, CA (December 1980).

Table 3.14-1. Differential potentials for Al_2O_3.

Trajectory Point (AU)	Differential Potential (V)
0.5	7
0.4	7.5
0.3	7
0.2	7
0.1	7.5
0.0443	3.8

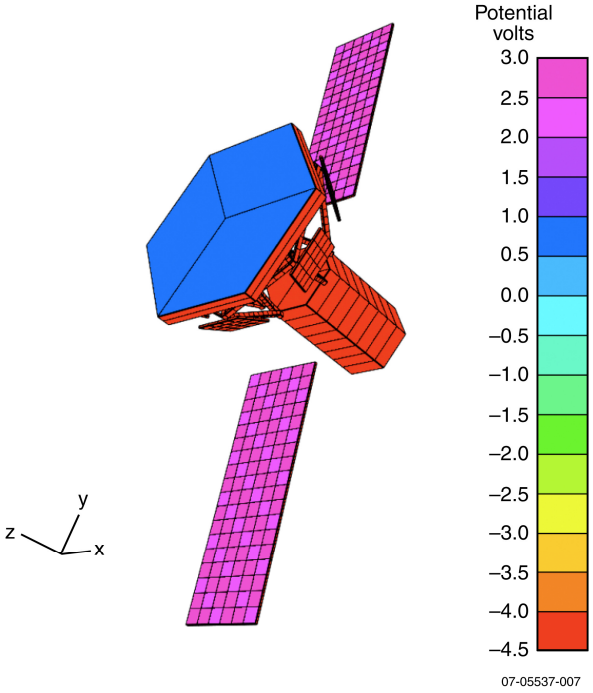

Figure 3.14-1. Differential charging for Al_2O_3 at 0.1 AU.

Table 3.14-2. Differential potentials for PBN.

Trajectory Point (AU)	Differential Potential (V)
0.5	7
0.4	7
0.3	6.5
0.2	7
0.1	4.5
0.0443	3.4

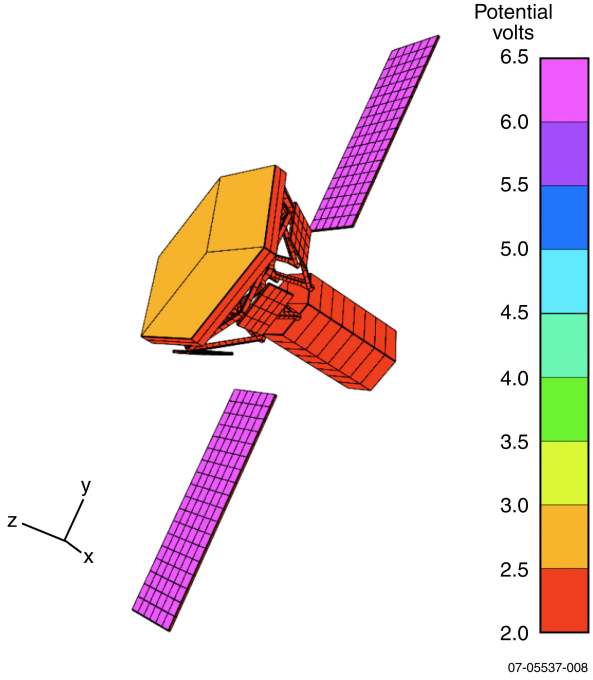

Figure 3.14-2. Differential charging for PBN at 0.1 AU.

values of α/ε, resulting in a higher resistivity and a change in the differential potential, so the results presented here are not worst case.

The differential charging results derived from NASCAP-2K are given in Tables 3.14-1 and 3.14-2. Both materials experience differential charging at low levels, below 10 V, for all of the trajectory points considered. The absolute surface charging relative to plasma ground also is below 10 V for all of these points. The NASCAP-2K plot of the spacecraft potentials for Al_2O_3 and PBN for at the 0.1 AU trajectory point for $\alpha/\varepsilon = 0.6$ are shown in Figures 3.14-1 and 3.14-2. The shaded portion of the spacecraft tends to charge to a few volts negative, whereas the heat shield coating charges slightly positive, and the solar cells charge to a few volts positive.

3.14.1.3. Impact of Spacecraft Charging

Typically, two major risk areas are studied in spacecraft charging efforts. If large differential potentials should build up between different sections of the spacecraft, there is the possibility of arcing, which could damage the spacecraft, including its electronics, communications devices, or instruments. Historical trends indicate that surface charging potentials should be limited to the low hundreds of volts in order to protect the spacecraft electronics. Even for low differential potentials, however, there is a risk of disrupting science data collection. The buildup of a significant potential on the spacecraft relative to plasma "ground" may cause measurement contamination by disrupting instrument function and by disturbing the local environment. The precise level of

charging that is tolerable from the perspective of science data collection is still under review but would best be kept to the low tens of volts.

3.14.1.4. Mitigation Strategies

The *Solar Probe Thermal Protection System Risk Mitigation Study: FY 2006 Final Report ITAR-Restricted Annex*[25] contains a summary of mitigation options that were studied for the previous Solar Probe+ design. These options presume that the ceramic-coated heat shield is the primary cause of surface charging, and they have not yet been studied in detail for Solar Probe+. However, the charging results above indicate the solar cells charge more positive than the heat shield. In order to mitigate their charging, it may be necessary to ensure that the solar arrays are conductive on the sunlit side, for example, by the use of transparent conductive oxides. If it also is necessary to mitigate charging by the ceramic coating, the principles involved in the earlier study should be applicable to the current heat shield design. In that case, one option to mitigate charging is to lower the resistivity of the heat shield coating by adding small quantities of impurities to the ceramic material. Another possible solution to reduce the differential charging of the heat shield is to expose small portions of the heat shield to be bare C-C. It should be noted that the effects of both approaches—the effect of dopants on ceramic optical properties and the effect of C-C exposure on outgassing—must be investigated before either approach could be implemented.

3.14.1.5. Conclusions

A preliminary charging analysis has been performed for the Solar Probe+ spacecraft design and for two different heat shield coating materials. Initial results indicate that the spacecraft charges to a potential of several volts relative to the plasma "ground." The differential charging situation is that the sunlit side of the solar arrays charge slightly positive, as does the heat shield, whereas the shaded portion of the spacecraft charges to a few volts negative. At these potential levels, arcing is not a concern, but mitigation strategies may be considered in order to prevent contamination of the data collected by the instruments. Possible mitigation approaches include, for the solar array, the use of conductive solar cells and, for the heat shield, doping ceramic coating or exposing portions of the shield to be bare C-C.

The Solar Probe+ spacecraft will include dust and micrometeoroid protection for the expected particle environment. The near-Sun dust environment and its impact on the Solar Probe spacecraft were a major focus of the 2005 Solar Probe STDT study.[26] Compared with that effort, the Solar Probe+ spacecraft will be subjected to a larger particle flux but at lower velocities. However, the spacecraft protection approach remains similar to the one described in the earlier study. It includes dust protection for the Thermal Protection System (TPS), spacecraft bus, and solar arrays. The Solar Probe+ approach is described below, but the planned effort includes a study both on the definition of the mission's dust exposure and a characterization of the protection approaches for the key areas.

The dust environment in the ecliptic portion of the trajectory was used in the STDT study to establish a statistical dust environmental model as shown in Figure 3.14-3. Within 1 AU, the dust density is highest near the ecliptic plane and falls off at higher inclinations. Parametric studies of particle impacts were used to define the protection level provided for designs subject to different particle velocities and angles of attack. In this region, there will be thousands of small particle impacts (submicrometer), but

[25] *Solar Probe Thermal Protection System Risk Mitigation Study: FY 2006 Final Report ITAR-Restricted Annex*, prepared by The Johns Hopkins University Applied Physics Laboratory under Contract NAS5-01072, Laurel, MD (September 17, 2007).

[26] *Solar Probe: Report of the Science and Technology Definition Team*, NASA/TM—2005–212786, National Aeronautics and Space Administration, Goddard Space Flight Center, Greenbelt, MD (2005).

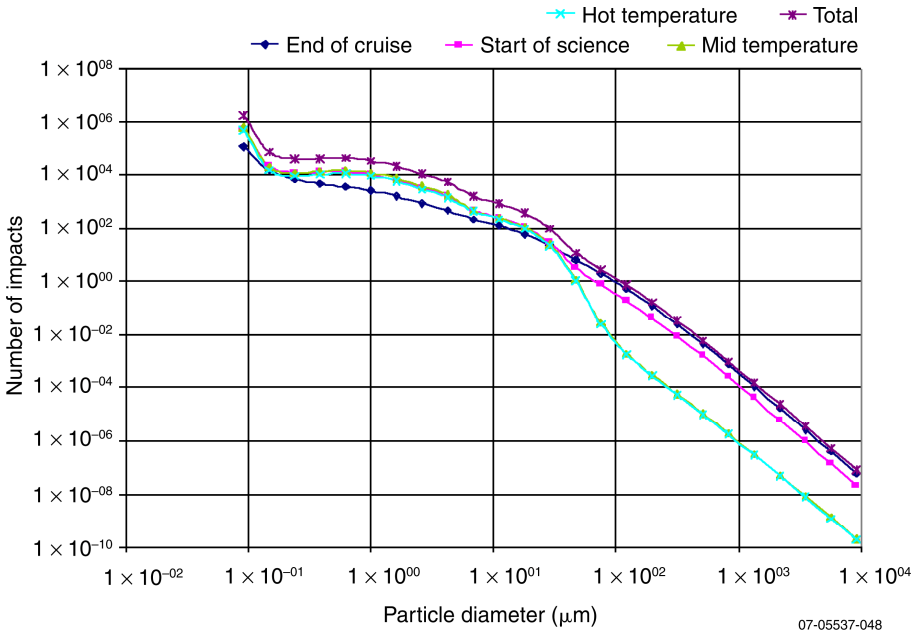

Figure 3.14-3. Distribution of dust impact with respect to particle size.

there will only be one or two particles large enough to penetrate the TPS C-C shell.

The Solar Probe+ study found that particle protection is required for three key areas: the TPS, the spacecraft bus, and the solar arrays. Compared with the earlier work, impacts on the TPS will be significantly reduced by the change from a conical to flat shield. The TPS cross-sectional area, in the ram direction, is reduced by a factor of almost 20. If there is a penetration of the TPS shell, the resulting damage could extend well into the insulating foam. To protect against this secondary damage, an extra C-C layer has been added to the TPS to shield the carbon foam. For the spacecraft bus, the Whipple-shield approach, where the multi-layer insulation (MLI) is spaced away from the underlying structure, will still provide the needed protection. The spacing between the MLI and spacecraft will be updated based on the new particle environment. The solar arrays are a new feature of the Solar Probe+ design; detailed dust environments will be generated for them in Phase A. However, there are several mitigating options that indicate adequate protection for them is available. Generally, the solar arrays are aligned parallel to the ram direction, reducing their exposure to the dust environment. Flight experience from the MESSENGER mission has shown that the effect of particle impacts on solar arrays between 1.0 and 0.3 AU is minimal; the Solar Probe+ spacecraft will spend 88% of its mission within this range. Inside 0.3 AU, potential protection options for the solar arrays have been identified, such as turning the cell face inward during storage, or oversizing the arrays. With a $1/r$ dust-particle dependency, the time spent within 0.3 AU is equivalent to a 6-year orbit at 1 AU. Existing solar array design rules, allowing for performance degradation factors, can account for the damage expected during the Solar Probe+ mission.

3.14.2. Methodology

An investigation was performed during the 2005 Solar Probe STDT study, using an analysis and prediction methodology similar to that used for other NASA missions (both low-Earth orbit and deep space), to assess the risk of dust to the spacecraft and to develop a methodology for dust protection. By using conservative, worst-case assumptions for particle size, velocity, and obliquity, this study was performed by Dr. Cesar Carasco (at the University of Texas at El Paso) using state-of-the–art hydrodynamic codes [e.g., Coupled Thermodynamic and Hydrodynamic (CTH) hydrocode][27] that resolve the highly dynamic, nonlinear impact physics and include constitutive models of the materials of construction. Carasco's findings predicted that Whipple shielding consisting of MLI (i.e., 18 layers of Kapton) at a stand-off distance of

[27]Boslough, M. B., *et al*., Hypervelocity testing of advanced shielding concepts for spacecraft against impacts to 10 km/s, *Int. J. Impact. Eng.* **14,** 96–106 (1993).

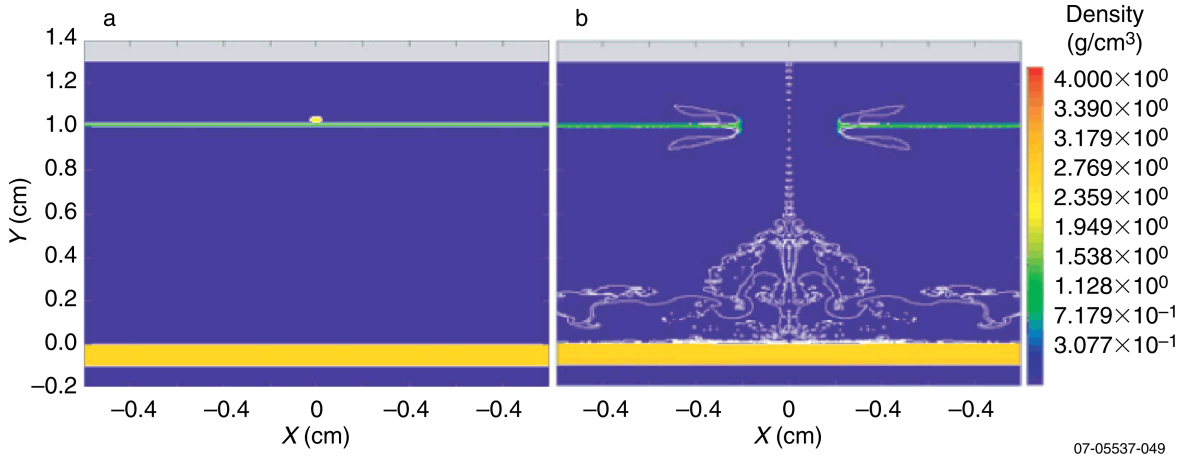

Figure 3.14-4. Large-particle, high-speed dust impact on Whipple shield.

10 mm would be sufficient to break up the largest particles and prevent penetration of the metallic spacecraft bus or instrument housings as illustrated in Figure 3.14-4. Because of similarities in both bus and instrument configurations and statistical dust environment models, it is believed that this approach also would be effective for the Solar Probe+ design. However, as the Solar Probe+ design and mission parameters mature, shielding studies need to be repeated with new trajectories (and corresponding dust environments) to predict whether MLI-based Whipple-shielding approaches remain appropriate.

During the 2005 Solar Probe STDT study and subsequent Solar Probe Risk Mitigation Studies in 2006 and 2007,[28,29] the TPS was analyzed to determine the thermal-structural performance after dust impact and to predict the resulting effects on mission performance with respect to mass loss and contamination of sensitive instruments. The TPS evaluated in these studies consisted of a thin-walled, conical, ceramic-coated C-C primary heat shield and a flat disk-shaped secondary heat shield (consisting of a thin-walled C-C shell packed with carbon foam insulation). The previous secondary heat shield is similar to the heat shield proposed in the current Solar Probe+ study with the exception that the new design incorporates a ceramic coating (like the primary heat shield) for temperature control. In follow-on work performed by Dr. Carasco at the University of Texas at El Paso, estimations of the structural response of the conical heat shield to a matrix of dust-particle size, impact speed, and impact angle of incidence were calculated by using high-performance hydrodynamic codes. These predictions indicated that localized spallation footprints were greater in size than that of the impact particle. For a given particle size and impact speed, the spallation footprint varied with angle of incidence; the largest footprints were developed for normal angle of incidence impacts as shown in Figure 3.14-5.

Although visually appearing large in the highly magnified Figure 3.14-5, the resulting spallation footprints are extremely small (tenths of square centimeters but several orders of magnitude greater than the diameter of the particle). Penetration through the heat shield includes both the ceramic coating and underlying C-C substrate. Predictions from thermal models of penetrated zones indicate localized temperature increases of several hundred degrees Kelvin, but the effect on pre-

[28] *Solar Probe Risk Mitigation Study*, prepared by The Johns Hopkins University Applied Physics Laboratory, 2006 Mid-Year Report.

[29] *Solar Probe Thermal Protection System Risk Mitigation Study: FY 2006 Final Report*, prepared by The Johns Hopkins University Applied Physics Laboratory under Contract NAS5-01072, Laurel, MD (November 30, 2006); and *ITAR-Restricted Annex* (September 17, 2007).

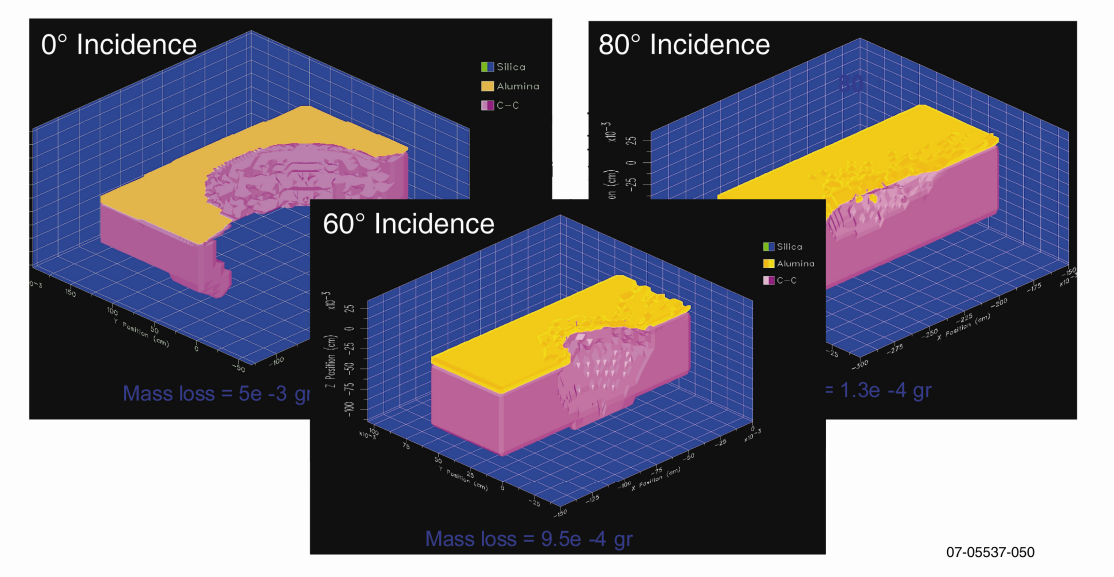

Figure 3.14-5. Predicted spallation footprints for particle impact of heat shield.

dicted equilibrium heat shield temperatures would be negligible. Predictions also indicated that large dust particles would be mostly consumed during the penetration event and that the remaining dust fragments would be vaporized within the large volume of the hot heat shield—no solid dust forms would impact the secondary heat shield. The small, submicrometer dust particles were predicted to be vaporized on impact and to not penetrate the conical heat shield.

By using analysis by similarity for the case of the Solar Probe+ design, it is shown that dust will impact the flat surface of the coated heat shield directly. However, in this case, the exposed heat shield will not be hollow but will be filled with foam essential to maintaining control of the equilibrium temperature of the bus. As before, small dust-particle impacts are not anticipated to be damaging; however, assessment of large-particle impact damage will be more complex. In this case, the heat shield will most likely experience similar spallation footprints; however, unconsumed dust particles will penetrate into the insulating foam structure, which will most likely not affect overall heat shield equilibrium temperatures but may induce localized hot spots with potential line of sight to the spacecraft bus. The number of impacts and size of the particles also will increase because of the increased number of orbits and the increased fluence.

Further studies will need to be conducted to define the number of dust fluence and the statistical size distribution of the particles predicted to impact the heat shield during the multiple ecliptic orbits and to quantify the effects of such impacts on thermal performance. Additional studies will be necessary to characterize the degree of insulation damage by large-particle impacts and the resulting increase in heat conduction through the heat shield. In addition, the effect of spallation on overall spacecraft mass loss rates and the interaction of spallation plumes with the local dust environment will need to be studied further.

3.15. Technical Challenges

Formal risk management begins in Phase A with risk identification. However, the Solar Probe+ mission involves significant new development. We have included in this study a preliminary assessment of program risks and identification of mitigations in order to develop a mission implementation that balances risk with the ability to achieve performance requirements at low cost and on schedule.

Secondary Solar Arrays. The secondary solar arrays are used to generate power during

solar encounters when the primary arrays cannot be used. The technology for this system exists at technology readiness levels (TRLs) 5–9 (depending on the element), including the temperature control system for the secondary arrays. However, Solar Probe+ presents unique environmental challenges, and thus the detailed design must accommodate this environment. In addition, the secondary solar array design includes solar cells and mechanisms that must be qualified for the Solar Probe+ program. If the design or qualification of the secondary solar arrays does not adequately address the near-Sun environment, the ability to generate sufficient power near perihelion may be compromised.

Mitigations include

- Increased power margin for the secondary solar arrays in the encounter operational modes to allow for greater than anticipated degradation (Phase A)
- Increased margin in the temperature control system in the secondary solar array subsystem to allow for greater than anticipated heat loads (Phase A)
- Detailed qualification program for mechanisms, temperature control elements, and solar cells (pre-Phase A/Phase A)
- More detailed thermal modeling to optimize the design of the secondary solar array, including the temperature control subsystem (Phase A)
- Mission design that allows for slow walk-in of perihelion to give opportunity for secondary solar array characterization and tailoring of operations concept before worst-case environmental exposure (incorporated into baseline concept)

Mass Margin. The Solar Probe+ orbit presented in this study requires a high C3, and maximum launch vehicle lift mass is constrained. We have baselined the Atlas V 551 launch vehicle with a STAR-48 third stage for cost; however, the margin on mass for this configuration is lower than usually required at this stage of a program. If significant mass growth occurs, the spacecraft may grow beyond the lift capability of the baselined launch vehicle and third stage.

Mitigations include

- Optimize mechanical structure mass by using composite elements instead of the baselined all-aluminum structure (Phase A)
- Optimize power usage on the spacecraft and the power subsystem design to shrink both primary and secondary solar arrays (Phase A)
- Optimize launch vehicle tailoring and margins to increase lift mass available to spacecraft (Phase A)
- Retain compatibility with Delta IVH launch vehicle with higher lift mass for this orbit (Phase A/B)

Thermal Protection System (TPS) Design and Manufacturing. The TPS is a critical element of the Solar Probe+ mission. Extensive risk mitigation work has been performed to ensure that the TPS concept will provide the needed protection from the solar environment. However, detailed design of the TPS has not been completed given the early phase of the program. If unforeseen problems occur during the design, manufacturing, or testing of the TPS occur, the ability to protect the spacecraft and payload from the near-Sun thermal environment may be compromised.

Mitigations include

- Longer than normal development phases for the Solar Probe+ program, with required schedule margin to allow for recovery should problems occur
- Detailed thermal modeling to be completed early in the program, with sufficient margins on thermal design maintained through program (Phase A)
- Full TPS qualification program included in the cost and schedule as early in the program as reasonably possible to allow for modifications that may be needed (pre-Phase A/Phase A)
- Modular design of TPS and spacecraft interface allows for late delivery of the shield to spacecraft integration (incorporated into baseline concept)

Mechanism Reliability. Mechanisms in the space environment carry some degree of risk, and failures in space of mechanisms have caused complications for missions in the past. In addition, the thermal environment of the near-Sun portion of the orbit provides challenges to the use of mechanisms. If Solar Probe+ mechanisms are inadequately designed, mechanism failure may occur, resulting in degradation or loss of mission.

Mitigations include

- Use of high-heritage mechanisms, including detailed analysis of the suitability of each mechanism for the Solar Probe+ environment (Phase A/B)
- Increased margins on mechanisms and detailed analysis of potential failure mechanisms, including wear and lifetime issues
- Trade study to eliminate mechanisms where possible (Phase A)
- Detailed qualification program for all mechanisms used in flight
- Study to identify workarounds for failure that may occur in flight (Phase A/B)

4.0. COST ESTIMATE

4.1. Cost Estimate Summary

A cost estimate for a complete Solar Probe+ mission was developed using the technical design described in Section 3 of this report. The cost estimate for Solar Probe+ is $739.5M in fiscal year 2007 dollars (FY07$). The Solar Probe+ cost estimate is provided in Table 4.1-1, broken down by NASA Level 2 Work Breakdown Structure (WBS) element and provided in FY07$ and real year dollars (RY$). This estimate is for the full mission cost and includes the launch vehicle and launch services, third stage, all science and scientist participation, and (DSN), environmental testing at the NASA/Goddard Space Flight Center (GSFC), and 7 years of Phase E operations.

Table 4.1-1. Solar Probe+ mission cost table. Reserves have not been applied to Kennedy Space Center (KSC) launch services, payload instruments, or DSN.

MISSION INSTITUTION SUMMARY FOR COST FOR SMD SOLAR PROBE+ ENGINEERING STUDY FY Costs in Real Year Dollars (to the Nearest Thousand); Totals in Real Year and Fixed Year 2007 Dollars						
Cost Element	**Phase A**	**Phase B**	**Phase C/D**	**Phase E**	**Total (Real Year)**	**Total (FY 2007)**
Task 01: Project Management	$1,420	$2,755	$6,955	$8,587	**$19,717**	**$15,636**
Task 02: Project Systems Engineering	$2,219	$5,962	$16,710	$22	**$24,912**	**$21,301**
Task 03: Safety and Mission Assurance	$432	$1,378	$6,666	$1,246	**$9,721**	**$8,015**
Task 04: Science/Technology	$833	$1,235	$3,135	$7,460	**$12,663**	**$9,751**
Task 05: Payload System	$636	$1,800	$4,846	$58	**$7,340**	**$6,264**
Task 06: Spacecraft Bus	$12,132	$57,215	$96,515	$896	**$166,758**	**$144,013**
Task 07: Mission Operations	$200	$1,028	$10,956	$40,835	**$53,020**	**$39,295**
Task 09: Ground Data System	$843	$2,507	$15,029	$295	**$18,674**	**$15,694**
Task 10: Systems Integration and Testing	$231	$2,123	$23,746	$371	**$26,471**	**$21,716**
Task 11: Education and Public Outreach	-	$384	$935	$323	**$1,643**	**$1,414**
Task 12: Mission Design	$496	$1,035	$2,874	$4,863	**$9,268**	**$7,209**
PI Mission Cost	**$19,441**	**$77,423**	**$188,367**	**$64,956**	**$350,187**	**$290,307**
Payload Instruments	$5,305	$33,437	$77,292	-	**$116,034**	**$100,000**
Environmental Testing at GSFC	-	-	$1,714	-	**$1,714**	**$1,398**
Navigation	$90	$210	$1,020	$1,680	**$3,000**	**$2,315**
KSC Launch Services	-	-	$225,100	-	**$225,100**	**$184,468**
Launch Vehicle Third Stage	-	-	$7,700	-	**$7,700**	**$6,078**
DSN	-	-	-	$22,940	**$22,940**	**$16,509**
External PI & Co-I Team, Phases A–D	$681	$2,443	$4,876	-	**$8,000**	**$6,882**
Science Ops. Preparations	-	-	-	$5,000	**$5,000**	**$3,539**
External PI & Co-I Team, Phase E	-	-	-	$50,000	**$50,000**	**$35,394**
Science Ops. Team	-	-	-	$8,000	**$8,000**	**$5,663**
Reserves	**$1,011**	**$24,023**	**$61,103**	**$19,445**	**$105,582**	**$86,933**
Total Mission Cost	**$26,528**	**$137,536**	**$567,172**	**$172,022**	**$903,257**	**$739,489**

Phase A: 5% Reserve
Phase B: 30% Reserve
Phase C/D: 30% Reserve
Phase E: 15% Reserve

4.2. Cost-Estimating Methodology and Independent Cost Estimate

4.2.1. Cost-Estimating Methodology

To determine mission cost feasibility, The Johns Hopkins University Applied Physics Laboratory (APL) conducted a rigorous "bottom-up" cost estimate and an independent parametric costs analysis. The bottom-up methodology was used to estimate the Solar Probe+ mission cost, integrating a top-level schedule, Work Breakdown Structure (WBS), resource-level identification, and risk assessment (see Section 3.15).

APL follows APL's Cost-Estimating Manual and APL's Product Assurance System (PAS) document SDO-11386 that outlines cost and schedule development and management standards for the Space Department. The cost-estimating process is described below, with detailed cost information presented in Section 4.5.

Experienced functional supervisors and lead engineers are responsible for estimating the required labor resources and skill mix. The labor estimate is based on the technical concept, engineering experience, an in-depth understanding of technical requirements, a disciplined engineering process to identify assumptions and cost sensitive areas, and experience on similar programs. Direct labor requirements are estimated by labor classification. Direct labor hours associated with all phases of Solar Probe+ are included in the cost estimate. APL direct (and indirect) labor rates are based on the forward-pricing rates submitted to the designated Administrative Contracting Officer (ACO) and the Defense Contract Management Command (DCMC) assigned to APL. These rates are applied to direct costs in accordance with APL practices. Procurement costs are based on vendor rough orders of magnitude (ROMs) or relevant recent experience. Estimates for miscellaneous other direct costs (MODC) are discrete for specific identified elements and based on a cost-estimating relationship (CER) for others. The CERs are based on actual values for similar programs and are adjusted by decrementing the CERs for like elements priced discretely. Travel has been estimated based on a CER of similar programs. For the purposes of this costing exercise, past experience included the MESSENGER, New Horizons, and STEREO missions.

This process resulted in a detailed bottom-up ("grass roots") cost estimate in which team members populate spreadsheet templates with resources against WBS elements that span the project schedule in 1-month increments. These lower-level inputs are quality-checked against historical data for omissions, overlaps, or inconsistencies. They also account for costs for APL payload administration, ground support equipment, and emulators. The internal and external WBS data are then incorporated into the project-level cost estimate using APL's Resource Management Information System (RMIS) to produce mission costs in fiscal year 2007 dollars (FY07$) and real year dollars (RY$).

Several detailed reviews are then conducted among the study manager, the technical leads, and their functional supervisors, and costs are revised accordingly. Near the end of this study period, an independent peer review evaluates the draft study final report for technical and costing completeness, followed by a Space Department management review of the final cost plan. These reviews allow management and senior staff to evaluate the final report, to review the costs and assumptions on which the costs are based, and to access cost realism. Any omissions or errors are exposed and corrected during this process.

The Solar Probe+ cost estimate, as with the entire engineering concept, assumes no contributions from foreign partners or non-NASA U.S. government agencies.

4.2.2. Cost Estimate Validation: Independent Cost Estimate

4.2.2.1. Summary

An independent cost estimate (ICE) was prepared for APL's portion of the Solar Probe+

spacecraft to validate the comprehensive, bottom-up Program Office estimate (POE), quantify cost risks, and determine the sufficiency of cost reserves. The ICE costing methodology is based on parametric cost-estimating models and risk estimation tools used throughout the space exploration and observation community. ICE results at the third WBS level enable detailed comparisons with the POE.

The ICE results correspond to approximately 85% of the total Solar Probe+ Phases A–D. They account for hardware and flight software costs for Phases A–D of the spacecraft and associated management, engineering, integration, and testing activities.They do not account for costs of ground systems or the mission and science operations centers, nor do they account for the costs of instrument design and development.

The Solar Probe+ program presents extremely challenging and unique performance requirements. Unfortunately, the most appropriate technical solutions are not captured in the space industry's cost databases and models used for generating ICEs. For instance, the solar environment in which Solar Probe+ will operate requires unique thermal shielding and solar array mechanisms. The ICE attempts to represent the costs of these solutions in several ways. For the Thermal Protection System (TPS), a complexity factor was developed from cost data on the Space Shuttle nose cone. A mechanism cost equation was used to estimate the cost of the solar array mechanism. To estimate the possible range of final subsystem costs, larger mass growth than typical for APL missions was assumed. When estimating flight software development, claims about the availability and applicability of heritage software code were discounted, and mostly new software code was assumed to be needed. All of these assumptions and modeling decisions resulted in conservative ICE results that capture the technical and cost-estimating risks inherent in such a unique mission.

Cost elements that were accounted for by the ICE include the following:

- Program management (PM; NASA WBS 01)
- Systems engineering, including mission analysis (SE; WBS 02)
- Mission and safety assurance (M&SA; WBS 03)
- Payload administration and emulators, APL's portion of payloads (WBS 05)
- Spacecraft elements (WBS 06)
- Attitude determination and control subsystem (ADACS)
- Flight software development
- Structural and mechanical, including harness
- Thermal control
- Propulsion
- Electrical power and distribution
- Command, control, communications, and data handling (CC&DH)
- Telecommunications
- Launch and early orbital operations (30 days), Phase D portion of mission operations (WBS 07)
- Integration and testing (I&T, WBS 10)

ICE results are generally consistent with the POE, where the ICE point estimates are based on the current best estimate (CBE) subsystem masses provided by APL systems engineers. POEs for the spacecraft integrating functions of PM, SE, and I&T are within 5% of the corresponding ICE point estimates. (The ICE point estimate bases estimated cost on the CBE masses.) The spacecraft POE and point-estimate ICE are within 3.1%. Estimates for smaller cost elements related to payload SE, mission operations support, and ground systems equipment do show larger variances, however. This is because of the conservativeness of our ICE assumptions and to ICE cost equations whose scope are broader than some POE elements.

When technical and cost-estimating risks are considered, ICE results indicate that properly managed reserves will likely be sufficient to complete Phase D without cost overruns. The spacecraft bus POE with 30% reserves falls at the 70th percentile of the corresponding ICE S curve. The S curve is a graphic representation of the cumulative probability distribution (CPD) of

likely costs that takes into account uncertainty related to mass growth and cost estimating. A 70th percentile value corresponds to a 30% likelihood of a cost overrun. The I&T POE with cost reserves falls at the 60th percentile; the SE/PM/M&SA POE falls at the 65th percentile. All of this suggests that the mission is achievable at proposed funding levels, although it will require careful management of cost reserves, shifting dollars to cover risks as they arise.

4.2.2.2. Methodology

4.2.2.2.1. Ground Rules and Assumptions

The following ground rules and assumptions guided preparation of the Solar Probe+ ICE:

- Solar Probe+ costs are presented in fiscal year 2007 (FY07) dollars. Because the ICE was estimated in FY08 dollars, a 3.1% annual deflation rate was used to adjust the Solar Probe+ ICE estimate from FY08 to FY07 dollars.
- Spacecraft estimates include the costs by subsystem to design, produce, integrate, and test a single spacecraft. Also included are estimated costs for management, SE, and I&T of spacecraft subsystems.
- The spacecraft estimate includes effort to design, code, and flight test and test bed software modules, software development management, and integration of software and hardware.
- Risk-adjusted technical and performance inputs to the model are provided by the Solar Probe+ system engineers, based on their technical assessments and judgments.
- Payload instrument costs were not estimated, but their cost provided a basis for estimating APL SE costs in support of instrument design and development.

4.2.2.2.2. Parametric Cost-Estimating Models and Data Used to Generate ICEs

Spacecraft Hardware, Launch Vehicle Adapter, and Other Program Costs. The ICE used the Eighth edition of the Air Force's Unmanned Spacecraft Cost Model (USCM8) to estimate nonrecurring and recurring costs at the subsystem level. USCM8 Version 1.1 was published by Tecolote Research, Inc., in October 2001.[1] USCM8 provides cost-estimating relationships (CERs) for estimating unmanned, Earth-orbiting space vehicle costs. According to the USCM documentation:

> Each CER was developed through rigorous statistical analysis of hypothesized cost drivers. This was done by generating hypotheses relating cost to those underlying parameters thought to be cost drivers. Each tested hypothesis was based on a sound understanding of the engineering principles that might drive cost. Selected CERs had to demonstrate favorable statistics and, from a behavior standpoint, be consistent with engineering expectations. As a result, CERs that did not make sound engineering sense were not selected despite having good statistical measures.

The USCM8 subsystem cost equations used for the Solar Probe+ ICE are mass-driven. Nonrecurring equations represent a "new design" effort and must be adjusted for heritage assumptions; therefore a factor (f_{ND}) based on percentage new design was applied to the nonrecurring CER to account for anticipated heritage as shown below:

$$f_{ND} = \frac{(2.8ND + 0.2)}{3},$$

where ND ($0.0 < ND < 1.0$) is the new design fraction.

This factor adjusts the USCM8 nonrecurring equation output to estimate more accurately the true costs of the nonrecurring effort experienced by programs in the USCM8 database. The USCM8 equations enable analysts to estimate quantitatively the contribution of design heritage to final cost and were used for all Solar Probe+ hardware subsystems.

[1] *Unmanned Space Vehicle Cost Model, Eighth Edition (USCM8)*, Tecolote Research, Inc., Goleta, CA, www.uscm8.com (October 2001).

Cost equations for such nonhardware elements as PM and SE are driven on the estimated costs of spacecraft hardware and software and I&T. The equations are derived from a total of 44 spacecraft missions. Eleven of the missions were funded by NASA, 20 were funded by the U.S., and the remaining 11 were funded commercially.

Three cost estimates, representing the best, most-likely, and worst cases, were generated for each spacecraft subsystem and cost element. The three estimates provide the bases for probabilistic cost estimates, described below, which enable the ICE to account for the effects of cost uncertainty. Based on a recent study by The Aerospace Corporation on spacecraft mass growth during the design and development phases, subsystem masses provided by APL system engineers were adjusted for the three estimates as follows: CBE masses were provided by the system engineer. The best-case estimates are based on the CBE masses plus 10%; the most-likely estimates, CBE masses plus 30%; and the worst-case estimates, CBE masses plus 50% (see Table 4.2-1).

The TPS is unique and more technologically complex than typical aluminum structural components. Accordingly, ICE analysts sought historical data on large carbon–carbon structures that could be used to adjust the USCM structure/mechanical CER. A search of the NASA–Air Force Cost Model (NAFCOM) data set identified the Space Shuttle nose cone as an analog. Detailed cost data was used to develop a complexity factor that adjusts the USCM structure cost equation for the relatively high cost per pound of carbon–carbon structures.

For the electrical power subsystem, ICE analysts applied the USCM structure/mechanical CER to estimate costs of the secondary solar array's complex mechanical components. The remainder of the subsystem's components was estimated with the USCM electrical power subsystem CER.

Estimating the cost of the telecommunications subsystem from historical data proved challenging. A check of the USCM8 and NAFCOM data sets identified only one mission, Tracking and Data Relay Satellite System (TDRSS), with dual Ka/X-band capabilities like those currently proposed for Solar Probe+. A new telecommunications cost equation was generated from USCM8 cost data that weighted more heavily the TDRSS historical data; that equation was used to estimate the Solar Probe+ telecommunications subsystem. Although the new equation is likely a better estimator for complex dual-band telecommunications subsystems, its statistical error is substantially larger than the standard equation, and cost results are less reliable.

Flight Software Development. The open-source COCOMO-II model developed by Barry Boehm's University of Southern California software research group was used to estimate costs of flight software development. COCOMO-II bases its cost estimate on the effective amount of code that must be developed, adjusted for heritage code that can be adapted, or used without change and productivity. COCOMO-II products include a time-phased profile of development effort and low, most-likely, and high cost estimates, which for Solar Probe+ are based on APL labor rates.

The estimated total number of source lines of code to be developed is 110,000; 75,000 of those lines of code serve guidance and control functions, and the remaining 35,000 lines serve command and data handling functions. ICE analysts chose not to discount the estimated effort for heritage code, including code that might be available from the Radiation Belt Storm Probes (RBSP) mission. Accordingly, the ICE results should be regarded as very conservative estimates of flight software development effort and costs.

Payload Systems Engineering. Although the Solar Probe+ instruments are outside the scope of the ICE, an ICE was generated for APL's effort for instrument SE and product assurance (specifically, APL WBS 210 Payload Administration and WBS 280 Payload Emulators). The SE cost factor from the NASA In-

strument Cost Model (NICM) was applied to the total instrument cost basis to estimate APL's instrument SE costs. Because the factor applied to all SE activities associated with instrument design, production, and I&T, the ICE result likely overestimates APL efforts directed at ensuring interoperability of spacecraft bus and payloads.

Accounting for Cost Uncertainty. Reuse of heritage designs from previous APL missions is critical to ensuring that the Solar Probe+ mission is executable and affordable, which leads to a pressure for adjusting cost estimates for likely heritage savings. However, recent analysis of NASA missions indicates that, after initial design, there is a trend for increases in mass and cost. Recent unpublished research of spacecraft mass growth finds 22–25% mass growth is typical, and mass growth of 50% or more is not uncommon. The ICE heritage design assumptions are conservative, in that we have assumed reuse will be minimal. Most functional subsystems within the spacecraft bus, for example, were modeled assuming new design would be 80–100%.

Our ICE approach tries to quantify the cost risk inherent in the estimated costs. It recognizes that cost estimates represent predictions about future costs and uses Monte Carlo simulation to assign probabilities to those predictions.

Two kinds of uncertainty contribute to discrepancies between predicted and actual costs:

1. Uncertainty in input variables such as mass and new design factor assumptions.
2. Statistical uncertainty in CERs and cost factors.

The Monte Carlo simulation accounts for both kinds of uncertainties as follows:

- Subsystem mass uncertainty is applied to all subsystem mass estimates without contingency. The uncertainty is modeled using a triangular probability density function (PDF) based on a study prepared by The Aerospace Corporation, which shows mass growth the minimum mass growth to be 10%, the most-likely mass growth to be 30%, and the maxi-

Table 4.2-1. Subsystem masses used in the ICE to estimate Solar Probe+ subsystem costs account for the likelihood during the design phases of mass growth. TT&C, telemetry, tracking, and control.

	Mass, kg			
	CBE	Low	Most Likely	High
Total Dry Mass	**452.4**	**497.7**	**588.1**	**678.6**
Payload	**54.6**	**60.1**	**71.0**	**81.9**
Instruments	***47.2***	***51.9***	***61.4***	***70.8***
Anticipated Instrument HW	***7.4***	***8.1***	***9.6***	***11.1***
Spacecraft Bus	**397.8**	**437.6**	**517.1**	**596.7**
Propulsion	21.0	23.1	27.3	31.5
ADACS/GCS	30.4	33.4	39.5	45.6
TT&C	10.4	11.4	13.5	15.6
C&DH	12.7	14.0	16.5	19.1
Thermal	15.7	17.3	20.4	23.6
Electrical Power	122.7	135.0	159.5	184.0
Primary Array	*25.1*	*27.6*	*32.6*	*37.6*
Secondary Array	*64.1*	*70.5*	*83.3*	*96.1*
Power Storage	*8.0*	*8.8*	*10.4*	*12.0*
Power Conditioning	*17.3*	*19.0*	*22.5*	*26.0*
Mechanisms	*8.2*	*9.1*	*10.7*	*12.3*
Harness	18.5	20.4	24.1	27.8
Heat Shield	70.5	77.6	91.7	105.8
Structure	72.9	80.2	94.8	109.4
Communications	23.0	25.3	29.9	34.5

mum mass growth to be 50%. The results of this study were published.[2]

- Uncertainty in the new design factor is modeled by using a log-normal PDF with a mean of 1.0 and a standard deviation in unit space of 0.30, which accounts for the uncertainty in the new design factor assumption.
- The uncertainty in the nonrecurring and recurring CERs were modeled by using a log-normal PDF with a mean of 1.0 and a standard deviation in unit space equal to the percentage standard error of the particular CER, which ranges from 0.12 to 0.44.
- To represent the observation that increases in one element's cost are reflected in increased costs for other cost elements—a frequently observed trend in the cost histories of space systems—the values selected during the Monte Carlo simulation with an intercorrelation matrix with all elements are statistically correlated at a low level (Pearson $r = 0.097$). The effect is that, for example, selection of a high (or low) structure costs will result in correspondingly higher (lower) costs for management, SE, I&T, etc.
- A Monte Carlo model is built by using the commercial Crystal Ball simulation tool. Inputs to the model include the subsystem PDFs and correlation matrix. The model simulates the mission being performed thousands of times. For each iteration, a cost prediction for each element is selected at random based on its PDF and correlation constraints.
- Adjusted cost predictions are summed at the completion of every iteration, after predictions have been drawn and adjusted for every cost element.
- Finally, after completion of 10,000 iterations, the element and aggregate outputs are characterized statistically.

The result is a CPD that reports the probability of each predicted cost's occurrence. The graphical representation of the CPD is sometimes called an S curve. CPDs offer three advantages over adding the costs of individual elements to predict total cost:

1. They avoid the bias inherent in arithmetic summing of point estimates, which tends to misstate total cost.
2. They provide a sense of the confidence we should associate with the proposed cost. If, for example, the cost proposal is at the 70th percentile, we would, if our model has faithfully represented the "known unknowns," expect to overrun that prediction 30% of the time.
3. The shape of CPDs suggests the size of the cost overrun that might be incurred in cases of where technical or other risks are not effectively controlled. All things considered, an estimate with a small difference between the 50th and 70th percentile predictions is preferable to one with a large difference because fewer cost reserves are required to assure mission success.

4.2.3. Results

The ICE results account for approximately 85% of APL's costs during Phases A–D. Figure 4.2-1 shows the ICE S curve for Solar Probe+ costs. Table 4.2-2 provides a summary of ICE results and comparison with the POE, by NASA WBS element.

The element POEs generally are consistent with the ICE point-estimate results. The estimates for the spacecraft integrating functions of PM, SE, and I&T are within 8%. The spacecraft bus POE and ICE point estimate are within 9%. Estimates for smaller cost elements related to payload SE and mission operations support show larger variances because of conservative ICE assumptions and ICE methods that include other costs in their calculations.

When technical and cost-estimating risks are considered, the ICE results indicate that reserves will likely be sufficient. The spacecraft bus POE with 30% reserves falls at the 70th percentile of the corresponding ICE S curve, a

[2]Covert, R., *Ten Common Things Wrong with Cost Risk Analysis*, Presented at 76th SSCAG, Hampton Roads, VA (October 22–23, 2002).

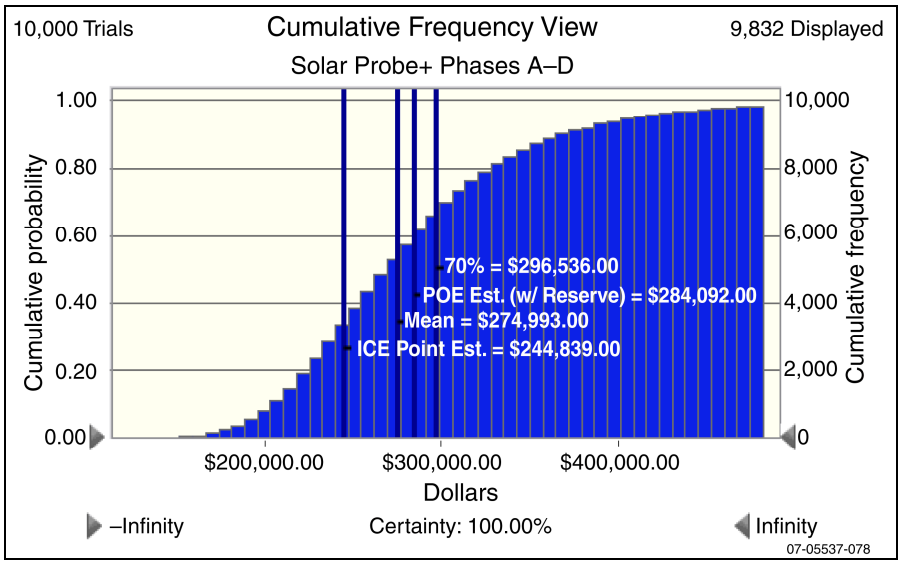

Figure 4.2-1. Solar Probe+ ICE S curve. (All costs are in FY07$M.)

graphic representation of the CPD of likely costs that takes into account uncertainty related to mass growth and cost estimating. The 70th percentile value corresponds to a 30% likelihood of a cost overrun. The I&T POE with cost reserves falls at the 60th percentile; the SE/PM/M&SA POE falls at the 65th percentile. All of this suggests that the mission is achievable at proposed funding levels although it will require careful management of cost reserves, shifting dollars to cover risks as they arise.

Key results from the ICE-POE comparison are highlighted below.

Program Management, Systems Engineering, and Safety and Mission Assurance (NASA WBS Cost Elements 01, 02, and 03). USCM8 provides a single cost equation for estimating costs of these three cost elements. Correspondence between the ICE and POE for the sum of three elements is high. The ICE point estimate, corresponding to the estimated cost using the CBE mass as input to the USCM cost equation, is $49.5 million, only 7% (or $3.4 million) more than the POE estimate of $46.1 million. The POE falls at the 47th percentile on the corresponding ICE S curve. The likelihood of the POE with 30% cost reserves rises to the 65th percentile on the ICE S curve. In other words, the POE with cost reserves will be sufficient is slightly less than two-thirds of most cases for APL's performance of its management and engineering functions.

Spacecraft Bus (WBS Element 06). The spacecraft ICE point estimate of $156.0 million is $12.7 million, or 9% higher than the spacecraft POE of $143.3 million. Some of the difference is attributable to the flight software development estimates. The flight software estimate difference of $10.1 million is a consequence of different assumptions about the reuse of RBSP and other heritage source code: The ICE does not discount effort for the availability of heritage code.

The largest cost difference among the hardware elements is associated with the electrical power subsystem. The ICE point estimate is $18.1 million, $8.5 million or 32% less than the POE of $26.2 million. The higher POE is attributed to the complexity of the secondary solar array.

The ICE for the avionics and telecommunications subsystems is $48.7 million, $9.1 million or 23.2% more than the POE of $39.5 million. The telecommunications ICE result is biased higher by the reliance on TDRSS as the most analogous spacecraft. Even with the abovementioned discrepancies among certain spacecraft subsystems, the POE with 30% cost reserves for the spacecraft bus falls at the 70th percentile of the ICE S curve.

Payload (WBS Element 05). Because NASA has budgeted separately for instruments, APL's payload costs are limited to Payload Administration (APL WBS 210) and Payload Emulators (APL WBS 280). The NICM SE cost

Table 4.2-2. Comparison of ICE point estimate and POE, by NASA WBS element. [All costs are in fiscal year 2007 millions of dollars (FY07$M).]

NASA WBS	Description	POE WBS Elements	ICE Results			POE		ICE-POEΔ		POE + Cost Reserve	
			Point Est. FY07$M	Mean Est. FY07$M	Std. Dev. FY07$M	FY07$M	ICE Percentile	FY07$M	Percentage	FY07$M	ICE Percentile
TOTAL	**(Spacecraft Only—No$100M Payload)**		**$244.8**	**$275.0**	**$69.5**	**$218.5**	**20%**	**$9.2**	**4.2%**	**$284.1**	**65%**
01, 02, 03	**PM, SE, S&MA**	**1xx**	**$49.5**	**$56.2**	**$29.7**	**$46.1**	**47th**	**$3.4**	**7.4%**	**$59.9**	**65%**
01	*Project Management*	11x	$24.7	$28.0	$15.0	$13.9	10th	$10.8	77.8%	$18.1	30%
02	*Systems Engineering*	12x, 13x	$24.7	$28.0	$15.0	$25.0	50th	$(0.3)	–1.2%	$32.5	75%
03	*Safety and Mission Assurance*	14x				$7.1		N/A	N/A	N/A	N/A
05	**Payload (Management Only)**	**210, 280 only**	**$12.4**	**$12.4**	**$5.0**	**$6.2**	**10th**	**$6.2**	**99.4%**	**$8.1**	**20%**
06	**Spacecraft**	**3xx**	**$156.0**	**$173.7**	**$28.9**	**$143.3**	**15th**	**$12.7**	**8.9%**	**$186.3**	**70%**
	ADACS	31x	$12.5	$14.1	$5.1	$11.5	30th	$1.0	8.3%	$15.0	65%
	Flight Software	38x	$24.1	$27.1	$4.5	$14.1	1st	$10.1	71.5%	$18.3	10%
	Structures/Thermal	34x, 35x	$47.3	$53.2	$18.6	$47.1	45%	$0.2	0.3%	$61.3	75%
	Propulsion	39x	$5.4	$5.9	$2.3	$4.5	30th	$0.9	19.4%	$5.9	60%
	Electrical Power	32x, 33x	$18.1	$19.6	$4.3	$26.6	90th	$(8.5)	–32.0%	$34.5	95%
	TT&C, C&DH, and Communications	36x, 37x	$48.7	$53.4	$13.6	$39.5	10th	$9.1	23.2%	$51.4	50%
07	**Mission Operations (Prelaunch)**	**5xx**	**$5.5**	**$5.4**	**$3.6**	**$3.2**	**30%**	**$2.3**	**71.2%**	**$4.2**	**50%**
10	**Systems I&T**	**4xx**	**$21.4**	**$28.0**	**$27.0**	**$19.7**	**50%**	**$1.7**	**8.7%**	**$25.6**	**60%**

factor used by the ICE predicts the cost of all instrument-related activities will be $12.4 million (point estimate), $6.2 million or 99% more than the POE of $6.2 million. With cost reserves included, the POE cost is $8.1 million. Given the ICE cost factor estimates all instrument-related SE, the difference is not surprising.

Mission Operations (WBS Element 07). The only mission operations element estimated by the ICE is launch operations and orbital support. The ICE point estimate, based on a cost factor, is $5.5 million, $2.3 million or 71% more than the POE of $3.2 million. The POE with cost reserves is $4.2 million.

Systems Integration and Testing (WBS Element 10). The ICE point estimate of $21.4 million is within $1.7 million, or 9%, of the POE of $19.7 million. Note, however, that the ICE does not include costs for integration of payloads with the spacecraft.

4.3. Schedule

For costing and engineering planning purposes, the Solar Probe+ mission used the top-level milestone schedule shown in Figure 4.3-1. The schedule consists of a 13-month Phase A, a 19-month Phase B, a 19-month Phase C, a 23-month Phase D, and a 7-year Phase E. Funded schedule reserves totaling 9.5 months [6.5 weeks for Phase B (1.0 month/year), 11.5 weeks for Phase C (1.8 months/year), and 20 weeks for Phase D (2.6 months/year)], as shown in the project master schedule, are funded at the peak burn rate for cost-estimating purposes.

The presented schedule is reasonable, based on recent experience. Table 4.3-1 compares the Solar Probe+ schedule with three recent, analogous, APL-led missions that successfully completed Phases A–D.

Solar Probe+ Summary Schedule

Task Name	Start	Finish
Mission Milestones		
Mission Confirmation Review (MCR)	**08/04/2009**	**08/04/2009**
Mission Design Review (MDR)	**03/23/2009**	**03/23/2009**
Preliminary Design Review (PDR)	**06/23/2011**	**06/23/2011**
Critical Design Review (CDR)	**12/18/2012**	**12/18/2012**
Integration and Testing (I&T) Start	**05/31/2013**	**05/31/2013**
Pre-Environmental Review (PER)	**04/08/2014**	**04/08/2014**
Pre-Ship Review (PSR)	**02/05/2015**	**02/05/2015**
Launch	**05/20/2015**	**05/20/2015**
Project Phases		
PHASE A	**04/01/2009**	**03/31/2010**
Instrument/Spacecraft Concept Design	04/01/2009	03/31/2010
PHASE B	**04/01/2010**	**10/31/2011**
Instrument/Spacecraft Preliminary Design	04/01/2010	09/14/2011
Funded Schedule Reserve	**09/15/2011**	**10/31/2011**
PHASE C	**11/01/2011**	**05/31/2013**
Instrument Design, Fabrication, and Assembly	11/01/2011	01/10/2013
Instrument Reserve	**01/11/2013**	**03/11/2013**
Spacecraft Design, Fabrication, and Assembly	11/01/2011	03/11/2013
Funded Schedule Reserve	**03/12/2013**	**05/31/2013**
PHASE D	**06/01/2013**	**06/18/2015**
Integration and Testing (APL)	06/01/2013	03/25/2014
Ship to GSFC	03/26/2014	04/08/2014
Environmental Test at GSFC	04/09/2014	08/06/2014
Final Performance Test at GSFC	08/07/2014	09/05/2014
Funded Schedule Reserve	**09/08/2014**	**02/05/2015**
Ship to KSC	02/06/2015	02/19/2015
Launch Campaign	02/20/2015	05/19/2015
Launch Checkout & Early Operations	05/20/2015	06/18/2015
PHASE E	**06/19/2015**	**04/29/22**

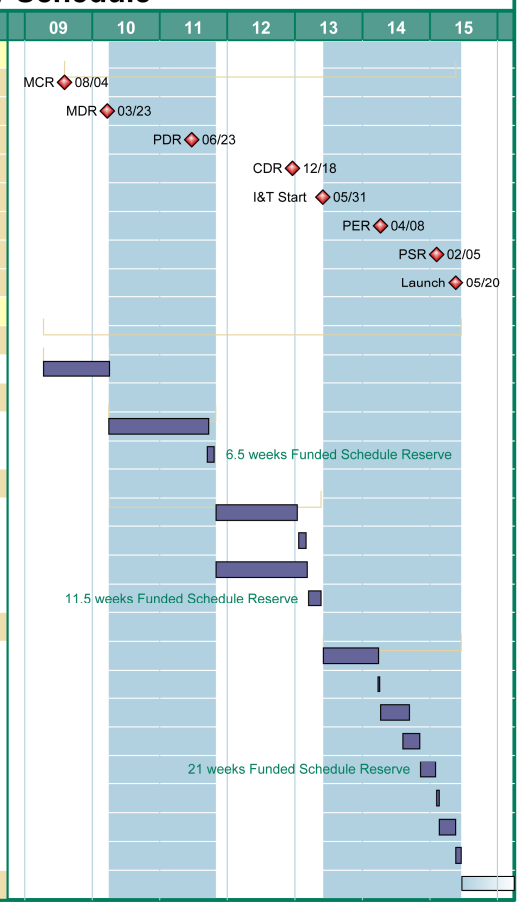

07-05537-077

Figure 4.3-1. Solar Probe+ summary schedule.

Table 4.3-1. Comparison of Solar Probe+ schedule with three recent missions.

Mission	Phases A/B (months)	Phases C/D (months)
MESSENGER	20	38
New Horizons	16	41
STEREO	29	60
Average	*22*	*46*
Solar Probe+ Schedule	**24**	**50**

Per NASA task order NNN07AA15T, Phase A is assumed to begin in 2009. Phases A and B will involve the activities typical to those phases, including instrument accommodation and development and documentation of the flowdown of the mission and science requirements to the subsystems, instruments, ground systems, and mission operations. During this phase, procurement activities for all major subcontracts will be initiated as the requirements for these components are determined. By the end of Phases A/B, subcontract selection should be complete, and all vendors should be under contract.

Phases C/D will include the initiation of the detailed design process and will end with the delivery of the fully integrated spacecraft to the launch site. The 50-month Phases C/D allow for ample reserve during integration and testing (I&T).

Phase E will start 30 days after launch and will continue for 7 years. Phase E will end 2 months after the 24th solar pass.

4.4. Work Breakdown Structure and Cost Detail

The Solar Probe+ mission cost estimation process used a level-three Work Breakdown Structure (WBS), shown in Figure 4.4-1. This WBS is consistent with the NASA standard WBS defined in Appendix G of NPR 7120.5D, and it will be used to allocate responsibility and resources during all phases of the Solar Probe+ project.

4.4.1. Work Breakdown Structure Dictionary

The following is a summary of the descriptions of each WBS element, along with top-level costing assumptions, as appropriate.

WBS 01: Project Management. This WBS includes project management and business management, administrative support and earned-value management, schedule and resource control, subcontract management, technology transfer, and reporting of technical and financial status to NASA. It also includes project scientist, export control issues, online documentation, and design review support. Project management staffing levels are based on actual expenditures on MESSENGER, New Horizons, and STEREO.

WBS 02: Project Systems Engineering. This WBS includes the mission system engineer, spacecraft system engineer, reliability engineering, system verification, electromagnetic compatibility (EMC)/electromagnetic interference (EMI) system engineering, interface control documentation, onboard fault protection, and precision onboard timekeeping. Systems engineering staffing levels are based on recent experience and have been augmented in recognition of the mission design complexity and reliability issues that are inherent to this mission.

WBS 03: Safety and Mission Assurance. This WBS includes performance assurance, contamination, safety, hardware quality assurance, spacecraft charging, reliability engineering (separate from that listed in WBS 02), parts engineering, software quality assurance, contamination, and configuration control. Staffing levels are based on past experience, but augmentations have been made to accommodate current NASA safety and mission assurance practices.

WBS 04: Science Team. This WBS includes the project scientist and deputy project scientist during Phases A–E as well as project support to science teams and payload interface

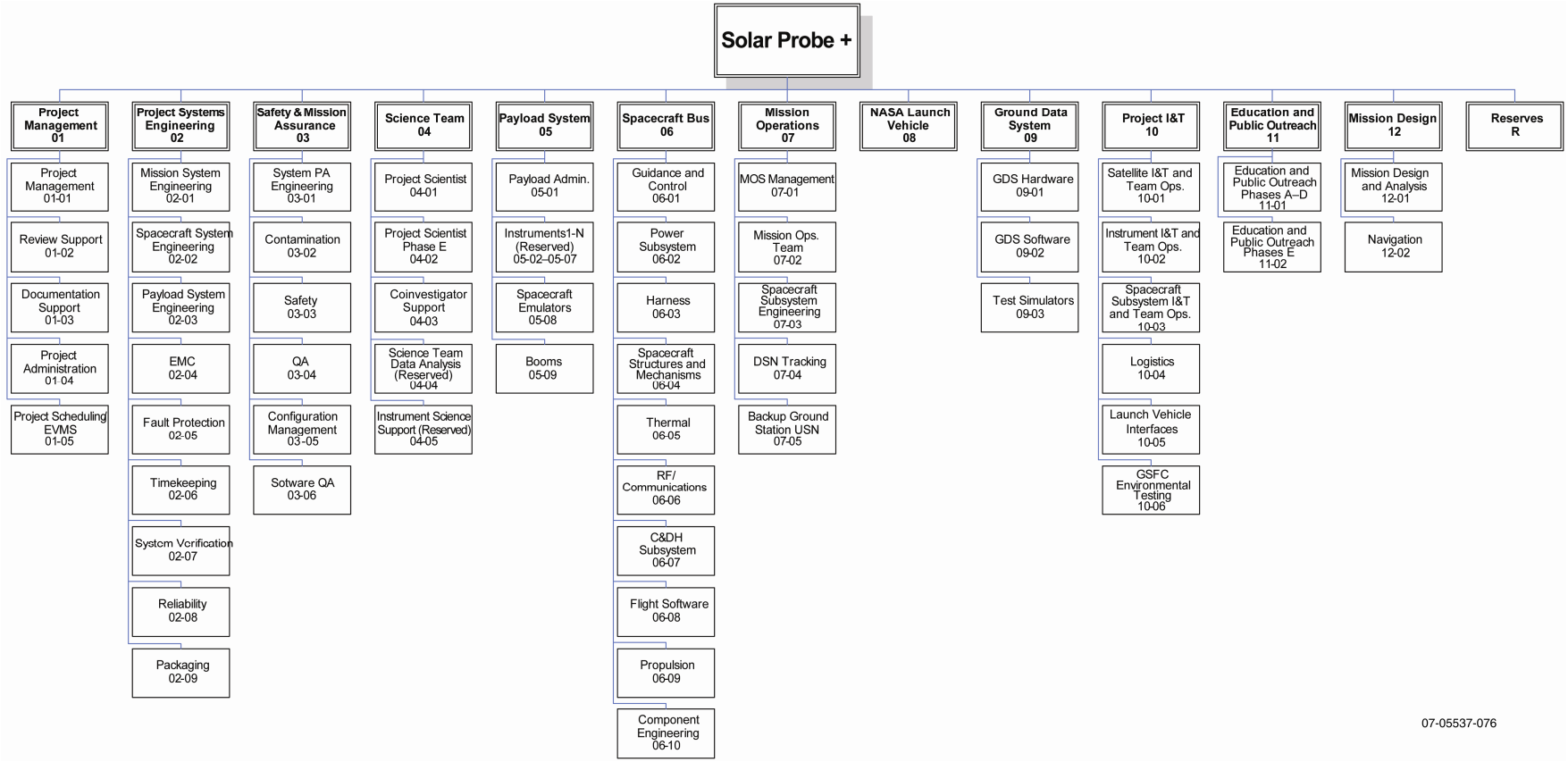

Figure 4.4-1. The level-three WBS for the Solar Probe+ mission.

engineering. It is assumed that the mission provider will have a project scientist and support staff. Staffing levels for this portion are based on recent experience with MESSENGER, New Horizons, and STEREO.

It is further assumed that the payload suite and associated principal investigator (PI) and coinvestigators (Co-Is) will be competitively selected and therefore will not necessarily be associated with the mission provider's institution. For this reason, costs that are directly associated with these portions of the science effort are shown separately from the rest of WBS 04 in Table 4.1-1. These "external" costed subelements are as follows:

- PI and Co-I team for Phases A–D
- PI and Co-I team for Phase E
- The effort required for the science team to prepare for science operations. This subelement is active in Phases C/D Science operations in Phase E

The costs for these subelements given in Table 4.1-1 were provided by the Solar Probe+ Science and Technology Definition Team (STDT). These costs are deemed by the STDT to be sufficient to produce the head-turning science expected of Solar Probe+.

In addition, the STDT strongly recommends that a Participating Science Program (PSP) be established in order to broaden the pool of contributors to Solar Probe+ science beyond those of the selected science team. The STDT has recommended that this PSP be funded at $8M, in real year dollars (RY$), during Phase E. However, because this recommendation falls outside the scope of this study, it is not included in Table 4.1-1.

WBS 05: Payload. This WBS includes payload administration as well as the NASA payload cost for the selected instruments for total mission cost reporting. This WBS also includes spacecraft emulators to be supplied to the instrument teams. The complete instrument payload package cost is held at $100M in fiscal year 2007 dollars (FY07$) per NASA task order NNN07AA15T. It is assumed that this cost includes any instrument-specific data processing units and cost reserves necessary to ensure on-cost delivery of the payload.

WBS 06: Spacecraft Bus. This WBS element is active in Phases A–D. It includes the effort associated with definition, engineering, design, fabrication, procurements, and assembly and testing of the spacecraft bus and components. After the subsystems are delivered to spacecraft-level I&T, the effort to support spacecraft integration is captured under a spacecraft I&T WBS.

WBS 07: Mission Operations. This WBS element contains the entire engineering team during Phase E and mission operations support during Phases A–D. It also includes Deep Space Network (DSN) costs. The mission operations phase for Solar Probe+ will indeed be complex. Costs for this WBS are based on the analogous efforts for MESSENGER (which has a similar numbers of planetary flybys) and has been augmented based on lessons learned from MESSENGER and the added complexity of Solar Probe+.

DSN costs were estimated by using the Jet Propulsion Laboratory DSN Aperture Fee Tool.

WBS 08: NASA Launch Vehicle. This WBS includes the NASA-supplied launch vehicle and is used for reporting total mission cost only. The mission design assumes an Atlas V 551 launch vehicle. The cost presented for the launch vehicle is from an estimate received in February 2008 from NASA/Kennedy Space Center (KSC).

In addition, Solar Probe+ will use a STAR-48BV third stage. A cost estimate was obtained from ATK for $5.6M in RY$. This estimate has been augmented in order to cover potential additional engineering activities associated with the third stage. (In addition, a full-time-equivalent I&T engineer dedicated to third-stage I&T has been included in WBS 10). Note also that, unlike with the Atlas V 551, ***30% reserve has been applied to the cost of the third stage***. A more complete discus-

sion of the third stage is provided in Section 3.1.7.

WBS 09: Ground Data System (GDS). This WBS element is active in Phases A–D. This effort contains the prelaunch GDS and mission operations system (MOS) efforts, including GDS hardware and software such as test simulators to support spacecraft and mission operations testing. For the costing purposes, we have assumed eight test beds. Based on past experience, this number seems prudent.

WBS 10: Project Integration and Testing. This WBS element is active in Phases A–D. This effort includes the I&T team and the subsystem engineers when they are supporting spacecraft-level I&T. Costing of the WBS element assumes all normal I&T functions will occur at APL with the exception of thermal vacuum and acoustic and shock testing. These test are assumed to take place at NASA/Goddard Space Flight Center (GSFC). The costs for these external activities are shown separately in Table 4.1-1.

WBS 11: Education and Public Outreach (E/PO). This WBS includes all E/PO costs associated with the Solar Probe+ mission. During this study., E/PO was not investigated in depth, but a program similar to that of STEREO is envisioned. A mission to the Sun offers many obvious exciting opportunities, especially with the in situ elements. For this study, the E/PO allocation was defined as 0.5% of the Phases A–E cost (less the launch system).

WBS 12: Mission Design. This WBS includes the APL effort and subcontractor support for mission design, navigation, and flight dynamics design and analysis in Phases A–E. It is based on experience with MESSENGER and New Horizons.

WBS R: Reserves. This WBS contains the project funding reserves.

Reserves are calculated as the percentage of funds to go within each phase. Although reserves are not normally held on Phase A activities, we felt it prudent to include 5% on the Solar Probe+ Phase A in recognition of the variability that risk reduction activities can introduce. Cost reserves of 30% are held against Phases B–D, which is commensurate with APL practices and seems appropriate given past experience, coupled with the more than 9 months of funded schedule reserves in the phases (that is, thereby reducing risk of overrunning due to falling behind schedule). In addition to these reserves, the estimated cost holds 15% in Phase E. Past experience throughout industry indicates 5% to 15% is the norm. Given the complexity of the trajectory and potential for real-time science discoveries, we felt it prudent to hold reserves at the high end of this range.

Funding reserves are held on all WBS elements, including all science activities, with the exception of the Atlas V 551 launch vehicle, payload (considered to be self-contained within the $100M cap), and DSN.

4.5. Subsystem Cost Detail

Table 4.5-1 provides Solar Probe+ subsystem cost detail. The cost element numbers refer to the APL internal Work Breakdown Structure (WBS) subelements. These have been mapped into the NASA WBS shown in Figure 4.4-1 in order to produce Table 4.1-1.

Table 4.5-1. Solar Probe+ subsystem cost detail. Reserves have not been applied to Kennedy Space Center (KSC) launch services, payload instruments, or DSN.

MISSION INSTITUTION SUMMARY FOR COST FOR SOLAR PROBE+ ENGINEERING STUDY FY Costs in Real Year Dollars (To The Nearest Thousand); Totals in Real Year and Fixed Year 2007 Dollars						
Cost Element	**Phase A**	**Phase B**	**Phase C/D**	**Phase E**	**Total (Real Year)**	**Total (FY 2007)**
Program Management 11*	$2,154	$3,990	$10,090	$16,005	**$32,239**	**$25,261**
System Engineering 12*	$2,219	$5,962	$16,710	$22	**$24,912**	**$21,301**
Mission Design and Analysis 13*	$496	$1,035	$2,874	$4,863	**$9,268**	**$7,209**
Performance Assurance Engineering 14*	$432	$1,378	$6,666	$1,246	**$9,721**	**$8,015**
Payload 2*	$636	$1,800	$4,846	$58	**$7,340**	**$6,264**
ADCS & GC 31*	$722	$7,398	$5,108	-	**$13,228**	**$11,508**
Power 32*	$1,955	$9,988	$15,973	-	**$27,915**	**$24,246**
Harness 33*	$71	$604	$2,039	-	**$2,714**	**$2,310**
Spacecraft Structures and Mechanisms 34*	$1,078	$3,084	$14,501	$90	**$18,754**	**$15,911**
Thermal 35*	$7,141	$12,650	$16,076	-	**$35,867**	**$31,305**
RF Communications 36*	$153	$10,351	$15,502	$156	**$26,163**	**$22,521**
C&DH 37*	$483	$10,403	$8,538	-	**$19,425**	**$17,105**
Flight Software 38*	$394	$1,283	$15,132	$649	**$17,458**	**$14,569**
Propulsion 39*	$134	$1,454	$3,646	-	**$5,235**	**$4,537**
I&T 4**	$329	$2,123	$19,701	$22	**$22,176**	**$18,339**
Launch Ops. & Early Orbital Ops. 5*	-	-	$4,045	$349	**$4,394**	**$3,470**
Ground Data System 7**	$1,043	$3,535	$25,973	$295	**$30,846**	**$25,801**
Mission Ops. and Data Analysis 8**	-	-	$12	$40,877	**$40,890**	**$29,222**
Education and Public Outreach	-	$384	$935	$323	**$1,643**	**$1,414**
APL Mission Cost	**$19,441**	**$77,423**	**$188,367**	**$64,956**	**$350,187**	**$290,307**
Payload Instruments	$5,305	$33,437	$77,292	-	**$116,034**	**$100,000**
Environmental Testing at GSFC	-	-	$1,714	-	**$1,714**	**$1,398**
Navigation	$90	$210	$1,020	$1,680	**$3,000**	**$2,315**
KSC Launch Services	-	-	$225,100	-	**$225,100**	**$184,468**
Launch Vehicle Third Stage	-	-	$7,700	-	**$7,700**	**$6,078**
DSN	-	-	-	$22,940	**$22,940**	**$16,509**
External PI & Co-I Team, Phases A–D	$681	$2,443	$4,876	-	**$8,000**	**$6,882**
Science Ops. Preparations	-	-	-	$5,000	**$5,000**	**$3,539**
External PI & Co-I Team, Phase E	-	-	-	$50,000	**$50,000**	**$35,394**
Science Ops. Team	-	-	-	$8,000	**$8,000**	**$5,663**
Reserves	$1,011	$24,023	$61,103	$19,445	**$105,582**	**$86,933**
Total Mission Cost	**$26,528**	**$137,536**	**$567,172**	**$172,022**	**$903,257**	**$739,489**

Phase A: 5% Reserve
Phase B: 30% Reserve
Phase C/D: 30% Reserve
Phase E: 15% Reserve

APPENDIX A:

SOLAR PROBE+ MASS AND POWER BUDGETS

Table A-1. Solar Probe+ mass budget.

Name	Qty	CBE Each (kg)	CBE Total (kg)	Contingency (%)	Total (kg)
Instruments					
Instruments Total:			47.2		51.9
Hemispheric Imager	1	1.5	1.5	10%	1.7
TBD Science Payload	1	5.0	5.0	10%	5.5
Fast Ion Analyzer	1	2.8	2.8	10%	3.1
Fast Electron Analyzer	2	2.5	5.0	10%	5.5
Ion Composition Analyzer	1	7.0	7.0	10%	7.7
Plasma Wave Electronics	1	2.0	2.0	10%	2.2
Plasma Wave Pre-amp	3	0.4	1.2	10%	1.3
Search Coils	3	0.6	1.8	10%	2.0
Magnetometer	1	2.5	2.5	10%	2.8
Energetic Particle Inst. High Energy	1	2.7	2.7	10%	3.0
Energetic Particle Inst. Low Energy	1	1.4	1.4	10%	1.5
Neutron-Gamma Spectrometer	1	2.0	2.0	10%	2.2
Coronal Dust Detector	1	1.5	1.5	10%	1.7
Common DPU	1	10.8	10.8	10%	11.9
Accommodation Hardware					
Accommodation Hardware Total:			7.4		8.4
Fast Plasma Actuator Bracket	1	2.2	2.2	15%	2.5
Plasma Wave Antenna, Actuator	3	1.2	3.6	15%	4.1
Magnetometer Boom	1	1.6	1.6	5%	1.7
Spacecraft					
Spacecraft Total:			373.7		420.1`
Telecommunications					
Telecommunications Total:			31.8		34.8
High Gain Antenna	1	3.8	3.8	10%	4.2
HGA Actuator	2	2.0	4.0	5%	4.2
High Gain Arm, mounting bracket, rotary joints, etc.	1	2.9	2.9	15%	3.3
HGA Actuator Electronics	1	1.0	1.0	5%	1.1
K-Band TWTA/EPC	2	3.0	6.0	5%	6.3
X-Band TWTA/EPC	2	2.5	4.9	5%	5.1
Low Gain Antenna Assembly	2	0.7	1.4	15%	1.6
RF Plate	1	1.0	1.0	15%	1.2
Hybrids/Components	1	1.0	1.0	15%	1.2
Transponder	2	1.6	3.2	15%	3.7
Coax/Waveguide	1	2.6	2.6	15%	3.0
Guidance and Control					
Guidance and Control Total:			30.4		32.0
Inertial Measurement Unit	1	6.6	6.6	5%	6.9

Name	Qty	CBE Each (kg)	CBE Total (kg)	Contingency (%)	Total (kg)
Reaction Wheel Assembly	4	4.2	16.8	5%	17.6
Star Tracker	3	2.0	6.0	5%	6.3
Solar Horizon Sensor	1	1.0	1.0	10%	1.1
Power					
Power Total:			117.2		132.2
Solar Array System (Primary)			25.1		27.2
SA Substrate	2	2.0	4.0	10%	4.4
SA Cells, wiring, etc	2	5.2	10.4	10%	11.4
Hinge/Damper	2	1.0	2.0	10%	2.2
Solar Array Drive	2	2.8	5.6	5%	5.9
Solar Array Drive Electronics	1	2.0	2.0	5%	2.1
Fasteners, pins, etc	2	0.6	1.1	10%	1.2
Solar Array System, Secondary			66.8		76.7
Radiator Panel, Al HC	6	1.5	9.0	15%	10.4
Radiator Panel, Heat Pipes	1	3.5	3.5	15%	4.0
Straps, Clamps, Inserts, Thermal Adhesive, etc.	1	3.0	3.0	15%	3.5
Cooling Tubes, fittings, flex lines, Fasteners, Fill/Drain Valves, etc.	1	8.6	8.6	15%	9.9
Pump	2	12.0	24.0	15%	27.6
Fluid	1	0.2	0.2	15%	0.2
Substrate Cooling/Mounting Deck	2	2.3	4.6	15%	5.3
Motor, Schaeffer-MOOG, Type 1	2	0.5	1.0	5%	1.0
Brackets, drive components, pins, fasteners, etc.	2	1.6	3.2	15%	3.7
Motor Drive Electronics	1	2.2	2.2	15%	2.5
Slider/Positioning System	2	0.91	1.8	15%	2.1
Substrate	2	1.0	2.0	15%	2.3
Cells/etc.	2	0.5	1.0	15%	1.2
Harness	2	0.8	1.5	15%	1.7
Center Deck Stiffener	1	1.2	1.2	15%	1.4
Power System Electronics			25.3		28.3
Power System Electronics	1	7.3	7.3	15%	8.4
Battery	1	8.0	8.0	5%	8.4
Power Distribution Unit	1	10.0	10.0	15%	11.5
Thermal Protection System					
Thermal Protection System Total:			68.5		78.8
Shield	1	52.0	52.0	15%	59.8
Support Structure	1	10.0	10.0	15%	11.5
Dust Protection	1	6.5	6.5	15%	7.5
Thermal Control					

Name	Qty	CBE Each (kg)	CBE Total (kg)	Contingency (%)	Total (kg)
Thermal Control Total:			15.7		18.1
Multi-Layer Insulation	1	10.0	10.0	15%	11.5
Radiators	1	0.3	0.3	15%	0.3
Heater/Thermistor Harness	1	2.5	2.5	15%	2.9
Diode Heat Pipe	1	0.9	0.9	15%	1.0
Doublers, Gaskets, etc	1	2.0	2.0	15%	2.3
Avionics					
Avionics Total:			12.7		14.0
Integrated Electronics Module	2	6.0	12.0	10%	13.2
TRIO Units	14	0.1	0.7	10%	0.8
Propulsion					
Propulsion Total:			20.5		21.9
Hydrazine Tank	1	6.4	6.4	5%	6.7
5-lbf Thruster	2	0.7	1.5	5%	1.5
0.2-lbf Thruster	12	0.3	3.6	5%	3.8
Latch Valve	2	0.3	0.6	5%	0.6
Filter	1	0.0	0.0	5%	0.0
Fill/Service Valve	2	0.2	0.3	5%	0.3
Pressure Transducers	2	0.2	0.4	5%	0.4
Tubing/Fasteners/Clamps	1	3.0	3.0	10%	3.3
Electrical Connectors	1	0.3	0.3	10%	0.3
Cabling	1	3.0	3.0	10%	3.3
Orifice	1	0.0	0.0	10%	0.0
Propulsion Diode Box	1	1.5	1.5	10%	1.7
Mechanical					
Mechanical Total:			58.9		67.7
Primary Structure =			53.4		61.5
Top Deck	1	6.5	6.5	15%	7.5
Aft Deck	1	14.7	14.7	15%	16.9
Side Panels	6	3.6	21.6	15%	24.8
Fasteners	1	1.8	1.8	15%	2.1
Payload Adaptor, Umbilical Brackets, etc.)	1	8.1	8.1	15%	9.3
Tank Mounting Structure	1	0.8	0.8	15%	0.9
Secondary Structure =			5.5		6.3
Reaction Wheel Brackets	4	0.3	1.2	15%	1.4
Low Gain Antenna Bracket	2	0.2	0.4	15%	0.5
Medium Gain Antenna Bracket	1	0.3	0.3	15%	0.3
Star Tracker Bracket	3	0.5	1.5	15%	1.7
Solar Array Tie Down Brackets (All)	8	0.2	1.6	15%	1.8

Name	Qty	CBE Each (kg)	CBE Total (kg)	Contingency (%)	Total (kg)
Balance Mass	0	8.0	0.0	15%	0.0
Purge Components	1	0.5	0.5	15%	0.5
Harness					
			Harness Total:	18.0	20.6
Main Harness	1	16.5	16.5	15%	19.0
Plugs	1	1.0	1.0	10%	1.1
Grounding Straps	1	0.5	0.5	10%	0.6
Observatory					
			Observatory Dry Mass	428.3	480.3
Propellant					
				Propellant Total:	52.7
Useable					52.3
Residual					0.3
Pressurant					0.1
				Observatory Wet Mass	533.0
				Launch Mass	610.0
				Unallocated Margin	77.0
				Total Mass Reserves	30.1%

Table A-2. Solar Probe+ power budget.

				Post-Separation		Maneuver		Cruise		Checkout/Calibration		Approach		Science		Science Momentum Dump	
Name	Qty	CBE Each (W)	CBE Total (W)	Duty Cycle (%)	Total (W)	Duty Cycle (%)	Total (W)	Duty Cycle (%)	Total (W)	Duty Cycle (%)	Total (W)	Duty Cycle (%)	Total (W)	Duty Cycle (%)	Total (W)	Duty Cycle (%)	Total (W)
Instruments																	
Instruments Total:					0.0		0.0		0.0		28.6		0.0		57.2		57.2
Hemispheric Imager	1	4.0	4.0	0%	0.0	0%	0.0	0%	0.0	50%	2.0	0%	0.0	100%	4.0	100%	4.0
Polar Source Region Imager	1	4.0	4.0	0%	0.0	0%	0.0	0%	0.0	50%	2.0	0%	0.0	100%	4.0	100%	4.0
Fast Ion Analyzer	1	3.7	3.7	0%	0.0	0%	0.0	0%	0.0	50%	1.9	0%	0.0	100%	3.7	100%	3.7
Fast Electron Analyzer	1	7.2	7.2	0%	0.0	0%	0.0	0%	0.0	50%	3.6	0%	0.0	100%	7.2	100%	7.2
Ion Composition Analyzer	1	6.0	6.0	0%	0.0	0%	0.0	0%	0.0	50%	3.0	0%	0.0	100%	6.0	100%	6.0
Plasma Wave Electronics	1	5.0	5.0	0%	0.0	0%	0.0	0%	0.0	50%	2.5	0%	0.0	100%	5.0	100%	5.0
Magnetometer	1	2.5	2.5	0%	0.0	0%	0.0	0%	0.0	50%	1.3	0%	0.0	100%	2.5	100%	2.5
Energetic Particle Inst. High Energy	1	2.3	2.3	0%	0.0	0%	0.0	0%	0.0	50%	1.2	0%	0.0	100%	2.3	100%	2.3
Energetic Particle Inst. Low Energy	1	1.7	1.7	0%	0.0	0%	0.0	0%	0.0	50%	0.9	0%	0.0	100%	1.7	100%	1.7
Neutron-Gamma Spectrometer	1	3.0	3.0	0%	0.0	0%	0.0	0%	0.0	50%	1.5	0%	0.0	100%	3.0	100%	3.0
Coronal Dust Detector	1	3.8	3.8	0%	0.0	0%	0.0	0%	0.0	50%	1.9	0%	0.0	100%	3.8	100%	3.8
Common DPU	1	14.0	14.0	0%	0.0	0%	0.0	0%	0.0	50%	7.0	0%	0.0	100%	14.0	100%	14.0
Accommodation Hardware																	
Accommodation Hardware Total:					0.0		0.0		0.0		0.3		0.0		0.3		0.3
Fast Plasma Actuator/Arm	1	0.0	0.0	0%	0.0	0%	0.0	0%	0.0	5%	0.0	0%	0.0	5%	0.0	5%	0.0
Plasma Wave Antenna, Actuator	1	5.0	5.0	0%	0.0	0%	0.0	0%	0.0	5%	0.3	0%	0.0	5%	0.3	5%	0.3
Spacecraft																	
Spacecraft Total:					201.6		325.8		292.8		244.8		245.1		245.1		253.3
Telecommunications																	
Telecommunications Total:					49.7		97.7		97.7		49.7		49.7		49.7		49.7
Ka-band TWT	2	80.0	160.0	0%	0.0	50%	80.0	50%	80.0	0%	0.0	0%	0.0	0%	0.0	0%	0.0
X-band TWTA	2	33.0	66.0	50%	33.0	0%	0.0	0%	0.0	50%	33.0	50%	33.0	50%	33.0	50%	33.0
Transponder rcv only	1	4.0	4.0	100%	4.0	100%	4.0	100%	4.0	100%	4.0	100%	4.0	100%	4.0	100%	4.0
Transponder (rcv+X only)	1	8.7	8.7	100%	8.7	0%	0.0	0%	0.0	100%	8.7	100%	8.7	100%	8.7	100%	8.7

				Post-Separation		Maneuver		Cruise		Checkout/Calibration		Approach		Science		Science Momentum Dump	
Name	Qty	CBE Each (W)	CBE Total (W)	Duty Cycle (%)	Total (W)	Duty Cycle (%)	Total (W)	Duty Cycle (%)	Total (W)	Duty Cycle (%)	Total (W)	Duty Cycle (%)	Total (W)	Duty Cycle (%)	Total (W)	Duty Cycle (%)	Total (W)
Transponder (rcv+Ka only)	1	9.7	9.7	0%	0.0	100%	9.7	100%	9.7	0%	0.0	0%	0.0	0%	0.0	0%	0.0
Transponder (rcv+X+Ka)	1	14.1	14.1	0%	0.0	0%	0.0	0%	0.0	0%	0.0	0%	0.0	0%	0.0	0%	0.0
USO	2	2.0	4.0	100%	4.0	100%	4.0	100%	4.0	100%	4.0	100%	4.0	100%	4.0	100%	4.0
Guidance and Control																	
Guidance and Control Total:					95.2		95.2		95.2		95.2		95.5		95.5		95.5
Inertial Measurement Unit	1	29.5	29.5	100%	29.5	100%	29.5	100%	29.5	100%	29.5	100%	29.5	100%	29.5	100%	29.5
Reaction Wheel Assembly	4	11.0	44.0	100%	44.0	100%	44.0	100%	44.0	100%	44.0	100%	44.0	100%	44.0	100%	44.0
Star Tracker	1	21.7	21.7	100%	21.7	100%	21.7	100%	21.7	100%	21.7	100%	21.7	100%	21.7	100%	21.7
Solar Horizon Sensor	1	0.3	0.3	0%	0.0	0%	0.0	0%	0.0	0%	0.0	100%	0.3	100%	0.3	100%	0.3
Power																	
Power Total:					18.8		18.8		18.8		18.8		18.8		18.8		18.8
Primary Solar Array Drive	2	18	36.0	1%	0.4	1%	0.4	1%	0.4	1%	0.4	0%	0.0	0%	0.0	0%	0.0
Secondary Solar Array Drive	2	18	36.0	0%	0.0	0%	0.0	0%	0.0	0%	0.0	1%	0.4	1%	0.4	1%	0.4
Power System Electronics	1	10.0	10.0	100%	10.0	100%	10.0	100%	10.0	100%	10.0	100%	10.0	100%	10.0	100%	10.0
Power Distribution Unit	1	8.8	8.8	100%	8.8	100%	8.8	100%	8.8	100%	8.8	100%	8.8	100%	8.8	100%	8.8
Thermal Control																	
Thermal Control Total:					0.0		43.2		43.2		43.2		43.2		43.2		43.2
Secondary Array Pumps	2	21.6	43.2	0%	0.0	100%	43.2	100%	43.2	100%	43.2	100%	43.2	100%	43.2	100%	43.2
Heaters	1	0.0	0.0	0%	0.0	100%	0.0	100%	0.0	100%	0.0	100%	0.0	100%	0.0	100%	0.0
Avionics																	
Avionics Total:					35.0		35.0		35.0		35.0		35.0		35.0		35.0
Primary IEM	1	30.0	30.0	100%	30.0	100%	30.0	100%	30.0	100%	30.0	100%	30.0	100%	30.0	100%	30.0
Secondary IEM	1	5.0	5.0	100%	5.0	100%	5.0	100%	5.0	100%	5.0	100%	5.0	100%	5.0	100%	5.0
Propulsion																	
Propulsion Total:					2.9		35.9		2.9		2.9		2.9		2.9		11.1
Thrusters	1	33.0	33.0	0%	0.0	100%	33.0	0%	0.0	0%	0.0	0%	0.0	0%	0.0	25%	8.3
Cat Bed Heaters	1	11.5	11.5	25%	2.9	25%	2.9	25%	2.9	25%	2.9	25%	2.9	25%	2.9	25%	2.9

				Post-Separation		Maneuver		Cruise		Checkout/Calibration		Approach		Science		Science Momentum Dump	
Name	Qty	CBE Each (W)	CBE Total (W)	Duty Cycle (%)	Total (W)	Duty Cycle (%)	Total (W)	Duty Cycle (%)	Total (W)	Duty Cycle (%)	Total (W)	Duty Cycle (%)	Total (W)	Duty Cycle (%)	Total (W)	Duty Cycle (%)	Total (W)
Pressure Transducers	1	1.8	1.8	100%	1.8	100%	1.8	100%	1.8	100%	1.8	100%	1.8	100%	1.8	100%	1.8
Observatory																	
Observatory Power					201.6		325.8		292.8		273.6		245.1		302.5		310.8
Radiated RF Power																	
TWT radiated power Ka-band	1	40	40.0		0.0		40.0		40.0		0.0		0.0		0.0		0.0
TWT radiated power X-band	1	12	12.0		12.0		0.0		0.0		12.0		12.0		12.0		12.0
Cooling pumps isolated from bus																	
Bus Subsystem Dissipated Power					189.6		242.6		209.6		218.4		189.9		247.3		255.6
Bus Heaters				0%	0.0	100%	27.4	100%	60.4	100%	51.6	100%	80.1	100%	22.7	100%	14.4
Harness Loss					3.0		5.3		5.3		4.9		4.9		4.9		4.9
Bus Power					192.6		275.3		275.3		274.9		274.9		274.9		274.9
Total S/C Consumed Power					204.6		358.5		358.5		330.1		330.1		330.1		330.1
Available Load Power							482.0		482.0		482.0		482.0		482.0		482.0
Power Reserves							123.5		123.5		151.9		151.9		151.9		151.9
Margin							34.45%		34.45%		46.03%		46.03%		46.03%		46.03%

APPENDIX B:

SOLAR PROBE+ LINK ANALYSIS

HGA 34m HEF Link Ver. 3.0 Name: DeBoy

SPACECRAFT COMMUNICATIONS LINK ANALYSIS Date: 1/6/2008

SPACECRAFT MISSION: Solar Probe Plus with Mast

LINK: X up Ka down HGA Link

Uplink Freq:	7.182	GHz	Wavlgth:	0.0418	meter
Downlink Freq:	32	GHz	Wavlgth:	0.0094	meter

Uplink Command Modulation: NRZ/PSK/PM (Data on a 16 kHz sine wave subcarrier)

Downlink Telemetry Modulation: NRZ/PSK/PM (Data on a 25.5 kHz square wave subcarrier)

Ranging Modulation: Off

HIGH GAIN ANTENNA UTILITY

Spacecraft HGA Diameter: 0.8 m Efficiency: 60.0 %

Spacecraft HGA Pointing Error (+/-): 0.20 Deg.

Calculated Parameter	Uplink		Downlink	
Spacecraft HGA Gain	33.37	dBic	46.35	dBic
Spacecraft HGA 3dB Beamwidth:	3.44	Deg.	0.77	Deg.
Spacecraft HGA Pointing Loss:	-0.04	dB	-0.81	dB

LEO SPACECRAFT SLANT RANGE UTILITY

Parameter	Value	Units
Spacecraft Altitude (Enter Re or km for units):	n/a	km
Ground Antenna Elevation Angle:	n/a	Deg.
Slant Range (Assumes average Re= 6370 km):	n/a	km

		Value	Units
Spacecraft range (enter AU, Re or km for units):		1.8	Au
UPLINK MODULATION CHARACTERISTICS			
Command data rate:		10	kbps
Command modulation index:		1.3	rad pk
Uplink ranging modulation index:		0.8	rad pk
RANGING CHANNEL CHARACTERISTICS			
Ranging channel turn-around (elbow/regenerative):		elbow	
DOWNLINK MODULATION CHARACTERISTICS			
Entered Parameters:			
Telemetry data rate:	info. Rate	72	kbps
Telemetry modulation index (enter BPSK, QPSK, or a value for PM):		QPSK	rad pk
Downlink ranging channel modulation index:		0.00001	rad pk
Downlink telemetry waveform (square/sine):		square	
Calculated Parameters:			
S/C ranging channel bandwidth:	Br=	1.5	MHz
Pwr in fundamental component of square ranging tone:	gamma=	0.8106	
Ranging SNR at output of S/C receiver filter:	alphar=	0.6108	
Cmd/noise ratio at output of S/C receiver filter:	alphac=	1.0075	
Effective downlink cmd modulation index:	t1=	0.0000	rad. pk
Effective downlink ranging modulation index:	t2=	0.0000	rad. pk
Effective downlink noise modulation index:	t3=	0.0000	rad. rms

Figure B-RF1. X-band/Ka-band link analysis (1 of 6): High-gain antenna (HGA) link parameters.

UPLINK CALCULATIONS 1/6/2008

Parameter	Notes	Units	Des.Value	Adv. Tol.	Fav. Tol.	Mean Val.	Variance	PDF
Gnd Station TX Power:	20 kW Mid-band	dBm	73.01	-1.00	0.00	72.68	0.06	tri
Gnd Station TX Antenna Gair	20 deg, vacuum, mod103 p22	dBic	67.06	-0.20	0.20	67.06	0.01	uni
Gnd Antenna Pointing Loss:	Con. Scan 30 mph wind, mod	dB	-0.40	0.00	0.30	-0.25	0.01	uni
Gnd Station Passive Loss:	810-005 mod103 p8	dB	-0.25	-0.05	0.05	-0.25	0.00	uni
EIRP:		dBm	139.42			139.24	0.08	
Uplink Path Loss:		dB	-278.17	0.00	0.00	-278.17	0.00	uni
S/C Antenna Gain:	HGA	dBic	33.37	-1.00	1.00	33.37	0.33	uni
S/C Antenna Pointing Loss:	included above	dB	-0.04	0.00	0.04	-0.03	0.00	tri
Atmospheric Loss:	90% wthr, 20 deg, mod103 p2	dB	-0.17	0.00	0.14	-0.10	0.00	uni
Polarization Mismatch Loss:	Included in S/C antenna gain	dB	0.00	0.00	0.00	0.00	0.00	tri
S/C Passive Loss: (Between	antenna port and rcvr input)	dB	-0.70	0.00	0.20	-0.60	0.00	gau
Total Received Power:	(At receiver input)	dBm	-106.29			-106.29	0.41	
S/C Antenna Noise Temp.	(At antenna port) RSB estir	K	100.00					
S/C Passive Loss Noise Temp.		K	50.72					
S/C Receiver Noise Figure:	LNA w/ filter loss	dB	2.00					
System Noise Temp:	(At receiver input)	K	297.90					
System Noise Density:	(At receiver input)	dBm/Hz	-173.86	0.90	-1.00	-173.91	0.10	gau
Carrier/Total Power:		dB	-7.29	-0.25	0.25	-7.29	0.01	tri
Received Carrier Power:		dBm	-113.58			-113.58	0.42	
Received Pc/No:		dB-Hz	60.28			60.33	0.52	
Tracking Loop Predetection Noise BW:	3 kHz	dBHz	34.77	0.40	-0.40	34.77	0.03	tri
Tracking Loop Predetection SNR:		dB	25.51			25.56	0.55	
Carrier Tracking Loop Bandwidth (BL):	50 Hz	dBHz	16.99	1.40	-1.50	16.96	0.35	tri
Received Carrier/Noise in Loop Bandwidth:		dB	43.29			43.37	0.87	
Required Carrier/Noise in Loop Bandwidth:		dB	10.00	0.00	0.00	10.00	0.00	uni
Carrier Margin:		**dB**	**33.29**			**33.37**	**0.87**	
	3sigma=	**dB**					**2.81**	
Command Subc/Total Power:		dB	-5.77	-0.25	0.25	-5.77	0.01	tri
Received Command Subc. Power:		dBm	-112.07			-112.07	0.42	
Subcarrier Demod. Predetection Noise E	3.84 kHz	dBHz	35.84	0.40	-0.40	35.84	0.03	tri
Subcarrier Demod. Predetection SNR:		dB	25.95			26.00	0.55	
Command Data Rate:		dBHz	40.00	0.00	0.00	40.00	0.00	tri
Received Command Eb/No:		dB	21.79			21.84	0.52	
Required Command Eb/No:	Pe=1.0E-06, PSK Yuen p205	dB	10.50	0.00	0.00	10.50	0.00	uni
Implementation Loss:	Card spec.	dB	-1.50	-0.50	0.50	-1.50	0.04	tri
Command Margin:		**dB**	**9.79**			**9.84**	**0.57**	
	3sigma=	**dB**					**2.26**	
Ranging/Total Power:		dB	-7.04	-0.25	0.25	-7.04	0.01	tri
Received Ranging Power:		dBm	-113.33			-113.33	0.42	
Uplink Pr/No:		dBHz	60.53			60.58	0.52	
S/C Ranging Channel Bandwidth:	1.5 MHz	dBHz	61.76	0.40	-0.40	61.76	0.03	tri
S/C Ranging Channel SNR:		dB	-1.23			-1.18	0.55	

Figure B-RF1 (cont.). X-band/Ka-band link analysis (2 of 6): X-band HGA uplink to 34 m at 1.8 AU.

DOWNLINK CALCULATIONS 1/6/2008

Parameter	Notes	Units	Des.Value	Adv. Tol.	Fav. Tol.	Mean Val.	Variance	PDF
S/C Transmitter Power:	40 watts	dBm	46.02	-0.50	0.50	46.02	0.04	tri
S/C Passive Loss:	Estimate	dB	-2.00	0.00	0.20	-1.90	0.00	gau
S/C Antenna Gain:	0.8m HGA	dBic	46.35	-0.50	0.50	46.35	0.04	tri
S/C Antenna Pointing Loss:	0.2° Pointing Error	dB	-0.81	0.00	0.81	-0.54	0.04	tri
EIRP:		dBm	89.56			89.93	0.12	
Path Loss:		dB	-291.15	0.00	0.00	-291.15	0.00	uni
Atmospheric Loss:	90% Weather 20 deg Elevation	dB	-1.00	0.00	0.14	-0.93	0.00	uni
Polarization Mismatch Loss:		dB	-0.10	0.00	0.00	-0.10	0.00	uni
Gnd Antenna Gain:	20 deg EL Angle	dBic	77.50	-0.20	0.20	77.50	0.01	uni
Gnd Antenna Pointing Loss:	20 MPH Wind + 90%	dB	-1.30	0.00	0.30	-1.15	0.01	uni
Total Received Power:		dBm	-126.49			-125.90	0.14	
		G/T	57.96					
Gnd Antenna Noise Temp.	90% wthr, 20 deg Elevation	K	90.00					
Solar/Planetary Noise:		K	0.00					
Gnd System Noise Temp:		K	90.00					
Gnd System Noise Density:		dBm/Hz	-179.06	0.25	-0.25	-179.06	0.01	gau
Carrier/Total Power:		dB	N/A	0.00	0.00	N/A	N/A	tri
Received Carrier Power:		dBm	N/A			N/A	N/A	
Received Pc/No:		dB-Hz	N/A			N/A	N/A	
Tracking Loop Predetection Noise BW:	1 kHz	dBHz	30.00	0.40	-0.40	30.00	0.03	tri
Tracking Loop Predetection SNR:		dB	22.57			23.16	0.18	
Tracking Loop Noise Bandwidth (BL):	1 Hz	dBHz	0.00	0.00	0.00	0.00	0.00	tri
Squaring/Quadrupling Loss:		dB	-12.25			-12.23	0.00	
Received Signal/Noise in Loop Bandwidth:		dB	40.32			40.93	0.15	
Required Signal/Noise in Loop Bandwidth:		dB	10.00	0.00	0.00	10.00	0.00	uni
Carrier Tracking Margin:		**dB**	**30.32**			**30.93**	**0.15**	
	3sigma=	**dB**					**1.16**	
TIm/Total Power:		dB	0.00	0.00	0.00	0.00	0.00	tri
Received TIm Power:		dBm	-126.49			-125.90	0.14	
TIm Data Rate:		dBHz	48.57	0.00	0.00	48.57	0.00	uni
Received Eb/No:		dB	4.00			4.58	0.15	
Required Eb/No:	Turbo Rate 1/2, 8920 frame baseline	dB	1.00	0.20	-0.20	1.00	0.01	uni
Implementation Loss:		dB	-1.00	0.00	0.00	-1.00	0.00	tri
Other gain/loss:		dB	0.00	-0.25	0.25	0.00	0.01	tri
Telemetry Margin:		**dB**	**2.00**			**2.58**	**0.17**	
	3sigma=	**dB**					**1.25**	
		SSNR	-3.79					
Rng/Total Power:		dB	n/a	0.00	0.00	n/a	0.00	tri
Received Ranging Power:		dBm	n/a			n/a	0.14	
Downlink Received Pr/No:		dBHz	n/a			n/a	0.15	
Tandem Pr/No (uplink and downlink):		dBHz	n/a			n/a	n/a	
Downlink Required Pr/No:		dBHz	-10.00	0.00	0.00	-10.00	0.00	uni
Ranging Demodulator Loss:		dB	-0.50	0.00	0.00	-0.50	0.00	tri
Ranging Margin:		**dB**	**n/a**			**n/a**	**n/a**	
	3sigma=	**dB**					**n/a**	

Figure B-RF1 (cont.). X-band/Ka-band link analysis (3 of 6): Ka-band HGA downlink to 34 m at 1.8 AU.

DOWNLINK CALCULATIONS 1/25/2008

Parameter	Notes	Units	Des.Value	Adv. Tol.	Fav. Tol.	Mean Val.	Variance	PDF
S/C Transmitter Power:	13 watts	dBm	41.14	-0.50	0.50	41.14	0.04	tri
S/C Passive Loss:	Estimate	dB	-3.00	0.00	0.20	-2.90	0.00	gau
S/C Antenna Gain:	0.8m HGA	dBic	34.78	-0.50	0.50	34.78	0.04	tri
S/C Antenna Pointing Loss:	0.2° Pointing Error	dB	-0.06	0.00	0.06	-0.04	0.00	tri
EIRP:		dBm	72.86			72.98	0.08	
Path Loss:		dB	-279.58	0.00	0.00	-279.58	0.00	uni
Atmospheric Loss:	10 deg EL, 90% Weather	dB	-0.31	0.00	0.14	-0.24	0.00	uni
Polarization Mismatch Loss:		dB	-0.10	0.00	0.00	-0.10	0.00	uni
Gnd Antenna Gain:	10 deg EL Angle	dBic	68.23	-0.20	0.20	68.23	0.01	uni
Gnd Antenna Pointing Loss:	90% weather	dB	-0.10	0.00	0.30	0.05	0.01	uni
Total Received Power:		dBm	-139.00			-138.66	0.11	
		G/T	52.21					
Gnd Antenna Noise Temp.	90% Weather, 10 deg EL	K	40.00					
Solar/Planetary Noise:		K	0.00					
Gnd System Noise Temp:		K	40.00					
Gnd System Noise Density:		dBm/Hz	-182.58	0.25	-0.25	-182.58	0.01	gau
Carrier/Total Power:		dB	N/A	0.00	0.00	N/A	N/A	tri
Received Carrier Power:		dBm	N/A			N/A	N/A	
Received Pc/No:		dB-Hz	N/A			N/A	N/A	
Tracking Loop Predetection Noise BW:	1 kHz	dBHz	30.00	0.40	-0.40	30.00	0.03	tri
Tracking Loop Predetection SNR:		dB	13.58			13.92	0.14	
Tracking Loop Noise Bandwidth (BL):	1 Hz	dBHz	0.00	0.00	0.00	0.00	0.00	tri
Squaring/Quadrupling Loss:		dB	-13.52			-13.42	0.00	
Received Signal/Noise in Loop Bandwidth:		dB	30.06			30.50	0.11	
Required Signal/Noise in Loop Bandwidth:		dB	10.00	0.00	0.00	10.00	0.00	uni
Carrier Tracking Margin:		**dB**	**20.06**			**20.50**	**0.11**	
	3sigma=	**dB**					**1.01**	
Tlm/Total Power:		dB	0.00	0.00	0.00	0.00	0.00	tri
Received Tlm Power:		dBm	-139.00			-138.66	0.11	
Tlm Data Rate:		dBHz	38.45	0.00	0.00	38.45	0.00	uni
Received Eb/No:		dB	5.13			5.47	0.11	
Required Eb/No:	Turbo Rate 1/2, 8920 frame baseline	dB	1.00	0.20	-0.20	1.00	0.01	uni
Implementation Loss:		dB	-1.00	0.00	0.00	-1.00	0.00	tri
Other gain/loss:		dB	0.00	-0.25	0.25	0.00	0.01	tri
Telemetry Margin:		**dB**	**3.13**			**3.47**	**0.14**	
	3sigma=	**dB**					**1.11**	
		SSNR	-2.65					
Rng/Total Power:		dB	n/a	0.00	0.00	n/a	0.00	tri
Received Ranging Power:		dBm	n/a			n/a	0.11	
Downlink Received Pr/No:		dBHz	n/a			n/a	0.11	
Tandem Pr/No (uplink and downlink):		dBHz	n/a			n/a	n/a	
Downlink Required Pr/No:		dBHz	-10.00	0.00	0.00	-10.00	0.00	uni
Ranging Demodulator Loss:		dB	-0.50	0.00	0.00	-0.50	0.00	tri
Ranging Margin:		**dB**	**n/a**			**n/a**	**n/a**	
	3sigma=	**dB**					**n/a**	

Figure B-RF1 (cont.). X-band/Ka-band link analysis (4 of 6): X-band HGA downlink to 34 m at 1.8 AU.

UPLINK CALCULATIONS 1/25/2008

Parameter	Notes	Units	Des.Value	Adv. Tol.	Fav. Tol.	Mean Val.	Variance	PDF
Gnd Station TX Power:	20 kW Mid-band	dBm	73.01	-1.00	0.00	72.68	0.06	tri
Gnd Station TX Antenna Gair	20 deg, vacuum, mod103 p22	dBic	72.62	-0.20	0.20	72.62	0.01	uni
Gnd Antenna Pointing Loss:	Con. Scan 30 mph wind, mod	dB	-0.40	0.00	0.30	-0.25	0.01	uni
Gnd Station Passive Loss:	810-005 mod103 p8	dB	-0.45	-0.05	0.05	-0.45	0.00	uni
EIRP:		dBm	144.78			144.60	0.08	
Uplink Path Loss:		dB	-278.89	0.00	0.00	-278.89	0.00	uni
S/C Antenna Gain:	Canted LGA	dBic	0.00	-1.00	1.00	0.00	0.33	uni
S/C Antenna Pointing Loss:		dB	0.00	0.00	0.00	0.00	0.00	tri
Atmospheric Loss:	90% wthr, 20 deg, mod103 p2	dB	-0.17	0.00	0.14	-0.10	0.00	uni
Polarization Mismatch Loss:	Included in S/C antenna gain	dB	0.00	0.00	0.00	0.00	0.00	tri
S/C Passive Loss: (Between antenna port and rcvr input)		dB	-3.00	0.00	0.20	-2.90	0.00	gau
Total Received Power:	(At receiver input)	dBm	-137.28			-137.29	0.41	
S/C Antenna Noise Temp.	(At antenna port)	K	100.00					
S/C Passive Loss Noise Temp.		K	288.63					
S/C Receiver Noise Figure:	LNA w/ filter loss	dB	2.00					
System Noise Temp:	(At receiver input)	K	364.39					
System Noise Density:	(At receiver input)	dBm/Hz	-172.99	0.90	-1.00	-173.04	0.10	gau
Carrier/Total Power:		dB	-1.45	-0.25	0.25	-1.45	0.01	tri
Received Carrier Power:		dBm	-138.73			-138.74	0.42	
Received Pc/No:		dB-Hz	34.26			34.30	0.52	
Tracking Loop Predetection Noise BW:	3 kHz	dBHz	34.77	0.40	-0.40	34.77	0.03	tri
Tracking Loop Predetection SNR:		dB	-0.51			-0.48	0.55	
Carrier Tracking Loop Bandwidth (BL):	50 Hz	dBHz	16.99	1.40	-1.50	16.96	0.35	tri
Received Carrier/Noise in Loop Bandwidth:		dB	17.27			17.34	0.87	
Required Carrier/Noise in Loop Bandwidth:		dB	10.00	0.00	0.00	10.00	0.00	uni
Carrier Margin:		**dB**	**7.27**			**7.34**	**0.87**	
	3sigma=	**dB**					**2.81**	
Command Subc/Total Power:		dB	-5.65	-0.25	0.25	-5.65	0.01	tri
Received Command Subc. Power:		dBm	-142.93			-142.94	0.42	
Subcarrier Demod. Predetection Noise E	3.84 kHz	dBHz	35.84	0.40	-0.40	35.84	0.03	tri
Subcarrier Demod. Predetection SNR:		dB	-5.79			-5.75	0.55	
Command Data Rate:	31 bps	dBHz	14.91	0.00	0.00	14.91	0.00	tri
Received Command Eb/No:		dB	15.14			15.18	0.52	
Required Command Eb/No:	Pe=1.0E-06, uncoded	dB	10.60	0.00	0.00	10.60	0.00	uni
Implementation Loss:		dB	-1.50	-0.50	0.50	-1.50	0.04	tri
Command Margin:		**dB**	**3.04**			**3.08**	**0.57**	
	3sigma=	**dB**					**2.26**	
Ranging/Total Power:		dB	-121.45	-0.25	0.25	-121.45	0.01	tri
Received Ranging Power:		dBm	-258.73			-258.74	0.42	
Uplink Pr/No:		dBHz	-85.74			-85.70	0.52	
S/C Ranging Channel Bandwidth:	1.5 MHz	dBHz	61.76	0.40	-0.40	61.76	0.03	tri
S/C Ranging Channel SNR:		dB	-147.50			-147.47	0.55	

Figure B-RF1 (cont.). X-band/Ka-band link analysis (5 of 6): X-band low-gain antenna (LGA) emergency uplink from Deep Space Network (DSN) 70 m, 1.8 AU.

DOWNLINK CALCULATIONS 1/25/2008

Parameter	Notes	Units	Des.Value	Adv. Tol.	Fav. Tol.	Mean Val.	Variance	PDF
S/C Transmitter Power:	13 watts	dBm	41.14	-0.50	0.50	41.14	0.04	tri
S/C Passive Loss:	Estimated	dB	-2.00	0.00	0.20	-1.90	0.00	gau
S/C Antenna Gain:	Canted LGA	dBic	0.00	-0.50	0.50	0.00	0.04	tri
S/C Antenna Pointing Loss:		dB	0.00	0.00	0.00	0.00	0.00	tri
EIRP:		dBm	39.14			39.24	0.08	
Path Loss:		dB	-278.00	0.00	0.00	-278.00	0.00	uni
Atmospheric Loss:	90% wthr, 20 deg, mod103 p2	dB	-0.17	0.00	0.14	-0.10	0.00	uni
Polarization Mismatch Loss:		dB	-0.10	0.00	0.00	-0.10	0.00	uni
Gnd Antenna Gain:	20 deg, vacuum, mod103 p22	dBic	73.92	-0.20	0.20	73.92	0.01	uni
Gnd Antenna Pointing Loss:	Con. Scan 30 mph wind, mod	dB	-0.40	0.00	0.30	-0.25	0.01	uni
Total Received Power:		dBm	-165.61			-165.29	0.11	
		G/T	58.13					
Gnd Antenna Noise Temp.	90% weather, 20 deg Elevatio	K	37.94					
Solar/Planetary Noise:		K	0.00					
Gnd System Noise Temp:		K	37.94					
Gnd System Noise Density:		dBm/Hz	-182.81	0.25	-0.25	-182.81	0.01	gau
Carrier/Total Power:		dB	-5.35	0.00	0.00	-5.35	0.00	tri
Received Carrier Power:		dBm	-170.96			-170.64	0.11	
Received Pc/No:		dB-Hz	11.85			12.17	0.11	
Tracking Loop Predetection Noise BW:	1 kHz	dBHz	30.00	0.40	-0.40	30.00	0.03	tri
Tracking Loop Predetection SNR:		dB	-18.15			-17.83	0.14	
Tracking Loop Noise Bandwidth (BL):	0.1 Hz	dBHz	-10.00	0.00	0.00	-10.00	0.00	tri
Squaring/Quadrupling Loss:		dB	0.00			0.00	0.00	
Received Signal/Noise in Loop Bandwidth:		dB	21.85			22.17	0.11	
Required Signal/Noise in Loop Bandwidth:	810-5	dB	16.00	0.00	0.00	16.00	0.00	uni
Carrier Tracking Margin:		**dB**	**5.85**			**6.17**	**0.11**	
	3sigma=	**dB**					**1.01**	
TIm/Total Power:		dB	-1.50	0.00	0.00	-1.50	0.00	tri
Received TIm Power:		dBm	-167.11			-166.79	0.11	
TIm Data Rate:	10 bps	dBHz	10.00	0.00	0.00	10.00	0.00	uni
Received Eb/No:		dB	5.70			6.02	0.11	
Required Eb/No:	Turbo code (R=1/6, 1784 frame)	dB	1.00	0.20	-0.20	1.00	0.01	uni
Implementation Loss:		dB	-1.50	0.00	0.00	-1.50	0.00	tri
Other gain/loss:		dB	0.00	-0.25	0.25	0.00	0.01	tri
Telemetry Margin:		**dB**	**3.20**			**3.52**	**0.14**	
	3sigma=	**dB**					**1.11**	
		SSNR	-2.08					
Rng/Total Power:		dB	-275.19	0.00	0.00	-275.19	0.00	tri
Received Ranging Power:		dBm	-440.80			-440.48	0.11	
Downlink Received Pr/No:		dBHz	-257.99			-257.67	0.11	
Tandem Pr/No (uplink and downlink):		dBHz	-257.99			-257.67	0.11	
Downlink Required Pr/No:		dBHz	-10.00	0.00	0.00	-10.00	0.00	uni
Ranging Demodulator Loss:		dB	-0.50	0.00	0.00	-0.50	0.00	tri
Ranging Margin:		**dB**	**-248.49**			**-248.17**	**0.11**	
	3sigma=	**dB**					**1.01**	

Figure B-RF1 (cont.). X-band/Ka-band link analysis (6 of 6): X-band LGA emergency downlink from DSN 70 m, 1.5 AU.

APPENDIX C:

SOLAR ENCOUNTER POWER GENERATION TRADE STUDY

C.1 Trade Study Definition

In the 2005 Solar Probe study,[1] the primary power source was a set of radioisotope thermal generators (RTGs) using plutonium as the heat source for thermoelectric power generation. Given the current concerns over the supply of plutonium available for space missions, the Solar Probe+ team was instructed to develop a mission using only non-nuclear power sources.

The bulk of the Solar Probe+ orbit can be powered with solar arrays. These arrays are sized to provide full power at aphelion and, as the spacecraft approaches the Sun, the arrays are off-pointed to maintain temperature while providing sufficient power including margin. Using MESSENGER heritage arrays, Solar Probe+ can be powered in this manner to ~0.25 AU. The heritage arrays cannot be used through the solar encounter where the solar distance at perihelion is 0.044 AU because of hypersensitivity of power and temperature versus off-pointing angle and solar panel edge effects at grazing incidence angles. During the solar encounter, some other means of storing and/or generating power must be used. The major activity of the Solar Probe+ study has been to determine the optimal power generation concept for the mission. In the subsequent discussion, the solar arrays used outside 0.25 AU are called the primary power generation system, and the power generation method used inside 0.25 AU is called the secondary power system. The segment of the orbit when the secondary power system is used is called the solar encounter.

The choice of secondary power generation is largely independent of the orbit trade study discussed in Section 4.1 except for the choice of perihelion. The choice of perihelion affects the trade in two ways: (*i*) the length of the solar encounter increases as the perihelion is raised from 4 R_S to 9.5 R_S and (*ii*) solar flux at perihelion is decreased for higher perihelion. The time spent in the solar encounter is slightly different for the orbit options, ~8 days for orbits with perihelion at 4 R_S and ~10 days for orbits with perihelion at 9.5 R_S. The major impact of this change is in sizing of options relying on energy storage. The magnitude of the maximum solar flux, however, is six times greater for a 4-R_S perihelion than for perihelion at 9.5 R_S. The major impact of this difference is to disallow the use at 4 R_S of photovoltaics and related concepts using mirrors to redirect light onto solar arrays because of the inability to prevent excessive thermal load on the bus from items directly exposed to the solar flux. In addition to these concerns, the solar flux time profile is similar for all orbits, peaking at perihelion ±1.5 days, as shown in Figure C-1. This environment determines the times when heat conversion systems can be used to generate electrical power during the solar encounter and generally means that all heat conversion concepts require the use of energy storage to power the spacecraft in at least some portion of the solar encounter.

The requirements for the secondary power system are as follows:

- Provide sufficient power to meet science measurement and spacecraft operations requirements through the entire solar encounter as constrained by the solar flux time profile. At the time the trade study was conducted, the total power required was estimated to be 350 W.
- Operate through repeated exposure to the maximum solar flux at perihelion, for which 3000 Suns was assumed for orbits with 4-R_S perihelion, and 512 Suns for orbits with 9.5-R_S perihelion.
- Limit heat load into the spacecraft bus to prevent temperature rises within the bus structure itself. The target for the trade

[1] *Solar Probe: Report of the Science and Technology Definition Team*, NASA/TM—2005–212786, National Aeronautics and Space Administration, Goddard Space Flight Center, Greenbelt, MD (2005).

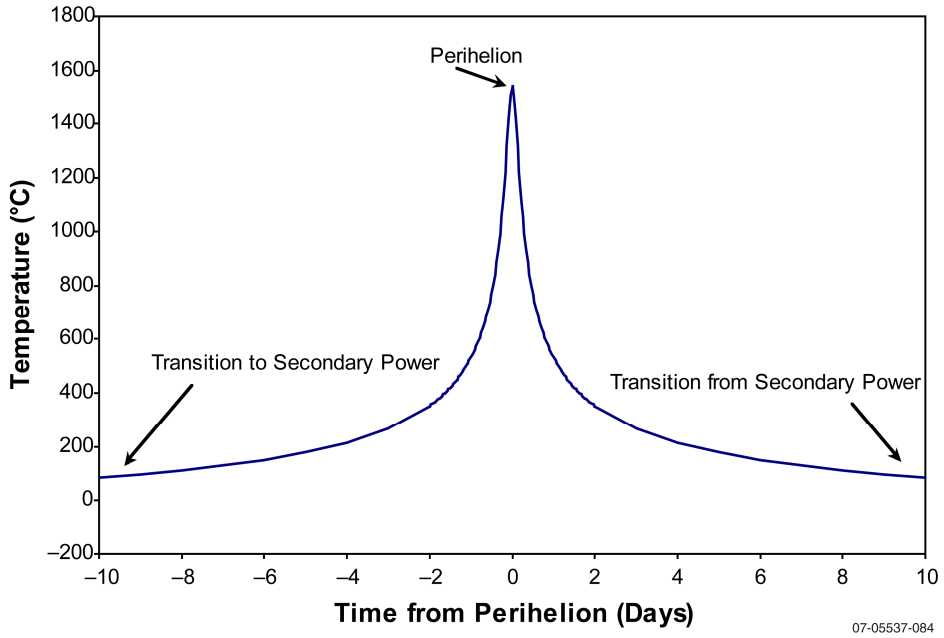

Figure C-1. Temperature profile for the front face of the Thermal Protection System (TPS) during a 4-R_S perihelion encounter.

study was to limit the heat load to 50 W, the heat load of the RTGs in the 2005 study.

- Limit mass to no more than the mass used by the RTGs in the 2005 study (120 kg), with a goal of reducing mass as much as feasible while meeting all other requirements.

In addition to the performance requirements above, the secondary power system should be of development status compatible with a 2015 launch. Although we did not exclude low-technology readiness level (TRL) solutions, the goal was to use a system that could be designed, manufactured, and qualified in the development cycle of the Solar Probe+ mission. All power system options included in the trade study required development at the system level but were designed using major components with flight heritage or significant recent investment in development for space flight.

C.2 Power System Options

In general, three types of system concepts were chosen for the trade study: conversion of solar heating to electric power, conversion of light to electric power, and energy storage. Consideration was given to other methods of power generation, such as electric power generation by collecting from the solar electromagnetic field with a tether extending from the spacecraft. These concepts were eliminated from the trade study as impractical and of very low development status with development schedules incompatible with a 2015 launch.

C.2.1. Battery Bank

Primary arrays are used to charge a battery bank prior to solar encounter, which is sized to provide sufficient energy for entire encounter. Multiple advanced battery types were investigated, as well as capacitor-based energy storage. Based on development status of battery technology and suitability for use in the Solar Probe+ environment, the engineering team chose a 2000-ampere-hour bank of lithium-ion batteries, assuming 80% depth of discharge, and a total encounter of 10 days with no use of solar arrays. The mass for this bank of batteries is ~800 kg. By using advanced battery technology and strict energy management during the encounter, the battery mass could be reduced to slightly more than 400 kg. Significant battery development investment will be required, and significant risk is incurred if this option is chosen.

C.2.2. Thermocouple-Based Energy Conversion

Commercially available thermocouples are embedded in the Thermal Protection System (TPS) such that the temperature difference between the front surface of the TPS and rear of the thermocouple is used to generate electric current. Thermocouples are semicon-

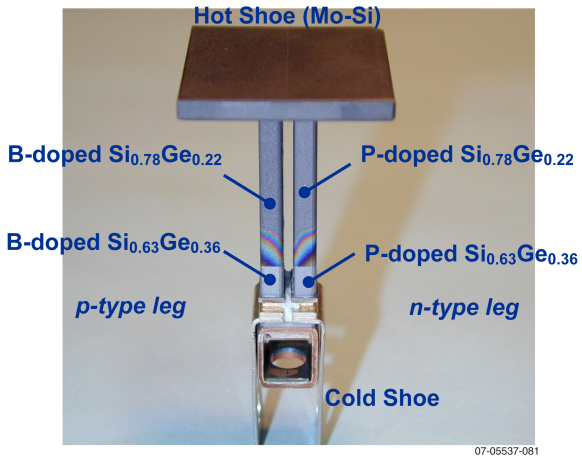

Figure C-2. Design of a typical thermocouple device.

ductor devices typically used in waste heat recovery (e.g., in jet engines), which are the energy conversion element used in radioisotope thermal generators (RTGs) in spaceflight missions. Figure C-2 shows a typical thermocouple design; this device is ~3-mm long and 6-mm across and has a mass of 20 g. The typical application for space flight is to embed the thermocouple such that the large collector is driven to hot temperature by some exterior source (the top surface of the heat shield in the case of Solar Probe+) while the cold legs are held at much lower temperature through connection to radiators. Conversion efficiency depends on the difference in temperature and on the temperature of the hot plate. At the Solar Probe+ perihelion, efficiency is ~6%, and decreases to match the thermal profile shown earlier in Figure C-1. Thermocouples will generate power only around perihelion ± 2 days for closest-approach orbits and may not generate power at all for early orbits in some mission design options with perihelion above 15 R_S or so. Some form of energy storage must be used in conjunction with thermoelectric generation.

The thermocouple-based design concept used ~500 devices embedded in the TPS around the circumference with attachment to radiators mounted on the support structure below the TPS. While the mass of the thermocouples themselves is quite low (~10 kg), the support structure needed to make the concept work is significant. Assuming strict power management when running on batteries, the ability to recharge batteries during closest approach and radiator size sufficient to hold the cold leg of the thermocouples to the required temperature, the mass of a thermocouple-based system to power Solar Probe+ is ~210 kg.

C.2.3. Stirling Engine Power Generation

Heat from the TPS front face is used to drive a set of Stirling engines such that the temperature difference between the hot and cold ends operates a mechanical electric generator. A Stirling engine uses the temperature difference between its hot end and cold end to establish a cycle of gas expansion and contraction within the engine, converting thermal energy into mechanical, and subsequently electric, power. The Advanced Stirling Converter is a nominal 35-W generator developed for the Advanced Stirling Radioisotope Generator program by Glenn Research Center. Figure C-3 shows a schematic of a pair of engines mounted in the configuration chosen for Solar Probe+. Two engines are driven by a common hot collector. In the case of Solar Probe+, this plate would be embedded in the TPS. The cold ends of these devices are controlled separately; the Solar Probe+ concept uses heat pipes and radiators to maintain the cold end temperature of the engines.

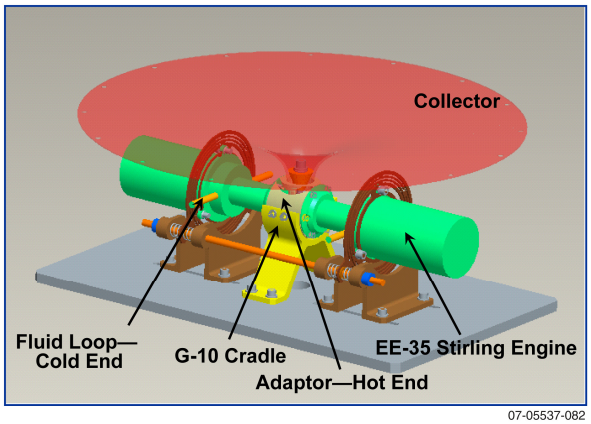

Figure C-3. Stirling engine module adopted for the Solar Probe+ concept.

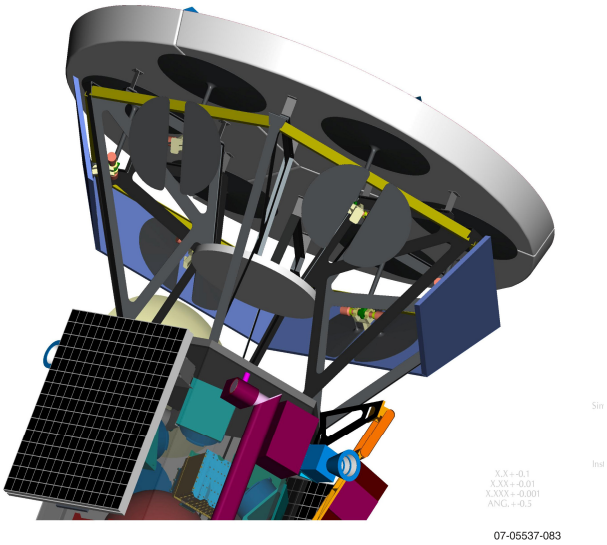

Figure C-4. Solar Probe+ concept using Stirling engine modules.

The Stirling power generation concept consist of six pairs of engine modules mounted under the TPS such that the collectors are embedded in the TPS in the region where the temperature of the collector will be near 650°C, at which the Stirling engines are highly efficient. The radiator for each Stirling engine pair is mounted on the outside of the TPS support structure near the engine module. Figure C-4 shows the system configuration for Solar Probe+, with two radiator panels hidden for clarity. As with the thermocouples, the Stirling engine concept depends on a large temperature difference between hot and cold ends, which limits ability of the Stirling engine system to provide sufficient power during the entire solar encounter and requires the use of energy storage as a supplementary system when the temperature of the TPS front face, as shown previously in Figure C-1, is too low to support power generation with the Stirling engines.

Assuming strict power management when running on batteries, the ability to fully recharge batteries during closest approach, and radiator size sufficient to maintain the cold end of the Stirling engine to the required temperature, the mass of the Stirling engine system is ~182 kg.

C.2.4. Photovoltaic-Based Energy Conversion

Solar cells designed for high-intensity illumination mounted on temperature-controlled solar array substrates. Direct illumination of solar cells will not meet the power system requirements given in Section C.1 without the use of some form of temperature control. Two types of photovoltaic concepts that perform this control were examined in detail for this trade study: (*i*) reduction of illumination impinging on cells and (*ii*) active temperature control of solar cell base plate. In the first case, the energy flux impinging on a set of solar cells is reduced by diffusing the solar input with slots or grids of holes in a shield protecting the arrays of solar cells or by using a reflector to illuminate cells with a reduced flux. In the second case, the cells are mounted on a base plate held at constant temperature using an active cooling loop. In practice, a photovoltaic-based system only works by using a combination of these two methods, and only for perihelia above 8.5–9 R_S. A large number of concepts using photovoltaics were proposed and discarded as untenable because of the physical limitations of the materials, overly difficult to manufacture (such as a grid of micrometer-sized holes through the TPS used to limit solar intensity on a solar array), or overly burdensome on the spacecraft bus (by adding extra heat leaks through the TPS to the bus, for instance).

An achievable photovoltaic concept emerged from preliminary engineering considerations. This concept uses a knife edge on the TPS to partially shadow an array of solar cells designed for high-intensity illumination. These cells use similar gridlines and contact metallization as used for concentrator photovoltaic cells, which have been used for terrestrial applications with optics having a very high concentration ratio. These cells are mounted to a base plate such that the cells are maintained at the proper temperature through a liquid cooling system, which moves excess heat to a set of radiators as described in Sec-

Table C-1. Power generation trade study summary.

Concept	Energy Storage	Thermocouple	Stirling Engine	Photovoltaic
Perihelion	>4 R_S	>4 R_S	>4 R_S	>9 R_S
Power Through Encounter?	Yes	Requires batteries	Requires batteries	Yes
Operational Range	Entire encounter	Perihelion ± 1.5 days	Perihelion ± 2 days	Entire encounter
Heat Load in Spacecraft Bus	<50 W	<50 W	<50 W	<50 W
Subsystem Mass	400–800 kg	210 kg	182 kg	66 kg
Advantages	• No mechanisms • Simple implementation • Highest TRL	• Well understood semiconductor devices • No mechanisms • High TRL	• Moderate TRL • Better energy conversion efficiency than thermocouples, slightly better than photovoltaics	• Lowest mass solution • Retractable arrays allow fine control of power generation and thermal control • No hardware embedded in TPS
Disadvantages	• Most massive concept • New battery chemistry may be required, significant development cost	• Difficult electrical interconnect scheme • Low efficiency means large radiator areas to maintain cold temperature end • Must be embedded into TPS, interface difficult	• Complicated interface to TPS and support structure • Potential for vibration from engines affecting pointing • Hot collector embedded into or attached to bottom surface of heat shield	• Low system TRL, most major components have flight heritage

tion 3 of this report. The photovoltaic concept will generate power throughout the solar encounter without the long-term need for batteries or other form of energy storage. The mass of this concept is estimated to be 66 kg. This concept was eventually chosen as a result of this trade study.

C.3 Trade Study Results

Table C-1 summarizes each concept and discusses advantages and disadvantages of each. Ultimately, the choice of concept for Solar Probe+ was driven by mass. Systems involving the use of energy storage were all more massive than the radioisotope thermal generator (RTG) system baselined for the 2005 study[2] (which was 120 kg), and none of the orbits under consideration in the mission design trade study could incorporate the increased mass and still achieve orbit, much less maintain the mass margin required as part of the overall Solar Probe+ study. The low mass of the photovoltaic concept relative to the others considered is an enabler for the Solar Probe+ mission concept as a whole.

[2] *Solar Probe: Report of the Science and Technology Definition Team*, NASA/TM—2005–212786, National Aeronautics and Space Administration, Goddard Space Flight Center, Greenbelt, MD (2005).

APPENDIX D:

REFERENCES

Atlas Launch Systems Mission Planner's Guide, Rev. 10a, Lockheed Martin Corporation (January 2007).

Boslough, M. B., *et al*., Hypervelocity testing of advanced shielding concepts for spacecraft against impacts to 10 km/s, *Int. J. Impact. Eng.* **14,** 96–106 (1993).

Covert, R., *Ten Common Things Wrong with Cost Risk Analysis*, Presented at 76th SSCAG, Hampton Roads, VA (October 22–23, 2002).

General Environmental Verification Standards (GEVS) for GSFC Flight Programs and Projects, GSFC-STD-7000, Goddard Space Flight Center (April 2005).

Gloeckler, G., *et al*., *Solar Probe: First Mission to the Nearest Star, Report of the NASA Science Definition Team for the Solar Probe Mission*, The Johns Hopkins University Applied Physics Laboratory, Laurel, MD (1999).

Goldstein *et al*., *Spacecraft Mass Loss and Electric Potential Requirements for the Starprobe Mission*, A Report of the Starprobe Mass Loss Requirements Group Meeting of September 29–30, 1980, NASA Jet Propulsion Laboratory, California Institute of Technology, Pasadena, CA (December 1980).

Ishimoto, H., Mann, I., Modeling the number density distribution of interplanetary dust on the ecliptic plane within 5 AU of the Sun, *Astron. Astrophys.* **362,** 1158–1173 (2000).

Load Analyses of Spacecraft and Payloads, NASA-STD-5002, National Aeronautics and Space Administration (June 21, 1996).

Mann, I., *et al*., Dust near the Sun, *Space Sci. Rev.* **110,** 269–305 (2004).

Payload Test Requirements, NASA-STD-7002, Rev A, National Aeronautics and Space Administration (September 10, 2004).

Payload Vibroacoustic Test Criteria, NASA-STD-7001, National Aeronautics and Space Administration (June 21, 1996).

Qualification and Quality Requirements for Space Solar Cells, AIAA Standard S-111-2005, American Institute of Aeronautics and Astronautics (January 2005).

Solar Probe Risk Mitigation Study, prepared by The Johns Hopkins University Applied Physics Laboratory, 2006 Mid-Year Report.

Solar Probe Thermal Protection System Risk Mitigation Study: FY 2006 Final Report, prepared by The Johns Hopkins University Applied Physics Laboratory under Contract NAS5-01072, Laurel, MD (November 30, 2006).

Solar Probe Thermal Protection System Risk Mitigation Study: FY 2006 Final Report ITAR-Restricted Annex, prepared by The Johns Hopkins University Applied Physics Laboratory under Contract NAS5-01072, Laurel, MD (September 17, 2007).

Solar Probe: An Engineering Study, prepared by The Johns Hopkins University Applied Physics Laboratory, in partnership with the Jet Propulsion Laboratory, under contract NAS5-01072, Laurel, MD (November 12, 2002).

Solar Probe: Report of the Science and Technology Definition Team, NASA/TM—2005–212786, National Aeronautics and Space Administration, Goddard Space Flight Center, Greenbelt, MD (2005).

Solar Probe+: Report of the Science and Technology Definition Team, Southwest Research Institute, San Antonio, TX, in press (2008).

Unmanned Space Vehicle Cost Model, Eighth Edition (USCM8), Tecolote Research, Inc., Goleta, CA, www.uscm8.com (October 2001).

APPENDIX E:

ACRONYMS AND ABBREVIATIONS

ACO	Administrative Contracting Officer
ADACS	Attitude Determination and Control Subsystem
AGE	Ground Support Equipment
AIAA	American Institute of Aeronautics and Astronautics
AICF	Aerogel Infiltrated Carbon Foam
AISC	Application-Specific Integrated Circuits
Al_2O_3	Aluminum Oxide, Alumina
AU	Astronomical Unit
C&DH	Command and Data Handling
CBE	Current Best Estimate
CC&DH	Command, Control, Communications, and Data Handling
CCD	Charge-Coupled Device
CCSDS	Consultative Committee for Space Data Systems
CD	Coronal Dust Detector
CDPU	Common Data Processing Unit
CDR	Critical Design Review
CER	Cost Estimating Relationship
CFDP	CCSDS File Delivery Protocol
cFE	Core Flight Executive
CFOV	Clear Field of View
CG	Center of Gravity
CIC	Cell-Interconnect-Cover
CLA	Coupled Loads Analysis
Co-I	Coinvestigator
CP	Center of Aerodynamic Pressure
cPCI	Compact Peripheral Component Interface
CPD	Cumulative Probability Distribution
CRISM	Compact Reconnaissance Imaging Spectrometer for Mars
CTE	Coefficient of Thermal Expansion
CTH	Coupled Thermodynamic and Hydrodynamic Hydrocode
DCMC	Defense Contract Management Command
Delta-DOR	Delta Differential One-Way Range
DOD	Depth of Discharge
DSMS	Deep Space Mission System
DSN	Deep Space Network
EMC	Electromagnetic Compatibility
EMCPM	Engineering Model Cell Positioning Mechanism
EMI	Electromagnetic Interference
EPI	Energetic Particle Instrument
EUV	Extreme Ultraviolet
FEA	Fast Electron Analyzers
FIA	Fast Ion Analyzer
FOV	Field of View
FPM	Fault Protection Module
FSW	Flight Software
FY07$	Fiscal Year 2007 Dollars
FY07$M	Fiscal Year 2007 Millions of Dollars
FY08	Fiscal Year 2008
g	Acceleration of Gravity
G&C	Guidance and Control
GaAs	Gallium Arsenide
GDS	Ground Data System
GEVS	General Environmental Verification Standard
Gr/CE	Carbon Graphite/Cyanate Ester
GSFC	Goddard Space Flight Center
HGA	High-Gain Antenna
HI	White-Light Hemispheric Imager
I&T	Integration and Testing
ICA	Ion Composition Analyzer
ICE	Independent Cost Estimate
IEM	Integrated Electronic Module
in.	Inch
I–V	Current–Voltage
JGA	Jupiter Gravity Assist
JSC	Johnson Space Center
kg	Kilogram
KSC	Kennedy Space Center
lb	Pound
lbf	Pound of Force
LGA	Low-Gain Antenna
LRO	Lunar Reconnaissance Orbiter
LVPS	Low-Voltage Power Supply

M&SA	Mission and Safety Assurance
MAG	Magnetometer
MCR	Mission Confirmation Review
MDR	Mission Design Review
MESSENGER	MErcury Surface, Space ENvironment, GEochemistry, and Ranging
MGSE	Mechanical Ground Handling Equipment
MLI	Multi-Layer Insulation
MODC	Miscellaneous Other Direct Costs
MOS	Mission Operations System
MRO	Mars Reconnaissance Orbiter
MSX	Midcourse Space Experiment
NAFCOM	NASA–Air Force Cost Model
NGS	Neutron/Gamma-Ray Spectrometer
NICM	NASA Instrument Cost Model
OD	Orbit Determination
PAS	Product Assurance System
PBN	Pyrolytic Boron Nitride
PDF	Probability Density Function
PDR	Preliminary Design Review
PDT	Pacific Design Technology
PDU	Power Distribution Unit
PER	Pre-Environmental Review
PI	Principal Investigator
PM	Program Management
POE	Program Office Estimate
PPT	Peak Power Tracker
PSE	Power System Electronics
psig	Pound-Force per Square Inch Gauge
PSP	Participating Science Program
PSR	Pre-Ship Review
PWI	Plasma-Wave Instrument
RBSP	Radiation Belt Storm Probes
RF	Radio Frequency
RHCP	Right-Hand Circularly Polarized
RIU	Remote Interface Unit
RMIS	Resource Management Information System
RMS	Root-Mean-Squared
ROM	Rough Order of Magnitude
R_S	Solar Radius
RTG	Radioisotope Thermoelectric Generator
RTW	Real-Time Workshop
RVC	Reticulated Vitreous Carbon
RY$	Real Year Dollars
S/N	Signal-to-Noise
SAJB	Solar Array Junction Box
SDO	Solar Dynamics Observatory
SEP	Sun–Earth–Probe
SEP	Systems Engineering
SPDT	Single-Pole-Double-Throw
SPE	Sun–Probe–Earth
SSR	Solid-State Recorder
STDT	Science and Technology Definition Team
STEREO	Solar TErrestrial RElations Observatory
SwRI	Southwest Research Institute
TCM	Trajectory Correction Maneuver
TDRSS	Tracking and Data Relay Satellite System
TIMED	Thermosphere, Ionosphere, Mesosphere Energetics and Dynamics
TPS	Thermal Protection System
TRL	Technology Readiness Level
TSA	Transition Structure Assembly
TT&C	Telemetry, Tracking, and Control
TVA	Thrust Vector Actuator
TWTA	Traveling Wave Tube Amplifier
USCM8	Air Force's Unmanned Spacecraft Cost Model
UTC	Coordinated Universal Time
W	Watt
WBS	Work Breakdown Structure
XFER Switch	Transfer Switch
α	Absorptivity
ε	Emissivity

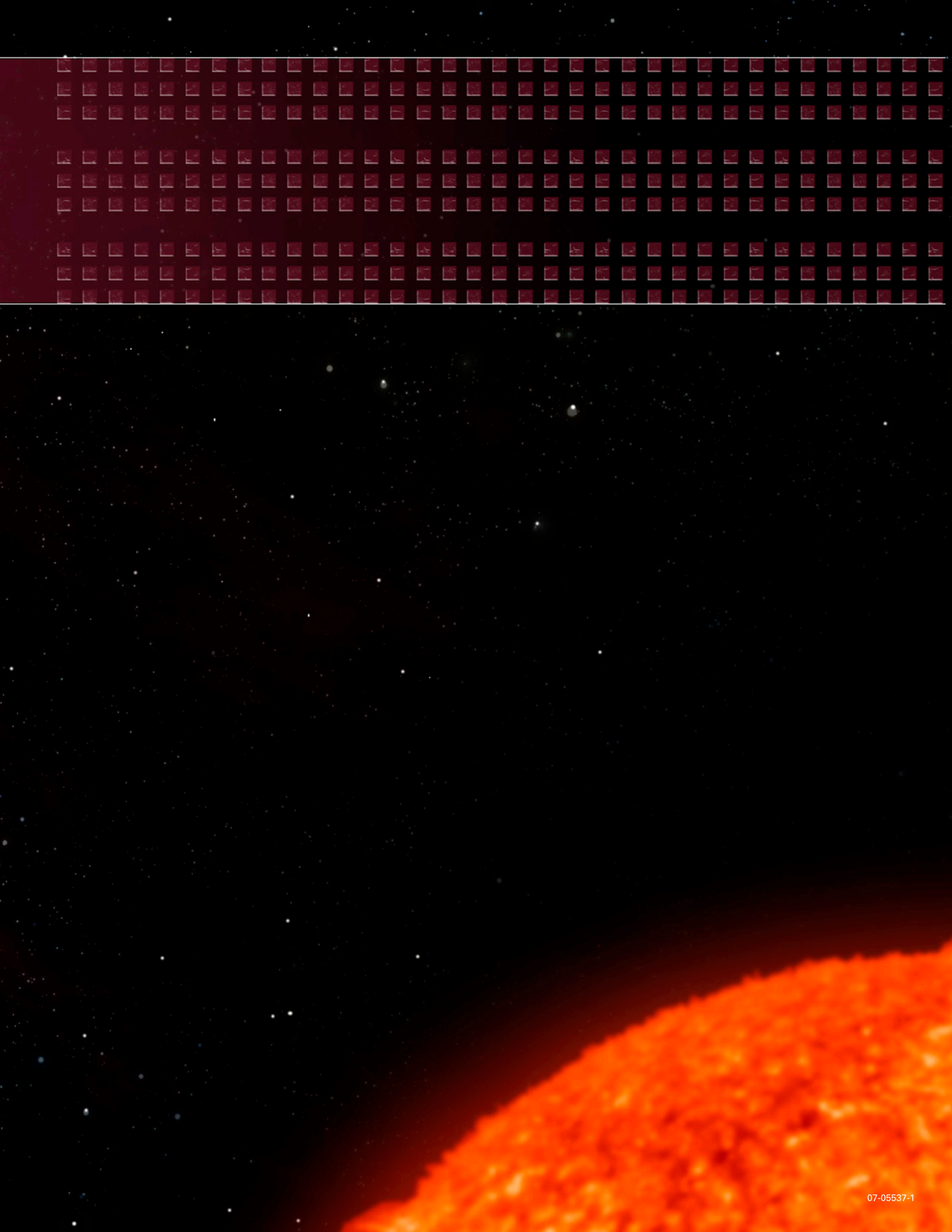

07-05537-1